NASA TECHNICAL TRANSLATION

NASA TT F-591

NASA TT F-591

PROBLEMS OF WAVE DIFFRACTION AND PROPAGATION, No. 7

E. M. Gyunninen, Editor

Leningrad State University Press, Leningrad, 1968

NATIONAL AERONAUTICS AND SPACE ADMINISTRATION • WASHINGTON, D. C. • NOVEMBER 1969

PROBLEMS OF WAVE DIFFRACTION AND PROPAGATION, No. 7

E. M. Gyunninen, Editor

Translation of: "Problemy Difraktsii i Rasprostraneniya Voln. VII"
Leningrad State University Press, Leningrad, 1968

NATIONAL AERONAUTICS AND SPACE ADMINISTRATION

For sale by the Clearinghouse for Federal Scientific and Technical Information
Springfield, Virginia 22151 – Price $3.00

The collection treats the problems of the propagation of radio waves in the waveguide channel Earth-ionosphere, as well as some questions on the diffraction of waves. One of the articles contains a review of asymptotic methods of solving differential equations with a reversal point.

The collection is of interest to specialists in radiophysics, and undergraduate and graduate students specializing in the field of the radiophysics of radio-wave propagation.

TABLE OF CONTENTS

CUT ALONG THIS LINE

FOLD LINE

NATIONAL AERONAUTICS AND SPACE ADMINISTRATION
WASHINGTON, D.C. 20546

OFFICIAL BUSINESS

POSTAGE AND FEES PAID
NATIONAL AERONAUTICS & SPACE ADMINISTRATION

NATIONAL AERONAUTICS AND SPACE ADMINISTRATION
CODE USS-T
WASHINGTON, D.C. 20546

NASA TTF No.
591

FOLD LINE

CUT ALONG THIS LINE

NATIONAL AERONAUTICS AND SPACE ADMINISTRATION

TECHNICAL TRANSLATION EVALUATION

Budget Bureau No. 104-R037
Approval Expires: Sept. 30, 1969

TO: THE USERS OF THIS TRANSLATION →

NASA TTF NO. 591

MAINTAINING THE QUALITY OF NASA TRANSLATIONS REQUIRES A CONTINUOUS EVALUATION PROGRAM. PLEASE COMPLETE AND MAIL THIS FORM TO AID IN THE EVALUATION OF THE USEFULNESS AND QUALITY OF THE TRANSLATING SERVICE.

THIS PUBLICATION *(Check one or more)*

- [ ] FURNISHED VALUABLE NEW DATA OR A NEW APPROACH TO RESEARCH.
- [ ] VERIFIED INFORMATION AVAILABLE FROM OTHER SOURCES.
- [ ] FURNISHED INTERESTING BACKGROUND INFORMATION.
- [ ] OTHER *(Explain)*: _____

FOLD LINE FOLD LINE

TRANSLATION TEXT *(Check one)*

- [ ] IS TECHNICALLY ACCURATE
- [ ] IS SUFFICIENTLY ACCURATE FOR OUR PURPOSE.
- [ ] IS SATISFACTORY, BUT CONTAINS MINOR ERRORS.
- [ ] IS UNSATISFACTORY BECAUSE OF *(Check one or more)*:
  - [ ] POOR TERMINOLOGY
  - [ ] NUMERICAL INACCURACIES.
  - [ ] INCOMPLETE TRANSLATION
  - [ ] ILLEGIBLE SYMBOLS, TABULATIONS, OR CURVES.
  - [ ] OTHER *(Explain)*: _____

FOLD LINE FOLD LINE

REMARKS

FROM

DATE

NOTE: REMOVE THIS SHEET FROM THE PUBLICATION, FOLD AS INDICATED, STAPLE OR TAPE, AND MAIL. NO POSTAGE NECESSARY.

NASA Form 1332 AUG 66

GPO 915-777

CUT ALONG THIS LINE

CUT ALONG THIS LINE

ASYMPTOTICS OF SOLUTIONS TO LINEAR SYSTEMS OF ORDINARY DIFFERENTIAL EQUATIONS WITH A LARGE PARAMETER IN THE PRESENCE OF REVERSAL POINTS

A.G. Alenitsyn

ABSTRACT: The article is basically a brief review of the results known from literature which touch on the asymptotic behavior of linear systems of ordinary differential equations with a large parameter. The basic facts from the classical theory, which is applicable when there are no reversal points, are first given for comparison (Section 1), and then the general method of approaching the problem of reversal points - the method of decomposition - is examined (Section 2). The asymptotics is obtained in Section 3 with the aid of a standardization method over the real interval containing the simplest reversal points. Examples from acoustics and the theory of elasticity are given in the article.

Section 1. Introduction and Classical Theory

An ordinary differential equation is often found in problems /3* of wave diffraction and propagation, i.e.,

$$-y''+k^2p(x)\,y+q(x)y=0, \tag{1.1}$$

and then the behavior of solutions to this equation must be known for $k \to \infty$.

Studies [1-3] in which asymptotic expansions of solutions to systems of ordinary differential equations with a large parameter[1] are used have recently appeared. For example, the following system is found in problems of wave propagation in a layered-nonhomogeneous elastic medium:

$$\vec{G}''+k\begin{pmatrix}0 & 1-\frac{1}{p}\\ 1-p & 0\end{pmatrix}\vec{G}'-k^2\begin{pmatrix}\frac{m_p^2}{p} & 0\\ 0 & pm_s^2\end{pmatrix}\vec{G}+ \\ +\begin{pmatrix}\frac{\mu'}{\mu} & 0\\ 0 & \frac{\nu'}{\nu}\end{pmatrix}\vec{G}'+k\begin{pmatrix}0 & -\frac{\mu'}{\mu}\\ \frac{\lambda'}{\nu} & 0\end{pmatrix}\vec{G}=0, \tag{1.2}$$

/4

---

* Numbers in the margin indicate pagination in the foreign text.

[1] Similar systems are found in some problems of quantum mechanics [28] and in the theory of an isotropic plasma [29].

where $\underline{p} = \mu/\nu$; $\nu = \lambda + 2\mu$; $\underline{m}_p^2 = 1 - \sigma^2\rho/\nu$; $\underline{m}_s^2 = 1 - \sigma^2\rho/\mu$; $\lambda = \lambda(\underline{x})$; $\mu = \mu(\underline{x})$; $\rho = \rho(\underline{x})$; $\underline{k}$ and σ are parameters of separation of variables ($\underline{k} \to \infty$); $\vec{\underline{G}}$ is a two-dimensional vector. This system is of the "connected" type, i.e., it cannot be reduced directly to two independent equations of second order. It is convenient to write out (1.2) in the form of a system

$$\vec{Z}' = [kA(x, \sigma) + B(x)]\vec{Z} \tag{1.3}$$

of four equations of first order, assuming the following:

$$\vec{Z} = (Z_1, Z_2, Z_3, Z_4) = (G_1, G_2, k\,{}^1G_1', k^{-1}G_2').$$

Here and further, the prime designates differentiation by $\underline{x}$.

We will consider the general case of a linear system

$$\vec{Z}' = k^m A(x, k)\vec{Z} \tag{1.4}$$

of $\underline{n}$ equations with a square matrix $\underline{A}(\underline{x}, \underline{k})$ of $\underline{n}$-th order; $\underline{m} > 0$ is an integer. Equation (1.1) is also reduced to a system of this type ($\underline{n} = 2$):

$$\vec{Z}' = k\begin{pmatrix} 0 & 1 \\ p & 0 \end{pmatrix}\vec{Z} + k^{-1}\begin{pmatrix} 0 & 0 \\ q & 0 \end{pmatrix}\vec{Z}, \quad \vec{Z} = \begin{pmatrix} y \\ k^{-1}y' \end{pmatrix} \tag{1.1a}$$

As regards the matrix $\underline{A}(\underline{x}, \underline{k})$ in (1.4), we will assume that it is expanded into a series by degrees of $\underline{k}^{-1}$:

$$A(x, k) = \sum_{\nu=0}^{\infty} A_\nu(x)k^{-\nu}, \tag{1.5}$$

This can be convergent or asymptotic. Even if the matrices $\underline{A}\nu(\underline{x})$ are assumed to be smooth (i.e., have several derivatives), $\underline{A}(\underline{x}, \underline{k})$ is continuous.

It is natural to assume that the higher term in (1.5) has most effect on the behavior of solutions to (1.4) for $\underline{k} >> 1$, i.e., that the matrix $\underline{A}(\underline{x}, \underline{k})$ can be replaced in first approximation by $\underline{A}_0(\underline{x})$ (or any matrix $\underline{B}(\underline{x}, \underline{k}) = \underline{A}(\underline{x}) + \sum_{\nu \neq 1}^{\infty} \underline{B}_\nu(\underline{x})\underline{k}^{-\nu}$). This idea is directed

in particular to the extensively studied [4-9] example of (1.1). Actually, it is found that this assumption is reliable in a sense, /5
although clarifications are needed even to find the first approximation. Moreover, the formulas (and corresponding proofs) differ greatly in the case when there are no reversal points in the interval for change in $\underline{x}$ under investigation, as well as in the case when there are such; in the latter case, the problem is much more complicated.

In studying the asymptotics of solutions to (1.4), the eigenvalues $\lambda_1(\underline{x})$, $\lambda_2(\underline{x})$, ..., $\lambda_n(\underline{x})$ of the matrix $\underline{A}_0(\underline{x})$ play a very important role.

The case when all the eigen-values are different is the simplest:

$$\lambda_i(x) \neq \lambda_j(x),\ i \neq j,\ i, j = 1, 2, \ldots, n. \tag{1.6}$$

The classical Birkhoff-Tamarkin theorem [10, 11] is famous for this case. It will be formulated here for $\underline{m} = 1$ and a real $\underline{x} \in [\underline{a}, \underline{b}]$ for the sake of simplicity.

We will call $\underline{S}$ the infinite, simple connected region on the complex $\underline{k}$-plane.

Birkhoff-Tamarkin Theorem. Let the following conditions be fulfilled in the interval $\underline{a} \leq \underline{x} \leq \underline{b}$ ($\underline{a}, \underline{b} \neq \infty$): (1) $\lambda_i(\underline{x}) \neq \lambda_j(\underline{x})$, $\underline{i} \neq \underline{j}$; (2) the $\underline{S}$ region is such that

$$\operatorname{Re}[k\lambda_j(x)] \leqslant \operatorname{Re}[k\lambda_{j+1}(x)],\quad j = 1, 2, \ldots, n-1;$$

(3) $\underline{A}_\nu(\underline{x}) \in \underline{C}^{N+1-\nu}[\underline{a}, \underline{b}]$, i.e., the elements of the matrix $\underline{A}_\nu$ have $\underline{N} + \underline{1} - \nu > 0$ continuous derivatives. Then there is a fundamental matrix $Z(\underline{x},\underline{k})$ in the interval $[\underline{a},\underline{b}]$ for (1.4) which had the following asymptotic expansion in the $\underline{S}$ region at $k \to \infty$

$$Z(x, k) = \left[\sum_{\nu=0}^{N-1} T_\nu(x)\, k^{-\nu} + O(k^{-N})\right] \times \exp\left\{\int [k\Lambda(x) + V(x)]\, dx\right\}, \tag{1.7}$$

where $\underline{T}_0(\underline{x})$ ($\det \underline{T}_0(\underline{x}) \neq 0$) reduces $\underline{A}_0(\underline{x})$ to the diagonal form $\Lambda(\underline{x}) = \underline{T}_0^{-1}\underline{A}_0\underline{T}_0$, the diagonal matrix $V(\underline{x})$ and the matrices $\underline{T}_1, \underline{T}_2, \ldots, \underline{T}_N - \underline{1}$ are calculated in the form of continuous functions by the recurrent formulas. The expansion of (1.7) is uniform for $[\underline{a}, \underline{b}]$.

There is a simple proof[2] to the general theorem (at $\underline{m} \geq 1$) in [12]. Different generalizations of this theorem can be found in [13-15]. With the aid of the classical asymptotic formulas, I solved in particular, the problem of high-frequency surface waves in a nonhomogeneous elastic space [1].

Section 2. Reversal Points. Decomposition Method /6

The term "reversal point" is used in different senses by different authors. Thus, any point on the real axis, during the passage through which the nature of solutions greatly changes, is sometimes called the reversal point. In this study, the term is used in a narrower sense.

Definition. The point $\underline{x}_0$ is called the reversal point for the system in (1.4) if two or more eigen-values of the matrix $\underline{A}_0(\underline{x})$ coincide at this point, while all the eigen-values are different in a certain neighborhood of $\underline{x}_0$; $\underline{A}_0(\underline{x})$ is continuous.[3]

Thus, very interesting problems linked with the poles and other particular points of the coefficients of this system are eliminated from this investigation. The definition of the reversal point used here naturally generalizes the ordinary definition for (1.1). Actually, for (1.1) $\lambda_1 = \sqrt{\underline{p}}$, $\lambda_2 = -\sqrt{\underline{p}}$, and $\lambda_1 = \lambda_2$ only if $\underline{p} = 0$.

The asymptotic theory for (1.1) in regions containing reversal points is relatively simple and has been analyzed in great detail ([4-9, 15, 16], etc.). A similar theory for general systems has not been developed to a great extent because of the great complexity of the problem.

The most general method for simplification of the problem is the so-called "decomposition method" [17, 18], which will be presented below.

Let us make a linear transformation, i.e.,

$$\vec{Z} = P(x, k)\vec{X}, \tag{2.1}$$

then

$$\vec{X}' = k^m B(x, k)\vec{X}, \quad B(x, k) = P^{-1}AP - P^{-1}P'k^{-m}. \tag{2.2}$$

---

[2] Inaccuracy was allowed in the proof and formulation of the theorem in [12]: there $A^{\nu} \in C^{N-1}$ is required, from which (1.7) is not obtained (a corrected formulation is given here).

[3] See the case of identically equal roots in [13].

It is found that, under certain conditions, we can select such a transformation of (2.1) that the system in (2.2) is quasi-diagonal.

Case 1. $\underline{x} \in \underline{D}$ is of a finite complex region We will consider $\underline{A}(\underline{x},\underline{k})$ to be regular in the region $|\underline{x} - \underline{x}_0| \leq \varepsilon, |\underline{k}| \geq \underline{k}_0 > 0, |\arg \underline{k}| \leq \alpha_0 > 0$; $\underline{A}_\nu(\underline{x})$ are regular at $|\underline{x} - \underline{x}_0| \varepsilon$. As is well known (see [19], for example), any constant square matrix $\underline{C}$ can be reduced by such transformation: $\underline{U}^{-1}\underline{C}\underline{U} = \underline{\widetilde{C}}$ to a canonical Jordan form, i.e.,

$$\widetilde{C} = [\widetilde{C}_1, \widetilde{C}_2, \ldots, \widetilde{C}_s], \quad s \leqslant n. \tag{2.3}$$

Here $\underline{C}$ is a quasi-diagcnal matrix, while the number $\underline{s}$ of diagonal blocks (cells) is equal to the number of various eigen-values of the matrix $\underline{C}$. Obviously, we can consider $\underline{A}_0(\underline{x}_0)$ to be reduced to the Jordan form.

Sibuya Theorem on Decomposition. In a certain subdomain /7

$$|x - x_0| \leqslant \varepsilon_1 \leqslant \varepsilon, \ |k| \geqslant k_1 \geqslant k_0, \ |\arg k| \leqslant \alpha_1 \leqslant \alpha_0 \tag{2.4}$$

there is a regular non-singular transformation of (2.1) such that the matrix $\underline{B}(\underline{x},\underline{k})$ in the corresponding system of (2.2) is quasi-diagonal, i.e.,

$$B(x, k) \quad [B_1(x, k), B_2(x, k), \ldots, B_s(x, k)], \quad s < n, \tag{2.5}$$

while the structure of $\underline{B}(\underline{x},\underline{k})$ coincides with the structure of the matrix $\underline{A}_0(\underline{x}_0)$. The matrices $\underline{P}(\underline{x},\underline{k})$ and $\underline{B}_i(\underline{x},\underline{k})$ ($\underline{i} = 1, \ldots, \underline{s}$) are expanded in the domain of (2.4) into asymptotic series, i.e.,

$$B_i(x, k) \sim \sum_{\nu=0}^{\infty} B_{i\nu}(x) k^{-\nu}, \tag{2.6}$$

$$P(x, k) \sim \sum_{\nu=0}^{\infty} P_\nu(x) k^{-\nu},$$

and $\underline{P}_0(\underline{x}_0) = \underline{E}$ is a unit matrix, while $\underline{P}_0(\underline{x})$ reduces $\underline{A}_0(\underline{x})$ to a quasi-diagonal form of the same structure as $\underline{A}_0(\underline{x}_0)$; the remaining $\underline{P}_\nu(\underline{x})$ and $\underline{B}_\nu(\underline{x})$ are calculated recurrently. All the matrices in (2.6) are regular in (2.4).

We can see that the Sibuya theorem aids in simplifying the system (1.4) in the neighborhood of any reversal point, reducing it to a selection of $\underline{s} \leq \underline{n}$ systems - cells with a smaller number of equations in each; actually, the number of equations in the system-cell No. $\underline{i}$

$$\vec{X}_i' = k^m B_i(x, k)\vec{X}_i, \quad i=1, \ldots, s \tag{2.7}$$

is equal to the multiplicity q_i of the eigen-value $\lambda_i(x_0)$.

The Sibuya theorem was applied, for example, to the system in (1.3) in [20]. In the case of (1.3), the reversal points $x_p(\sigma)$ and $x_s(\sigma)$ satisfied the following equations, respectively:

$$\sigma = \pm v_p(x), \ \sigma = \pm v_s(x).$$

where

$$v_p^2(x) = \frac{\lambda+2\mu}{\rho}, \ v_s^2(x) = \frac{\mu}{\rho}.$$

The following system of two equations is obtained for the neighborhood of the point $x_p(\sigma)$ as a result of decomposition:

$$\vec{X}_1' = \left\{k\begin{pmatrix}0 & 1\\ m_p^2 & 0\end{pmatrix} + L + O(k^{-1})\right\}\vec{X}_1 \tag{2.8}$$

and two individual scaler equations, i.e.,

$$X_{2,3}' = \{\mp km_s + M + O(k^{-1})\}X_{2,3}. \tag{2.9}$$

Here

$$M = -\frac{1}{2}\frac{(\rho m_s)'}{\rho m_s}, \quad L = \begin{pmatrix}\alpha & 0\\ 0 & \beta\end{pmatrix},$$
$$\alpha = -\frac{\rho'}{\rho} - \frac{2v_s^2}{\sigma^2}\frac{\mu'}{\mu}, \quad \beta = \frac{2v_s^2}{\sigma^2}\frac{\mu'}{\mu}$$

The equations in (2.9) are integrated directly, and the system of (2.8) is easily reduced to one second-order equation of the type in (1.1). /8

Although the Sibuya theorem is universal, it has a local nature, which is inconvenient in practice. In the case of a real x, decomposition over an arbitrary finite interval can be carried out (see [17, 21]).

Case 2. $x \in [a, b]$ for a real interval. We will consider that $A(x,k)$ and $A_0(x)$ are infinitely differentiable by x and that the matrix $A_0(x)$ has the following property: the eigen-values of the matrix $A_0(x)$ can be divided into groups in such a way that the eigen-values of one group (for any x) are not equal to the eigen-values

of another group (the condition of S.F. Feshchenko).

With these assumptions[4], there is non-degenerate, infinitely differentiable transformation of $\underline{P}(\underline{x},\underline{k})$ over the entire interval $[\underline{a}, \underline{b}]$, which reduces the system of (1.4) into the form of (2.2) with a quasi-diagonal matrix, i.e.,

$$B(x, k)=[B_1(x, k), B_2(x, k), \ldots, B_s(x, k)], \quad s\leqslant n. \tag{2.10}$$

The matrices $\underline{P}(\underline{x},\underline{k})$ and $\underline{B}(\underline{x},\underline{k})$ are expanded into asymptotic series with coefficients which satisfy the recurrence formulas. The structure of $\underline{B}(\underline{x},\underline{k})$ is determined by dividing the eigen-values of the matrix $\underline{A}_0(\underline{x})$ into groups: if there are $\underline{q}_{\underline{i}}$ eigen-values in group No. $\underline{i}$ ($\underline{i}$ = 1, 2, ..., $\underline{s}$),

$$\lambda_{i1}(x), \ldots, \lambda_{iq_i}(x), \tag{2.11}$$

then the following system-cell corresponds to this group:

$$X_i'=k^m[B_{i0}(x)+B_{i1}(x)k^{-1}+\ldots]\vec{X}_i, \tag{2.12}$$

and the eigen-values of the matrix $\underline{B}_{\underline{i}0}(\underline{x})$ coincide with (2.11). Here again, as in the Sibuya theorem, the matrix $\underline{P}_0(\underline{x})$ reduces the matrix $\underline{A}_0(\underline{x})$ to a quasi-diagonal form:

$$P_0^{-1}A_0P_0\equiv B_0(x)=[B_{10}(x), \ldots, B_{s0}(x)]. \tag{2.13}$$

Let us emphasize the varying nature of decomposition in the complex and real cases: in the first case we are examining the total neighborhood of an individual reversal point, and in the second there can be any coincidences of eigen-values at any number of points inside the given group.

The decomposition method is not always suitable for practice, since, first of all, very stringent conditions are imposed on $\underline{A}(\underline{x},\underline{k})$ (regularity in the complex case, infinite smoothness in the real case); secondly, after decomposition there must be a special study of the decomposed systems, and this, generally speaking, is a complicated problem (see [22-24]);[5] thirdly, in order to compute the further terms in expansions of the solutions, we must make a large number of calculations, since the recurrence formulas appear twice - in obtaining the decomposed system and in its solution. /9

---

[4] And some additional ones which we will not formulate here (see [17] and [21]).

[5] In the cases encountered in practice, the decomposed systems usually have a simple form.

Sometimes asymptotic formulas can be obtained without the decomposition method. In the following section, we will prove a theorem which, in a sense, is similar to the classical one, for the case of the so-called "simplest" reversal point. The method for the proof is a standardization equation; a regular proof of the classical theorem [12] is carried out essentially by the standardization method. Some new instances appear in the proof given below.

Section 3. Uniform Asymptotics in a Real Interval Containing the Simplest Reversal Point

Let us consider the system

$$\vec{Z}' = kA(x, k)\vec{Z} \tag{3.1}$$

of $\underline{n} > 1$ equations with a square $\underline{n} \times \underline{n}$ complex-value matrix, continuous over $(\underline{x}, \underline{k})$ in the region $\underline{a} \leq \underline{x} \leq \underline{b}$, $\underline{k} \leq \underline{k}_0 > 0$ and smooth over $\underline{x}$ for a fixed $\underline{k}$. Let

$$A(x, k) \sim \sum_{\nu=0}^{\infty} A_\nu(x)\, k^{-\nu} \tag{3.2}$$

with smooth $\underline{A}_\nu(\underline{x})$ [the series in (3.2) is convergent or asymptotic]. The eigen-values of $\underline{A}_0(\underline{x})$ will be $\lambda_1(\underline{x}), \ldots, \lambda_{\underline{n}}(\underline{x})$.

Definition. A reversal point $\underline{x} = \underline{x}_0$ is called the simplest one if the following hold for $|\underline{x} - \underline{x}_0| \leq \varepsilon$:

$$\begin{aligned} &a)\ \lambda_1(x),\ \lambda_2(x) \neq \lambda_j(x),\ j = 3, 4, \ldots, n; \\ &b)\ \lambda_i(x) \neq \lambda_j(x) \text{ for } i \neq j,\ i, j = 3, 4, \ldots, n; \\ &c)\ p(x) \equiv \tfrac{1}{4}[\lambda_1(x) - \lambda_2(x)]^2 = (x - x_0)\, p_1(x),\ p_1(x) \neq 0,\ \operatorname{Im} p(x) = 0. \end{aligned}$$

For (1.1), this definition coincides with the ordinary definition of a simple reversal point: $\underline{p}(\underline{x})$ has a simple zero for $\underline{x} = \underline{x}_0$.

We will assume, without losing the generality, that $\underline{x}_0 = 0$, $\underline{a} \leq 0 \leq \underline{b}$ and $\underline{p}_1(\underline{x}) > 0$. Let us make the symmetrizing transformation

$$\vec{Z} = \vec{\widetilde{Z}} \exp\left[\frac{k}{2}\int(\lambda_1 + \lambda_2)\, dx\right], \tag{3.3}$$

Then the system acquires a form

$$\vec{\widetilde{Z}}' = k\left[A(x, k) - \frac{1}{2}(\lambda_1 + \lambda_2)\, E\right]\vec{\widetilde{Z}} \equiv k\widetilde{A}(x, k)\vec{\widetilde{Z}},$$

which is convenient in that $\tilde{\lambda}_1(\underline{x}) \equiv -\tilde{\lambda}_2(\underline{x})$, since

$$\tilde{\lambda}_j(x)=\lambda_j(x)-\frac{1}{2}(\lambda_1(x)+\lambda_2(x)), \quad j=1, 2, \ldots, n. \tag{3.4}$$

We will consider that the transformation of (3.3) is already done, and then $\lambda_1(\underline{x}) \equiv -\lambda_2(\underline{x})$. Obviously, the transformation of (3.3) does not change the nature of the reversal point. /10

Since the eigen-values of $\underline{A}_0(\underline{x})$ are divided into $(\underline{n}-1)$ groups: λ_1 and λ_2; $\lambda_3, \ldots, \lambda_n$, such that the eigen-values can coincide only inside the group, then, as is well known [17], there is a smooth non-singular matrix $\underline{U}_0(\underline{x})$ which reduces $\underline{A}_0(\underline{x})$ to a quasi-diagonal form, i.e.,

$$U_0^{-1}A_0U_0=[S; \lambda_3, \ldots, \lambda_n], \tag{3.5}$$

where 2×2 matrix $\underline{S}(\underline{x})$ has the eigen-values $\lambda_1(\underline{x})$ and $\lambda_2(\underline{x})$.

Let us attempt to reduce $\underline{S}(\underline{x})$ by smooth non-singular transformation of $\underline{L}(\underline{x})$ to the following special form:

$$L^{-1}SL=\begin{pmatrix} 0 & 1 \\ p(x) & 0 \end{pmatrix}. \tag{3.6}$$

Let

$$S(x)=\begin{pmatrix} s_1 & s_2 \\ s_3 & s_4 \end{pmatrix}, \quad L(x)=\begin{pmatrix} l_1 & l_2 \\ l_3 & l_4 \end{pmatrix}$$

Since $\lambda_1 \equiv -\lambda_2$, then $\underline{s}_4 \equiv -\underline{s}_1$, $\underline{s}_1^2 + \underline{s}_2\underline{s}_3 \equiv \underline{p}(\underline{x})$. It is easy to see that we can assume the following (for arbitrary and smooth $\underline{l}_2$, $\underline{l}_4$):

$$L=\begin{pmatrix} s_1l_2+s_2l_4 & l_2 \\ s_3l_2-s_1l_4 & l_4 \end{pmatrix}. \tag{3.7}$$

The matrix of (3.7) is non-singular if

$$l=2s_1l_2l_4+s_2l_4^2-s_3l_2^2 \neq 0, \quad a \leq x \leq b. \tag{3.8}$$

It is easy to show a simple sufficient condition for the existence of a smooth non-singular $\underline{L}(\underline{x})$: if $\underline{s}_2(\underline{x}) \neq 0$, then we can assume that $\underline{l}_4 = 1$, $\underline{l}_2 = 0$; if $\underline{s}_3(\underline{x}) \neq 0$, then $\underline{l}_4 = 0$, $\underline{l}_2 = 1$.[6] If $\underline{s}_2$ and $\underline{s}_3$

[6] In the case of the system of (1.3), $\underline{s}_2(\underline{x}) \neq 0$.

can vanish, then the sufficient conditions are complicated and we will not derive them. In the general case, it can be said that $|\underline{s}_1|+|\underline{s}_2|+|\underline{s}_3|>0$ for all $\underline{x} \in [\underline{a}, \underline{b}]$; it follows, and is easy to show, that $\underline{S}(\underline{x})$ is reduced to the form of (3.6) locally, i.e., in the neighborhood of any point of $[\underline{a}, \underline{b}]$.

Thus, the transformation

$$\vec{Z}=U_0[L;\ E]\vec{X}\equiv U\vec{X} \tag{3.9}$$

reduces the system of (3.1) to the form of

$$X'=(kH_0(x)+B_1(x)+k^{-1}B_2(x)+\dots)\vec{X}, \tag{3.10}$$

where

$$H_0(x)=\left[\begin{pmatrix}0 & 1\\ p & 0\end{pmatrix};\ \lambda_3,\ \lambda_4,\ \dots,\ \lambda_n\right];$$
$$B_1(x)=U^{-1}A_1U-U^{-1}U';\quad B_\nu(x)=A_\nu(x),\ \nu=2,\ 3,\ \dots$$

In the matrix form, (3.10) has the following form: /1

$$X'=(kH_0(x)+B_1(x)+k^{-1}B_2(x)+\dots)X. \tag{3.10a}$$

On the other hand, the quasi-diagonal matrix

$$W(x,\ k)\equiv[Y;\ w_3,\ w_4,\ \dots,\ w_n] \tag{3.11}$$

satisfies the differential matrix equation

$$W'=(kH_1(x)+k^{-1}H_2(x))W, \tag{3.12}$$

if

$$w_j=\exp\left[k\int_a^x\lambda_j(t)\,dt\right],\ j=3,\ 4,\ \dots,\ n;\ H_2(x)=\left[\begin{pmatrix}0 & 0\\ r & 0\end{pmatrix};\ 0\right],$$

while $\underline{Y}$ satisfies the matrix equation

$$Y'=\left\{k\begin{pmatrix}0 & 1\\ p & 0\end{pmatrix}+k^{-1}\begin{pmatrix}0 & 0\\ r & 0\end{pmatrix}\right\}Y. \tag{3.13}$$

Since (3.13) is an equation of the type in (1.1) in a matrix form, we can assume the following:

$$Y=\begin{pmatrix} y_1 & y_2 \\ k^{-1}y_1' & k^{-1}y_2' \end{pmatrix},\quad y_j=\frac{c_j}{\sqrt{\varphi'}}\,\mathrm{Ai}_j\left(k^{2/3}\varphi\right),\quad j=1,\ 2;$$

$$\varphi=\varphi(x)=\left(\frac{3}{2}\int_0^x |p(t)|^{1/2}\,dt\right)^{2/3}\operatorname{sign} x;\quad r=\frac{\psi''}{\psi},\quad \psi=\frac{1}{\sqrt{\varphi'}}.$$

Here $\mathrm{Ai}_j(\underline{t})$ are linearly independent solutions to the Airy equation $\mathrm{Ai}''(\underline{t}) \equiv \underline{t}\mathrm{Ai}(\underline{t})$. It is convenient to take $\mathrm{Ai}_1(\underline{t}) = \underline{u}(\underline{t})$, $\mathrm{Ai}_2(\underline{t}) = \underline{v}(\underline{t})$, where $\underline{u}$ and $\underline{v}$ are Airy functions in the definition by V. A. Fok [25].

The matrix equation in (3.12) can be called a standard equation for the original system of (3.1) or for (3.10a). It can be seen that (3.12) and (3.10a) coincide in the higher terms; however, this is insufficient even for proof of the coincidence of the higher terms for the asymptotics of solutions to these equations. Moreover, if we eliminate $\underline{B}_1(\underline{x})$, then, as will be seen below, even the first term changes asymptotically. Therefore, we will consider a formal expression of the following type:

$$\hat{X}=\sum_{\nu=0} P_\nu(x)\,k^{-\nu}W. \tag{3.14}$$

Having substituted (3.14) into (3.10a) and having equated the coefficients for identical degrees $\underline{k}^{-1}$, we will obtain the recurrence system

$$P_0H_0=H_0P_0, \tag{3.15}$$

$$P_\nu'+P_{\nu+1}H_0-H_0P_{\nu+1}=\sum_{s=0}^{\nu} B_{\nu+1-s}P_s-P_{\nu-1}H_2, \tag{3.16}$$

where $\nu=0,\ 1,\ 2,\ \ldots;\ P_{-1}\equiv 0$.

Equation (3.15) has a matrix of the following type as a general solution: /12

$$P_0=\left[\begin{pmatrix} \alpha_0 & \beta_0 \\ p\beta_0 & \alpha_0 \end{pmatrix};\ a_{03},\ a_{04},\ \ldots,\ a_{0n}\right] \tag{3.17}$$

with arbitrary $\alpha_0(\underline{x})$, $\beta_0(\underline{x})$ and $\underline{a}_{0\underline{i}}(\underline{x})$, $\underline{i} = 3,\ 4,\ \ldots,\ \underline{n}$.

We will examine (3.16) by blocks. Each $\underline{n} \times \underline{n}$ matrix will be divided into four blocks; we will number the blocks in the following

way:

$$H_0=\begin{pmatrix} H_{01} & H_{02} \\ H_{03} & H_{04} \end{pmatrix},\ P_\nu=\begin{pmatrix} P_{\nu 1} & P_{\nu 2} \\ P_{\nu 3} & P_{\nu 4} \end{pmatrix}\ \text{etc.}$$

Here $\underline{H}_{01}$ and $\underline{P}_{\nu 1}$ - are matrices 2 × 2 with elements $(\underline{H}_{01})_{\underline{i}\underline{k}}$ and $(\underline{P}_{\nu 1})_{\underline{i}\underline{k}}$, $\underline{i}$, $\underline{k}$ = 1, 2; $\underline{H}_{02} = \underline{H}_{03} = 0$.

At $\nu = 0$, (3.16) is equivalent to the system of equations for the blocks:

$$1)\ P_{01}'+P_{11}H_{01}=H_{01}P_{11}+B_{11}P_{01};\ 2)\ P_{12}H_{04}=H_{01}P_{12}+B_{12}P_{04};$$

$$3)\ P_{13}H_{01}=H_{04}P_{13}+B_{13}P_{01};\ 4)\ P_{04}'+P_{14}H_{04}=H_{04}P_{14}+B_{14}P_{04}. \qquad (3.18)$$

We find, in particular, from the force equation in (3.18) that

$$a_{0j}(x)=\exp\int (B_1)_{jj}dx,\ j=3,\ 4,\ \ldots,\ n. \qquad (3.19)$$

The non-diagonal elements $\underline{P}_{14}$ are determined uniquely from this equation in terms of the elements of the matrices $\underline{B}_{12}$, $\underline{H}_{04}$, as well as the already-known elements of the matrix $\underline{P}_{04}$. This part of the procedure coincides with the classical one.

The second equation in (3.18) defines $\underline{P}_{12}$ singularly in terms of $\underline{B}_{12}$, $\underline{H}_{01}$, $\underline{H}_{04}$ and $\underline{P}_{04}$, since the eigen-values of $\underline{H}_{01}$ are not equal to those of $\underline{H}_{04}$.[7] For the same reason, the third equation in (3.18) determines $\underline{P}_{13}$, if $\underline{P}_{01}$ is known. The matrix $\underline{P}_{01}$ contains the unknown functions α_0 and β_0; we will find them from the first equation in (3.18). Let

$$P_{11}=\begin{pmatrix} \alpha_1 & \beta_1 \\ \gamma_1 & \delta_1 \end{pmatrix},\ B_{11}=\begin{pmatrix} b_1 & c_1 \\ d_1 & e_1 \end{pmatrix},$$

then the first equation of (3.18) gives the following system:

$$\begin{aligned} &\alpha_0'+\beta_1 p=\gamma_1+b_1\alpha_0+c_1\beta_0 p,\\ &\beta_0'+\alpha_1=\delta_1+b_1\beta_0+c_1\alpha_0,\\ &(\beta_0 p)'+\delta_1 p=p\alpha_1+d_1\alpha_0+e_1\beta_0 p,\\ &\alpha_0'+\gamma_1=p\beta_1+d_1\beta_0+e_1\alpha_0. \end{aligned} \qquad (3.20)$$

---

7 It is well known that, if the square matrices V_1 and V_2 do not have general eigen-values, then the matrix equation $V_1X = XV_2$ has a unique solution $X = 0$ (see [17], for example).

This yields the following, in particular: /13

$$2\alpha_0' = (b_1 + e_1)\alpha_0 + (d_1 + c_1 p)\beta_0,$$
$$2p\beta_0' = d_1\alpha_0 + p[(b_1 + e_1)\beta_0 + c_1\alpha_0] - p'\beta_0. \qquad (3.21)$$

If $\underline{d}_1 + \underline{c}_1\underline{p} \equiv 0$, then we can take $\beta_0 \equiv 0$, $\alpha_0 = \exp \times \left[\frac{1}{2}\int (\underline{b}_1 + \underline{e}_1)\,d\underline{x}\right]$ (for (1.3), $\underline{c}_1 \equiv \underline{d}_1 \equiv 0$). We will assume that $\vec{\omega}_0 = (\alpha_0, \beta_0)$ in the general case. It is easy to show that the basic matrix $\omega_0(\underline{x})$ of (3.21) has the following form:

$$\omega_0(x) = Q(x)\left[1,\ x^{-\frac{1}{2}}\right], \qquad (3.22)$$

where $\underline{Q}(\underline{x})$ is smooth if $\underline{p}(\underline{x})$ and $\underline{B}_{11}(\underline{x})$ are smooth functions. We can take the components of the first vector from (3.22) as α_0 and β_0 and obtain a (smooth) $\underline{P}_{01}(\underline{x})$. The following also follows from (3.20):

$$\gamma_1 = p\beta_1 + \alpha_0' - b_1\alpha_0 - c_1 p\beta_0,$$
$$\delta_1 = \alpha_1 + \beta_0' - b_1\beta_0 - c_1\alpha_0$$

where $\alpha_1(\underline{x})$ and $\beta_1(\underline{x})$ are still arbitrary.

For $\nu = 1$, a nonuniform system of the type in (3.21) is obtained from the first block of (3.16) for $\alpha_1(\underline{x})$ and $\beta_1(\underline{x})$, while the free term contains the already-known functions. It follows from (3.22) for the basic matrix that the nonuniform system has a unique smooth vector solution, i.e.,

$$\vec{\omega}_1(x) = \omega_0(x)\int_a^x \omega_0^{-1}(t)\vec{F}(t)\,dt, \qquad (3.23)$$

where $\vec{\underline{f}}$ is a free term of the nonuniform system. For the rest, the procedure for $\nu = 1$ repeats the procedure with $\nu = 0$. For $\nu > 1$, the arguments are similar.

It is important to note that, if the initial system of (3.1) has infinitely differentiable coefficients, then all the coefficients of the formal solution are infinitely differentiable; if (3.1) has finite smoothness, then only a finite number of continuous $\underline{P}_\nu(\underline{x})$ can be found (this is sufficient for our purposes). In other words,

$P_\mu(x) \in C^{M-\mu}[a, b]$, if $A_\nu(x) \in C^{M-\mu}[a, b]$ $(0 \leq \nu, \mu \leq M)$.

Let us turn to a justification of the formal expansion. As usual, we will construct an approximating solution, i.e.,

$$\widetilde{X}=\sum_{\nu=0}^{N}P_\nu(x)\,k^{-\nu}W(x,\,k),\ N>0. \tag{3.24}$$

It is easy to see that (3.24) satisfies the equation /14

$$\widetilde{X}'=\{kA(x,\,k)+k^{-N}\Gamma(x,\,k)\}\widetilde{X}, \tag{3.25}$$

where the continuous[8] matrix $\Gamma(\underline{x},\,\underline{k})=0(1)$ at $\underline{k}\to\infty$. We still show that there is a real solution $\underline{X}(\underline{x},\,\underline{k})$ to (3.10a) which is close to (3.24) for $\underline{k}>>1$.

Let us find the following integral equation for $\underline{X}(\underline{x},\,\underline{k})$ by the method of variation of constants:

$$X(x)=\widetilde{X}(x)\,C_0-k^{-N}\int^{x}\widetilde{X}(x)\,\widetilde{X}^{-1}(x')\,\Gamma(x')\,X(x')\,dx'. \tag{3.26}$$

Here $\underline{C}_0$ is a constant matrix; integration is carried out from a certain fixed point (for each column of the matrix $\underline{X}$) to a variable point $\underline{x}$; part of the arguments of the functions are omitted for the sake of brevity.

Having introduced

$$F\equiv\left(\sum_{\nu=0}^{N}P_\nu(x)\,k^{-\nu}\right)^{-1}X,\quad \widetilde{\Gamma}\equiv\left(\sum_{\nu=0}^{N}P_\nu(x)\,k^{-\nu}\right)^{-1}\times$$
$$\times\,\Gamma(x)\sum_{\nu=0}^{N}P_\nu(x)k^{-\nu},$$

we will write (3.26) in the following form:

$$F(x)=W(x)-k^{-N}\int_{a}^{x}W_1(x)\,W^{-1}(x')\,\widetilde{\Gamma}(x')F(x')\,dx'-$$
$$-\,k^{-N}\int_{b}^{x}W_2(x)\,W^{-1}(x')\,\widetilde{\Gamma}(x')\,F(x')\,dx'. \tag{3.27}$$

Here it is assumed that $\underline{C}_0=\underline{E}$ and $\underline{W}=\underline{W}_1+\underline{W}_2$; the specific division of $\underline{W}$ is one for each $\underline{j}$ (see below).

---

[8] It is assumed that P_ν has a sufficient number of derivatives. Since Γ contains P_ν and P_ν', then it is sufficient that $M=N+1$.

We will assume the following:

$$\chi_j(\tau, t) \equiv \exp\left[k \int_\tau^t \lambda_j(x)\, dx\right], \quad j = 1, 2, \ldots, n;$$

$$w_j(x, k) \equiv \frac{k^{1/6}}{1 + k^{1/6} |\varphi(x)|^{1+}} \chi_j(0, x), \quad j = 1, 2.$$

It follows from the properties of the Airy functions (see [16], for example) for $\underline{x} \in [\underline{a}, \underline{b}]$ that, for $\underline{j} = 1, 2$.

$$|y_j(x, k)| \leqslant C |w_j(x, k)|,$$
$$|k^{-1} y_j'(x, k)| \leqslant C_1 |w_j(x, k)|, \; C \quad C_1 > 0. \tag{3.28}$$

Since det $\underline{Y} = 1$, /15

$$Y^{-1} = \begin{pmatrix} -k^{-1} y_2' & y_2 \\ k^{-1} y_1' & -y_1 \end{pmatrix}, \; Y(x) Y^{-1}(x') = O(w_1(x, k) w_2(x', k)) +$$
$$+ O(w_2(x, k) w_1(x', k)).$$

whence

$$W(x) W^{-1}(x') =$$
$$= \left[\frac{|\varphi(x')|^{-\frac{1}{4}}}{k^{-\frac{1}{6}} + |\varphi(x)|^{\frac{1}{4}}} O(|\chi_1(x', x)| + |\chi_2(x', x)|); \right.$$
$$\left. \chi_3(x', x), \ldots, \chi_n(x', x) \right],$$

since

$$|w_j(x', k)| \leqslant |\varphi(x')|^{-\frac{1}{4}} |\chi_j(0, x')|.$$

Let us introduce new unknown vectors $\vec{\Phi}_{\underline{j}} = \vec{F}^{\underline{j}} \underline{W}_{\underline{j}}(\underline{x}, \underline{k})$. Then

$$\vec{\Phi}^j(x) = \vec{W}^j(x) w_j^{-1}(x) - k^{-N} \times$$
$$\times \int_a^x W_1(x) W^{-1}(x') w_j(x') w_j^{-1}(x) \widetilde{\Gamma}(x') \vec{\Phi}^j(x') dx' -$$
$$- k^{-N} \int_b^x W_2(x) W^{-1}(x') w_j(x') w_j^{-1}(x) \widetilde{\Gamma}(x') \vec{\Phi}^j(x') dx'. \tag{3.29}$$

It is obvious that, for $\underline{j}$ = 1, 2,

$$|w_j(x')\, w_j(x)| \leqslant |\varphi(x')|^{-\frac{1}{4}}\left(k^{-\frac{1}{6}} + |\varphi(x)|^{\frac{1}{4}}\right)|\chi_j(x, x')|$$

Therefore, it follows from (3.29) that, for $\underline{j}$=1,...,$\underline{n}$,

$$W(x)\, W^{-1}(x')\frac{w_j(x')}{w_j(x)} = O\left\{|\varphi(x')|^{-\frac{1}{2}}\left[e^{k\int_{x'}^{x}\mathrm{Re}(\lambda_1-\lambda_j)dt}\right.\right.$$

$$\left.\left. + e^{k\int_{x'}^{x}\mathrm{Re}(\lambda_2-\lambda_j)dt};\ e^{k\int_{x'}^{x}\mathrm{Re}(\lambda_3-\lambda_j)dt}, \ldots, e^{k\int_{x'}^{x}\mathrm{Re}(\lambda_n-\lambda_j)dt}\right]\right\} \qquad (3.30)$$

Let us now impose the following condition on the eigen-values of $\underline{A}_0(\underline{x})$: for a fixed pair of subscripts $\underline{i}$, $\underline{j}$ = 1, 2, ..., $\underline{n}$, with all $\underline{x} \in [\underline{a}, \underline{b}]$,

$$\mathrm{Re}(\lambda_i - \lambda_j) \geqslant 0 \ (\text{ or } \leqslant 0).$$

It is obvious that this is the same condition as the second condition in the Birkhoff-Tamarkin theorem. Because of this condition, for a fixed $\underline{j}$, $\underline{W} = \underline{W}_1 + \underline{W}_2$ can be divided in such a way that all the exponents in the core are limited for $\underline{k} \to +\infty$: if $\mathrm{Re}(\lambda_{\underline{i}} - \lambda_{\underline{j}}) \geq 0$, then the $\underline{i}$-th column of $\underline{W}(\underline{x})$ will be put under the sign $\int_{\underline{b}}^{\underline{x}}$ (the $\underline{i}$-th column of $\underline{W}_1$ then consists of zeros); if $\mathrm{Re}(\lambda_{\underline{i}} - \lambda_{\underline{j}}) \leq 0$, then the $\underline{i}$-th zero column in in $\underline{W}_2$ (here the proof does not differ from that in the classical case, see [12]). Further, the function $|\phi(\underline{x}')|^{-\frac{1}{2}}$ can be integrated, and therefore the integrals from the core have (together with the factor $\underline{k}^{-\underline{N}}$) order of $\underline{k}^{-\underline{N}}$, while the free term is limited. The method of successive equations immediately leads to the following asymptotic formulas: /16

$$\vec{\Phi}^j(x, k) = \vec{W}^j(x, k)\, w_j^{-1}(x, k) + O(k^{-N}), \qquad (3.31)$$

$$\vec{F}^j(x, k) = \vec{W}^j(x, k) + O(k^{-N})\, w_j(x, k), \qquad (3.32)$$

or

$$\vec{Z}^j(x, k) = U(x)\left\{\sum_{\nu=0}^{N-1} P_\nu(x)\, k^{-\nu}\, \vec{W}^j(x, k) + O(k^{-N})\, w_j(x, k)\right\}, \qquad (3.33)$$

which are valid for $\underline{j} = 1, 2, \ldots, \underline{n}$; $\underline{a} \leq \underline{x} \leq \underline{b}$. For $\underline{j} = 3, 4, \ldots, \underline{n}$, (3.33) means that

$$\vec{Z}^j(x, k) = U(x)\left\{\sum_{\nu=0}^{N-1} P_\nu(x) k^{-\nu} + O(k^{-N})\right\} \vec{W}^j(x, k). \tag{3.34}$$

Using the vectors $\underline{F}^{\underline{j}}/y_{\underline{j}}$, it is easy to find that (3.34) is also valid for $\underline{j} = 1, 2$ at $\underline{x} \geq \overline{0}$ (the functions $\underline{y}_{1,2}$ do not have zeros at $\underline{x} \geq 0$). At $\underline{x} \geq 0$, $|\underline{W}_{1,2}| \geq \underline{k}^{1/6}$. Therefore, it follows from (3.33) that, in the case under investigation,

$$\vec{Z}^j(x, k) = U(x)\left\{\sum_{\nu=0}^{N-1} P_\nu(x) k^{-\nu} \vec{W}^j(x, k) + O\left(k^{-N+\frac{1}{6}}\right)\right\}, j = 1, 2. \tag{3.35}$$

Thus, we have obtained the theorem.

Theorem. If: (1) the point $\underline{x} = 0$ is unique and the simplest reversal point in the interval $\underline{x} \in [\underline{a}, \underline{b}]$; (2) $\mathrm{Re}(\lambda_{\underline{i}} - \lambda_{\underline{j}})$ do not change sign ($\underline{i}$ and $\underline{j}$ are fixed); (3) $\underline{A}_\nu(\underline{x}) \in \underline{C}^{N+1-\nu}[\underline{a}, \underline{b}]$; (4) the matrix $\underline{S}(\underline{x})$ is reduced to the form of (3.6), then the basic matrix of (3.1) has asymptotic expansion determined by (3.33)-(3.35) for $\underline{k} \to +\infty$.

Based on (3.33) and using the obvious equality $0 < \underline{k}^{-1/6} + |\phi(\underline{x})|^{1/4} \leq \underline{C}_2$, it is easy to obtain the asymptotic formula for the basic matrix /17

$$Z(x, k) = U(x)\left\{\sum_{\nu=0}^{N-1} P_\nu(x) k^{-\nu} + O\left(\frac{k^{-N}}{\left(k^{-\frac{1}{6}} + |\varphi(x)|^{\frac{1}{4}}\right)^2}\right)\right\} W(x, k), \tag{3.36}$$

which is valid for all $\underline{x} \in [\underline{a}, \underline{b}]$. It follows from this formula, in particular, that at $|\underline{x}| \geq \varepsilon > 0$,

$$Z(x, k) = U(x)\left\{\sum_{\nu=0}^{N-1} P_\nu(x) k^{-\nu} + O(k^{-N})\right\} W(x, k). \tag{3.37}$$

It also follows from (3.36) that at $\underline{a} \leq \underline{x} \leq \underline{b}$,

$$Z(x, k) = U(x)\left\{\sum_{\nu=0}^{N-1} P_\nu(x) k^{-\nu} + O(k^{-N+1})\right\} W(x, k). \tag{3.38}$$

Formulas of the type in (3.37) and (3.38), which were proven in [2] for the system of (1.3), were used there in order to investigate the problem of the natural vibrations of a nonhomogeneous elastic film. It was found in this study that the presence of a reversal point causes the arisal of "quasi-intersection" of the dispersion curves, i.e., resonance frequencies of their own type.

Final Comments

1. If the reversal point $\underline{x} = 0$ is not simple, i.e., $(\lambda_1 - \lambda_2)^2 = \underline{x}^{\alpha}\underline{p}_1(\underline{x})$, $0 < \alpha \neq 1$, then we can act in a similar way, using the solutions to the equation $\underline{y}'' - \underline{k}^2\underline{x}^{\alpha}\underline{p}_1(\underline{x})\underline{y} = 0$ in order to construct the standard equations; this equation was studied in [8].

2. In some cases an infinite $\underline{x}$-interval must be investigated, the corresponding generalization of that proposed in Section 1 can be found in [14, 15]. That presented in Section 3 can also be expanded for this case, and in this regard certain conditions must be imposed on the behavior of the matrices $\underline{A}_{\nu}(\underline{x})$ for $\underline{x} \to \infty$.

REFERENCES

1. Alenitsyn, A.G.: Volny Releya v neodnorodnom uprugom poluprostranstve (Rayleigh Waves in a Inhomogeneous Elastic Space). Prikladnaya Matematika i Mekhanika, Vol. 27, No. 3, 1963.
2. Alenitsyn, A.G.: Volny Releya v neodnorodnom uprugom sloye (Rayleigh Waves in an Inhomogeneous Elastic Film). Prikladnaya Matematika i Mekhanika, Vol. 28, No. 5, 1964.
3. Zavadskiy, V. Yu.: Asimptoticheskiye priblizheniya v dinamike uprugoy sloisto-neodnorodnoy sredy (Asymptotic Approximations in the Dynamics of an Elastic Nonuniformly-Layered Medium). Abstract of Address III at the Simposium on Diffraction of Waves. "Nauka", 1964, pp. 72-74; Author's Abstract of a Candidate's Dissertation of the Acoustics Institute, Moscow, 1965.
4. Langer, R.E.: On the Asymptotic Solutions of Differential Equations. Trans. Amer. Math. Soc., Vol. 34, No. 3, 1932. /18
5. Fok, V.A.: Tablitsy funktsiy Eyri (Tables of Airy Functions). Izdat. Akad. Nauk S.S.S.R., 1946.
6. Langer, R.E.: The Asymptotic Solutions of Ordinary Linear Differential Equations. Trans. Amer. Math. Soc. Vol. 67, No. 3, 1949.
7. Cherry, T.M.: Uniform Asymptotic Formulae for Functions with Transition Points. Trans. Amer. Math. Soc., Vol. 68, No. 2, 1950.
8. Dorodnitsyn, A.A.: Asimptoticheskiye zakony raspredeleniya sobstvennykh znacheniy (Asymptotic Laws for the Distribution of Eigen-Values). Uspekhi Matem. Nauk, Vol. 7, No. 6, 1952.
9. Olver, F.W.J.: Uniform Asymptotic Expansions of Solutions of Linear Second-Order Differential Equations. Philos. Trans. Roy. Soc. London, Ser. A, No. 981, 1958; Error Bounds for

Asymptotic Expansions. J. Soc. Industr. Appl. Math., Vol. 12, No. 1, 1964.
10. Birkhoff, G.D.: On the Asymptotic Character of the Solutions of Certain Linear Differential Equations. Trans. Amer. Math. Soc. Vol. 9, 1908.
11. Tamarkin, J.D.: Some General Problems of the Theory of Ordinary Linear Differential Equations. Math. Zs., Bd. 27, 1928.
12. Coddington, E.A. and N. Levinson: Teoriya obyknovennykh differentsial'nykh uravneniy (Theory of Ordinary Differential Equations). Foreign Literature Publishing House, 1958.
13. Turritin, H.L.: Asymptotic Solutions of Certain Ordinary Differential Equations. Amer. J. Math., Vol. 58, No. 2, 1936.
14. Pugachev, V.S.: Ob asimptoticheskikh predstavleniyakh integralov (On Asymptotic Representations of Integrals). Matem. Sb., Vol. 15 (57), No. 1, 1944.
15. Fedoryuk, M.V.: Supplement 1 to the Book: J. Heding: Introduction to the Phase Integral Method. "Mir", 1965; Asimptotika resheniy obyknovennykh lineynykh differentsial'nykh uravneniy n-go poryadka (Asymptotics of Solutions to Ordinary Linear Differential Equations of the n-th Order). Doklady Akad. Nauk S.S.S.R., Vol. 165, No. 4, 1965.
16. Erdeyi, A.: Asimptoticheskiye razlozheniya (Asymptotic Expansions)."Fizmatgiz", 1962.
17. Feshchenko, S.F.: Ob asimptoticheskom rasshchepleniy sistemy lineynykh differentsial'nykh uravneniy (Asymptotic Decomposition of a System of Linear Differential Equations). Ukr. Matem. Zhur., Vol. 7, No. 2; Vol. 7, No. 4, 1955.
18. Sibuya, Y.: Sur reduction analytique d'un systeme d'equations differentielles ordinaires linéaires (On the Analytical Reduction of a System of Ordinary Linear Differential Equations). J. Fac, Sci. Univ. Tokyo, Vol. 7, No. 5, 1958.
19. Smirnov, V.I.: Kurs vysshey matematiki (Course in Higher Mathematics), Vol. 3, Part 2. "GITTL", 1953.
20. Alenitsyn,A.G.: O zadache Lemba dlya neodnorodnogo uprugogo prostranstva (On the Lamb Problem for a Nonuniform Elastic Space). Collection: Problemy matematicheskoy fiziki (Problems of Mathematical Physics), No. 1. Izdat. Leningrad State Univ. Press, 1966.
21. Ilyukhin, A.G.: Pro zvedennya sistemi zvichaynikh liniynikh differentsial'nikh rivnyan' (Reducing a System of Ordinary Linear Differential Equations). Dopovidy Akad. Nauk Ukr. S.S. R., No. 8, 1961.
22. Wasow, W.: Turning Pcint Problems for Systems of Linear Differential Equations. Comm. Pure Appl. Math., Vol. 14, No. 3, 1961; Vol. 15, No. 2. 1962.
23. Okubo, K.: On Certain Reduction Theorems for Systems of Differential Equations. Proc. Jap. Acad., Vol. 37, No. 9, 1961.
24. Wasow, W.: Simplification of Turning Point Problems. Trans. Amer. Math. Soc., Vol. 106, No. 1, 1963.
25. Fok, V.A.: Difraktsiya radiovoln vokrug zemnoy poverkhnosti (Diffraction of Radio-Waves Around the Earth's Surface). Izdat. Akad. Nauk S.S.S.R., 1946.

26. Asymptotic Solutions of Differential Equations (Red. Vilcox). New York, 1964.
27. Langer, R.E.: Turning Points in Linear Asymptotic Theory. Bol. Soc. Math. Mexico, Vol. 5, No. 1, 1960.
28. Dubrovskiy, V.: Author's Abstract of a Candidate's Dissertation of Leningrad State University, 1964.
29. Budden, K.G.: Radio-Waves in the Ionosphere. Cambridge Univ. Press, 1961.

PROPAGATION OF ELECTROMAGNETIC WAVES IN PLANES AND SPHERICAL IMPEDANCE WAVEGUIDES

Part I. Construction of the Solution

G.I. Makarov and V.V. Novikov

ABSTRACT: The Problems of the propagation of superlong radio-waves in a surface waveguide channel formed by the surface of the Earth and the ionosphere, by two parallel planes or two concentric spheres, are formulated in this study. The general concepts on the methods of constructing the solutions are discussed, and a formal solution by the method of normal waves is presented for the case of plane and spherical waveguides.

A great deal of literature has treated the problems of propagation of electromagnetic waves in waveguides of various types. The principal efforts of researchers were directed toward a solution of two problems: /19

(1) A consideration of various irregularities in waveguides and a study of the propagation processes in waveguides of a complex geometric shape [1] (boundary conditions of the simplest type corresponding to infinite conductivity of the waveguide walls are usually used in their study because of the complexity of this group of problems):

(2) A study of the field in waveguides of the simplest geometric shape, but with a consideration of more complex boundary conditions, as a rule, of the impedance type.

The second group of problems is investigated most frequently in works which treat the problems of propagation of superlong radio-waves in a surface waveguide channel [2-5] formed by the surface of the Earth and the ionosphere. A formulation of problems of this type in terms of impedance is convenient in that it permits a consideration of the structure of the Earth and the ionosphere which is not uniform in depth, as well as the anisotropic nature of the latter, when necessary, which is rather simple but not entirely ordered from the mathematical point of view.

We will be interested in the second group of problems, and we will limit ourselves to an investigation of waveguides formed by two parallel planes or two concentric spheres. We divided this work into three independent parts for the sake of convenience in reading. In the first part we will discuss general concepts on methods of constructing the solution, and we will construct a for-

mal solution by the method of normal waves. The second and third parts of the study will treat the problems of the eigen-values of the problem, using one of the variation methods (method of instances) and a study of the fields in plane and spherical waveguides. /20

Section 1. Methods of Constructing the Solution

The solution to the problem of a field of given sources in waveguides of the simplest geometric shape, when the walls of the waveguides coincide with the coordinate surfaces and there is separation of variables in the differential equation for the problem, was used to construct each of the following diagrams.

1. The given system of sources is expanded by eigen-functions of the ordinary differential operator connected with the longitudinal coordinate, which is directed along the waveguide axis. In this regard, the solution to the problem is also represented in the form of expansion by eigen-functions of this operator. It can be seen that this form of the solution is most convenient for investigating it at relatively small distances from the source. Using this, after corresponding transformation we have a solution in the form of the sum of waves reflected once and repeatedly from the surface of the earth and the ionosphere. The asymptotic expressions for these waves correspond to a geometric-optical image in the illuminated region, and diffraction beams in the region of the penumbra and the umbra.

2. Spectral expansions of the source and fields are constructed according to the eigen-functions of the operator created by the transverse coordinate. In this regard, one of the transverse coordinates will be considered to be cyclical, so that the corresponding differential operator will be an ordinary one. Using the terminology of P. Ye. Krasnushkin, we will call the representation of the solution obtained an expansion by normal waves (modes). Formulas of this type are particularly convenient if the observation site is sufficiently removed from the source.

We should mention that both forms of the solution are equivalent to each other and expansion of the solution by normal waves can be obtained from expansion of the first type with the aid of integral transformation. In the case of a sperical waveguide, this transformation is called a Watson transformation. The Watson transformation is often used in order to obtain an expansion of the solution by normal waves from an expansion of the first type in those cases when a direct approach is complicated for some reason (for example, in the case of the ionosotropic ionosphere).

In the future, we will consider only expansion by normal waves. The basic difficulty in this regard is to find in the eigen-values of the transverse operator of the problem. In order to find them, it is necessary to solve a complex transcendental equation which contains spherical Bessel functions in the case of a spherical /21

waveguide [6]. This equation can be solved only when numerical methods are involved. The need for using numerical methods complicates investigations and does not make it possible to explain the qualitative picture of the propagation processes and their principal laws with sufficient simplicity. In the second and third parts of this work, we attempted to construct approximative solutions in a closed analytical form with the aid of the method of instances. In this regard, we will not try to obtain approximating expressions of high accuracy, but we will look for relatively simple analytical formulas for the eigen-values which describe the character of the solution qualitatively.

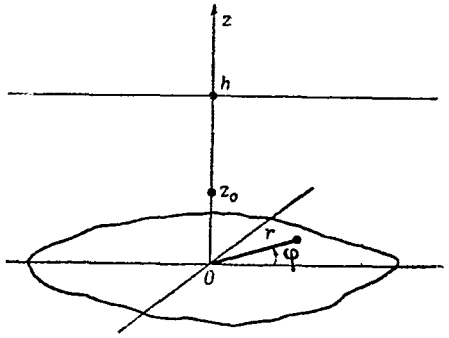

Fig. 1.

The possibility of using variation methods in order to solve the problem is due to the following circumstance. In the case of boundary conditions of the impedance type, the transverse differential operator is half-limited in the corresponding manner by an outlined Hilbert space. If it is expanded and the Green functions of the differential operator are used, then we can convert to an integral equation of the second type from the differential equation with impedance boundary conditions. The integral operator obtained here is found to be not only limited but also completely continuous, which guarantees discreteness in the spectrum of the problem under investigation. This also permits us to use direct variation methods in solving the problem: the Galerkin method [7] or the method of instances [8].

Section 2. Construction of the Solution for a Plane Waveguide

Let us consider the problem of the field of a vertical electric bipole used between two horizontal parallel planes z = 0 and z = h (Fig. 1), which correspond to the surface of the Earch and that of the ionosphere. We will consider that impedance boundary conditions of the following type are fulfilled on these surfaces:

$$E_\tau = Z_{sur} H_\tau, \qquad (1)$$

where E_τ and H_τ are tangential components of the electromagnetic field; Z_{sur} is the surface impedance of the Earth or ionosphere, and does not depend on the coordinates. The medium constituting the region between surfaces is assumed to be isotropic and has a relative permittivity at ε_m which depends on the vertical coordinate z. /22

The problem amounts to a construction of the solution to Maxwellian equations for the corresponding boundary conditions of (1). In the case under investigation, the electromagnetic field contains three components - H_ϕ, E_z and E_r, while E_r and E_z are expressed in terms of H_ϕ[1], i.e.,

$$E_r = -i\frac{Z_0}{\varepsilon_m}\frac{\partial H_\varphi}{\partial x},$$
$$E_z = i\frac{Z_0}{\varepsilon_m}\cdot\frac{1}{\rho}\cdot\frac{\partial}{\partial\rho}(\rho H_\varphi) - \frac{i}{\omega\varepsilon_0\varepsilon_m}j, \qquad (2)$$

where H_ϕ satisfies the following equation:

$$\frac{\partial^2 H_\varphi}{\partial x^2} + \varepsilon_m\frac{\partial}{\partial x}\left(\frac{1}{\varepsilon_m}\right)\frac{\partial H_\varphi}{\partial x} + \frac{\partial}{\partial\rho}\left[\frac{1}{\rho}\cdot\frac{\partial}{\partial\rho}(\rho H_\varphi)\right] + \varepsilon_m H_\varphi = \frac{1}{k}\cdot\frac{\partial j}{\partial\rho}. \qquad (3)$$

Here the following designations are used: $x = kz$; $\rho = kr$, or dimensionless coordinates: $k = \frac{\omega}{c}$, or the wave number under vacuum; $E_0 = \sqrt{\frac{\mu_0}{\varepsilon_0}}$, or the characteristic vacuum impedance; ε_0 and μ_0 are the permittivity and magnetic susceptibility of the vacuum ($\varepsilon_0 \approx 8{,}854\cdot10^{-12}$ F/m, $\mu_0 = 4\ 10^{-7}$ H/m); j is the volume density of extraneous vertical currents.

The boundary conditions of (1) have the following form for H_ϕ, considering (2):

$$\frac{\partial H_\varphi}{\partial x} = -i\varepsilon_m\delta_g H_\varphi \quad \text{at } x = 0,$$
$$\frac{\partial H_\varphi}{\partial x} = i\varepsilon_m\delta_i H_\varphi \quad \text{at } x = \beta = kh. \qquad (4)$$

In (4) the values δ_g and δ_i are reduced surface impedances of the Earth and ionosphere, respectively, i.e.,

---

[1] We are using the International System of Units and are examining a stationary regime corresponding to a harmonic dependence on time of the type $e^{-i\omega t}$.

$$\delta_g = \frac{Z_{sur\,g}}{Z_0}, \quad \delta_i = \frac{Z_{sur\,i}}{Z_0}$$

It is reasonable to reduce (3) to a form which does not contain the first derivative for the coordinate x, for which we must introduce a new unknown function Z by the following formula;

$$H_\varphi = \sqrt{\varepsilon_m}\, Z. \tag{5}$$

Consequently, this problem is reduced to the construction of a solution to the equation /23

$$L_x Z + L_\rho Z = \varphi \tag{6}$$

under the boundary conditions of

$$\begin{aligned} \frac{\partial Z}{\partial x} &= -i\delta_g^* Z \quad \text{at} \quad x = 0, \\ \frac{\partial Z}{\partial x} &= i\delta_i^* Z \quad \text{at} \quad x = \beta. \end{aligned} \tag{7}$$

In (6) and (7) $L_x = \frac{\partial^2}{\partial x^2} + \psi(x)$ is the transverse differential operator; $L\rho = \frac{\partial}{\partial \rho} \cdot \frac{1}{\rho} \cdot \frac{\partial}{\partial \rho}\, \rho + 1$ is the longitudinal differential operator;

$$\psi(x) = \varepsilon_m^* - 1:$$

$$\varepsilon_m^* = \varepsilon_m + \frac{1}{2\varepsilon_m} \cdot \frac{d^2\varepsilon_m}{dx^2} - \frac{3}{4\varepsilon_m^2}\left(\frac{d\varepsilon_m}{dx}\right)^2;$$

under the boundary conditions of

$\phi = \frac{1}{k\sqrt{\varepsilon_m}} \cdot \frac{\partial i}{\partial \rho}$ is the source function;

$$\delta_g^* = \delta_g \varepsilon_m(0) - \frac{i}{2\varepsilon_m(0)} \cdot \frac{d\varepsilon_m}{dx}\Big|_{x=0};$$
$$\delta_i^* = \delta_i \varepsilon_m(\beta) + \frac{i}{2\varepsilon_m} \cdot \frac{d\varepsilon_m}{dx}\Big|_{x=\beta}.$$

In the case of a homogeneous medium with $\varepsilon_m = 1$, the following equation holds:

$$\varepsilon_m^* = \varepsilon_m = 1, \quad \delta_g^* = \delta_g, \quad \delta_i^* = \delta_i, \quad \psi(x) = 0.$$

In constructing the solution to (6), we will base our arguments on the eigen-functions μ_n of the transverse differential operation

$$\begin{aligned} L_x u_n &= -\mu_n u_n, \\ \frac{\partial u_n}{\partial x} &= -i\delta_g^* u_n \quad \text{at} \quad x = 0, \\ \frac{\partial u_n}{\partial x} &= i\delta_i^* u_n \quad \text{at} \quad x = \beta, \end{aligned} \tag{8}$$

where the value - μ_n is an eigen-value.

The operator L_x, which is not self-conjugate, has a point spectrum [9] and its eigen-functions are orthogonal to the eigen-functions of the conjugate operator u_m^*, so that

$$(u_n, u_m^*) = \int_0^\beta u_n \overline{u_m^*} dx = 0 \quad \text{at} \quad n \neq m$$

In this case, the eigen-values and eigen-functions of the conjugate /24 operator coincide with the complex-conjugate eigen-values and eigen-functions of the initial operator, and the condition of orthogonality ultimately acquires the following form:

$$(u_n,\ u_m^*)=(u_n,\ \overline{u_m})=\int_0^\beta u_n u_m dx=0 \text{ for } n\neq m. \tag{9}$$

We will look for a solution to the initial differential equation in (6) in the form of an expansion by eigen-functions of the transverse differential operator[2], i.e.,

$$Z=\sum_n a_n(\rho)\,u_n(x), \tag{10}$$

where a_n (ρ) are certain still unknown coefficients of the expansion. Having substituted the series in (10) into (6) and having used the condition of orthogonality in (9), we will arrive at an ordinary differential equation for determining the coefficients of expansion a_n (ρ), i.e.,

$$L_\rho a_n-\mu_n a_\rho=d_n, \tag{11}$$

where

$$d_n\equiv\frac{(\varphi,\ \overline{u_n})}{(u_n,\ \overline{u_n})} \tag{12}$$

In finding the solution to (11), we will first select as a source a ring of vertical electric dipoles arranged at $r = r_0$ and $z = z_0$, i.e., we will assume that

---

[2] We will assume that the operator L_x has a simple spectrum. In the case of a multiple spectrum the expansion will have a more complex appearance [11].

$$j = \frac{Ih_g \delta (r - r_0)\, \delta (z - z_0)}{2\pi r}.$$

Here δ (x) is a delta-function, while $Ih_g = \int j dV$, where I can mean the maximum value of the current, and H_g means the effective height of the antenna. We will construct the solution by the Lagrange method. The solution should be limited at $\rho = 0$ and $\rho = \infty$, which is necessary to select a Bessel function and a Hankel function as linear independent solutions to the uniform equation in (11):

$$\varphi_1 = J_1(\sqrt{1 - \mu_n}\,\rho),\ \varphi_2 = H_1^{(1)}(\sqrt{1 - \mu_n}\,\rho),\ (\operatorname{Im}\sqrt{1 - \mu_n} > 0),$$

Each of these satisfy one of the conditions. Consequently, the solution to (11) is constructed in a standard manner. With r_0 in the expression obtained tending to 0, we will ultimately find the expression of interest to us for a_n (ρ) corresponding to the source in the form of a vertical electric dipole at the point $r = 0$ and $z = z_0$:

$$a_n(\rho) = \frac{ik^2 Ih_g \sqrt{1 - \mu_n}}{4\sqrt{\varepsilon_m(x_0)}} \cdot \frac{u_n(x_0)}{(u_n, \bar{u}_n)} H_1^{(1)}(\sqrt{1 - \mu_n}\,\rho).$$

The expression for a_n (ρ), together with (10) and (5), make it pos- /25
sible to write out the solution to the problem for the component H_ϕ in the form of expansion by normal waves. The solution constructed should be understood in a general sense.

Since the solution for the component H_ϕ has been constructed there are no difficulties in finding the expression for other field exponents according to (2). In application, the vertical component of the electrical field is of greatest interest; expansion by normal waves for this component has the following form:

$$E_z = -\frac{k^2 Z_0 Ih_g}{4\sqrt{\varepsilon_m(x_0)\varepsilon_m(x)}} \sum_{n=0}^{\infty} (1 - \mu_n) \frac{u_n(x)\, u_n(x_0)}{(u_n, \bar{u}_n)} H_0^{(1)}(\sqrt{1 - \mu_n}\,\rho). \qquad (13)$$

If the observation site is sufficiently removed from the source, so that there is an inequality

$$|kr\sqrt{1-\mu_n}| \gg 1,$$

then we can use an asymptotic representation for the Hankel functions, and

$$E_z \approx -\frac{i\omega\mu Ihg}{2h}\sqrt{\frac{2}{\pi kr}}\,e^{i\frac{\pi}{4}}\sum_{n=0}^{\infty}\Lambda_n f_n(z)f_n(z_0)e^{ikS_n r}, \qquad (14)$$

with the following symbols:

$$S_n = \sqrt{1-\mu_n}; \qquad (15)$$

$$\Lambda_n = S_n^{3,2}\frac{u_n^2(0)}{\varepsilon_m(0)\frac{2}{kh}(u_n,\ \bar{u}_n)} \qquad (16)$$

as the so-called coefficient of excitation of the n-th normal wave (mode):

$$f_n(z_0) = \sqrt{\frac{\varepsilon_m(0)}{\varepsilon_m(x_0)}}\cdot\frac{u_n(x_0)}{u_n(0)} \text{ и } f_n(z) = \sqrt{\frac{\varepsilon_m(0)}{\varepsilon_m(x)}}\cdot\frac{u_n(x)}{u_n(0)} \qquad (17)$$

as the altitude factor.

It follows from (14) that the phase velocity of the n-th mode along the Earth's surface is equal to

$$v_{\text{pn}}^{(n)} = \frac{c}{\operatorname{Re} S_n} = \frac{c}{\operatorname{Re}\sqrt{1-\mu_n}}. \qquad (18)$$

The change in amplitude of a single normal wave in dependence on the distance is caused first of all, by the cylindrical divergence of the wave (factor of $1/\sqrt{r}$) and, secondly, by exponential attenuation ($e^{-\alpha_n r}$) because of energy losses due to the impedance boundary conditions (absorption of energy on the Earth and ionosphere). The coefficient of attenuation α_n is determined by the following expression: /26

$$\alpha_n = k \operatorname{Im} S_n = k \operatorname{Im} \sqrt{1 - \mu_n}. \qquad (19)$$

The expressions in (13) and (14) represent a formal solution in the form of expansion by normal waves. For a further study of the solution we must determine the eigen-functions $u_n(x)$ and the eigen-values - μ_n of the transverse differential operator, c.f. (8). This is usually done in the following manner.

We will assume that we know two linearly independent solutions to the equation

$$L_x u + \mu u = 0,$$

which we will call

$$u^{(1)} = \psi_1(x, \mu), \; u^{(2)} = \psi_2(x, \mu).$$

Thus, in the case of a homogenuous atmosphere ($\varepsilon_m = 1$), such solutions are trigonometrical functions, i.e.,

$$\psi_1(x, \mu) = \sin \sqrt{\mu}\, x, \;\; \psi_2(x, \mu) = \cos \sqrt{\mu}\, x.$$

We will look for the eigen-function u_n in the form of a linear combination, i.e.,

$$u_n(x) = C_1 \psi_1(x, \mu) + C_2 \psi_2(x, \mu). \qquad (20)$$

Having substituted (20) into the boundary conditions for the operator L_x, c.f. (8), we will obtain a system of two uniform algebraic equations relative to C_1 and C_2. In order that this system might have a non-trivial solution, its determinant should be equal to zero:

$$\begin{aligned}&[\psi_1'(0,\ \mu)+i\delta_g^*\psi_2(0,\ \mu)]\,[\psi_2'(\beta,\ \mu)-i\delta_1^*\psi_2(\beta,\ \mu)]-\\&-[\psi_1'(\beta,\ \mu)-i\delta_1^*\psi_2(\beta,\ \mu)]\,[\psi_2'(0,\ \mu)+i\delta_g^*\psi_2(0,\ \mu)]=0.\end{aligned}\qquad(21)$$

Here the prime designates the derivative for x.

Equation (21) is a transcendental equation used for finding the eigen-values μ_n. In the case of $\varepsilon_m = 1$, it is reduced to the following form:

$$\tan\sqrt{\mu}\beta=-\frac{i\sqrt{\mu}(\delta_g+\delta_1)}{\mu+\delta_g\delta_1}.\qquad(22)$$

Thus, the problem of determining the eigen-values of the operator L_x (as well as its eigen-functions) is based on a solution to the transcendental equation (21).

However, in order to find the eigen-values of the operator L_x, c.f. (8), we can also use other methods, particularly direct variation methods. It is these problems which we will examine in the subsequent parts of our study.

Section 3. Solution in the Case of a Spherical Waveguide

A solution to the problem of a spherical waveguide is constructed according to the same scheme as that for a plane one. In the case of a radial electric dipole in an electromagnetic field, there are three components - H_ϕ, E_θ and E_R (we will use a spherical system of coordinates) (Fig. 2.). The components E_θ and E_R are linked with H_θ in the following way:

$$\begin{aligned}E_\theta&=-i\frac{Z_0}{\varepsilon_m}\cdot\frac{1}{\partial X}(XH_\varphi),\\E_R&=i\frac{Z_0}{\varepsilon_m}\cdot\frac{1}{X\sin\theta}\cdot\frac{\partial}{\partial\theta}(\sin\theta H_\varphi)-\frac{i}{\omega\varepsilon_0\varepsilon_m}J.\end{aligned}\qquad(23)$$

The following equation holds for H_ϕ:

$$\frac{1}{X}\cdot\frac{\partial^2}{\partial X^2}(XH_\varphi)+ \varepsilon_m\frac{d}{dX}\left(\frac{1}{\varepsilon_m}\right)\frac{1}{X}\cdot\frac{\partial}{\partial X}(XH_\varphi)+ \frac{1}{X^2}\cdot\frac{\partial}{\partial\theta}\left[\frac{1}{\sin\theta}\cdot\frac{\partial}{\partial\theta}(\sin\theta H_\varphi)\right]+ +\varepsilon_m H_\varphi=\frac{1}{kX}\cdot\frac{\partial j}{\partial\theta}, \tag{24}$$

We will consider that ε_m depends on the radial coordinate R, i.e., that $\varepsilon_m = \varepsilon_m(X)$. In (23) and (24), X is a dimensionless radial coordinate:

$$X=kR. \tag{25}$$

Boundary conditions of the impedance type, such as in (1), are fulfilled on the surface of the Earch (R = a) and the ionosphere (R = d = a + h). They lead to the following boundary conditions for H_ϕ:

$$\begin{aligned}&\frac{\partial}{\partial X}(XH_\varphi)=-i\varepsilon_m\delta_g XH_\varphi \quad \text{at} \quad X=ka\equiv\beta_0,\\ &\frac{\partial}{\partial X}(XH_\varphi)=i\varepsilon_m\delta_i XH_\varphi \quad \text{at} \quad X=ka=\beta_0+\beta\ (\beta=kh).\end{aligned} \tag{26}$$

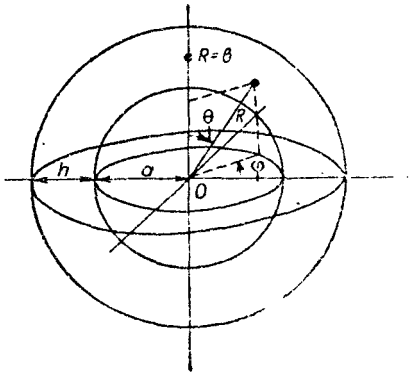

Fig. 2.

In solving (23), a new unknown function U with the following formula must be used instead of H_ϕ:

$$U=\frac{R}{a}\frac{H_\varphi}{\sqrt{\varepsilon_m}} \tag{27}$$

Consequently, we arrive at the following equation for U, based on (24) and (26):

$$L_X U+L_\theta U=f \tag{28}$$

as well as the boundary conditions /28

$$\begin{aligned}&\frac{\partial U}{\partial X}=-i\delta_g^* U \quad \text{at} \quad X=\beta_0,\\ &\frac{\partial U}{\partial X}=i\delta_i^* U \quad \text{at} \quad X=\beta_0+\beta,\end{aligned} \tag{29}$$

where the following symbols are used:

$$L_X=X^2\frac{\partial^2}{\partial X^2}+\varepsilon_m^*(X)X^2$$

or the radial (transverse) differential operator;

$$L_\theta = \frac{\partial}{\partial\theta}\cdot\frac{1}{\sin\theta}\cdot\frac{\partial}{\partial\theta}\sin\theta$$

or the angular (longitudinal) differential operator;

$$\varepsilon_m^*(X) = \varepsilon_m(X) + \frac{1}{2\varepsilon_m}\cdot\frac{d^2\varepsilon_m}{dX^2} - \frac{4}{4\varepsilon_m^2}\left(\frac{d\varepsilon_m}{dX}\right)^2;$$

$f = \frac{X^2}{k\beta_0\sqrt{\varepsilon_m}}\cdot\frac{\partial j}{\partial\theta}$ is the first function:

$$\delta_g^* = \delta_g\varepsilon_m(\beta_0) - \frac{i}{2\varepsilon_m}\cdot\frac{d\varepsilon_m}{dX}\Big|_{X=\beta_0};$$
$$\delta_i^* = \delta_i\varepsilon_m(\beta_0+\beta) + \frac{i}{2\varepsilon_m}\cdot\frac{d\varepsilon_m}{dX}\Big|_{X=\beta_0+\beta},$$

We will look for a solution to (28) in the form of an expansion by eigen-functions of the radial differential operator;

$$U = \sum_n b_n(\theta)v_n(X),$$
$$L_X v_n = \lambda_n^{\text{sph}} v_n, \qquad (30)$$

$$\frac{\partial v_n}{\partial X} = -i\delta_g^* v_n \quad \text{at} \quad X=\beta_0, \qquad (31)$$

$$\frac{\partial v_n}{\partial X} = i\delta_i^* v_n \quad \text{at} \quad X=\beta_0+\beta.$$

The operator L_X is not self-conjugate and has a point spectrum [3].[3] Its eigen-functions are orthogonal to the eigen-functions of the conjugate operator v_m^* with $1/X^2$, i.e.,

$$\left(v_n, \frac{1}{X^2}v_m^*\right) = \int_{\beta_0}^{\beta_0+\beta}\frac{v_n\overline{v_n^*}}{X^2}dX = 0 \quad \text{at} \quad n\neq m. \qquad (32)$$

Since the eigen-functions and the eigen-values of the conjugate operator under investigation are equal to the complex-conjugate eigen-functions and eigen-values of the initial operator, the condition of orthogonality of (32) is reduced to the following form: /29

$$\left(v_n, \frac{1}{X^2}\overline{v_n}\right) = \int_{\beta_0}^{\beta_0+\beta}\frac{v_n v_m}{X^2}dX = 0 \quad \text{at} \quad n\neq m. \qquad (33)$$

---

[3] We are assuming that the spectrum is simple.

Using (28) and (33) for the coefficients of expansion $b_n(\theta)$ [see (30)], it is easy to obtain an ordinary differential equation

$$L_\theta b_n + \left(\nu_n^2 - \frac{1}{4}\right) b_n = e_n, \tag{34}$$

where

$$e_n = \frac{\left(f, \overline{\frac{v_n}{X}}\right)}{\left(v_n, \overline{\frac{v_n}{X}}\right)},$$

and, instead of λ_n^{sph}, we are using ν_n, according to the following formula, for the sake of convenience in further computations:

$$\lambda_n^{sph} = \nu_n^2 - \frac{1}{4}, \tag{35}$$

whereas the condition $Re\nu_n \geq 0$ is imposed on ν_n for the sake of definiteness.

Let us construct the solution to (34) for this source in the form of

$$j = \frac{I h_g \delta(\theta - \theta_0)\delta(R - b)}{2\pi R^2 \sin\theta},$$

representing a ring of radial dipoles at R = b and $\theta = \theta_0$. We will construct the solution by the Lagrange method. Since the solution should satisfy the requirements of limitedness at the end of the interval $(0,\pi)$, we will select associated Legendre functions of the first type as linearly independent solutions to the uniform equation of (34), i.e.,

$$\varphi_1 = P^1_{\nu_n - \frac{1}{2}}(\cos\theta) \quad \text{и} \quad \varphi_2 = P^1_{\nu_n - \frac{1}{2}}[\cos(\pi - \theta)],$$

each of which satisfies the condition of limitedness at one of the ends of the interval. Having completed standard computations, it is easy to obtain a solution to (34). Transferring to the limit $\theta \to 0$ in the solution obtained, we can find the expression of interest to us $b_n(\theta)$ for the radial electric dipole at the point $\theta = 0$ and R = b:

$$b_n(\theta) = \frac{k^2 I h_g v_n(X_0) P^1_{\nu_n - \frac{1}{2}}[\cos(\pi - \theta)]}{4\beta_0 X_0^2 \sqrt{\varepsilon_{m.}(X_0)} \left(v_n, \overline{\frac{v_n}{X^2}}\right) \sin\left(\nu_n - \frac{1}{2}\right)\pi}, \tag{36}$$

where $X_0 = kb$.

Formulas (27),(30) and (36) also yield a solution to the problem under investigation for the component H_ϕ in the form of an expansion by normal waves. Using (23) it is easy to find the expansion by normal waves for the radial components of the electrical field, i.e., /30

$$E_R = -\frac{i\omega\mu I h_g}{4\sqrt{\varepsilon_m(X)\,\varepsilon_m(X_0)}} \times$$

$$\times \sum_{n=0}^{\infty} \frac{k\left(\nu_n^2 - \frac{1}{4}\right) v_n(X)\, v_n(X_0)}{X^2 X_0^2 \left(v_n, \frac{v_n}{X^2}\right)} \frac{P_{\nu_n - \frac{1}{2}}[\cos(\pi - \theta)]}{\sin\left(\nu_n - \frac{1}{2}\right)\pi}. \qquad (37)$$

If the observation site is sufficiently removed from the emitter and from its antipode, so that the inequalities below are fulfilled simultaneously,

$$|\nu_n|\theta \gg 1 \text{ and } |\nu_n|(\pi - \theta) \gg 1^4, \qquad (38)$$

then we can use their assymptotic representation for the Legendre functions. Moreover, since the eigen-values of ν_n have a positive imaginary part because of energy losses due to the impedance boundary conditions, then, with the additional condition of

$$\operatorname{Im} \nu_n(\pi - \theta) > 1$$

the following relationship holds:

$$\frac{P_{\nu_n - \frac{1}{2}}[\cos(\pi - \theta)]}{\sin\left(\nu_n - \frac{1}{2}\right)\pi} \simeq -\sqrt{\frac{2}{\pi\nu_n \sin\theta}}\, e^{i\frac{\pi}{4} + i\nu_n\theta}$$

Considering this relationship, we can represent the expression for E_p in a far-removed zone in the following form:

$$E_R \simeq \frac{i\omega\mu I_g}{2h} \sqrt{\frac{2}{\pi kr}} \sqrt{\frac{\theta}{\sin\theta}}\, e^{i\frac{\pi}{4}} \sum_{n=0}^{\infty} \tilde{\Lambda}_n \tilde{f}_n(X) \tilde{f}_n(X_0) e^{ikS_n r}. \qquad (39)$$

Here the following symbols are used: $r = a\theta$, or the distance between emitter and observation site, reading along the ground;

$$\tilde{S}_n = \frac{\nu_n}{\beta_0} = \frac{\nu_n}{ka};$$

$$\tilde{\Lambda}_n = \tilde{S}_n^{3/2} \frac{v_n^2(\beta_0)}{\varepsilon_m(\beta_0) \frac{2}{kh} \beta_0^2 \left(v_n, \frac{v_n}{X^2}\right)}$$

or the coefficient of excitation of the n-th mode; /31

4 In the problem under investigation $|\nu_n| \sim 0(ka)$ and, consequently, $|\nu_n| >> 1$ for frequencies of $f >> 10$ Hz.

$$\tilde{f}_n(X_0)=\sqrt{\frac{\varepsilon_m(\beta_0)}{\varepsilon_m(X_0)}}\cdot\frac{\beta_0^2}{X_0}\cdot\frac{v_n(X_0)}{v_n(\beta_0)},$$
$$\tilde{f}_n(X)=\sqrt{\frac{\varepsilon_m(\beta_0)}{\varepsilon_m(X)}}\cdot\frac{\beta_0^2}{X^2}\cdot\frac{v_n(X)}{v_n(\beta_0)}$$

or the altitude factors.

Having compared (39) and (14), we see that they have an identical general structure, except for the factor $\sqrt{\theta/\sin\theta}$ in the solution for a spherical waveguide. This factor considers the additional geometric convergence of the field of the electromagnetic wave due to the sphericity of the waveguide channel.

The phase velocity of the n-th normal wave along the ground surface is given by the following expression for a spherical waveguide:

$$v_{\text{ph}}^{(n)}=\frac{c}{\operatorname{Re}\tilde{S}_n}=\frac{ka}{\operatorname{Re}\nu_n}, \tag{40}$$

The coefficient of continuation is equal to

$$\alpha_n=k\operatorname{Im}\tilde{S}_n=\frac{\operatorname{Im}\nu_n}{a}. \tag{41}$$

The expressions in (37) and (39) represent a formal solution to the problem for a spherical waveguide. For a further study, we must find the eigen-functions and eigen-values of the radial differential operator in (31). Here, just as in the case of a plane waveguide, it is easy to obtain a transcendental equation for the eigen-values. The basic difficulty in the investigation of this solution is finding the roots of this equation. In the third part of this work, we will examine the problems of determining the eigen-values of the radial operator with the aid of the method of instances for the purpose of obtaining approximative analytical expressions.

In concluding this section, let us touch briefly on the limit transition from a spherical to a plane waveguide. Instead of the variable X we will use a new variable x with the formula

$$X=\beta_0+x,$$

where $X = kR$; $\beta_0 = ka$; $x = kz$; $z = R - a$, while x lies in the interval $(0, \beta = kh)$. We will now rewrite (31) for the eigen-functions of the operator L_x in the following way:

$$\begin{aligned}
&Av_n=\frac{\lambda_n^{\text{sph}}}{(\beta_0+x)^2}v_n,\\
&\frac{\partial v_n}{\partial x}=-i\delta_g^* v_n \qquad \text{at} \quad x=0,\\
&\frac{\partial v_n}{\partial x}=i\delta_l^* v_n \qquad \text{at} \quad x=\beta,
\end{aligned} \tag{42}$$

where

$$A \equiv \frac{\partial^2}{\partial x^2} + \varepsilon_m^*(x); \tag{43}$$

/32

$$\delta_g^* = \delta_g \varepsilon_m(\vartheta) - \frac{i}{2\varepsilon_m} \cdot \frac{d\varepsilon_m}{dx}\Big|_{x=0};$$

$$\delta_l^* = \delta_l \varepsilon_m(\vartheta) + \frac{i}{2\varepsilon_m} \cdot \frac{d\varepsilon_m}{dx}\Big|_{x=\vartheta_0}; \tag{44}$$

$$\varepsilon_m^*(x) = \varepsilon_m(x) + \frac{1}{2\varepsilon_m} \cdot \frac{d^2\varepsilon_m}{dx^2} - \frac{3}{4\varepsilon_m^2}\left(\frac{d\varepsilon_m}{dx}\right)^2. \tag{45}$$

We should mention that we replaced $\varepsilon_m(\vartheta_0 + x)$ by $\varepsilon_m(x)$ in (43) - (45) - this simply is a change in the origin in the reading.

With the radius of the Earth a tending toward infinity, we can obtain the following form of (42);

$$A\tilde{v}_n = \lambda_n^{pl}\tilde{v}_n,$$

$$\frac{\partial \tilde{v}_n}{\partial x} = -i\delta_g^*\tilde{v}_n \quad \text{at} \quad x=0, \tag{46}$$

$$\frac{\partial \tilde{v}_n}{\partial x} = i\delta_l^*\tilde{v} \quad \text{at} \quad x=\beta.$$

In this regard, in (46),

$$\lambda_n^{pl} = \lim_{a\to\infty} \frac{\lambda_n^{sph}}{\beta_0^2} = \lim_{a\to\infty} \frac{\lambda_n^{sph}}{(ka)^2}, \tag{47}$$

while all the remaining symbols correspond to (43) - (46). Having compared the operators L_x [see (8)] and A [see (46)], we can see that they are equivalent to each other, i.e., their eigen-functions coincide:

$$\tilde{v}_n = \lim_{a\to\infty} v_n = u_n.$$

The eigen-values are linked by the following relationships:

$$1 - \mu_n = \lambda_n^{pl} = \lim_{a\to\infty} \frac{\lambda_n^{sph}}{(ka)^2} = \lim_{a\to\infty} \frac{\nu_n^2}{(ka)^2}.$$

It follows from this relationship, in particular, that ν_n is a value of order ka. If we now consider the limit to the expression in (37) for E_φ at $a \to \infty$, then we can show that it converts into (13) for E_z. In this regard, we must keep (48) and (43) in mind, as well as the asymptotic representation of [10] for $a \to \infty$:

$$\frac{P_{kaS}[\cos(\pi-\theta)]}{\sin(kaS\pi)}=\frac{P_{kaS}\left[\cos\left(\pi-\frac{r}{a}\right)\right]}{\sin(kaS\pi)}=-iH_0^{(1)}(kSr)+O\left(\frac{r}{a}\right),$$
$$\operatorname{Im}S>0.$$

REFERENCES

1. Katsenelenbaum, B.Z.: Teoriya neregulyarnykh volnovodov s medlenno menyayushchimisya parametrami (Theory of Irregular Waveguides with Slowly Changing Parameters). Academy of Sciences U.S.S.R. Press.
2. Krasnushkin, P.Ye.: Metod normal'nykh voln i ego primeneniye k dal'ney radiosvyazi (Method of Normal Waves and its Application in Long-Range Radio Communications). Moscow State Univ., 1947.
3. Krasnushkin, P.Ye. and N.A. Yablochkin: Teoriya rasprostraneniya sverkhdlinnykh voln (Theory of the Propagation of Superlong Waves). Computation Center, Acad. of Sci. U.S.S.R., 1963.
4. Wait, J.R. Terrestrial propagation of very low frequency radiowaves. J. Res. NBS, Vol. 64D, 1960.
5. Wait, J.R. A new approach to the mode theory of VLF propagation, J. Res. NBS, Vol. 65D, 1961.
6. Rybachek, S.R.: This Collection, p. 152.
7. Mikhlin, S.G.: Variatsionnyye metody v matematicheskoy fizike (Variation Methods in Mathematical Physics). "Gostekhizdat", 1957.
8. Vorob'yev, Yu.V.: Metod momentov v prikladnoy matematike (Method of Instances in Applied Mathematics). "GIFML", 1958.
9. Titchmarsh, Ye.: Razlozheniya po sobstvennym funktsiyam, svyazannyye s differentsial'nymi uravneniyami vtorogo poryadka (Expansions by Eigen-Functions Connected with Differential Equations of the Second Order), Vol. 1. Foreign Literature Publishing House, 1961.
10. Beytmen, G. and A. Erdeyi: Vysshiye transtsendentnyye funktsii (Higher Transcendental Functions), Vol. 2. "Nauka", 1966.
11. Keldysh, M.V.: Doklady Akad. Nauk S.S.S.R., Vol. 87, p. 95, 1951.

PROPAGATION OF ELECTROMAGNETIC WAVES IN PLANE AND SPHERICAL IMPEDANCE WAVEGUIDES. PART II. PROPAGATION OF ELECTROMAGNETIC WAVES IN A PLANE IMPEDANCE WAVEGUIDE

G.I. Makarov and V.V. Novikov

ABSTRACT: The problems of finding and investigating the behavior of the eigen-values of a tranverse differential operator in the case of a plane waveguide are discussed in terms of the method of direct variations and the method of instances. The method of instances aids in obtaining rather simple analytical expressions for the eigen-values of the transverse differential operator with relatively wide limits to applicability. These expressions can be used for a qualitative study of the principal rules for the structure of an electromagnetic field in plane impedance waveguides.

In this part of the study, we will discuss the problems of finding and investigating the behavior of the eigen-values of a transverse differential operator in the case of a plane waveguide. In order to obtain clearer physical results, we will assume that the lower waveguide wall ($x = 0$) has infinite conductivity ($\delta_g = 0$). As for the normalized surface impedance $\delta = \delta_i$ of the upper wall of the waveguide ($x = \beta$), we will not impose any limitations on it, except for the requirement of physical practicability $\operatorname{Re}\delta \geq 0$ [1]. Moreover, in this study the medium filling in the waveguide is considered to be homogeneous with $\varepsilon_m = 1$. /34

Section 1. Applying Direct Variation Methods in Order to Determine Eigen-Values

A formal solution to the problem of the field of a vertical electric dipole in a plane waveguide was constructed in the first part of the study [2]. A further investigation of the solution is based on a determination of the eigen-values of the transverse differential operator L_x, i.e.,

$$L_x u + \mu u = 0, \quad L_x \equiv \frac{d^2}{dx^2}, \quad \left.\frac{du}{dx}\right|_{x=0} = 0, \quad \left.\left(\frac{du}{dx} - i\delta u\right)\right|_{x=\beta} = 0. \tag{1.1}$$

The operator L_x is not self-conjugate and has a point spectrum [3], which we will consider to be simple.

Let us reduce the problem of finding the eigen-values of the differential operator L_x to that of determining the spectrum of a certain integral operator. We will select a complex number μ_0^m in such a way that it does not belong to the spectrum of the operator L_x. We will formulate further limitations on μ_0^m at a later time. Let us consider a differential operator of the following type:

$$L_m u = \frac{d^2u}{dx^2} + \mu_0^m u, \quad \frac{du}{dx}\Big|_{x=0} = 0, \quad \left(\frac{du}{dx} - i\delta u\right)\Big|_{x=\beta} = 0. \tag{1.2}$$

Since μ_0^m does not belong to the spectrum of L_x, there is a limited inverse operator, i.e.,

$$K^m \equiv L_m^{-1}, \tag{1.3}$$

which is entirely continuous in L_2 at the same time. If we now use the operator K^m on (1.1), then the latter will acquire the following form:

$$u + \mu^{(m)'} K^m u = 0, \tag{1.4}$$

where

$$\mu^{(m)'} \equiv \mu - \mu_0^m. \tag{1.5}$$

Thus, the problem of (1.1) is reduced to the problem of (1.4) of determining the eigen-values of the completely continuous operator K^m. In order to solve the latter problem, we can use one of the direct variation methods, for example the Galerkin method [4] or the method of instances [5]. We will discuss the plan of the method of instances briefly below.

According to this method [5], the operator K^m acting in L_2 is replaced by a finite-dimensional operator K_n^m acting in a finite-dimensional space H_n formed by the elements

$$z_0^m \in L_2, \quad z_1^m = K^m z_0^m, \ \ldots, \ z_{n-1}^m = K^m z_{n-2}^m,$$

In this regard,

$$K_n^m = E_n K^m E_n,$$

where E_n is the projector on H_n. The eigen-values $\mu_n^{(m)}$ of the operator K_n^m

$$u_n^{(m)} + \mu_n^{(m)'} K_n^m u_n^{(m)} = 0, \ \frac{du_n^{(m)}}{dx}\bigg|_{x=0} = 0, \left(\frac{du_n^{(m)}}{dx} - i\delta u_n^{(m)}\right)\bigg|_{x=\beta} = 0$$

on the condition that the operator K^m is completely continuous, satisfy the limiting relation

$$\mu_{n,i}^{(m)'} \to \mu_i^{(m)'} \quad \text{при} \quad n \to \infty \ (i = 1, 2, \ldots)$$

for any selection of z_0^m. The convergence of $\mu_{n,i}^{(m)'}$ to $\mu_i^{(m)'}$ is found to be more rapid than that of the geometric progression with a decreasing denominator tending to zero.

The eigen-values of the operator K_n^m are linked with the roots of the algebraic equation of $\lambda_{n,i}^{(m)}$ as

$$\sum_{k=0}^{n} \alpha_k [\lambda_n^{(m)}]^k = 0, \quad \alpha_n = 1, \quad \mu_{n,i}^{(m)} = -\frac{1}{\lambda_{n,i}^{(m)}} \quad (i = 1, 2, \ldots, n),$$

where the coefficients α_k are determined by the following system of equations: /38

$$\begin{gathered}\alpha_0(z_0^m, z_0^m) + \alpha_1(z_1^m, z_0^m) + \ldots + \alpha_{n-1}(z_{n-1}^m, z_0^m) = -(z_n^m, z_0^m), \\ \cdots\cdots\cdots\cdots\cdots\cdots \\ \alpha_0(z_0^m, z_{n-1}^m) + \alpha_1(z_1^m, z_{n-1}^m) + \ldots + \alpha_{n-1}(z_{n-1}^m, z_{n-1}^m) = -(z_n^m, z_{n-1}^m),\end{gathered}$$

and $z_n^m \equiv K^m z_{n-1}^m$. In the future, we will be interested in obtaining rather simple approximative analytical forumulas for the eigen-values, and thus it is necessary that a good approximation be attained for a small number of steps (n = 1 or, in the extreme case, n = 2). The latter can be obtained by a corresponding selection of the number μ_0^m and element z_0^m. In order to understand better how they should be selected, we will consider the expression for $\mu_1^{(m)'}$ in first approximation, i.e.,

$$\mu_{1,1}^{(m)'} = -\frac{(z_0^m, z_0^m)}{(z_1^m, z_0^m)}. \tag{1.6}$$

Let u_i^m be normalized characteristic elements of the operator K^m, while $\mu_i^{(m)'} = \mu_i - \mu_0^m$ are its eigen-values. Obviously, the eigen-functions of the operator K^m coincide in this case with the eigen-functions of the operator L_x of (1.1). Let us represent the element z_0^m in the form of an expansion

$$z_0^m = \sum_{i=0}^{\infty} a_i u_i^m, \tag{1.7}$$

Then

$$z_1^m = -\sum_{i=0}^{\infty} \frac{a_i}{\mu_i^{(m)'}} u_i^m = -\sum_{i=0}^{\infty} \frac{a_i}{\mu_i - \mu_0^m} u_i^m. \tag{1.8}$$

The p-th term in the series of (1.7) is the principal one if the element z_0^m is closest to the eigen-function u_p^m (for $z_0^m = u_p^m$ this term is unique). Generally speaking, there are two principal terms in the series of (1.8) in this case: first of all, the p-th term, as in (1.7), because of the coefficient of expansion a_p; secondly, the term with number s, for which the difference $\mu_s - \mu_0^m$ is minimal in modulus. The presence of two prinicpal terms in (1.8) results in a situation where $\mu_{1,1}^{(m)'}$ is linked with μ_p and μ_s, or with $\mu_p^{(m)'}$ and $\mu_s^{(m)'}$, which is the same ($\mu_{1,1}^{(m)'}$ depends, obviously, on the entire spectrum of $\mu_i^{(m)'}$, but the greatest dependence holds for the cited eigen-values). Consequently, $\mu_{1,1}^{(m)'}$ can have a value which differs greatly from $\mu_p^{(m)'}$, as well as from $\mu_s^{(m)'}$. In order to have the value $\mu_{1,1}^{(m)'}$ approximate one of the cited eigen-values, it is necessary either to select the element z_0^m as closest to the eigen- /37
function u_s^m (for a fixed value of μ_0^m), or to select μ_0^m as nearest to μ_p (for a fixed selection of z_0^m). Thus, the selection of z_0^m should agree with the selection of μ_0^m (or the inverse). In such a case, there will be one principal term with the same number s in each of the series of (1.7) and (1.8), so that $\mu_{1,1}^{(m)'}$ from (1.6) is close to the eigen-value $\mu_s^{(m)'}$. Then, in first approximation,

$$\mu_s^{(1)} = \mu_0^m + \mu_{1,1}^{(m)'}, \tag{1.9}$$

while it is easy to obtain an estimate of the closeness of $\mu_s^{(1)}$ to μ_s on the basis of (1.6) and the expansions of (1.7) and (1.8), on the condition that the coefficients of expansion of (1.7) decrease rather rapidly:

$$|\mu_s - \mu_s^{(1)}| \simeq \left| \frac{\mu_s - \mu_0^m}{\mu_{s-1} - \mu_0^m} (\mu_{s-1} - \mu_s) \frac{a_{s-1}}{a_s} (u_{s-1}^m, u_s^m) + \right.$$
$$\left. + \frac{\mu_s - \mu_0^m}{\mu_{s+1} - \mu_0^m} (\mu_{s+1} - \mu_s) \frac{a_{s+1}}{a_s} (u_{s+1}^m, u_s^m) \right| \tag{1.10}$$

It follows from (1.10) that the degree of closeness of $\mu_s^{(1)}$ to μ_s depends on the closeness of z_0^m to the characteristic element u_s^m of the operator L_x [see (1.1)] (a sufficient smallness of the ratios $\frac{a_{s-1}}{a_s}$ and $\frac{a_{s+1}}{a_s}$) and on the closeness of μ_0^m to the eigen-value μ_s. If we can guarantee these two conditions, then we can expect that the eigen-values will be found with rather high accuracy in first approximation of the method of instances.

Thus, in order to obtain rather simple approximative formulas, it is necessary to present the expansion of eigen-values of the operator of (1.1). Therefore, before carrying out computations according to the plan described above, it is necessary to study the problem of the distribution of eigen-values of the transverse operator for a plane waveguide and their behavior, in dependence on the surface impedance of the upper waveguide wall, the height of the waveguide and the frequency of electromagnetic oscillations. The following section will treat these problems.

Section 2. Qualitative Investigation of the Ordering of Eigen-Values for a Plane Waveguide

A transcendental equation was presented in the first part of the study for the eigen-values μ of the transverse operator of the problem in the case of a plane waveguide [(22) of Part I]. For ideal conductivity of the lower wall of the waveguide ($\delta_g = 0$), it /38
acquires the following form:

$$\eta \tan \eta = t, \qquad (2.1)$$

where

$$\eta \equiv \sqrt{\mu}\beta; \quad t \equiv -i\delta\beta; \quad \delta \equiv \delta_i; \quad \beta \equiv kh.$$

Let us examine (2.1) on a complex plane (η) and let us study the behavior of its roots in dependence on the value t. The modulus and argument of t are determined by the frequency, the height of the waveguide and the nature of the surface impedance of the upper waveguide wall. Since the only condition imposed on the surface impedance is the requirement that Re $\delta \geq 0$, then Im $t \leq 0$. In this regard, positive values of t correspond to purely capacitive impedance, while the negative values correspond to purely inductive impedance, and the imaginary values correspond to active impedance of the ionosphere (Fig. 1).

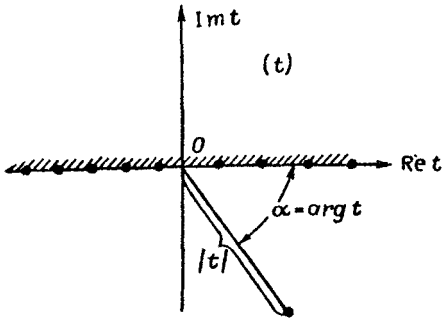

Fig. 1.

Before turning to a detailed analysis of (2.1), we should mention two of its general properties: (1) the roots of the equation for the plane (η) are expanded symmetrically relative to the origin of the coordinates: (2) Equation (2.1) has a double root which satisfies the following equation additionally, for certain values of t:

$$\eta + \sin \eta \cos \eta = 0, \qquad (2.2)$$

As is easy to see, the latter, when in the band $m\pi + \frac{\pi}{2} \leq \text{Re } \eta \leq m\pi + \frac{3\pi}{4}$, where m is a whole number. In order to find t corresponding to the double root, we must substitute the solution to (2.2) into (2.1).

Let us now rewrite (2.1) in the form of two equations, i.e.,

$$\tan \alpha = \frac{\tau \sin \sigma \cos \sigma + \sigma \operatorname{sh} \tau \operatorname{ch} \tau}{\sigma \sin \sigma \cos \sigma - \tau \operatorname{sh} \tau \operatorname{ch} \tau}; \qquad (2.3)$$

$$|t|^2 = \frac{(\sigma^2 + \tau^2)(\sin^2 \sigma \cos^2 \sigma + \operatorname{sh}^2 \pi \operatorname{ch}^2 \tau)}{(\cos^2 \sigma + \operatorname{sh}^2 \tau)^2}, \qquad (2.4)$$

where $\alpha = \arg t$, $\eta = \sigma + i\tau$, while (2.3) should be supplemented by conditions defining the sign of the numerator and denominator of the right-hand part:

$$\begin{aligned}\operatorname{sign}\cos\alpha &= \operatorname{sign}\left[\sigma\sin\sigma\cos\sigma - \tau\,\mathrm{sh}\,\tau\,\mathrm{ch}\,\tau\right],\\ \operatorname{sign}\sin\alpha &= \operatorname{sign}\left[\tau\sin\sigma\cos\sigma + \sigma\,\mathrm{sh}\,\tau\,\mathrm{ch}\,\tau\right].\end{aligned} \tag{2.5}$$

Equation (2.3) can be called the equation of the line of zeros. /39
It shows on what line on the plane (η) the beam α = const on the plane (t) transfers. Equation (2.4) makes it possible to determine the distribution of zeros on the zero line (2.3).

It was mentioned above that the roots of (2.1) are arranged symmetrically relative to the origin of the coordinates. Therefore, we will consider only the case of $\sigma \geq 0$ below. We will begin the analysis of (2.3) and (2.4) with an investigation of the particular cases $\alpha = 0$ (purely capacitive surface impedance) and $\alpha = -\pi$ (purely inductive surface impedance). In both cases, (2.3) acquires the form of

$$\tau\sin\sigma\cos\sigma + \sigma\,\mathrm{sh}\,\tau\,\mathrm{ch}\,\tau = 0 \tag{2.6}$$

and has the possible solutions of $\tau = 0$ and $\sigma = 0$. The first of the supplementary conditions of (2.5) makes the solutions more precise:

$$\text{for } \alpha = 0 \quad \tau = 0 \quad \text{at} \quad n\pi \leqslant \sigma \leqslant \frac{2n+1}{2}\pi, \tag{2.7}$$

$$\text{for } \alpha = -\pi \quad \tau = 0 \quad \text{at} \quad \frac{2n+1}{2}\pi \leqslant \sigma \leqslant (n+1)\pi \tag{2.8}$$

$$\text{and } \sigma = 0 \text{ at any } \tau. \tag{2.9}$$

Rewriting (2.6),

$$\frac{\sin\sigma}{\sigma}\cos\sigma = -\frac{\mathrm{sh}\,\tau}{\tau}\mathrm{ch}\,\tau,$$

it is easy to see that it does not have roots in the range of $\sigma \neq 0$ and $\tau \neq 0$, i.e., the solutions found above are unique.

Let us now turn to (2.4). On the zero lines of (2.7) and

(2.8), where $\tau = 0$, it converts into the following:

$$|t| = \sigma |\tan \sigma|.$$

It can be seen from this that the point $|\tau| = 0$ on the plane (η) corresponds to the point $\sigma = 0$ and $\sigma = \eta\pi$, while for $|\tau| \to \infty$ it corresponds to the point $\sigma \to \frac{2n + 1}{2} \pi$. On the zero line of (2.9), where $\sigma = 0$, (2.4) acquires the form of

$$|t| = \tau \operatorname{sh} \tau,$$

so that $\tau = 0$ at $|\tau| = 0$ and $\tau \to \pm \infty$ for $|\tau| \to \infty$. Figure 2 shows the zero lines for the cases under investigation of $\alpha = 0$ and $\alpha = -\pi$ and points out the direction where the zeros displace along these lines in measure with the increase of $|\tau|$.

Let us now examine (2.2) in the general case, considering $\sin \alpha < 0$ and $\sigma \neq 0$, $\tau \neq 0$, since the limiting case $\sin \alpha = 0$ and $\sigma = 0$, $\tau = 0$ has already been investigated. According to the second additional condition of (2.5), the following inequality should be fulfilled:

$$\tau \sin \sigma \cos \sigma + \sigma \operatorname{sh} \tau \operatorname{ch} \tau < 0.$$

An elementary analysis shows that this inequality takes place only in the range of $\tau < 0$ (for us, $\sigma > 0$).

The possible ranges for distribution of roots of (2.1) can be /40
clarified in more detail. Let us consider the case of capacitive surface impedance ($\cos \alpha > 0$). In this regard the first additional condition of (2.5) should be fulfilled, i.e.,

$$\sigma \sin \sigma \cos \sigma > \tau \operatorname{sh} \tau \operatorname{ch} \tau. \qquad (2.10)$$

In the range of $\sigma > 0$ and $\tau < 0$, (2.10) can take place only in the interval of

$$n\pi < \sigma < \frac{2n+1}{2} \pi. \qquad (2.11)$$

If the surface impedance has an inductive nature ($\cos \alpha < 0$), then the first condition of (2.5)

$$\sigma \sin \sigma \cos \sigma < \tau \operatorname{sh} \tau \operatorname{ch} \tau$$

can be fulfilled for any τ in the intervals of

$$\frac{2n+1}{2}\pi < \sigma < (n+1)\pi, \qquad (2.12)$$

as well as in the intervals of (2.11) for values of τ which are rather great in modulus.

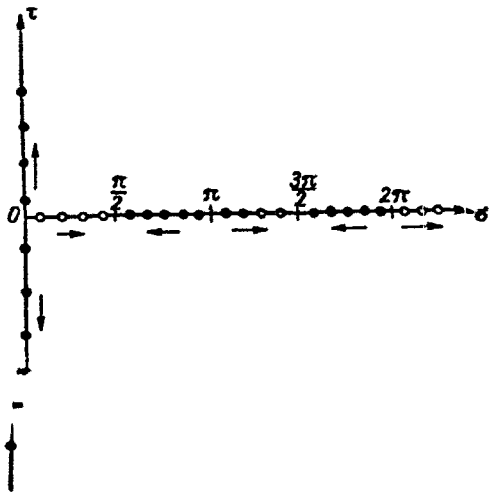

Fig. 2.

In order to explain the behavior of the zero lines on the plane (η), it is necessary to find the arrangement of the initial and final points corresponding to $|\tau| = 0$ and $|\tau| = \infty$. According to (2.4), the value $|\tau| = 0$ corresponds to the "output" points $\sigma = 0$, $\tau = 0$ and $\sigma = \eta\pi$, $\tau = 0$. The "input" points, for which $|\tau| = \infty$, are arranged at $\sigma = \frac{2n+1}{2}\pi$, $\tau = 0$, while one of these points is at $|\tau| = \infty$. Using (2.3), it is easy to clarify the arrangement of this last "input" point, finding the asymptote of the zero line for $\tau \to -\infty$ from it: /41

$$\tau = -\frac{\sigma}{\tan \alpha} \qquad (2.13)$$

It follows that the corresponding "input" point takes place only in the case of inductive surface impedance ($\tan \alpha > 0$).

Basing our discussions on (2.3), we can find the first derivatives along the zero lines at the "output" and "input" points:

$$\left.\frac{d\tau}{d\sigma}\right|_{\sigma,\ \tau=0} = \tan\frac{\alpha}{2}, \quad \left.\frac{d\tau}{d\sigma}\right|_{\substack{\sigma=\frac{m\pi}{2} \\ \tau=0}} = (-)^m \tan\alpha.$$

Thus, the zero lines go out from the point $\sigma, \tau = 0$ at angles which are twice less than the angles α at which the beams on the plane

(t) go out. The zero lines go out from the points $\sigma = n\pi$ and $\tau = 0$ at the same angles as do the corresponding beams on the plane (t). The angles of input of the zero lines at the points $\sigma = \frac{2n+1}{2}\pi$, $\tau = 0$ are found to be equal to $-\alpha$.

We should mention one general property of the zero line. Since any given values of σ and τ, except the points of "input" and "output" correspond to one value of α, according to (2.3), then the zero lines relating to various values of α cannot intersect one another. Consequently, the zero lines corresponding to the same value of α also do not intersect. Only their tangency is possible.

The qualitative ideas presented above allow us to represent the behavior of the zero lines in the case of capacitive impedance. The zero lines go from the "output" points $\sigma_0 = m\pi$, $\tau_0 = 0$ to the "input" points $\sigma_{in} = \frac{2m+1}{2}\pi$, $\tau_{in} = 0$, arranged entirely in the bands

$$m\pi \leqslant \sigma \leqslant \frac{2m+1}{2}\pi.$$

In each such band, the zero lines trace the region between the real axis $\sigma = 0$ and the line

$$\sigma \sin 2\sigma = \tau \operatorname{sh} 2\tau, \qquad (2.14)$$

representing the zero line for purely active impedance ($\alpha = -\frac{\pi}{2}$). It follows from (2.14) that, with an increase in the number m, this range takes on higher and higher values of $|\tau|$. A qualitative picture for the zero lines for capacitive impedance is given in Figure 3.

In the case of inductive impedance, the course of the zero lines is more complex, and it is necessary to have additional materials for a final explanation of their behavior. First of all, let us examine the course of the zero lines in the range of /42

$$\sigma \gg 1, \quad \tau \ll 1. \qquad (2.15)$$

In this case, it is easy to find the approximating equation of the

zero lines from (2.3):

$$\tau \simeq \frac{1}{2} \sin 2\sigma \tan \alpha. \qquad (2.16)$$

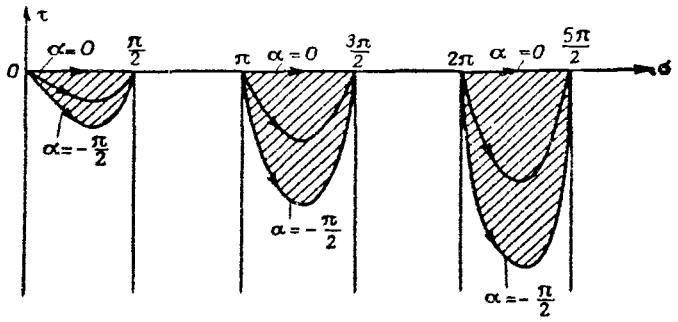

Fig. 3.

Expression (2.16) describes the behavior of the zero lines in the range of (2.15) rather precisely for the condition of $|\tan \alpha| \ll 1$, and is suitable both for capacitive ($\tan \alpha < 0$) and inductive ($\tan \alpha > 0$) impedance. Consequently, in the case of inductive impedance the zero lines are arranged in the bands

$$\frac{2m-1}{2}\pi \leqslant \sigma \leqslant m\pi$$

and go from the "output" points $\sigma_0 = m\pi$, $\tau_0 = 0$ to the "input" points $\sigma_{in} = \frac{2m-1}{2}\pi$, $\tau_{in} = 0$ for rather high numbers m and $\tan \alpha \ll 1$ (Fig. 4).

Secondly, let us study the zero lines in the neighborhood of the "input" and "output" points in more detail, i.e.,

$$\sigma = \frac{n\pi}{2} + \beta_0, \quad |\beta_0| \ll 1, \quad |\tau| \ll 1$$

for the condition of $\tan \alpha > 0$. We can find an approximating equation for the zero lines in this range from (2.3):

$$(-)^n \tan\alpha \cdot \beta_0 = \tau + \frac{2\tan\alpha}{n\pi}\tau^2. \qquad (2.17)$$

If $\tan\alpha \ll 1$, then we arrive at the following equation:

$$\tau = (-)^n \tan\alpha \cdot \beta_0,$$

In the case under investigation ($|\beta_0| \ll 1$), the latter also follows from the relationship (2.16) examined above. However, if $\tan\alpha \gg 1$, then it is necessary to consider the second right-hand term in (2.17), so that /43

$$\beta_0 = \frac{2(-)^n}{n\pi}\tau\left(\tau + \frac{n\pi}{\tan\alpha}\right) \qquad (2.18)$$

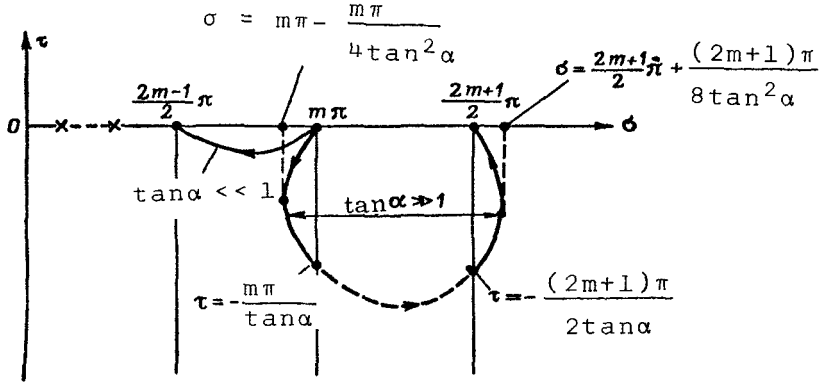

Fig. 4.

In this case, the zero lines are parabolas, the qualitative course of which is represented in Figure 4 for the neighborhood of the points of "output" (n = 2m) and "input" (n = 2m + 1). We should mention that the curves presented in Figure 4 which correspond to the parabolas of (2.18) in the case of $\tan\alpha \gg 1$ describe the zero lines rather well all the way to the points of intersection with the lines $\sigma = m\pi$ and $\sigma = \frac{2m+1}{2}\pi$ on the condition that the stricter inequality is fulfilled, i.e.,

$$\tan\alpha \gg m\pi.$$

If the zero line intersects the lines $\sigma = m\pi$ and $\sigma = \frac{2m+1}{2}\pi$, as is depicted in Figure 4, then it necessarily goes from the point

$\sigma = m\pi$, $\tau = 0$ to the point $\sigma = \frac{2m+1}{2}\pi$, $\tau = 0$ (dotted line in Fig. 4), since it follows from (2.3) that the lines $\sigma = \frac{n\pi}{2}$ intersect the zero lines only at the following points:

$$\tau = -\frac{n\pi}{2\tan\alpha}.$$

Considering the above, we can see that the zero lines behave in qualitatively different ways for a fixed value of m in the case of weakly inductive ($\tan\alpha >> 1$) and strongly inductive ($\tan\alpha << 1$) impedance. The process of the change in course of the zero lines as $\tan\alpha$ decreases can be explained in the following way. For some fixed value of m and a rather high value of $\tan\alpha$ ($\tan\alpha >> m\pi$), the zero lines relating to the two neighboring "output" points $\sigma_0 = (m-1)\pi$, $\tau_0 = 0$ and $\sigma_0 = m\pi$, $\tau_0 = 0$ are loops going from the "output points to the corresponding "input" points $\sigma_{in} = \frac{2m-1}{2}\pi$, $\tau_{in} = 0$ and $\sigma_{in} = \frac{2m+1}{2}\pi$, $\tau_{in} = 0$ (Fig. 5). Let us follow the change in course of the zero lines relating to the left-hand "output" points. As $\tan\alpha$ decreases, the loops representing the zero lines going from the neighboring "output" points are more and more "inflated", coming closer to each other. For some critical value of $\tan\alpha_{cr}$ depending on the number m, there is tangency of the zero lines coming out of the neighboring "output" points, which corresponds to the arisal of a two-fold root of the characteristic equation in (2.1). In a further (small) decrease of $\tan\alpha$,

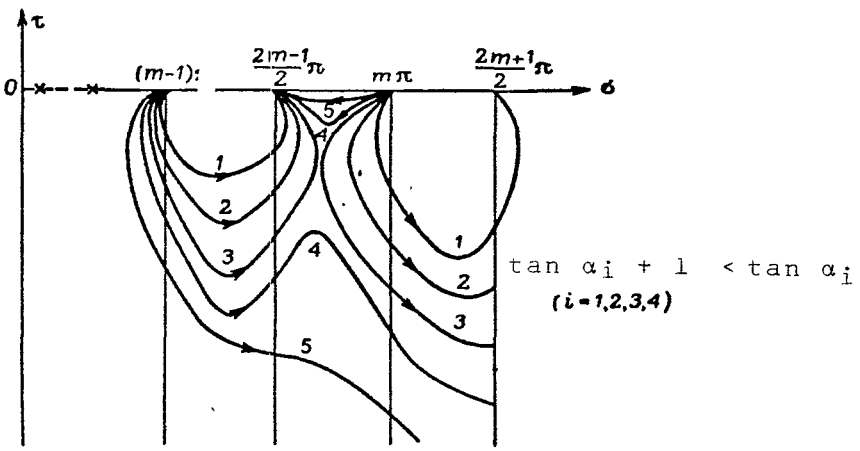

Fig. 5.

there is a splitting of the zero line going from the left-hand "output" points. This line now goes to infinity and has the asymptote of (2.13) found above. The zero line going from the

right-hand "output" point now ends at the left-hand "input" point, where the zero line corresponding to the left-hand "output" point had ended previously (for tan $\alpha >>$ tan α_{cr}).

The process of change in course of the zero line we examined depends on the number m. From (2.2), which defines the position of multiple zeros, we can find the approximative coordinates of the points of tangency of the zero lines for $m >> 1$, and we can calculate the value of tan α_{cr} on the basis of (2.1):

$$\sigma_\kappa \simeq \frac{4m+3}{4}\pi, \quad \frac{\ln(4m+3)\pi}{(4m+3)\pi}, \quad \tau_\kappa \simeq -\frac{1}{2}\ln(4m+3)\pi; \qquad (2.19)$$

$$\tan \alpha_{cr} \simeq \frac{(4m+3)\pi}{2\ln(4m+3)\pi}$$

/45

Thus, the greater the value of m the greater the values of tan α for which there is tangency and further splitting of the zero lines. With a value of tan α as high as wanted but still finite, we can find that number $\underline{m}$ for which tangency and splitting of the zero lines already took place. With a decrease in tan α, the splitting process encompasses smaller and smaller values of m. The qualitative course of the zero lines in the case of inductive impedance is depicted in Figure 6. The arrows show the direction of dislocation of zeros along the lines with an increase of $|\tau|$. We should mention that, for a specific value of surface impedance which has an inductive nature, there is always only one zero line going to infinity and corresponding to a certain "output" point, the number m of which depends on the argument of the surface impedance.

The ideas on the behavior of the zero lines presented above are of a qualitative nature. Numerical calculations confirm the validity of the picture for the dynamics of the zero lines we have drawn. Figure 7 shows zero lines in the band $(0,\pi)$ found with the aid of a numerical solution to (2.3). The numbers around the zero lines on this figure correspond to values of tan α. Tangency of the zero lines coming from the points $\sigma = 0$, $\tau = 0$ and $\sigma = \pi$, $\tau = 0$ takes place at tan $\alpha_{cr} \simeq 1.24$, which corresponds to weakly inductive surface impedance of the upper wall of the waveguide with argument equal to -39°. In this regard, the multiple root of (2.1) for the cited value of the argument of impedance appears in the case when $|\tau| = |\delta\beta| \simeq 2.64$.

The following results are derived from the general picture we have examined for the behavior of the eigen-values of μ_i (or, more precisely, $\eta_i = \sqrt{\mu_i}\beta$) of the transverse operator of the problem concerning the field in a plane waveguide.

First of all, an interesting fact is seen in the possibility

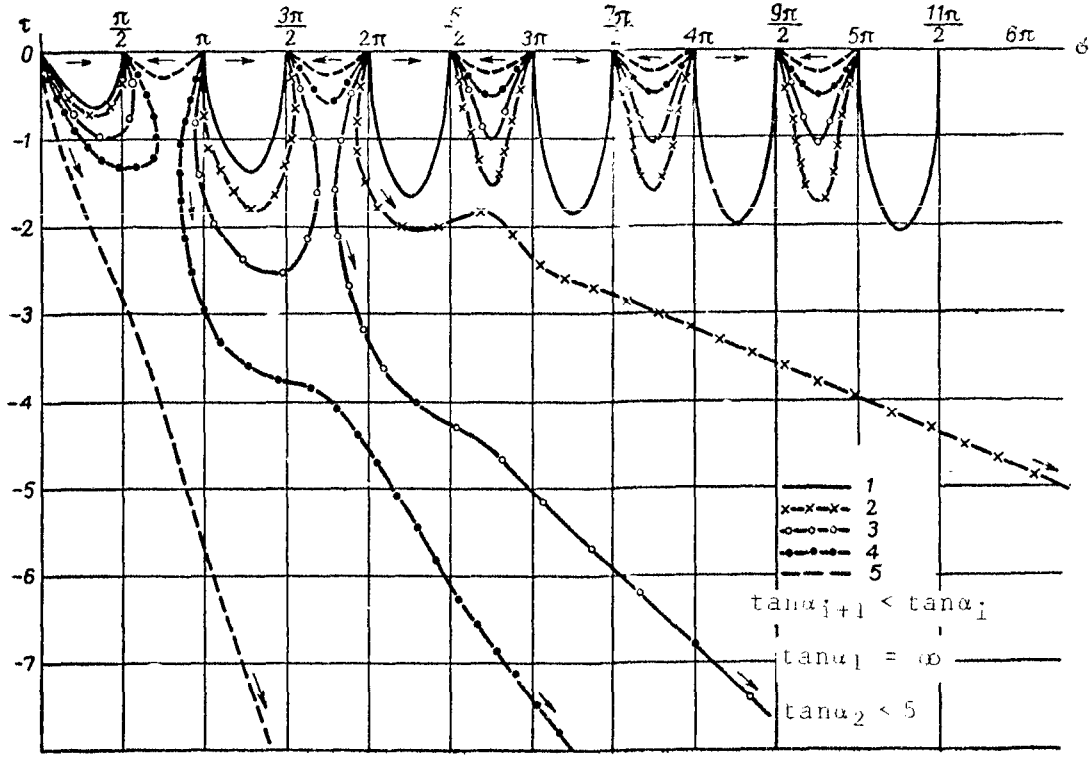
τ
0
-1
-2
-3
-4
-5
-6
-7
π/2
π
3π/2
2π
5/2
3π
7π/2
4π
9π/2
5π
11π/2
6π
δ
1
2
3
4
5
tanα_{i+1} < tanα_i
tanα_1 = ∞
tanα_2 < 5

Fig. 6.

9h7

of degeneration of the spectrum of the transverse operator, i.e., the presence of a multiple eigen-value under certain conditions.[1] This takes place only in the case of weakly inductive surface impedance of the upper environment (ionosphere). For example, in the case of a uniform upper environment with reduced surface impedance of

$$\delta = \frac{1}{\sqrt{\varepsilon_m + 1 + i\frac{\sigma}{\omega\varepsilon_0}}},$$

where ε_m and σ are the relative permittivity and conductivity of the upper environment, respectively, the eigen-value which is least in modulus is found to be degenerate on the condition that the frequency of vibrations and the height of the waveguide are linked with the properties of the upper environment by the following relationships: /47

$$f\,[\text{KHz}] \simeq \frac{3{,}8\cdot 10^6}{\varepsilon_m + 1}\,\sigma\left[\frac{1}{\text{Ohm}\cdot\text{m}}\right], \quad h\,[\text{km}] \simeq 7{,}2\cdot 10^{-5}\,\frac{(\varepsilon_m+1)^{3/2}}{\sigma\left[\frac{1}{\text{Ohm}\cdot\text{m}}\right]}$$

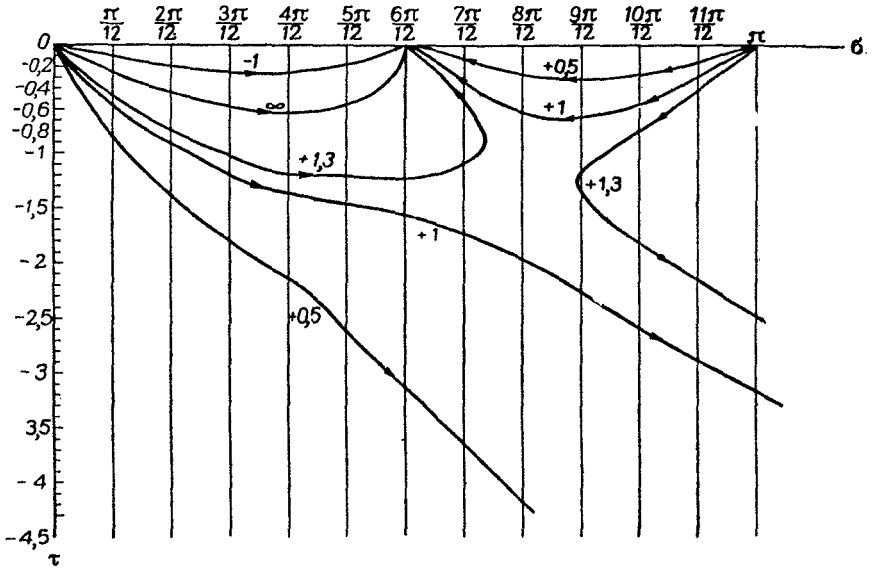

Fig. 7.

[1] K. Budden [6] first noted such a possibility.

If $\varepsilon_m = 1$ and $\sigma = 2.5 \cdot 10^{-6} \frac{1}{\text{Ohm} \cdot \text{m}}$, then degeneracy can hold for $f \simeq 4.75$ KHz and $h \simeq 80$ km. These data indicate that degeneration can apparently be observed under real conditions of the propagation of superlong waves in a ground waveguide; however, this question needs separate investigation with a consideration of the sphericity of the waveguide channel.

Let us turn to the problem of the numeration of normal waves (modes). As follows from Figure 6, the problem of numeration of modes in the case of capacitive impedance does not cause any difficulties. Here it is natural to call the m-th mode that normal wave whose eigen-value satisfies the following condition:

$$m\pi \leqslant \operatorname{Re} \sqrt{\mu\beta} \leqslant m\pi + \frac{\pi}{2} \tag{2.20}$$

For such numeration, the modulus of the eigen-value μ_m increases monotonously with an increase of the number m, so that /48

$$|\mu_0| < |\mu_1| < |\mu_2| \tag{2.21}$$

Thus, in the case of capacitive impedance the numeration of modes can be carried out in order of the increase of $|\mu_m|$, which corresponds to numeration of the eigen-values used in the mathematical literature.

For inductive impedance, the situation is more complex, and, generally speaking, the condition of (2.20) is not fulfilled, while the conditions of (2.21) are inconvenient for numeration, since, if they are kept, then numeration of the modes is dependent both on the surface impedance of the upper wall of the waveguide and on the height of the latter. From our point of view, the simplest and most purposeful numeration of modes corresponds to the "output" points of the zero lines $\sigma_0 = m\pi$, $\tau_0 = 0$ (see Fig. 6), so that the m-th mode represents that normal wave for which

$$\sqrt{\mu m}\beta \to m\pi \text{ for } h \to 0 (|t| \to 0). \tag{2.22}$$

The proposed numeration is valid for any nature of surface impedance, and, in the case of capacitive impedance, coincides with the numeration based on (2.20) or (2.21). Moreover, with such numeration [see (2.22)], the eigen-value of the mode of a fixed number describes a continuous curve with a change in the height of the waveguide for given surface impedance.

Finally, we should mention the instability of single eigen-values of the transverse operator relative to small changes in the argument of surface impedance in that case where it is inductive. For an example of this phenomenon, we can consider the eigen-value of the first mode (Fig. 6). For values of $t = \delta\beta$ which are rather high in modulus, the eigen-value corresponding in our numeration to the first mode can lie in completely different ranges of the complex plane (μ), depending on the specific value of the argument of surface impedance. This can be seen from the fact that the value $\eta_1 = \sqrt{\mu_1}\beta$ in this case is either in the neighborhood of the point $\sigma = \frac{3\pi}{2}$, $\tau = 0$ (Curves 1,2 and 3 in Fig. 6), in a range with a rather high value of $|\tau|$ (Curve 4 on Fig. 6), or in the neighborhood of the point $\sigma = \frac{\pi}{2}$, $\tau = 0$ (Curve 5 on Fig. 6). Consequently, with small changes in the argument of surface impedance around certain critical values (corresponding to the points of tangency of the zero lines closest to the output point of the mode under investigation), there is a discontinuous change in the eigen-value of a single mode for rather high values of $|\tau|$ exceeding $|\tau|_{cr}$ at the cited points of tangency. However, such a change in the eigen-value of a single mode does not result in instability of the spectrum of eigen-values on the whole, and is simply a disadvantage of the numeration of modes we assumed. Actually, it is easy to see that, in a discontinuous change in the eigen-value of any mode there is a discontinuous change in the eigen-value of the mode neighboring it (on the left or right), so that as a result, as the argument of surface impedance around a critical value changes, the eigen-value of one mode converts continuously into the eigen-value of another mode (only the number of this eigen-value changes in the discontinuity, which is not fundamental and is linked with the terminology we used). /49

Up to now, we have actually been speaking of the eigen-values of the transverse operator of the problem for fixed frequency with given surface impedance, and of the change in these values during an increase or decrease in the height of the waveguide. Therefore, the curves on Figures 6 and 7 represent the zero lines along which the eigen-values (more precisely, $\sqrt{\mu_i}\beta$) displace with a change in the height of the waveguide h for any given values of the frequency of electromagnetic vibrations and the surface impedance of the ionosphere. In application, it is usually of interest to study the dependence of the eigen-values on the frequency of electromagnetic vibrations for given height of the waveguide and given surface impedance of its upper wall. If the surface impedance did not depend on the frequency, its change would be entirely equivalent to the change in height of the waveguide in respect to the effect on the eiger-values (2.1). In this regard, the course of the zero lines would remain as before (see Figs. 6 and 7). Actually (particularly if we are speaking of the propagation of

superlong waves), the surface impedance most often has a relatively sharply expressed frequency dispersion, so that both the modulus and argument of the surface impedance change with a change in frequency. In this case, the modulus and argument of the value $t = -i\delta\beta$ also change with an increase in frequency, so that the depicted point t on the complex plane (t) (see Fig. 1) displaces, not along arg $t = \alpha = \text{const}$, but over some complex curve whose specific course depends on the given frequency dispersion of the surface impedance. This curve on the plane (n) (Figs. 6 and 7) corresponds to zero lines which apparently do not coincide with any of the zero lines depicted on Figures 6 and 7. However, using the data on the course of the zero lines in the latter case and knowing the values of $|\tau|$ along these lines, it is easy to find the behavior of the zero lines for frequency-dependent impedance.

The zero lines for frequency-dependent impedance will intersect the zero lines corresponding to arg $t = \text{const}$. In this regard, if the zero line for arg $t = \text{const}$ goes out from the "output" point $\sigma = m\pi$, $\tau = 0$, ends at neighboring "input" points (on the left or right), or goes to infinity, then the zero line can go either to infinity or, generally speaking, to any "input" point, with an increase of $|\tau|$ for frequency-dependent impedance. As a result, with a change in frequency the continuously-changing eigen-value for some frequencies should be related to one certain mode in the numeration used, while for other frequencies it shoud be related to another mode. It is necessary to find whether or not this phenomenon takes place specially in each specific case. /50

The possible change in number with a change in frequency for a continuously-changing eigen-value noted is one more disadvantage of the numeration of modes we used above. Undoubtedly we could have carried out numeration of modes in another way in the case of frequency-dependent impedance, for example with the condition of

$$\sqrt{\mu m}\beta \to m\pi \quad \text{for } f \to 0 \ (|t| \to 0). \tag{2.23}$$

The eigen-value which changes continuously with an increase in frequency would then correspond to the same normal wave in this numeration. However, the numeration of modes which is based on (2.23) also has its disadvantages; in particular, it depends on the height of the waveguide as well as the specific frequency dispersion of the surface impedance.

It follows from the above that the numeration of modes which is based on the conditions of (2.22) or (2.23) is generally different. It is important to emphasize that the problem of numeration of modes is not fundamental, being purely a matter of terminology, and we can use any numeration of modes, noting the numeration procedure used each time. We gave specific attention to this problem only because there has been no real clarity con-

cerning it in the literature to this time, and some authors have related the same eigen-value to different modes [6,7] without clearly indicating the principle of the mode numeration. In the future we will keep the numeration of modes which results from the condition of (2.22).

Section 3. Constructing Approximative Formulas for the Eigen-Values of a Plane Impedance Waveguide

In the preceding section we studied the qualitative picture of the behavior of eigen-values of a plane impedance waveguide. Using the scheme of the variation methods, we can attempt to give this picture a quantitative nature. Undoubtedly we could solve the transcendental equation of (2.1) numerically and study the behavior of the eigen-values numerically, in dependence on the frequency of electromagnetic vibrations, the height of the waveguide and the surface impedance of its upper wall. However, this /5 study would involve a great deal of time-consuming calculations. This is why it is of interest to obtain rather simple approximative analytical formulas for the eigen-values, on the basis of which we could study their dependence on the parameters of the problem analytically. Moreover, such approximative formulas would have value in a numerical solution to the transcendental equation of (2.1), since the results they would give could be used as the initial values of the unknown eigen-values.

In obtaining the approximative analytical formulas for the eigen-values with the variation methods, we will keep the following goals in mind:

(1) Obtaining simple analytical formulas based on one-dimensional approximations of the operator K^m. In this case, the variation methods give a value of one eigen-value closest to the selected "center" of μ_0^m (see Section 1). If there are two eigen-values which differ slightly from one another in the neighborhood of this "center", then the accuracy of a one-dimensional approximation decreases abruptly. Therefore, the formulas of a one-dimensional approximation do not permit describing the phenomenon of degeneration of which we spoke above.

(2) A further examination of the problems of degeneration and numeration of modes. For this purpose, we will use two-dimensional approximations of the operator K^m, and we will obtain the formulas of second approximation for the eigen-values, with the aid of which we can also estimate the limits to applicability of the first-approximation formulas.

We will give a great deal of attention to the study of the behavior of eigen-values of the zero and first modes below.

Calculations with the aid of the variation methods are carried out according to the standard plan of [4,5]; however, the accuracy

and limits to applicability of the formulas obtained will depend largely on a successful selection of the "center" μ_0^m and the subspace H_n, with the aid of which the approximation of the operator K^m is carried out. First of all, as mentioned in Section 1, we must have the selection of the number μ_0^m and the support element z_0^m agree. It is natural to select the following:

$$z_0^m = \cos \sqrt{\mu_0^m}\, x, \tag{3.1}$$

since, in that case when the eigen-value of the operator L_x of (1.1) tends toward μ_0^m, its eigen-function, and thus the eigen-function of the operator K^m, tend toward the expression of (3.1). With this selection of z_0^m, the operator K^m of (1.3) acquires the following form:

$$K^m u \equiv \int_\delta^\beta K^m(x, y)\, u(y)\, dy,$$

$$K^m(x, y) = \frac{1}{\sqrt{\mu_0^m}} \begin{cases} \cos \sqrt{\mu_0^m}\, x \left(\sin \sqrt{\mu_0^m}\, y + R^m \cos \sqrt{\mu_0^m}\, y\right), & x \leqslant y, \\ \cos \sqrt{\mu_0^m}\, y \left(\sin \sqrt{\mu_0^m}\, x + R^m \cos \sqrt{\mu_0^m}\, x\right), & x \geqslant y, \end{cases} \tag{3.2}$$

$$R^m = \frac{\sqrt{\mu_0^m} - i\delta \operatorname{tg} \sqrt{\mu_0^m}\, \beta}{i\delta + \sqrt{\mu_0^m} \operatorname{tg} \sqrt{\mu_0^m}\, \beta}.$$

/52

The operator K^m determined by these relationships is found to be completely continuous, which validates application of the Galerkin method or the method of instances for finding its eigen-values.

Further, the question of selecting μ_0^m is raised. In order to obtain simple formulas, the "center" of μ_0^m must be selected as the simplest one and, as follows from the results of the preceding section, we must examine two cases - the cases of "small" and "large" values of $|\delta\beta|$.

In the first case, it is natural to take for μ_0^m its value obtained in solving the problem with $\delta = 0$ (the upper wall of the waveguide, as the lower one, has infinite conductivity),

$$\sqrt{\mu_{0,0}^m} = \frac{m\pi}{\beta}. \tag{3.3}$$

Since we agreed to numerate the modes in correspondence with the

"output" points [see (2.22)], the number m in (3.3) relates to the m-th mode.

In the second case, for μ_0^m we will select a value corresponding to $|\delta| = \infty$ (so-called magnetic wall),

$$\sqrt{\mu_{0,\infty}^m} = \frac{(2m+1)\pi}{2\beta}. \qquad (3.4)$$

In this formula the superscript m means the number of the "input" point. The fixation of the "input" point does not permit determining the number of the mode unambiguously; therefore, we must use qualitative results concerning the dynamics of the eigen-values as obtained in the preceding section in order to compare the number m of some mode in this case. These results show that the eigen-value of the m-th and the m + 1-th modes can be in the neighborhood of a given "input" point, with number m depending on the argument of the surface impedance δ. Thus, for $\arg\delta > -39°$, the eigen-value of the zero mode is in the neighborhood of the "input" point with m = 0. However, if $\arg\delta < -39°$, then we find the eigen-value of the first mode, while the eigen-value of the zero mode is far removed from this "input" point and goes to infinity of $\beta \to \infty$. An analogous situation also takes place for other "input" points. We can find from (2.19) that m = 1 in (3.4) relates to the first mode for $\arg\delta > -16°$ and to the second mode for $\arg\delta < -16°$; in this regard, the eigen-value of the first mode tends toward infinity for $\beta \to \infty$ in the range of $-39° < \arg\delta < -16°$, i.e., the first mode does not have a finite "input" point, etc. /5

We should mention that, when the eigen-value of some mode does not have a finite "input" point, it is difficult to construct simple analytical formulas. However, this case is not of interest from the practical point of view, since the attenuation of the corresponding mode is great in this regard, and it can simply be disregarded in calculations of the field. The exception is the zero mode for purely inductive surface impedance of the upper wall of the waveguide.

Let us now turn to the results for eigen-values obtained with the aid of the method of instances. We will begin with the study of a one-dimensional approximation of the operator K^m, i.e.,

$$K_1^m = E_1 K^m E_1,$$

where E_1 is the projector onto space with basis vector of (3.1). In the case of a one-dimensional approximation the schemes of the method of instances and the Galerkin method coincide.

Going by the scheme presented in Section 1, simple but rather cumbersome calculation, it is easy to find the following formulas:

(a) Case of "small" $|\delta\beta|$

$$\sqrt{\mu_{1,0}^{0}}\beta=\sqrt{\frac{-i\delta\beta}{1-\frac{i\delta\beta}{3}}} \tag{3.5}$$

- for the zero mode,

$$\sqrt{\mu_{1,0}^{m}}\beta=m\pi\sqrt{1-\frac{4i\delta\beta}{2(m\pi)^2-i\delta\beta}} \tag{3.6}$$

- for the m-th mode;

(b) Case of "large" $|\delta\beta|$

$$\sqrt{\mu_{1,\infty}^{m}}\beta=\frac{2m+1}{2}\pi\sqrt{1-\frac{4}{3-2i\delta\beta}} \tag{3.7}$$

In (3.5)-(3.7) the branches of the roots were fixed by the following condition for the sake of definiteness:

$$\operatorname{Im}\sqrt{\mu_1^m}\beta\leqslant 0.$$

A very simple evaluation of the accuracy for the expressions obtained with (3.5)-(3.7) can be carried out for purely imaginary values of the surface impedance. In this case, the operator K^m becomes self-conjugate, and it is possible to make two-sided evaluations of the eigen-values [4]. The estimate below of the eigen-value is given by the following inequality:

$$\left|\sqrt{\mu_1^m}\right|\beta>\left\{\int_0^\beta\int_0^\beta |K^m(x,y)|^2\,dxdy\right\}^{-\frac{1}{4}}$$

As is well known, (3.5)-(3.7) give increased (in modulus) values of the eigen-values in this case. Having made the corresponding /54

calculations for the zero mode and the "small" $|\delta\beta|$, we can obtain the following two-sided estimate of the eigen-value of zero mode:

$$\sqrt{\frac{|\delta|\beta}{1\pm\frac{|\delta|\beta}{3}}} < |\sqrt{\mu_1^0}|\beta > \sqrt{\frac{|\delta|\beta}{1\pm\frac{2|\delta|\beta}{3}+\frac{2}{3}(|\delta|\beta)^2}}, \qquad (3.8)$$

where Re $\delta = 0$, while the "+" and "-" signs relate to Im $\delta > 0$ and Im $\delta < 0$ respectively, and in the first case $|\sqrt{\mu_0^1}| = \sqrt{\mu_1^0}$, while in the second $|\sqrt{\mu_1^0} = i\sqrt{\mu_1^0}$.

Using (3.8), we can evaluate the values of $\delta\beta$ for which (3.5) is valied with a certain given accuracy, assuming that the precise value of the eigen-value is in the middle between the boundaries given by the inequality in (3.8). For example, if we are interested in the values of $\delta\beta$ for which the error in (3.5) does not exceed 10%, then these values lie within the following interval, according to (3.8):

$$-5{,}5 < i\delta\beta < 1{,}1 \ (\mathrm{Re}\,\delta = 0). \qquad (3.9)$$

The results of a comparison of the eigen-values given by (3.5) and the values obtained as a result of numerical solutions to (2.1) are given in Table 1.

TABLE 1

$i\delta\beta$	$\lvert\sqrt{\mu^0}\rvert\beta_{\text{precise}}$	$\lvert\sqrt{\mu^0_{1,0}}\rvert\beta$	Error %
$-\infty$	1,571	1,732	10
−4	1,265	1,309	3
−2	1,077	1,095	2
−1	0,860	0,866	0,7
1	1,200	1,225	2
1,5	1,630	1,730	6
1,7	1,80	1,98	10
1,8	1,89	2,12	12
2	2,07	2,45	18
3	3,015	∞	∞

A comparison of the two-sided estimates of (3.9) and the results of numerical calculations (Table 1) shows that the inequality in (3.9) gives somewhat decreased limits to the applicability of (3.5); the precise limits to applicability (for relative error no greater than 10%) in (3.5) are determined by the following conditions:

$$-\infty < i\delta\beta < 1.7 \quad (\mathrm{Re}\,\delta = 0), \tag{3.10}$$

i.e., are very broad.

We can evaluate the limits to applicability of (3.6) in the case/55 of "small" $|\delta\beta|$ for the m-th mode at Re δ = 0 in a similar way. The two-sided estimates in this case have the following form:

$$m\pi\sqrt{1-\frac{4i\delta\beta}{2(m\pi)^2-i\delta\beta}} > \sqrt{\mu_1^m\beta} > \\ > m\pi\sqrt{1-\frac{2i\delta\beta}{m^2\pi^2\left(1-\frac{i\delta\beta}{(m\pi)^2}+\frac{(i\delta\beta)^2}{(m\pi)^2}\right)}} \tag{3.11}$$

Let us now stipulate that the difference between the precise values of $\sqrt{\mu_1^0\beta}$, which we will consider halfway between the limits given by (3.11) as before, and the approximate value given by (3.6) must not exceed 0.1.[2] Using (3.11), we can then obtain the following limitation on $\delta\beta$ for m $\geq$ 2:

$$|\delta|\beta < 0.6(m\pi)^{4/3} \quad (\mathrm{Re}\,\delta = 0). \tag{3.12}$$

As for the first mode, it is more convenient to evaluate the accuracy in (3.6) for it by a direct comparison of the precise values of $\sqrt{\mu^1\beta}$ found numerically and the approximate values obtained with the aid of this formula. The result of such a comparison is given in Table 2.

TABLE 2

$i\delta\beta$	$\sqrt{\mu^1\beta}$ precise	$\sqrt{\mu_{1,0}^1\beta}$
$-\infty$	4,71	7
−10	4,39	4,81
− 4	4,03	4,06
− 2	3,66	3,67
− 1	3,42	3,42
1	2,80	2,78
2	2,16	2,32
3	2,20	1,67

[2] In examining the m-th mode it is not necessary to find the relative error, since the relative error tends to vanish with an increase in the number m, as seen from the inequality in (3.11).

It follows from Table 2 that, on the condition that

$$-5 \leqslant \delta\beta \leqslant 1{,}7 \quad (\mathrm{Re}\,\delta = 0)$$

the difference between the approximative and precise results does not exceed 0.1.

The estimates given for the approximating formulas in (3.5) and (3.6) for "small" $|\delta\beta|$ show that they describe the behavior of the eigen-values rather well for Re δ = 0, all the way to values of $|\delta\beta|$ which exceed unity. We can expect that this conclusion will also be valid for Re $\delta \neq 0$.

We were speaking above of the accuracy in formulas (3.5) and (3.6) for "small" $|\delta\beta|$. The accuracy of (3.7) for "large" $|\delta\beta|$ at Re δ = 0 can be examined in a similar way. We will limit ourselves here to an investigation of (3.7) for m = 1 in the case of Re δ = 0. For Im $\delta > 0$, (3.7) gives the eigen-value of the zero mode, and for Im $\delta < 0$, it gives that of the first mode. Tables 3 and 4 show the precise and approximate figures of the eigen-values of the zero and first modes, as well as the eigen-values obtained by (3.5) and (3.6) for "small" $|\delta\beta|$, for the sake of a comparison. /56

TABLE 3

$\delta\beta$	$\sqrt{\mu^0}\beta$ precise	$\sqrt{\mu^0_{1,\infty}}\beta$	$\sqrt{\mu^0_{1,0}}\beta$
−1	0,860	0,703	0,866
−2	1,077	1,020	1,095
−4	1,265	1,254	1,309
−∞	1,571	1,571	1,732

TABLE 4

$\delta\beta$	$\sqrt{\mu^1}\beta$ precise	$\sqrt{\mu^0_{1,\infty}}\beta$	$\sqrt{\mu^1_{1,0}}\beta$
2	2,46	3,50	2,32
3	2,20	2,71	1,67
4	2,05	2,10	—
6	1,88	1,89	—
∞	1,57	1,57	—

It can be seen from Table 3 that, in the case of capacitive surface impedance, the ranges of applicability for (3.5) and (3.7) are superposed rather well, and their combined usage [for $|\delta\beta| < 3$, Formula (3.5); for $|\delta\beta| > 3$, Formula (3.7)] leads to a result which differs by no more than 3% from the precise value. For inductive surface impedance, the matter is somewhat different, as follows from Table 4. Formula (3.7) for m = 1 gives the eigen-value of the first mode differing from the precise one by no more than 0.1 at $|\delta\beta| > 4$, while (3.6) is applicable for the same accuracy at $|\delta\beta| < 1.7$.

Having finished an analysis of the elementary formulas corresponding to the one-dimensional approximation, it is interesting to find the regions on the plane $(\delta\beta)$ in which the formulas for the "small" and "large" $|\delta\beta|$ superpose with given accuracy. These regions are depicted in Figure 8 for the zero mode. In region I, the relationship between the modulus of the difference in eigen-values /57 given by (3.5) and (3.7) and the modulus of one of them does not exceed 10%, and in the region II, it does not exceed 7%.

Thus, in the case of capacitive surface impedances the simplest formulas guarantee accuracy which is sufficient for qualitative investigations, and they make it possible to find the eigen-values for practically any $|\delta\beta|$. However, for inductive surface impedances the range of applicability of the simplest approximating formulas is narrower. This is connected with the possible arisal of degeneration of the spectrum for inductive impedance. In order to describe this phenomenon, as well as to clarify the limits to applicability of (3.5)-(3.7) further, it is necessary to examine the following, second approximation, using the method of instances.

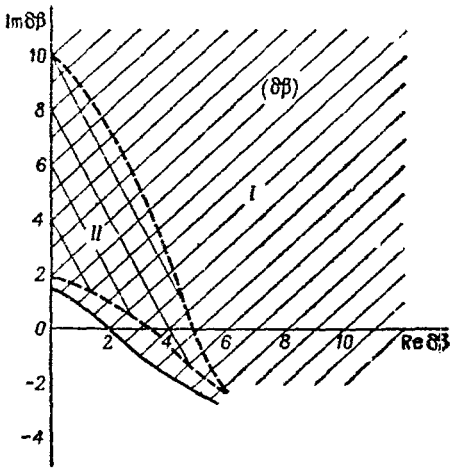

Fig. 8

We will illustrate the second approximation with the example of the "center" of $\mu_0^m = \mu_0^\circ = 0$, and the selection of that center will lead us to the approximative formulas for the eigen-values of the zero and first modes in the case of "small" $|\delta\beta|$. In order to obtain the second approximation, we will use the two-dimensional approximation of the operator K°

$$K_2^\circ = E_2 K^\circ E_2,$$

where E_2 is the projector onto space given by the basis vectors

$$z_0^\circ = 1,\ z_1^\circ = K^\circ z_0^\circ = \frac{x^2 - \beta^2}{2} + \frac{\beta^2}{i\delta\beta}.$$

As a result of elementary but cumbersome calculations, we can obtain the following formula:

$$\sqrt{\mu^{\circ}_{2,0}}\beta = \sqrt{\frac{1-\frac{3}{7}i\delta\beta-\sqrt{1-\frac{10}{21}i\delta\beta-\frac{107}{735}\delta^2\beta^2}}{\frac{4}{21}\left(1-\frac{1}{10}i\delta\beta\right)}} \qquad (3.13)$$

The branch of the outer radical is fixed as before by the condition $\operatorname{Im}\sqrt{\mu^{\circ}_{2,0}} \leq 0$. As for the inner radical, we will introduce a two-/58 sheeted Riemann surface for its uniformization, and, from the branching point

$$(i\delta\beta)_b = 1{,}64 + i2{,}05\ ^{3} \qquad (3.14)$$

we will plot on the plane $(i\delta\beta)$ a break to infinity along the continuation of the line coming from the origin of the coordinates (Fig. 9). We will call the upper sheet of the Riemann surface that sheet on which the inner radical acquires the values of +1 at the origin of the coordinates. In this case, the real and imaginary parts of the radical on the upper sheet have signs as shown in Figure 9. Obviously, on the lower sheet, all the signs are the inverse.

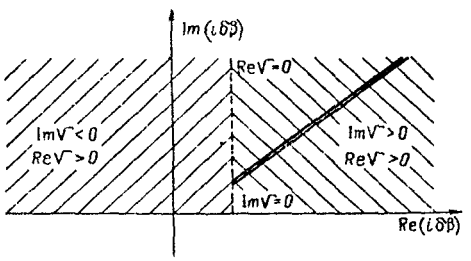

Fig. 9

For such a fixation of the branches of the inner radical in (3.13), the upper sheet of the Riemann surface corresponds to the eigen-values of the zero mode, while the lower sheet corresponds to those of the first mode. Actually, for $\beta \to 0$ we have

$$\sqrt{\mu^{\circ}_{2,0}}\beta \simeq \sqrt{\frac{-i\delta\beta}{1-\frac{i\delta\beta}{3}}} \to 0$$

on the upper sheet and

$$\sqrt{\mu^{\circ}_{2,0}}\beta \simeq \sqrt{\frac{21}{2}}\left[1+\frac{21}{90}(i\delta\beta)^2\right]^{-\frac{1}{2}} \to 3{,}24$$

---

[3] The inner radical in (3.13) has a second branching point which is complex-conjugate with (3.14); however, we will not examine it, since the upper half-plane of the plane $(i\delta\beta)$ corresponds to physically practicable structures.

on the lower sheet, which corresponds to the "output" points of the zero and first modes (o and π, respectively).

Obviously, the branching point of (3.14) corresponds to the case of degeneracy, i.e., coincidence of the eigen-values of the first and zero modes. At the branching point of (3.14), $|\delta\beta| \approx 2.64$ and $\arg\delta \approx -38°40'$, which coincides well with the results obtained in Section 2 of this study by the numerical method. This coincidence shows that (3.13) of second approximation describes the behavior of the eigen-values of the zero and first modes with a high degree of accuracy for any arguments of the surface impedance all the way to /59 $|\delta\beta| \sim 3$, including the phenomenon of degeneracy of the zero and first modes. Moreover, we should mention that (3.13) gives numbers for the eigen-value of the zero mode for $\arg\delta > -38°40'$ and the first mode for $\arg\delta < -38°40'$ for $|\delta\beta| \to \infty$, which differ from the precise value ($\pi/2$) by 0.6%.

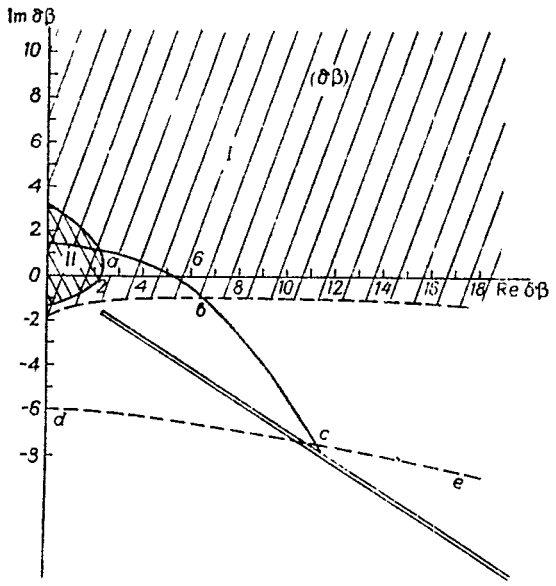

Fig. 10

As we already mentioned in the preceding section, there was a discussion between Wait and Budden concerning the numeration of modes and, particularly, the following question: is the zero or the first mode the principal one in the range of superlong waves? (Budden considered that the zero mode was the basic one, and Wait considered it to be the first mode.) Using (3.13) and keeping the numeration of modes we introduced, we can find an answer to this question. A rather simple analysis of (3.13) shows that the mutual role of the zero and first modes depends on what ratio between the conductivity of the ionosphere σ and the following value is found:

$$\sigma_{cr}\left[\frac{1}{\text{Ohm}\cdot\text{m}}\right] \simeq \frac{0{,}14\,(\varepsilon_m+1)^2}{h\,[\text{km}]}.$$

If $\sigma > \sigma_{cr}$, then the first mode (in our numeration) plays the principal role in the range of superlong waves, and if $\sigma < \sigma_{cr}$, it is the zero mode. The zero mode is then the principal one under the /60 diurnal conditions for propagation ($h \simeq 70$km, $\sigma_{cr} = 8\cdot10^{-6}$ $\frac{1}{\text{Ohm}\cdot\text{m}}$), $\sigma = 2\cdot10^{-6}$ $\frac{1}{\text{Ohm}\cdot\text{m}}$), and the first mode is principal under the nocturnal conditions ($h \approx 90$ km, $\sigma_{cr} = 6\cdot10^{-6}$ $\frac{1}{\text{Ohm}\cdot\text{m}}$, $\sigma = 8\cdot10^{-6}$ $\frac{1}{\text{Ohm}\cdot\text{m}}$).

In concluding this section, we will touch briefly on an evaluation of the limits to practicability of the first-approximation

formulas (3.5) and (3.7) for the zero mode with the aid of the second-approximation formula in (3.13). Figure 10 shows regions I and II in which the difference between results given by (3.5) and (3.13) does not exceed 10 and 5%, respectively. As for (3.7), the results obtained with it differ from those obtained according to (3.13) by no more than 10% in the range above and to the right of the line abc on Figure 10. In the same figure, the region where the error in the second-approximation formula does not exceed 10% is found above the line dce.

Thus, as has been shown in this section, the method of instances permits us to obtain rather simple analytical expressions for the eigen-values of the transverse differential operator with relatively wide limits to applicability. These expressions can be used for a qualitative study of the principal rules for the structure of the electromagnetic field in plane impedance waveguides.

Section 4. Discussion of Some Qualitative Rules for the Structure of the Field in Plane Impedance Waveguides

In this section we will discuss some rules for the behavior of the electromagnetic field in plane impedance waveguides; the rules will follow from the topological characteristics of the behavior of the eigen-values examined above and the simple analytical formulas of the preceding section.

Of all the laws of general order, we should mention the phenomenon of degeneration discussed above. It consists of a situation where some two modes, all of whose properties coincide, exist for certain parameters of the waveguides defined by (3.14) and (2.19). If the degenerate modes are the principal ones in this case (and this can take place if the modes with small numbers degenerate), then the instability phenomenon characteristic of the degenerated state can arise; the instability phenomenon consists in the elimination of degeneration with small disturbance of the properties of the wall (or frequency), and two modes with close properties exist in the waveguide. If in this case the disturbance of the boundary conditions is such that the wave attenuations are identical, while the velocities differ, then an interference picture arises and points are found where the field produced by these modes can vanish. In order to evaluate this effect, we will consider a case close to degeneration for the zero and first modes, so that the parameters are defined by the following formula: /61

$$i\delta\beta = i(\delta\beta)_0 + \Delta\eta, \qquad (4.1)$$

where $(\delta\beta)_0 = 2.05 - i1.64$. The magnitude of the disturbance is determined by the complex number $\Delta\eta$, and

$$|\Delta\eta| \ll 1. \qquad (4.2)$$

The nature of propagation of the modes is determined, as is well known, by the function exp ($iK_m r$), where K_m is the constant of propagation of the m-th mode, i.e.,

$$K_m \equiv k\sqrt{1-\mu^m}.$$

Having substituted (4.1) into (3.13) and having used (4.2), for the case of

$$\beta > 2{,}5$$

we can obtain the following simple formulas for the constant of propagation of the zero and first modes, which are valid in the neighborhood of the degeneration point:

$$K_{0,1} \simeq k\left[1 + \frac{1}{\beta^2}(-1{,}5 + i\ 2{,}4) \pm \frac{2{,}3}{\beta^2}\sqrt{\Delta\eta}\, e^{i\varphi_0}\right],$$
$$\varphi_0 \simeq 59^\circ$$

If arg $\Delta\eta$ = -118°, then the attenuations of both modes are equal for such disturbance of the boundary conditions, and, assuming that their coefficients of excitation have not changed greatly, we can find that the modulus of their summary field is proportional to the following value:

$$e^{-\frac{2{,}4}{\beta}\cdot\frac{z}{h}} \cos\left(\frac{2{,}3}{\beta}\cdot\frac{z}{h}\left|\sqrt{\Delta\eta}\right|\right).$$

Thus, as the result of the disturbance of $\Delta\eta$ at a distance from the source of

$$r \simeq \frac{0{,}7h\sqrt{\beta}}{\sqrt{|\Delta\delta|}}$$

the field produced by the zero and first modes vanishes.

Another interesting effect is the attenuation of waves at $|\delta\beta| \to \infty$. It follows from the general picture for the movement of the eigen-values (Section 2) that all the eigen-values except perhaps one tend toward some real "input" point. A more detailed analysis shows that in this case and with $\mathrm{Im}K_m \to 0$[4] (the modes are propagated without losses). However, if $\mathrm{Im}\,\delta < 0$, then there is always a mode for which the "input" point is at infinity. The attenuation of this mode tends toward infinity in this limit transition.[5] As has already been mentioned, this situation arises for the zero mode at /62

$$90^\circ < \arg\delta < -39^\circ,$$

and for the first mode at

$$-16^\circ < \arg\delta < -12^\circ$$

and so forth, see (2.19).

Together with the general rules mentioned above, it is of interest to discuss the properties of the zero mode in more detail, since it is the principal one in problems of the propagation of superlong waves in a waveguide channel. For it,

$$K_0 = k\sqrt{1+\frac{i\delta\beta}{\beta^2\left(1-\frac{i\delta\beta}{3}\right)}} \qquad (4.3)$$

We should mention that if $\delta = i|\delta|$, then a boundary frequency equal to the following arises for the zero mode:

$$\omega_{rp} = \frac{c}{h}\left[\sqrt{\frac{2{,}25}{|\delta|^2}+3} - \frac{1{,}5}{|\delta|}\right]$$

---

[4] If the frequency exceeds the critical one in this regard.

5 The exception is the zero mode at $\delta = -i|\delta|$. If in this case $|\delta| \to \infty$, then the field is concentrated around the upper wall, while the phase velocity tends to vanish.

In the future, in order to obtain simpler and clearer results, we will consider that

$$\frac{|\delta|}{\beta}\cdot\frac{1}{\left|1-\frac{i\delta\beta}{3}\right|}<1. \tag{4.4}$$

We will then obtain the following from (4.3):

$$K_0\simeq k+\frac{1}{2h}\cdot\frac{i\delta}{1-\frac{i\delta\beta}{3}} \tag{4.5}$$

Let us explain the problem of the phase velocity of the zero mode. The latter is equal to the speed of light if

$$\mathrm{Re}\frac{i\delta\beta}{1-\frac{i\delta\beta}{3}}=0,$$

i.e., the real and imaginary parts of $\delta\beta$ should satisfy the following equation:

$$(\delta'\beta)^2+\left(\delta''\beta+\frac{3}{2}\right)^2=\left(\frac{3}{2}\right)^2,$$

where $\delta = \delta' + i\delta''$.

Thus, $v_{ph} = c$ on the plane $(\delta\beta)$ has the form of a semi-circle with center at the point $\mathrm{Im}\,\delta\beta = -\frac{3}{2}$ and radium $\frac{3}{2}$ (Fig. 11). However, only its initial region, the size of which is determined by the condition in (4.4) and the limits to applicability of (3.5), can be given physical significance. /63

Let us turn to an analysis of the attenuation of the zero mode. Using (4.5), it is easy to find the following formula:

$$\mathrm{Im}\,K_0\approx\frac{1}{2h}\cdot\frac{|\delta|\cos\varphi}{1+\frac{2}{3}|\delta|\beta\sin\varphi+\frac{|\delta|^2\beta^2}{9}},$$

where $\phi = \arg \delta$.

Having considered the dependence of Im K_0 on $|\delta|$, it is easy to see that at

$$|\delta| = \frac{3}{\beta}$$

the attenuation is maximum and equal to

$$(\mathrm{Im}\, K_0)_{\max} = \frac{3}{4\beta h} \cdot \frac{\cos\varphi}{1+\sin\varphi},$$

i.e., the losses are greater for inductive surfaces than for capacitive ones.

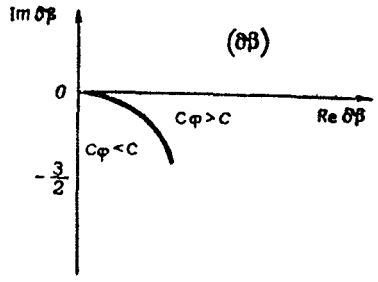

Fig. 11.

If we consider that δ does not depend on the frequency, it is found that the frequency at which attenuation is maximum is determined by the following formula:

$$\omega_{\max} = -\frac{3c}{|\delta| h}\sin\varphi,$$

$$(\mathrm{Im}\, K_0)_{\max} = \frac{1}{2h} \cdot \frac{|\delta|}{\cos\varphi}.$$

This means that the extremal point in the particular dependence of attenuation of the zero mode is found only in the case of inductive grounds. In the case of capacitive surfaces and $\omega > \omega_{gr}$, the attenuation decreases monotonously with an increase in frequency.

A consideration of the frequency dependence of δ is of somewhat greater interest for some specific model of the medium. For example, let us consider the simplest case, considering that a homogeneous conducting half-space forms the upper boundary of the waveguide, the conductivity currents in which greatly exceed the displacement currents (this corresponds roughly to a model of the ionosphere for low frequencies). Then

$$|\delta| = \gamma_0 \sqrt{\beta}, \quad \gamma_0 \equiv \sqrt{\frac{\varepsilon_0 c}{\sigma h}}, \quad \varphi = -\frac{\pi}{4}$$

and it is found that attenuation is maximum at a frequency of

$$\omega_{max} = \frac{c}{h} \cdot \frac{1,7}{\sqrt[3]{\gamma_0}}, \qquad (4.6)$$

In this case, /64

$$(\mathrm{Im}\, K_0)_{max} \approx \frac{1,45\gamma_0^{5,6}}{h}$$

Having substituted the parameters characteristic of the D layer of the ionosphere $\sigma \approx 10^{-6} \frac{1}{\mathrm{Ohm \cdot m}}$, h ≈ 60 km into (4.6), we find that the attenuation is maximum for frequency of f = 3.6 KHz, which corresponds roughly to the experimental data. For this frequency $(\mathrm{Im}K_0)_{max} \approx \frac{0.3}{h}$.

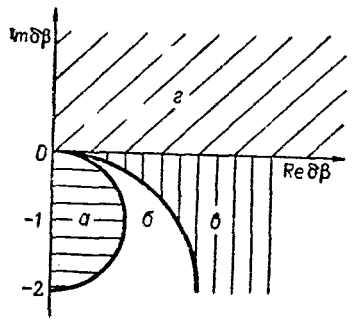

Fig. 12.

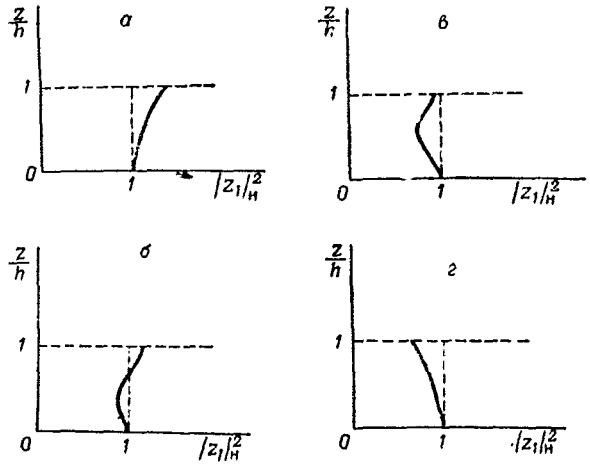

Fig. 13.

Let us turn now to a study of the structure of the field in a cross section. For the characteristic element of the zero mode, we will take the function z_1^0 as the initial approximation (see Section 3). We will study its modulus, numbering it so that on the surface x = 0

$$|z_1^0|_{x=0} = 1,$$

Then

$$|z_{1H}^{0}|^2 = \frac{\frac{1}{4}\left(1-\frac{x^2}{\beta^2}\right)^2 + \left(1-\frac{x^2}{\beta^2}\right)\frac{\delta''\beta}{|\delta\beta|^2} + \frac{1}{|\delta\beta|^2}}{\frac{1}{4} + \frac{\delta''\beta}{|\delta\beta|^2} + \frac{1}{|\delta\beta|^2}}$$

We will examine the complex plane ($\delta\beta$) and draw on it two semi- /6
circles: one with center of Re $\delta\beta$ = 0, Im $\delta\beta$ = -2 and radius equal to 2, and the second with center of Re $\delta\beta$ = 0, Im $\delta\beta$ = -1 and radius equal to 1, as shown in Figure 12. As a result, the complex plane ($\delta\beta$) divided into a number of regions - regions a, b, c and d. Depending on where the point characterizing the properties of the upper wall of the waveguide is found on the complex plane ($\delta\beta$), we will find the following structures of the fields in cross section (Fig. 13). For region a, the field increases monotonously in approaching the upper wall. For region b, the field at the upper wall is greater than that at the lower wall, but its change with a change in height is not monotonous. For region c, the field at the upper wall is less than that at the lower wall, but, as in Case b, the change in field with height is not monotonous. Finally, for region d, the field decreases monotonously with the height.

FINDING COMPLEX EIGEN-VALUES OF SOME BOUNDARY-VALUE PROBLEMS BY THE METHOD OF ANALYTICAL EXTENSION OF FUNCTIONS WITH A REAL AXIS ONTO THE COMPLEX RANGE OF THE ARGUMENT. APPLYING THE METHOD TO PROBLEMS OF SUPER-LONG WAVE PROPAGATION, WITH A CONSIDERATION OF THE EARTH'S MAGNETIC FIELD

G.F. Remenets

ABSTRACT: The author shows how difficulties encountered in applying some results of the theory of super-long wave propagation based on the apparatus of boundary-value problems are overcome with the aid of an approach based on an analytical continuation of the functions with a real axis of the argument into a complex range of regularity. Particular emphasis is given to the "correctness" of algorithms in the computational sense.

Section 1. Mathematical Formulation of the Problem

Practical applications of some results of the theory of super- /66
long wave propagation based on the apparatus of boundary-value problems are connected with great computational difficulties. These difficulties are generated by the complexity of calculations of special functions in the complex range of parameters and the arguments.

The computational problem was greatly simplified when the approach to it was changed. One approach, which was based on the variation method of instances [1] and which did not use a digital computer, was discussed in [2]. Our approach is based on an analytical continuation of the functions with real axis of the argument into a complex range of regularity. In this study we will discuss this approach in connection with the fact that it has made our ideas about the so-called correct and incorrect problems of mathematical physics more concrete, has decreased the requisite machine time by 2-3 orders in comparison to the old methods for calculations, and has aided in solving a group of numerical problems which had not been solved before because of the complexity of calculations.

Let us consider the following three boundary-value problems applied to a model of super-long wave propagation in three waveguides, respectively:

(a) In a plane waveguide with incidence boundary conditions on the walls "air-earth" and "air-ionosphere", i.e.,

$$\frac{d^2U}{dx^2}+k^2\cos^2\psi U=0,$$
$$\left.\frac{dU}{dx}\right|_{x_1}=-i\Delta_1 U,\quad \left.\frac{dU}{dx}\right|_{x_2}=+i\Delta_2 U, \tag{1.1}$$

(b) In a spherical waveguide with scalar impedance boundary conditions on the walls "air-earth" and "air-ionsophere", i.e.,

$$\frac{d^2U}{dr^2}+\left(k^2-\frac{\nu^2-\frac{1}{4}}{r^2}\right)U=0,$$
$$\left.\frac{dU}{dr}\right|_{r_1}=-i\delta_1 U, \tag{1.2}$$
$$\left.\frac{dU}{dr}\right|_{r_2}=+i\delta_2 U;$$

/67

(c) In a spherical waveguide with scalar impedance boundary conditions at the "air-earth" boundary and matrix impedance boundary conditions at the "air-ionosphere" boundary; matrix boundary conditions arise as a result of a consideration of the anisotropy of the ionosphere, which appears as an effect of the Earth's magnetic field [3], i.e.,

$$\left(\frac{d^2}{dr^2}+\frac{1}{r}\cdot\frac{d}{dr}+k^2-\frac{\nu^2}{r^2}\right)\begin{bmatrix}U\\ \widetilde{V}\end{bmatrix}=0,$$
$$\frac{d}{dx}\begin{bmatrix}xU\\ x\widetilde{V}\end{bmatrix}_{x=kr_1}=\begin{bmatrix}-i\Delta_g, & 0\\ 0, & i\Delta_g^{-1}\end{bmatrix}\begin{bmatrix}xU\\ x\widetilde{V}\end{bmatrix}, \tag{1.3}$$
$$\begin{bmatrix}\frac{d}{dx}, & 0\\ 0, & i\end{bmatrix}\begin{bmatrix}xU\\ x\widetilde{V}\end{bmatrix}_{x=kr_2}=\begin{bmatrix}\Delta_{11}, & \Delta_{12}\\ \Delta_{21}, & \Delta_{22}\end{bmatrix}\begin{bmatrix}\frac{d}{dx}, & 0\\ 0, & i\end{bmatrix}\begin{bmatrix}x\widetilde{V}\\ xU\end{bmatrix},$$

where $\widetilde{V} = V\cdot 120\pi$; k is the wave number; Δ_1, Δ_2, Δg, δ_1, δ_2, $\Delta i,k$ (i,k = 1, 2) are complex constants in the general case; U and V are certain scalar values by which the components of the intensity of the electric and magnetic fields in the waveguide are expressed; x and r are scalar variables.

The eigen-values for the boundary-value problems of (1.1), (1.2) and (1.3) are found from three characteristic equations:

$$1-R_{v1}R_{v2}e^{+2ik(x_2-x_1)\cos\psi}=0; \tag{1.1a}$$

$$1-\tilde{R}_{v1}\tilde{R}_{v2}I=0; \tag{1.2a}$$

$$\left(1-{}_{\parallel}R_{\parallel}\tilde{R}_{v}I\right)\left(1-{}_{\perp}R_{\perp}R_{h}I\right)-{}_{\parallel}R_{\perp}\,{}_{\perp}R_{\parallel}\tilde{R}_{v}\tilde{R}_{h}I^{2}=0, \tag{1.3a}$$

where ψ is the angle of incidence of the wave at the boundary of the division; R_{v1} and R_{v2} are the coefficients of reflection of a plane vertically-polarized wave from the first and second plane boundaries; $\tilde{R}_{v1}$ and $\tilde{R}_{v2}$ are the reflection coefficients of a spherical vertically-polarized wave from the first and second spherical boundaries; $\tilde{R}_{v}$ and $\tilde{R}_{h}$ are the coefficients of reflection of vertically and horizontally polarized spherical waves from the first spherical boundary "Earth-air"; ${}_{\parallel}R_{\parallel}$, ${}_{\perp}R_{\perp}$, ${}_{\perp}R_{\parallel}$ and ${}_{\parallel}R_{\perp}$ are four coefficients of reflection of plane waves from the plane boundary "air-anisotropic ionosphere, non-uniform in electron concentration $N(r)$ and number of collisions $\nu(r)$" [5]; I is a combination of Han- /68
kel functions, i.e.,

$$I=\frac{H_{\nu}^{(2)}(kr_1)H_{\nu}^{(1)}(kr_2)}{H_{\nu}^{(1)}(kr_1)H_{\nu}^{(2)}(kr_2)}$$

The argument of (1.1a) is the angle of incidence of the wave at the boundary ψ. The argument of Equations (1.2a) and (1.3a) is the index of the cylindrical functions ν, which is connected asymptotically with the angle of incidence of the wave at the boundary of the division by the following equation [3]:

$$\nu=kr_2\sin\psi.$$

All further discussions will be directed toward a construction of an algorithm for the solution to (1.1a), (1.2a) and (1.3a).

Section 2. Incorrectness of the Problems of Mathematical Physics According to Adamar

An understanding of classical correctness in problems of mathematical physics was given by Adamar at the beginning of this century In modern functional language, it can be defined [6] as the practicability, for the equation

$$\begin{gathered}A\varphi=f,\\ \varphi\in\Phi,\\ f\in F\end{gathered} \tag{2.1}$$

of three conditions:

(1) There is a solution to (2.1) for any $\underline{f} \in \underline{F}$;

(2) The solution to (2.1) is unique in Φ;

(3) The solution to (2.1) depends continuously on the right-hand part of $\underline{f}$.

Here Φ and $\underline{F}$ are complete metric functional spaces, for example $\underline{C}^1$ or $\underline{L}_p$ or $\underline{W}_p^1$, while $\underline{A}\phi$ is a function with range of defintion of $\Phi' \subset \Phi$ and with range of values of $\underline{F}' \subset \underline{F}$.

In other words, condition (3) means that case when infinitely small variations in the solution correspond to infinitely small variations in the right-hand part of $\underline{f}$. The variations change by the distance function of that space from which the elements are drawn.

The problem for which the condition of continuity of (3) is not fulfilled in any of the spaces $\underline{C}^1$, $\underline{L}_p$, $\underline{W}_2^1$ is the following Cauchy problem presented by Adamar for Laplace equations [7]:

$$\begin{gathered}\frac{\partial^2 U}{\partial x^2}+\frac{\partial^2 U}{\partial y^2}=0, \quad -\frac{\pi}{2}\leqslant x\leqslant\frac{\pi}{2},\\ U|_{x=-\frac{\pi}{2}}=U|_{x=\frac{\pi}{2}}=U|_{y=0}=0,\\ \frac{\partial U}{\partial y}\Big|_{y=0}=e^{-\sqrt{n}}\cos nx.\end{gathered} \tag{2.2a}$$

It can be seen from a solution to this problem, i.e., /69

$$U=\frac{1}{n}\,e^{-\sqrt{n}}\cos nx\,\mathrm{sh}\,(ny) \tag{2.2b}$$

that in any of the enumerated spaces there are always those elements which are as great as desired in moving into the range $\underline{y} \neq 0$, despite their values on the $\underline{x}$ axis, which are as low as desired.

For the calculator, the incorrectness means the following according to Adamar. An arbitrarily small error in the initial data for the problem can add to the solution elements which increase more rapidly in the process of computations than does the sought-for solution, and then the relative error increases rapidly. We will show that this danger can be avoided in the computational problems we have investigated.

Section 3. Determining the Computational Correctness of the Algorithm

Let us define the computational correctness. We will call a computational algorithm correct if the ratio between the disturbance and the element itself decreases or remains unchanged during the calculation process, and we will call it incorrect if this condition is not fulfilled. Numerical integration of an ordinary linear differential equation of second order in the range of exponential changes in the solutions is an example of a correct and incorrect procedure, depending on what particular solution is required. If we calculate an exponentially decreasing solution, then the error in the initial data generates a second linearly independent solution, which increases exponentially. Therefore, the relative error increases exponentially in the process of calculation, and this procedure is incorrect in the computational sense. If we calculate an exponentially increasing solution, then the error in the initial data generates two supplements to the solution - both exponentially increasing and exponentially decreasing. The first addition and the sought-for solution increase just as rapidly, and the relative error remains unchanged. This procedure is correct in the computational sense.

Similar examples can be taken from the practice of calculating special functions according to recurrence formulas [8] and a solution to ordinary differential equations of second order by asymptotic methods [9].

We should mention that, in the cited examples, the rate of increase in error does not depend on the relative value in the initial data, and is limited by the rate of increase of the general solution to the ordinary differential equation.

The essential difference between the two-dimensional Cauchy problem for the Laplace equation and the one-dimensional examples pre-/70
sented above is that the magnitude of the increase in absolute error does not depend on the solution, as follows from Adamar's idea of incorrectness, and is determined by the magnitude of an increase in elements introduced into the problem by an error in initial data. Therefore, if we can avoid elements which increase more rapidly than the solution in the process of constructing the algorithm, then we can find an algorithm which is correct in the computational sense. Consequently, in order to construct a correct computational procedure for a problem which is incorrect according to Adamar, we can approximate, for example, the initial data of the problem by elements from the set of functions with the same type of change as that which the unknown solution has, and we can construct an approximation of the latter from elements of this set. The set of functions described will be called correct in relation to the unknown solution.

As is well known, the problem of analytical extension of functions with a real axis into a complex range of the argument is equivalent to the Cauchy problem for the Laplace equation. Therefore, speaking of one of these problems, we will keep in mind the second one, its equivalent, without special clarifications.

In the following sections we will give numerical examples of a solution to problems which are incorrect according to Adamar and which are solved correctly in the computational sense. A set of Chebyshev polynomials [10] was taken as a correcting set. It can be seen from these examples that, when we solve a problem of analytical extension for functions of the polynomial type, the results are very good; when we solve a problem for functions which increase exponentially, the results are worse, but satisfactory in the neighborhood of the real axis. In order to improve the results of calculations in the second case, functions which increase exponentially in the complex range of the argument, for example the set sin $\underline{nx}$ and cos $\underline{nx}$, should be taken as the correcting set.

Since the computational recommendations presented above are of a qualitative nature, the computational correctness of any algorithm is established ultimately by numerical experiments.

Section 4. Analysis of a Computational Problem from Section 1

Let us turn to our problem of finding the first roots of Equations (1.1a), (1.2a) and (1.3a). In order to overcome the already-cited difficulties, we applied the following algorithm: according to the tables of values for the functions R_{v1}, R_{v2}, $\tilde{R}_{v1}$, $\tilde{R}_{v2}$, $\tilde{R}_{v}$, $\tilde{R}_{h}$, $||^{R}||$, $_{\perp}R_{\perp}$, $_{\perp}R_{||}$, $||^{R}_{\perp}$ and $\underline{I}$, we constructed approximating polynomials [11] on the real axis of the argument and used them in the complex range of the argument.

As a rather simple analysis shows, all these functions, except the last, preserve their numerical order (with the exception of the neighborhood of zeros and poles) in going from the real axis to the complex range of the argument. The latter function I is a function of exponential order.

The theory of approximation by rational functions in the complex range of the argument [12, 13] gives us the following proof. Let $\underline{p}_n(\underline{x})$ be an orthonormalized system of polynomials, and $\underline{f}(\underline{x})$ an analytical function which is regular in the segments (-1, +1), and let

$$f(x)=f_0p_0(x)+f_1p_1(x)+\ldots,$$
$$f_n=\int_{-1}^{1}f(x)\,p_n(x)\,dx \qquad (4.1)$$

be its expansion into a Fourier series. If R is the sum of semi-axes of the greatest ellipse with focuses at the point ± 1, in which $\underline{f}(\underline{x})$ is regular, then the Fourier series of (4.1) converges [to the sum $\underline{f}(\underline{x})$] inside and is arranged outside this ellipse. The convergence is uniform in each closed set inside the ellipse. Moreover,

$$\lim|f_n|^{-1/n}=R,\ n\to\infty, \qquad (4.2)$$

and if $\underline{p}_{\underline{n}}(\underline{x})$ are Chebyshev's polynomials, then we will have the best approximation in the sense of the least squares.

It follows from this theorem that the results of calculations according to the algorithm proposed will be satisfactory until we are sufficie. tly removed from the singularities of the functions.

In order to illustrate what we have said in the preceding sections, we will give results of calculations of the first roots of Equations (1.1a), (1.2a) and (1.3a) according tc the method described.

Section 5. Numerical Results

The results of a calculation of the first roots for Equation (1.1a) according to the algorithm described (second to eighth rows of the table) for $\underline{k}\,(\underline{x}_2 - \underline{x}_1) = 4$ are given in Table 1. In order to evaluate the effectiveness of the method, we had the first row contain the same root, but that found by direct calculation of the coefficients $R_{\underline{v}1}$ and $R_{\underline{v}2}$ in the complex range of the angle of incidence ψ of the wave of the boundary of the division according to the following formulas:

$$R_{vj}=\frac{\cos\psi-\omega_j}{\cos\psi+\Delta_j},\quad j=1,\ 2.$$

The constants $\Delta_{\underline{j}}$ were assumed to be equal to $0.1-\underline{i}0.1$. The second through eighth rows of the table differ from one another by the accuracy in approximation of the functions $R_{\underline{vj}}$ on the real axis (number of units, the step, the relative root-mean-square error in /72

the units). It can be seen from a comparison of the first and last rows that, in going from the real axis to the complex range at a distance of x one order with an interval for the functions $R_{\nu j}$ on the real axis, the method used guarantees accuracy up to the seventh sign (with nine significant digits on a digital computer).

Table 2 compares a calculation of the first eigen-value for (1.2a) for frequency $f = kc/2\pi = 4$ KHz, and $k(r_2 - r_1) = 5.36165$, by the direct method of [14] and the method of analytical extension of the functions $\tilde{R}_{\nu 1}$, $\tilde{R}_{\nu 2}$ and I, where

$$\tilde{R}_{\nu 1} = -\left[\frac{\ln' H_\nu^{(2)}(x) + \frac{1}{2x} + i\delta_1}{\ln' H_\nu^{(1)}(x) + \frac{1}{2x} + i\delta_1}\right]_{x=kr_1}; \qquad (5.1)$$

$$\tilde{R}_{\nu 2} = -\left[\frac{\ln' H_\nu^{(1)}(x) + \frac{1}{2x} - i\delta_2}{\ln' H_\nu^{(2)}(x) + \frac{1}{2x} - i\delta_2}\right]_{x=kr_2}; \qquad (5.2)$$

$$\delta_1 = (0{,}1530809 - i0{,}2122646)\,10^{-2},$$

$$\delta_2 = 0{,}754 - i0{,}214.$$

TABLE 1.

Re and Im Parts of the Eigen-Value of ψ, rad	Approximation Interval, rad	Number of Units	Step, rad	Mean-Square Error of Approximation, ε	Powers of Approximating Polynomials $\mathrm{Re}R_\nu$ and $\mathrm{Im}R_\nu$
0,76869269 +0,10756792	—	—	—	—	—
0,79 +0,12	0,6—1,6	6	0,2	10^{-1}	5, 5
0,7683 +0,109	0,6—1,6	11	0,1	10^{-5}	—
+0,76868 +0,10753	0,72—0,82	6	0,02	10^{-5}	3, 3
0,76868 +0,10753	0,72—0,82	11	0,01	10^{-5}	3, 3
0,768692 +0,107567	0,72—0,92	11	0,02	10^{-5}	5, 5
0,768698 +0,107566	0,70—0,87	34	0,005	10^{-5}	4, 4
0,76869262 +0,10756793	0,70—0,87	34	,005	10^{-6}	5, 4

TABLE 2.

Re and Im Parts of the Eigen-Value of ν	Re ν/kr_1 and Im ν/kr_1	Re ψ and Im ψ	Mean-Square Accuracy of Approxi-mation, ε	Tabulation by ν: Approxi-mation Interval	Step $\Delta\nu$	Number of Units	Power of Polynomials Approxi-mating the Re and Im Parts of the Functions: R_{v1}	R_{v2}	I	$I \times e^{i2k(r_2-r_1)} \frac{\nu}{kr_1}$
513,378 13,1637	0,962009 0,02466718	—	—	—	—	—	—	—	—	—
513,384 13,173	0,96202 0,024684	1,25186 0,077862	10^{-7}	501—520	1	20	10 9	8 6	10 10	—
513,379 13,1630	—	1,251850 0,0778015	10^{-8}	501—520	1	20	12 11	10 9	— —	10 10

TABLE 3.

Re and Im Parts of the Eigen-Value of ν	Re ν/kr_1 and Im ν/kr_1	Re ψ and Im ψ, rad	Magnetic Field H	Mean-Square Accuracy of Approximation ε	Tabulation by Angle ψ: Approximation Interval, rad	Step $\Delta\psi$	Number of Units	Powers of Polynomials Approximating the Re and Im Parts of the Functions: $\parallel R_\parallel$	$\perp R_\perp$	$\perp R_\parallel = \parallel R_\perp$	Tabulation by Sign of ν: Approximation Interval	Step $\Delta\nu$	Number of Units	Powers of Polynomials Approximating the Re and Im Parts of the Functions: R_v	R_h	$I \times e^{i2k(r_2-r_1)} \frac{\nu}{kr_1}$
509,95 16,20	0,95559 0,03036	1,2294 0,08966	=0	10^{-5}	1,21— —1,37	0,02	9	4 5	4 4	—	495— —522	3	10	8 8	3 3	8 8
509,48 11,29	0,95471 0,021169	1,23255 0,06312	≠0	10^{-6}	1,17— —1,34	0,01	18	5 6	5 7	4 5	501— —520	1	20	9 9	4 4	8 8

TABLE 4.

Angle of Incidence ψ, rad	$\lvert R_{\parallel}\rvert$		$\arg R_{\parallel}$		$\lvert R_{\perp}\rvert$		$\arg R_{\perp}$		$\lvert R_{\perp}\rvert - \lvert R_{\parallel}\rvert$		$\arg R_{\perp} - \arg R_{\parallel}$	
	$H \neq 0$	$H = 0$	$H \neq 0$	$H = 0$	$H \neq 0$	$H = 0$	$H \neq 0$	$H = 0$	$H \neq 0$	$H = 0$	$H \neq 0$	$H = 0$
1,21	0,534	0,449	2,76	2,64	0,815	0,826	3,53	3,81	0,0801	0	0,291	0
1,23	0,548	0,463	2,79	2,68	0,824	0,834	3,50	3,78	0,0773	0	0,272	0
1,25	0,563	0,479	2,81	2,72	0,833	0,843	3,46	3,74	0,0741	0	0,253	0
1,27	0,580	0,496	2,81	2,72	0,843	0,853	3,42	3,72	0,0681	0	0,237	0
1,29	0,598	0,515	2,86	2,79	0,852	0,862	3,38	3,67	0,0637	0	0,219	0
1,31	0,617	0,536	2,88	2,80	0,861	0,869	3,33	3,63	0,0581	0	0,201	0
1,33	0,638	0,559	2,91	2,85	0,871	0,879	3,31	3,59	0,0523	0	0,181	0
1,35	0,660	0,583	2,93	2,88	0,881	0,888	3,27	3,56	0,0466	0	0,164	0
1,37	0,683	0,611	2,95	2,91	0,891	0,897	3,23	3,52	0,0414	0	0,147	0

S.T. Rybachek calculated the expressions for (5.1) and (5.2) in the range of complex ν in terms of the value of $H_\nu^{(1,2)}(x)$, which were calculated in terms of the integral representation by Sommerfield. In our algorithm, these expressions are used only for real ν in tabulation of $R_{\nu 1}$ and $R_{\nu 2}$, and recurrence formulas are applied according to the index for $H_\nu^{(1,2)}(x)$.

/74

The function I changes as the exponential curve decreases for Im $\nu < 0$ and increases for Im $\nu > 0$. This can be confirmed by using the asymptotic representations for the Hankel functions $H_\gamma^{(1,2)}(x)$.

The eigen-value obtained by extension of the exponentially increasing function I for Im $\nu > 0$ is given in the second row in Table 2.

In the third row, it was obtained by extension of the function $Ie^{2ik(r_2-r_1)} \nu / kr_1$, which preserves its numerical order in moving to the upper half-plane.

It can be seen from a comparison between the results of the first row and those of the second and third rows in Table 2 that the relative error of the method is equal to $0(10^{-6})$ for the real part and $0(10^{-5})$ for the imaginary part of the roots. The necessary machine time for calculations according to the method discussed decreased by two orders in comparison to the direct method of [14].

The calculational algorithm described aided in finding the first eigen-value of (1.3a), which is generated by the problem of propagation of super-long waves

with a consideration of the Earth's magnetic field. Up to the present, such problems had been solved by Wait [3,4] for two strong limitations: (a) in the case of applicability of the quasi-longitudinal approximation; (b) in the case of glancing angles of incidence of the wave at the boundary of the division "air-ionosphere". The method we used eliminates these limitations and permits a control of the accuracy in all the computational stages. /75

The results of the calculation of the first eigen-value of (1.3a) for frequency $f = kc/2\pi = 4$ KHz and $k(r_2-r_1) = 5.36165$ are given in Table 3. The coefficients of reflection of electromagnetic waves from the "diurnal" ionosphere, which is non-uniform in altitude, were calculated according to the program of N.S. Gavrilova [5], with and without a consideration of the Earth's magnetic field, and are given in Table 4. The coefficients $\tilde{R}_\nu$ and $\tilde{R}_h$ were tabulated according to the following formulas:

$$\widetilde{R}_v = -\left[\frac{\ln' H_\nu^{(2)}(x) + \frac{1}{2x} + i\delta_1}{\ln' H_\nu^{(1)}(x) + \frac{1}{2x} + i\delta_1}\right]_{x=r_1 k}$$

$$\widetilde{R}_h = -\left[\frac{\ln' H_\nu^{(2)}(x) + \frac{1}{2x} + \frac{i}{\delta_1}}{\ln' H_\nu^{(1)}(x) + \frac{1}{2x} + \frac{i}{\delta_1}}\right]_{x=r_1 k}$$

for $\delta_1 = (0.1530809 - i0.2122646)\cdot 10^{-2}$.

We would like to take advantage of this opportunity to express our appreciation to G.I. Makarov and V.V. Novikov for formulating the problem, to G.I. Makarov for discussions which determined the final variation of the article, to B.A. Samokish for valuable consultation on the incorrect problems of mathematical physics, and to N.S. Gavrilova for the program of the calculation of coefficients of reflection from a non-uniform and isotropic ionosphere.

REFERENCES

1. Vorob'yev, Yu.V.: Metod momentov v prikladnoy matematike (Method of Instances in Applied Mathematics). "Fizmatgiz", 1958.
2. Makarov, G.I. and V.V. Novikov: This Collection, p. 19.
3. Wait, J.R.: The Mode Theory of VLF Radio Propagation for a Spherical Earth and a Concentric Anisotropic Ionosphere. Canad. J. Phys., Vol. 41, No. 2, 1963.
4. Wait, J.R., and K.P. Spies: Influence of Finite Ground Conductivity on the Propagation of VLF Radio-Waves. J. NBS, Vol. 69D, No. 10, 1965.
5. Gavrilova, N.S. and V.V. Kirillov: Superlong Wave Propagation. Calculation of the Coefficients of Reflection of plane Waves from a Non-uniform Anisotropic Plasma. In the

Collection: Problemy difraktsii i rasprostraneniya voln (Problems of Wave Diffraction and Propagation), No. V. Leningrad State Univ. Press, 1966.

6. Lavrent'yev, M.M. and V.G. Vasil'yev: Formulating Some Incorrect Problems of Mathematical Physics. Sibirskiy Matem. Zhur., Vol. VII, No. 3, 1966.
7. Sobolev, S.L.: Uravneniye matematicheskoy fiziki (The Equation in Mathematical Physics). "Nauka", 1966.
8. Goldstein, M., and R.M. Thaler: Recurrence Techniques for the Calculation of Bessel Functions. Math. Tables and Other Aids to Computation, Vol. XIII, No. 66, 1959.
9. Fröman, N., and P.O. Fröman: IWKB Approximation Contributions to the Theory. Amsterdam, 1965.
10. Berezin, I.S. and N.P. Zhidkov: Metody vychisleniy (Methods for Computations), Vol. I. "Gizmatgiz", 1962.
11. Reznik, T.L.: Standartnaya programma approksimatsii algebraicheskimi mnogochlenami (Standard Program for Approximation of Algebraic Polynomials). Computer Center of Siberian Dept. of Academy of Sciences U.S.S.R. Press, 1964.
12. Sege, G.: Ortogonal'nyye mnogochleny (Orthogonal Polynomials). "Fizmatgiz", 1962.
13. Walsh, J.L.: Interpolyatsiya i approksimatsiya ratsional'nymi funktsiyami v kompleksnoy oblasti (Interpolation and Approximation by Rational Functions in the Complex Range). Foreign Literature Publishing House, 1961.
14. Rybachek, S.T. and E.M. Gyunninen: Propagation of Long and Superlong Radio Waves in the Waveguide Channel Earth-Ionosphere. In the Collection: Problemy difraktsii i rasprostraneniya voln (Problems of Wave Diffraction and Propagation), No. VI, 1966.
15. Krasnushkin, N.Ye.: Method of Solving the General Boundary Problem of the Propagation of Long and Superlong Radio Waves Around the Earth. Doklady Akad. Nauk S.S.S.R., Vol. 171, No. 1, 1966.

A SOLUTION TO A WAVE EQUATION IN A SPHERICAL SYSTEM OF COORDINATES

V.N. Krasil'nikov

ABSTRACT: The author shows why the method of separation of variables which is often used in solving diffraction problems in a spherical system of coordinates needs modifications in certain particular cases. The requisite modifications are presented, and examples are cited.

The scheme of solving diffraction problems in a spherical system of coordinates by the method of separation of variables is well known [1]. Essentially, a wave field is subjected to spectral analysis according to time t. However, there can be situations where an assumption that the field sources are monochromatic does not simplify the solution to the problem. For an example, we could mention the diffraction of waves on a sphere with radius changing in time - a description of this phenomenon with the aid of ordinary expansions into spherical and temporal harmonics is extremely inconvenient. The standard scheme of the method of separation of variables needs (in this case) some modification. This study discusses the latter in detail. /77

Section 1. Principal Relationships

Let us consider a scalar field $u(\vec{r}, t)$ which satisfies the following uniform wave equation:

$$\nabla^2 u - \frac{1}{c^2} \cdot \frac{\partial^2 u}{\partial t^2} = 0, \tag{1}$$

where c is the velocity of wave propagation, assumed to be constant. In a spherical system of coordinates (r, θ, ϕ), it is natural to represent the field in the form of a series by spherical angular functions $Y_n(\theta, \phi)$, i.e.,

$$u(r, \theta, \varphi, t) = \sum_{n=0}^{\infty} u_n(r, t) Y_n(\theta, \varphi). \tag{2}$$

Since $Y_n(\theta, \phi)$ form a complete and orthogonal system of functions, and each of these satisfies the equatic

$$\nabla_1^2 Y_n + n(n+1) Y_n = 0,$$

where ∇_1^2 is the angular part of the Laplace operator [1], the coefficients of the series in (2) obey the following equation: /78

$$M_n\{u_n(r, t)\}=0, \tag{3}$$

where the symbol below was introduced for the sake of brevity:

$$M_n \equiv \frac{\partial^2}{\partial r^2}+\frac{2}{r}\frac{\partial}{\partial r}-\frac{(n+1)n}{r^2}-\frac{1}{c^2}\cdot\frac{\partial^2}{\partial t^2}. \tag{3a}$$

The assumption usually made about the monochromatism of the process reduces (3) to an equation for spherical Bessel functions. However, it is more convenient for our purposes to use some auxiliary differential operator L_m which satisfies the commutative relationship

$$M_nL_n=L_n\Box, \tag{4}$$

where $\Box$ is a uniform wave operator for the coordinate r, i.e.,

$$\Box=\frac{\partial^2}{\partial r^2}-\frac{1}{c^2}\cdot\frac{\partial^2}{\partial t^2}.$$

If there is such an operator L_n, then, by the substitution

$$u_n=L_n\{v_n\}$$

we will reduce the problem of integration of (3) to that of solving a uniform wave equation, i.e.,

$$\Box v_n=f_n, \tag{5}$$

where f_n is the general solution to the uniform equation

$$L_n\{f_n\}=0. \tag{5a}$$

It is found that the operator L_n is not very complex and, what is particularly important, it acts only in respect to the coordinate r; as a result, the auxiliary equations of the type in (5a) which arise are ordinary differential equations.

Section 2. The Operator L_n and its Properties

First of all, we will assume that the differential operator which has the form of

$$L_n = r^n \frac{\partial^n}{(r\partial r)^n} \cdot \frac{1}{r}. \tag{6}$$

actually satisfies the requirement in (4). This can be done conveniently with the method of mathematical induction. Since the equation below holds for any function F,

$$\left\{\frac{\partial}{\partial r^2} + \frac{2}{r} \cdot \frac{\partial}{\partial r} - \frac{1}{c^2} \cdot \frac{\partial^2}{\partial t^2}\right\} \frac{F}{r} = \frac{1}{r}\left\{\frac{\partial^2 F}{\partial r^2} - \frac{1}{c^2} \cdot \frac{\partial^2 F}{\partial t^2}\right\}$$

the validity of the commutative relationship in (4) for n = 0 is obvious; the existence of identity for an arbitrary n is required for its fulfillment,

$$\left\{r^2 \frac{\partial^{n+2}}{(r\partial r)^{n+2}} + (2n+3) \frac{\partial^{n+1}}{(r\partial r)^{n+1}}\right\} \frac{F}{r} = \frac{\partial^n}{(r\partial r)^n}\left\{\frac{1}{r} \cdot \frac{\partial^2 F}{\partial r^2}\right\}. \tag{7}$$

This is easy to see if we recall the clear form of the operator M_n in (3a). Let (7) be valid for some n; then, using the operator $\sim \left(\frac{\partial}{r\,\partial r}\right)$ on it and carrying out termwise differentiation of the first term in the left-hand part, we find that /79

$$\left\{r^2 \frac{\partial^{n+3}}{(r\partial r)^{n+3}} + (2n+5) \frac{\partial^{n+2}}{(r\partial r)^{n+2}}\right\} \frac{F}{r} = \frac{\partial^{n+1}}{(r\partial r)^{n+1}}\left\{\frac{1}{r} \cdot \frac{\partial^2 F}{\partial r^2}\right\}, \tag{7a}$$

i.e., the same identity as (7), but written in a different way for the superscript n + 1. It turns out that the operator of (6) has the property we want.

It is obvious that the operator L_n is not unique. The commutative relationship in (4) will also hold for the operator $\tilde{L}_n = LK$, where K is any operator commutating with the wave one, i.e., satisfying the following condition:

$$K\Box = \Box K.$$

However, we will use the simplest form of the operator in (6) in the future.

The operator L_n is a linear n-th-order differential operator. It is sometimes useful to have an explicit expression for it which includes derivatives for r (and not for $r^2/2$). The following formula is proven without difficulty by the method of mathematical induction:

$$L_n = \sum_{k=0}^{n} \frac{(n+k)!}{k!\,(n-k)!} \frac{(-1)^k}{2^k r^{k+1}} \cdot \frac{\partial^{n-k}}{\partial r^{n-k}}. \qquad (8)$$

Section 3. Expansion of the Field into Non-Stationary Spherical Waves

In order to find the auxiliary functions $v_n(r, t)$, we must solve the non-uniform wave equation in (5); the function in its right-hand part is found from the condition in (5a). If we take the operator L_n in the form in (6), then it becomes obvious that

$$f_n(r, t) = \sum_{k=0}^{n=1} C_k(t)\, r^{2k+1}, \qquad (9)$$

where $C_k(t)$ are arbitrary time functions. However, logical considerations show what has been derived, what has been introduced into the solution to the problem by the functions in (9), what was due to the artificial mathematical method - introduction of the operator L_n - and what should not affect the ultimate form of the solution. Let us prove this.

The auxiliary functions v_n, as the solutions to (5), have th following form:

$$v_n = \Box^{-1} f_n, \qquad (10)$$

where $\Box^{-1}$ is the inverse operator of the wave one. It follows from /80 the commutation relationship in (4) that

$$L_n = M_n^{-1} L_n \Box \qquad (11)$$

(M_n^{-1} is also an inverse operator). Let us turn to the functions $u_n(r, t)$ introduced directly into the solution of the wave problems,

$$u_n = L_n\{v_n\}. \tag{12}$$

A consideration of (10) and (11) gives the following:

$$u_n = M_n^{-1} L_n\{f_n\}, \tag{12a}$$

However, in view of (5a) $L_n\{f_n\} = 0$ and, consequently, the functions u_n do not depend on the selection of f_n. Therefore, limiting ourselves solely to an investigation of the uniform equation in (5), we will take its general solution in a d'Alambertian form, i.e.,

$$v_n(r, t) = \Phi_n\left(t - \frac{r}{c}\right) + \Psi_n\left(t + \frac{r}{c}\right), \tag{13}$$

where Φ_n and Ψ_n are arbitrary functions of its arguments. Expansion by spherical functions of (2) then acquires the following form:

$$u(r, \theta, \varphi, t) = \sum_{n=0}^{\infty} L_n\left\{\Phi_n\left(t - \frac{r}{c}\right) + \Psi_n\left(t + \frac{r}{c}\right)\right\} Y_n(\theta, \varphi). \tag{14}$$

Formula (14) represents the general solution to the three-dimensional uniform wave equation in (1). A single term in the series of (14) can be called a non-stationary spherical wave; naturally, it is a particular solution to (1).

The expansion by stationary spherical waves is well known [1] for monochromatic ($e^{-i\omega t}$) fields:

$$u(r, \theta, \varphi, t) = e^{-i\omega t} \sum_{n=0}^{\infty} \left\{A_n h_n^{(1)}(kr) + B_n h_n^{(1)}(kr)\right\} Y_n(\theta, \varphi), \tag{15}$$

where $h_n^{(1)}(kr)$ are spherical Bessel functions; $k = \frac{\omega}{c}$, while A_n and B_n are arbitrary constants. It is obvious that this expansion is a particular case of our formula in (14). If we assume that

$$\Phi_n\left(t - \frac{r}{c}\right) = A_n \frac{i}{(-k)^{n+1}} e^{-i\omega\left(t - \frac{r}{c}\right)},$$
$$\Psi_n\left(t + \frac{r}{c}\right) = B_n \frac{i}{(-k)^{n+1}} e^{-i\omega t - ikr},$$

we recall the explicity form of the operator L_n in (6), and we consider that the spherical Bessel functions have representations [1] such as

$$h_n^{(1)}(z) = i(-1)^{n+1} z^n \frac{\partial^n}{(z\partial z)^n}\left(\frac{e^{iz}}{z}\right),$$
$$h_n^{(2)}(z) = i(-1)^n z^n \frac{\partial^n}{(z\partial z)^n}\left(\frac{e^{-iz}}{z}\right),$$

then it is easy to see that the expansion of (14) converts precisely /8 into (15).

One more comment which should be made touches on the behavior of the solution to (14) in the neighborhood of the origin of the coordinates. The operator L_n includes the inverse power of r and, therefore, even acting on the analytical function, it yields a result which generally becomes infinity at the origin of the coordinates. If the latter cannot be eliminated from the region where expansion of (14) has force, then it is necessary to impose a special condition on the functions Φ_n and Ψ_n. In order to explain this property, we should mention that the effect of the operator L_n on some function F(r) can be represented in the following form, considering (6):

$$L_n\{F\} = 2^n r^n \frac{\partial^n}{(\partial r^2)^n} \cdot \frac{F(r)}{r}.$$

If $\frac{F(r)}{r}$ is an even and limited function of the coordinate r, then $L_n\{F\}$ does not go to infinity for r = 0 (since $\frac{F(r)}{r}$ is expanded into a series by non-negative powers of r^2). The function F(r) itself should be limited and odd. As regards the expansion of (14), this means that the wave field which is finite at the origin of the coordinates can be represented in the following form:

$$u(r, \theta, \varphi, t) = \sum_{n=0}^{\infty} L_n\left\{\Phi_n\left(t - \frac{r}{c}\right) - \Phi_n\left(t + \frac{r}{c}\right)\right\} Y_n(\theta, \varphi), \qquad (16)$$

where each member of the series contains only one arbitrary function Φ_n, which is assumed to be limited.

Section 4. Expansion Theorem for a Plane Wave

Let there by a plane wave which is propagated in space in a direction coinciding with the polar axis of the spherical system of coordinates, and for which

$$u(r,\ \theta,\ t)=f\left(t-\frac{r\cos\theta}{c}\right), \tag{17}$$

where $f(t - \frac{r \cos \theta}{c})$ is some arbitrary (for example, piece-wise continuous) function. The independence of the field from the coordinate ϕ allows that the expansion of (16) be written in the form of a series by Legendre polynominals $P_n(\cos \theta)$.

$$f\left(t-\frac{r\cos\theta}{c}\right)=\sum_{n=0}^{\infty}u_n(r,\ t)\,P_n(\cos\theta). \tag{18}$$

The convergence of such an expansion is guaranteed by the corresponding theorems in the theory of spherical functions of [2], and the coefficients $u_n(r, t)$ are determined by the integrals /82

$$u_n(r,\ t)=\frac{2n+1}{2}\int_{-1}^{+1}f\left(t-\frac{rx}{c}\right)P_n(x)\,dx. \tag{19}$$

Here $x = \cos\theta$. For Legendre polynomials, the following Rodrigues formula is valid:

$$P_n(x)=\frac{1}{2^n n!}\cdot\frac{\partial^n}{\partial x^n}(x^2-1)^n,$$

This shows that, if we carry out multiple integration by parts in (19), then, considering that

$$\frac{\partial^{2n+1}}{\partial x^{2n+1}}(1-x^2)^n=0,$$

we will reduce the integral of (19) to the sum of the (n+1)-th integrated term. The result of this operation has the following form:

$$u_n(r,\ t)=\frac{2n+1}{n!2^{n+1}}\sum_{k=0}^{n}(-1)^k D_x^{-(k+1)}f\left(t-\frac{rx}{c}\right)D_x^{n+k}(x^2-1)^n\Big|_{x=-1}^{x=+1}, \tag{20}$$

where the symbolic operator $D_x = \frac{\partial}{\partial x}$ was used. According to the Leibniz formula of [1],

$$D_x^{n+k}(x^2-1)^n=\sum_{s=0}^{n+k}C_{n+k}^{s}D_x^{n+k-s}(x-1)^n D_x^s(x+1)^n.$$

However, $D_x^{n+k-s}(x-1)^n = 0$ at $x = 1$ for all s, except $s = k$; and $D_x^n(x-1)^n = n!$ Similarly, $D_x^s(x+1)^n = 0$ at $x = -1$ for all s, except $s = n$; in the latter case, $D_x^n(x+1)^n = n!$ This means that

$$\left.\begin{aligned} D_k^{n+k}(x^2-1)^n\big|_{x=1} &= C_{n+k}^k n!\, n(n-1)\ldots(n-k+1)2^{n-k}, \\ D_x^{n+k}(x^2-1)^n\big|_{x=-1} &= C_{n+k}^n n!\, n(n-1)\ldots \\ &\quad \ldots(n-k+1)2^{n-k}(-1)^{n-k}. \end{aligned}\right\}$$

It is convenient to express the cofactors $D_x^{-(k+1)}f(t - \frac{rx}{c})$ with the aid of the symbolic operator for differentiation by time $D = \frac{\partial}{\partial t}$. In this regard, it is obvious that

$$D_x^{-(k+1)} f\left(t - \frac{rx}{c}\right) = \left(-\frac{c}{r}\right)^{k+1} D^{-(k+1)} f\left(t - \frac{rx}{c}\right),$$

and the series of (20) is rewritten thus: /83

$$u_n(r, t) = \frac{2n+1}{2}\sum_{k=0}^{n}(-1)^k C_{n+k}^n \frac{n(n-1)\ldots(n-k+1)}{2^k\, r^{k+1}} \times$$
$$\times (-c)^{k+1} D^{-(k+1)} f\left(t - \frac{r}{c}\right) - \frac{2n+1}{2}\sum_{k=0}^{n}(-1)^k C_{n+k}^n \times$$
$$\times \frac{n(n-1)\ldots(n-k+1)}{2^k\, r^{k+1}}(-c)^{k+1} D^{-(k+1)} f\left(t + \frac{r}{c}\right).$$

Let us now consider the possibility of the followi g identity conversion:

$$D^{-(k+1)} f\left(t \pm \frac{r}{c}\right) = \frac{\partial^{n-k}}{\partial t^{n-k}} D^{-(n+1)} f\left(t \pm \frac{r}{c}\right) =$$
$$= (\pm c)^{n-k} \frac{\partial^{n-k}}{\partial r^{n-k}} D^{-(n+1)} f\left(t \pm \frac{r}{c}\right),$$

and, using the formula for the number of combinations $C_{n+k}^n = \frac{(n+k)!}{n!k!}$, we find this representation for the coefficients $u_n(r, t)$:

$$u_n(r,\ t)=\frac{2n+1}{2}(-1)^{n+1}c^{n+1}\sum_{k=0}^{n}\frac{(n+k)!}{k!\,(n-k)!}\cdot\frac{(-1)^k}{2^k r^{k+1}}\times$$
$$\times\frac{\partial^{n-k}}{\partial r^{n-k}}D^{-(n+1)}f\left(t-\frac{r}{c}\right)+\frac{2n+1}{2}(-1)^{n+1}c^{n+1}\sum_{k=0}^{n}\frac{(n+k)!}{k!\,(n-k)!}\times \qquad (21)$$
$$\times\frac{(-1)^k}{2^k r^{k+1}}\cdot\frac{\partial^{n-k}}{\partial r^{n-k}}D^{-(n+1)}f\left(t+\frac{r}{c}\right)$$

If we now recall the explicit form of the operator L_n [Formula (8)] from Section 2, then the expression in (21) is simplified in this way:

$$u_n(r,\ t)=\left(n+\frac{1}{2}\right)(-1)^{n+1}\ c^{n+1}L_n\left\{D^{-(n+1)}f\left(t-\frac{r}{c}\right)-\right.$$
$$\left.-D^{-(n+1)}f\left(t+\frac{r}{c}\right)\right\},$$

and the expansion theorem for the plane wave in terms of nonstationary spherical harmonics acquires the ultimate form of

$$f\left(t-\frac{z}{c}\right)=\sum_{n=0}\left(n+\frac{1}{2}\right)(-c)^{n+1}L_nD^{-(n+1)}\left\{f\left(t-\frac{r}{c}\right)-\right. \qquad (22)$$
$$\left.-f\left(t+\frac{r}{c}\right)\right\}P_n(\cos\theta).$$

where the operator $D^{-(n+1)}$ signifies integration of (n+1)-th multiplicity in time t.

We could raise the question of the arbitrary constants which arise when this type of integration is carried out. It is rather obvious that their selection should not affect our final results; the operator $D^{-(n+1)}$ arose in the process of integration by parts of (19). However, it is well known that the result of this operation does not depend on the specific selection of the antiderivatives. We can arrive at such a conclusion precisely by analyzing (22) directly. The functions $D^{-(n+1)}f(t\pm\frac{r}{c})$ differ from each other by polynomials of degree n with arbitrary coefficients A_k, so that the difference

/84

$$D^{-(n+1)}\left\{f\left(t-\frac{r}{c}\right)-f\left(t+\frac{r}{c}\right)\right\}$$

has the following form in the general case:

$$\sum_{k=0}^{n}A_k\left(t-\frac{r}{c}\right)^k-\sum_{k=0}^{n}A_k\left(t+\frac{r}{c}\right)^k,$$

i.e., is a polynomial by r of degree no higher than n, and includes only odd powers of r. Because of the properties of the operator L_n already discussed at the end of Section 3, this difference vanishes and the coefficients in the expansion of (22) do not depend on the selection of the constant A_K.

Section 5. Field of Concentrated Source

In the preceding sections we considered solutions to a uniform wave equation in (1), but it is also of interest to apply the apparatus developed to a calculation of wave fields which have sources. Let a concentrated emitter whose effect is described by an arbitrary time function f(t) be propagated at the point $\vec{r} = \vec{r}_0$. The field $g(\vec{r},t)$ produced by it in free space is a partial solution to the equation

$$\nabla^2 g - \frac{1}{c^2}\cdot\frac{\partial^2 g}{\partial t^2} = -4\pi f(t)\,\delta(\vec{r}-\vec{r}_0), \tag{23}$$

which disappears as f(t) tends toward zero. It is well known [3] that

$$g(\vec{r}, t) = \frac{f\left(t-\frac{R}{c}\right)}{R}, \tag{24}$$

where R is the distance between the observation site $\vec{r}$ and the point $\vec{r}_0$. However, we are interested in the expansion of the function in (24) into a series by non-stationary spherical waves. Considering the source to be ordered on the polar axis of the spher- /85
ical system of coordinates - $\vec{r}_0$ (r_0, 0, 0), - we can find $g(\vec{r},t)$ in the form of

$$g(\vec{r}, t) \quad \sum_{n=0}^{\infty} g_n(r, r_0, t)\, P_n(\cos\theta). \tag{25}$$

Using (23) and the fact of orthogonality of the Legendre polynomials, it is easy to show that the functions g_n are solutions to the equations

$$M_n\{g_n\} = \cdot(2n+1)\frac{f(t)}{r^2}\,\delta(r-r_0),$$

where the differential operator M_n is determined by (3a). We will use the ordinary substitution $g_n = L_n \{V_n\}$ and the principal property of the operator L_n in (4); the auxiliary functions $v_n(r,t)$ then satisfy the non-uniform one-dimensional wave equation

$$\Box v_n = -(2n+1) f(t) L_n^{-1}\left\{\frac{\delta(r-r_0)}{r^2}\right\}, \tag{26}$$

where L_n^{-1} is an inverse operator whose explicit form is given in the Appendix. After considering this, (26) is written thus:

$$\begin{aligned} &\frac{\partial^2 v_0}{\partial r^2} - \frac{1}{c^2}\cdot\frac{\partial^2 v_0}{\partial t^2} = -f(t)\frac{\delta(r-r_0)}{r}, \\ &\frac{\partial^2 v_n}{\partial r^2} - \frac{1}{c^2}\cdot\frac{\partial^2 v_n}{\partial t^2} = \begin{cases} -(2n+1) f(t) \dfrac{r}{2^{n-1}} \dfrac{(r^2-r_0^2)^{n-1}}{(n-1)! r_0^{n+1}}, & r<r_0, \\ 0 & r>r_0, \end{cases} \end{aligned} \tag{26a}$$

i.e., for the auxiliary function v_n the sources are distributed in the interval $(0 - r_0)$. The following expression is a particular solution to the equations in (26a) [1] [Φ (t), below, is the antiderivative for f(t)]:

$$\begin{aligned} v_n'(r,t) = &\begin{cases} \dfrac{(2n+1)c}{r_0^{n+1}2^n}\displaystyle\int_0^{r_0} x\frac{(x^2-r_0^2)^{n-1}}{(n-1)!}\Phi\left(t-\frac{r-x}{c}\right)dx, & r>r_0, \\ \dfrac{(2n+1)c}{r_0^{n+1}2^n}\left[\displaystyle\int_0^{r} x\frac{(x^2-r_0^2)^{n-1}}{(n-1)!}\Phi\left(t-\frac{r-x}{c}\right)dx + \right. \\ \left. + \displaystyle\int_r^{r_0} x\frac{(x^2-r_0^2)^{n-1}}{(n-1)!}\Phi\left(t+\frac{r-x}{c}\right)dx\right], & r<r_0, \end{cases} \\ v_0'(r,t) = &\begin{cases} \dfrac{c}{2r_0}\Phi\left(t-\dfrac{r-r_0}{c}\right), & r>r_0, \\ \dfrac{c}{2r_0}\Phi\left(t+\dfrac{r-r_0}{c}\right), & r<r_0. \end{cases} \end{aligned} \tag{27}$$

However, the solution of (27) does not guarantee finiteness of the field at the origin of the coordinates. Therefore, $v_n'(r,t)$ must be supplemented by a solution to the uniform equation $v_n''(r,t)$ in such a way that their combination /86

$$v_n(r,t) = v_n'(r,t) + v_n''(r,t)$$

is an odd function of r. Considering Section 3, this causes finiteness of the field at r = 0. Let us show that $v_n''(r,t)$ should be

taken in the form of

$$v_n^*(r,\ t) = -\frac{(2n+1)\,c}{2^n r_0^{n+1}} \int_0^{r_0} x \frac{(x^2 - r_0^2)^{n-1}}{(n-1)!} \Phi\left[t - \frac{(r+x)}{c}\right] dx \qquad (28)$$

[The wave of (28) can be interpreted as produced by auxiliary sources obtained by mirror reflection of real ones relative to the point r = 0].

The complete solution for $r < r_0$ can be written in the following form:

$$\begin{aligned} v_n(r,\ t) = \frac{2n+1}{2^n} \frac{c}{r_0^{n+1}} \Bigg\{ & \int_0^{r_0} x \frac{(x^2 - r_0^2)^{n-1}}{(n-1)!} \Phi\left(t + \frac{r-x}{c}\right) dx - \\ & - \int_0^{r_0} x \frac{(x^2 - r_0^2)^{n-1}}{(n-1)!} \Phi\left(t - \frac{r+x}{c}\right) dx + \\ & + \int_0^{r} x \frac{(x^2 - r_0^2)^{n-1}}{(n-1)!} \Phi\left(t - \frac{r-x}{c}\right) dx - \\ & - \int_0^{r} x \frac{(x^2 - r_0^2)^{n-1}}{(n-1)!} \Phi\left(t + \frac{r-x}{c}\right) dx \Bigg\}. \end{aligned}$$

It is obvious that the first two integrals give the odd function of r in the sum; this is easily demonstrated for the last two by replacing the variable of integration x by -x.

The ultimate form of expansion of a field of a point source into a series by spherical waves is found as such:

$$\begin{aligned} g(\vec{r},\ t) = c \sum_{n=1}^{\infty} \frac{2n+1}{r_0^{n+1} 2^n} \int_0^{r_0} x \frac{(x^2 - r_0^2)^{n-1}}{(n-1)!} L_n \Bigg[& \Phi\left(t - \frac{r-x}{c}\right) - \\ & - \Phi\left(t - \frac{r+x}{c}\right) \Bigg] dx P_n(\cos\theta) + \frac{c}{2r_0} \left[\Phi\left(t - \frac{r-r_0}{c}\right) - \Phi\left(t - \frac{r+r_0}{c}\right) \right] \\ \text{for } r > r_0, & \\ g(\vec{r},\ t) = c \sum_{n=1}^{\infty} \frac{(2n+1)}{r_0^{n+1} 2^n} \Bigg\{ \int_0^{r_0} x \frac{(x^2 - r_0^2)^{n-1}}{(n-1)!} L_n \Bigg[& \Phi\left(t + \frac{r-x}{c}\right) - \\ & - \Phi\left(t - \frac{r+x}{c}\right) \Bigg] dx + \int_0^{r} x \frac{(x^2 - r_0^2)^{n-1}}{(n-1)!} L_n \Bigg[\Phi\left(t - \frac{r-x}{c}\right) - \\ & \Phi\left(t - \frac{\quad x}{c}\right) \Bigg] dx \Bigg\} P_n(\cos\theta) + \frac{c}{2r_0} \left\{ \Phi\left(t + \frac{r-r_0}{c}\right) - \right. \\ & \left. \Phi\left(t - \frac{r+r_0}{c}\right) \right\} \text{ for } r < r_0. \end{aligned} \qquad (29)$$

/87

Let us recall that the function $\Phi(t) = \int f(t)dt$; a selection of the integration constant, as follows from the form of the formulas in (29), is not essential; this constant is preserved.

We should mention that the assumption we made about the position of the emitter on the polar axis is not a fundamental limitation: we can write the relationships in (29) for an arbitrarily arranged source by simple use of the theorem of addition for Legendre polynomials [1].

APPENDIX

Operator Inverse to L_n

Together with the effect of the principal operator

$$L_n = r^n \left(\frac{\partial}{r\partial r}\right)^n \frac{1}{r} \qquad (I)$$

it is sometimes necessary to consider the results of applying the inverse operator L_n^{-1}. If the operation

$$\varphi = L_n(\psi) \qquad (II)$$

is an unambiguous differential transition from the function ψ to the function ϕ, then the converse effect

$$\psi = L_n^{-1}(\varphi) \qquad (III)$$

is essentially reduced to integration of a differential equation of n-th order, and its result is determined with accuracy up to the solution χ_n of the uniform equation $L_n\{\chi_n\} = 0$. It follows directly from the explicit form of L_n that

$$\chi_n = \sum_{k=1}^{n} C_k r^{2k-1}, \qquad (IV)$$

where C_k are arbitrary constants, the definitions of which can be drawn from various conditions.

Considering (I), we will again write out (III) as the following:

$$\psi = r\int_{r}^{r_n} r_n dr_n \int_{r_n}^{r_{n-1}} r_{n-1} dr_{n-1} \cdots \int_{r_2}^{r_1} \frac{\varphi}{r_1^{n-1}}\, dr_1 + \chi_n(r). \qquad (V)$$

The presence of an arbitrary function in (IV) allows us to consider the integrals in (V) as non-definite. A substitution of the variables $r^2 = x$ reduces (V) to n-multiple integration of the function $\phi(\sqrt{x})/x^{n/2}$. Using the well-known formula which reduces the iterative integral to the single one [1], and again turning to the variable r, we can write the following:

$$\psi = \frac{r}{2^{n-1}} \int_a^r \frac{(r^2 - s^2)^{n-1}}{(n-1)!} \cdot \frac{\varphi(s)}{s^{n-1}} ds + \chi_n(r), \qquad \text{(VI)}$$

where the lower limit in the integral and the coefficients of the polynomial $\chi_n(r)$ are arbitrary, as before.

In Section 5, we had to use the operator L_n^{-1} in a specific problem concerning expansion into series by spherical waves of the field of a point emitter. In this regard, the emitter, which was connected not infinitely long ago, cannot produce fields at arbitrarily great distances from itself. This physical condition permits us to define the operator L_n^{-1} unambiguously. The zero conditions at great distances are guaranteed if we assume that $\chi_n(r) = 0$ and $a = \infty$ in (VI). Therefore, L_n^{-1} meant the following operation in Section 5: /88

$$L_n^{-1}\{\varphi\} = \frac{r}{2^{n-1}} \int_\infty^r \frac{(r^2 - s^2)^{n-1}}{(n-1)!} \cdot \frac{\varphi(s)}{s^{n-1}} ds, \qquad \text{(VII)}$$

and $L_0^{-1}\{\phi\} = r\phi$.

REFERENCES

1. Smirnov, V.I.: Kurs vysshey matematiki (Course in Higher Mathematics), Vol. II, III. "OGIZ", 1953.
2. Hobson, E.V.: Teoriya sfericheskikh i ellipsoidnykh funktsiy (Theory of Spherical and Ellipsoidal Functions). Foreign Literature Publishing House, 1952.
3. Morse, F. and F. Feshbach: Metody teoreticheskoy fiziki (Methods of Theoretical Physics). Foreign Literature Publishing House, 1958.

DIFFRACTION OF A PLANE ELECTROMAGNETIC WAVE ON AN IMPEDANCE SPHERE WITH RADIUS CHANGING IN TIME

V. N. Krasil'nikov

ABSTRACT: The diffraction of a plane electromagnetic wave on an impedance sphere with radius changing in time is analyzed mathematically. Even the simplest examples presented clearly show the uniqueness of the process of wave diffraction on bodies of variable size. The Debye potentials corresponding to an incident linearly-polarized plane electromagnetic wave are defined.

Section 1. Formulation of the Problem

/89

Let there by a spherical body which changes its radius in time t according to a certain law a(t) in an inorganic uniform nonconducting isotropic medium with electrodynamic characteristics of $\varepsilon = \mu = 1$. Moreover, let a linearly-polarized plane electromagnetic wave be propagated at a velocity of c in the direction of the axis OZ of the Cartesian system of coordinates, i.e.,

$$\vec{E}_a = f\left(t - \frac{z}{c}\right)\vec{e}_x, \quad \vec{H}_0 = f\left(t - \frac{z}{c}\right)\vec{e}_y, \tag{1}$$

where $f(t - \frac{z}{c})$ is a known function describing the shape of the wave, while $\vec{e}_i$ are the unit vectors of the system of coordinates (we will also use the spherical system of coordinates r, θ, φ, the polar axis of which coincides with the axis OZ, while the center is located at the center of the pulsing sphere).

At the surface of the spherical body which causes the diffraction of the incident wave of (1), we will impose an impedance boundary condition on the tangential components of the field vectors, i.e.,

$$\vec{E}_\tau = w\left[H_\tau \times \vec{n}\right]\big|_{r=a(t)}, \quad \vec{n} = -\vec{e}_r. \tag{2a}$$

Here w is the surface impedance determined according to the physical properties of the body; its magnitude can change in time, but should not depend on the angular coordinates θ and φ. From the electrodynamic point of view, the surface of the body is uniform and isotropic.

The condition of (2a) requires some physical remarks. We should differentiate between the motion of the boundary (surface

at which the properties of the medium change irregularly) and the motion of the substance itself. For example, a unique ionization wave can be propagated along the substance by the effect of a pulsed source of hard radiation. In this case, the free electrons arising as a result of the photoelectric effect, which basically determine the electrodynamic properties of the medium, do not have a mean directed velocity. On the contrary, in the motion of a metal conductor its electrons have a certain directed velocity and, from the point of view of the immobile observer, are subjected to the effect of Lorentz forces, of which there are none in the first case. The difference between the motion of the substance and the motion of its state is partly reminiscent of the relationship which exists between group and phase velocities. In quantitative terms, this difference amounts to the fact that the usual electrodynamic characteristics of the medium (including the surface impedance) can be used directly only in that reading system relative to which the substance (or, more precisely, its current carriers) is at rest. A conversion of the relationships of interest to us into another system of coordinates can be carried out by using the Lorentz transformation for the field. /90

Let us consider such a small part of the surface that it cannot be considered plane; let the rate of movement of the boundary be directed along the normal $\vec{n}$, and at a given moment of time be equal to V, while the velocity of the substance moving behind it is equal to U in respect to our "immobile" reading system K. In a system of coordinates K' which moves together with the substance, the condition at the boundary S acquires the following form:

$$\vec{E}'_\tau = w_0 [\vec{H}'_\tau \times \vec{n}]\big|_S, \qquad (2b)$$

where $\vec{E}'$ and $\vec{H}'$ are the electromagnetic fields in the system K', while w_0 is the ordinary value of the surface impedance. Using the law for the conversion of fields in [1], we will write out (2b) in the following way:

$$\left(\vec{E}_\tau - \frac{U}{c}[\vec{H}_\tau \times \vec{n}]\right) = w_0\left(\vec{H}_\tau + \frac{U}{c}[[\vec{E}_\tau \times \vec{n}] \times \vec{n}]\right)\Big|_S,$$

where $\vec{E}$ and $\vec{H}$ are the electromagnetic fields in our reading system.

The latter relationship converts into the boundary condition of (2a) if we use the value of the surface impedance w according to the formula

$$w = w_0 \frac{1 - U/cw_0}{1 - Uw_0/c}, \qquad (3)$$

which defines the rule for conversion of the surface impedance into the "immobile" system of coordinates. Formula (3) includes the directed velocity of the current carriers U, and not the rate of displacement of the boundary V.

The surface impedance is often a function of the frequency (for example, in considering the skin effect), and in this case is usually complex. A direct application of these values of w_0 in our problem is inadmissible, since the wave diffraction is of a /91
parametric nature and the spectrum of the field is converted in this regard. However, if we can disregard the dispersion of surface impedance in the frequency band arising in the diffraction process (this is realized for slow movements and a sinusoidal incident wave), then in constructing the model we can use the value of w_0 at some mean frequency. The fact that, despite its parametric aspect, the problem remains linear, allows us to describe the dependence of the fields on time with a symbolic factor exp $\{-i\omega t\}$, and to use the complex surface impedance derived from it.

In concluding this section, we should note that, since the theorem of singularity of the solution to the electrodynamic boundary problem also holds in our case [2], the sought-for diffracted field should satisfy (1) either the zero initial conditions, if the wave of (1) is of a non-stationary nature, i.e., $f(x) = 0$ at $x < x_0$, where x_0 is some integer, or (2) the conditions for infinite emission, if the incident field of (1) is a periodic function of the time.

Section 2. Construction of the Formal Solution.

It is convenient to describe both the incidence (1) and the diffracted field ($\vec{E}$, $\vec{H}$) in correspondence with the principle of polarization duality, with the electric ($\vec{\Pi}_e$) and magnetic ($\vec{\Pi}_h$) Hertz vectors having only one radial component in the spherical system of coordinates. The Maxwellian equations in the space outside the sphere are equivalent to

$$\operatorname{grad}\operatorname{div}\vec{\Pi}_i - \operatorname{rot}\operatorname{rot}\vec{\Pi}_i - \frac{1}{c^2}\cdot\frac{\partial^2\vec{\Pi}_i}{\partial t^2} = 0, \quad i = e,\ h, \tag{4}$$

while the fields $\vec{E}$ and $\vec{H}$ are determined according to the Hertz vectors by the following:

$$\vec{E} = \operatorname{rot}\operatorname{rot}\vec{\Pi}_e - \frac{1}{c}\cdot\frac{\partial}{\partial t}\operatorname{rot}\vec{\Pi}_h, \quad \vec{H} = \operatorname{rot}\operatorname{rot}\vec{\Pi}_h + \frac{1}{c}\cdot\frac{\partial}{\partial t}\operatorname{rot}\vec{\Pi}_e. \tag{5}$$

Let us introduce the traditional Debye potentials u and v, which are connected with the Hertz vectors in the following way:

$$\vec{\Pi}_e = ru\vec{e}_r, \quad \vec{\Pi}_h = rv\vec{e}_r. \tag{6}$$

It is well known [3] that ordinary wave equations are obtained from (4) for the functions of u and v, i.e.,

$$\left(\nabla^2 - \frac{1}{c^2}\cdot\frac{\partial^2}{\partial t^2}\right)\begin{Bmatrix} u \\ v \end{Bmatrix} = 0. \tag{7}$$

It is natural to look for the potentials u and v for the diffracted field in the following way, considering the results of our study in [4]: /92

$$\begin{aligned} u(\vec{r}, t) &= \sum_{n=1}^{\infty} u_n(r, t)\, P_n^{(1)}(\cos\theta)\cos\varphi, \\ v(\vec{r}, t) &= \sum_{n=1}^{\infty} v_n(r, t)\, P_n^{(1)}(\cos\theta)\sin\varphi, \end{aligned} \tag{8}$$

where

$$u_n(r, t) = L_n\left\{\Phi_n\left(t - \frac{r}{c}\right)\right\}, \quad v_n = L_n\left\{\Psi_n\left(t - \frac{r}{c}\right)\right\},$$

while the operator $L_n = r^n\left(\frac{\partial}{r\partial r}\right)^n \frac{1}{r}$. The corresponding expansions for the incident wave are found in the Appendix (Formulas IV and V).

A selection of the arguments for the still-unknown functions Φ_n and Ψ_n corresponds to the fulfillment of the zero initial conditions in the non-stationary problem, and it guarantees satisfaction of the principle of emission in the stationary case. The potentials in (8) satisfy the equations in (7) derived from the principal Maxwellian rules.

The components of the vectors of the diffracted field in the space outside the sphere - r > a(t) - are determined by the following group of formulas, based on (5), (6) and (8):

$$\begin{aligned} E_r &= \sum_{n=1}^{\infty}\left(\frac{\partial^2}{\partial r^2} - \frac{1}{c^2}\cdot\frac{\partial^2}{\partial t^2}\right)(ru_n)\, P_n^{(1)}(\cos\theta)\cos\varphi, \\ E_\theta &= \sum_{n=1}^{\infty}\frac{1}{r}\cdot\frac{\partial}{\partial r}(ru_n)\frac{\partial}{\partial\theta}\, P_n^{(1)}(\cos\theta)\cos\varphi + \\ &\quad + \sum_{n=1}^{\infty}\frac{1}{c}\cdot\frac{\partial}{\partial t}(v_n)\frac{P_n^{(1)}(\cos\theta)}{\sin\theta}\cos\varphi, \\ E_\varphi &= -\sum_{n=1}^{\infty}\frac{1}{r}\cdot\frac{\partial}{\partial r}(ru_n)\frac{P_n^{(1)}(\cos\theta)}{\sin\theta}\sin\varphi - \end{aligned} \tag{9}$$

$$\sum_{n=1}^{\infty} \frac{1}{c} \cdot \frac{\partial}{\partial t}(v_n) \frac{\partial}{\partial \theta} P_n^{(1)}(\cos\theta) \sin\varphi,$$

$$H_r = \sum_{n=1}^{\infty} \left(\frac{\partial^2}{\partial r^2} - \frac{1}{c^2} \cdot \frac{\partial^2}{\partial t^2}\right)(r v_n) P_n^{(1)}(\cos\theta) \sin\varphi,$$

$$H_\theta = \sum_{n=1}^{\infty} \frac{1}{r} \cdot \frac{\partial}{\partial r}(r v_n) \frac{\partial P_n^{(1)}(\cos\theta)}{\partial \theta} \sin\varphi +$$

$$+ \frac{1}{c} \sum_{n=1}^{\infty} \frac{\partial}{\partial t}(u_n) \frac{P_n^{(1)}(\cos\theta)}{\sin\theta} \sin\varphi,$$

$$H_\varphi = \sum_{n=1}^{\infty} \frac{1}{r} \cdot \frac{\partial}{\partial r}(r v_n) \frac{P_n^{(1)}(\cos\theta)}{\sin\theta} \cos\varphi +$$

$$+ \frac{1}{c} \sum_{n=1}^{\infty} \frac{\partial}{\partial t}(u_n) \frac{\partial}{\partial \theta} P_n^{(1)}(\cos\theta) \cos\varphi.$$

Similar relationships also occur for the incident wave $(\vec{E}_0, \vec{H}_0)$. /93

In order to find the unknown functions, we should use the boundary conditions on the surface of a sphere of variable radius. It follows from (2a) that

$$(E_0 + E)_\theta = -w(H_0 + H)_\varphi, \quad (E_0 + E)_\varphi = w(H_0 + H)_\theta \qquad (10)$$
$$\text{at } r = a(t).$$

Having compared (9) and (10), it is easy to see that the boundary conditions are fulfilled if

$$\begin{cases} \frac{1}{r} \cdot \frac{\partial}{\partial r}[r(u_{0n} + u_n)] - \frac{w}{c} \cdot \frac{\partial}{\partial t}(u_{0n} + u_n) = 0, \\ \frac{1}{r} \cdot \frac{\partial}{\partial r}[r(v_{0n} + v_n)] - \frac{1}{wc} \cdot \frac{\partial}{\partial t}(v_{0n} + v_n) = 0, \end{cases} \qquad (11)$$

n = 1, 2, 3, ... at r = a(t).

The existence of separate conditions for the first and second Debye potential shows that, in the case under investigation, the effect of the boundary does not result in a connection between fields of the types TE and TM.

In an explicit form, the equations used for finding Φ_n and Ψ_n are such:

$$\left\{L_{n+1}+\frac{n+1}{r}L_n-\frac{w}{c}\cdot\frac{\partial}{\partial t}L_n\right\}\Phi_n\left(t-\frac{r}{c}\right)=$$

$$=\left\{L_{n+1}+\frac{n+1}{r}L_n-\frac{w}{c}\cdot\frac{\partial}{\partial t}L_n\right\}\frac{\left(n+\frac{1}{2}\right)}{n(n+1)}(-c)^{n+1}D^{-(n+2)}\times$$

$$\times\left\{f\left(t-\frac{r}{c}\right)-f\left(t+\frac{r}{c}\right)\right\},\qquad(12)$$

$$\left\{L_{n+1}+\frac{n+1}{r}L_n-\frac{1}{cw}\cdot\frac{\partial}{\partial t}L_n\right\}\Psi_n\left(t-\frac{r}{c}\right)=$$

$$=\left\{L_{n+1}+\frac{n+1}{r}L_n-\frac{1}{cw}\cdot\frac{\partial}{\partial t}L_n\right\}\frac{\left(n+\frac{1}{2}\right)}{n(n+1)}(-c)^{n+1}D^{-(n+2)}\times$$

$$\times\left\{f\left(t-\frac{r}{c}\right)-f\left(t+\frac{r}{c}\right)\right\},$$

n = 1, 2, 3, ... at r = a(t).

The boundary conditions are reduced to an infinite set of ordinary linear differential equations with variable coefficients. This proves that the comments we made earlier about the linear and parametric nature of our problem are correct. Each of the equations has order of (n+1) and is uniform: if we find those particular solutions for Φ_n and Ψ_n which vanish as f(t-r/c) tends toward zero, then the diffraction problem is formally solved. /94

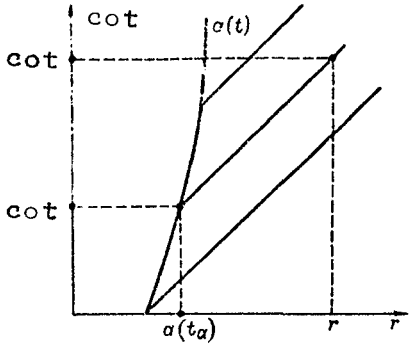

Fig. 1

We should mention the order of inversion with the relationships in (12). At first, we must perform all the operations of integration and differentiation by t and r, considering that the functions Φ_n, Ψ_n and f depend on the combinations $t-\frac{r}{c}$ or $t+\frac{r}{c}$.

As a result, the derivatives of these functions are introduced into (12) by their complete arguments.

Then these arguments must be considered (at the boundary surface) as equal to $t - \frac{a(t)}{c} = \xi(t)$ and $t + \frac{a(t)}{c} = \eta(t)$. The powers $\underline{r}$ introduced to the coefficients in front of the derivatives are replaced by the power $a(t)$.

A solution to the differential equation thus obtained defines the functions $\Phi_n(\xi)$ and $\Psi_n(\xi)$ only on the surface of the sphere $r = a(t)$. In order to obtain the diffracted field in space, we must extend Φ_n and Ψ_n into the region $r > a(t)$, using the propagation of these functions by characteristics of the uniform wave equation. In this case, we must distinguish between the "start" time t_a of a certain wave phase with surface $r = a(t)$ and the time $\underline{t}$ it is observed at a certain point at a distance of $\underline{r}$. The equation for the characteristic is

$$t - \frac{r}{c} = t_a - \frac{a(t_a)}{c}, \qquad (13)$$

and, obviously, the functions on the characteristic satisfy the following condition: /95

$$\Phi_n\left(t - \frac{r}{c}\right) = \Phi_n\left(t_a - \frac{a(t_a)}{c}\right), \quad \Psi_n\left(t - \frac{r}{c}\right) = \Psi_n\left(t_a - \frac{a(t_a)}{c}\right). \qquad (14)$$

An extension of the wave field into space by characteristics, as illustrated in Figure 1, is impossible if the velocity of the boundary $\left(\frac{da}{dt}\right)$ exceeds $\underline{c}$. In this case, the boundary advances the wave reflected by it, the diffracted field does not arise, and the energy of the incident wave undergoes transformation into other types of energy connected with the specific physical mechanism for displacement of the boundary.

Section 3. Long-Wave Approximation.

A precise solution to the equations in (12) can hardly be shown for any arbitrary law of the motion of the boundary. It is true that, in the case of uniform expansion (or compression), the expressions in (12) can be reduced to non-uniform Euler equations, but the functions Φ_n and Ψ_n thus found would have too complex a representation, preventing us from obtaining physical results. Therefore, an approximating analytical study of the equations in (12) is more intelligent for a number of particular situations. In this work, we will discuss the case of "long-wave approximation", when the relative changes of the function $f(t)$ determining the time dependence of the incident field are small for a time on the order of a_0/c, where a_0 is the maximum value of the radius of the sphere at the stage of the process under investigation.

Since the incident wave is generally not sinusoidal, then, instead of the ordinary inequality $\lambda >> a_0$, we will require that the function f(t) has N continuous derivatives which satisfy the following inequalities:

$$\overline{\left(\frac{\partial^{k+1} f}{\partial t^{k+1}}\right)^2 \left(\frac{a_0}{c}\right)^2} \ll \overline{\left(\frac{\partial^k f}{\partial t^k}\right)^2}, \qquad (15)$$

where k = 0, 1, ..., N - 1. The line signifies averaging over the interval of time between two neighboring zeros of the averaged function. Let us emphasize that the criterion of (15) relates only to the incident field; since we will not impose any limitations on the velocity of the boundary, and the values on the order of c are admissible, the result could be that the secondary, diffracted field does not satisfy the requirement of (15).

The existence of the inequality in (15) shows that $f(t \pm \frac{a}{c})$ can be expanded around the point a = 0 into a Taylor series with a remainder term of number N, and this series is a good mean description of the function $f\left(t \pm \frac{a}{c}\right)$, even with some of its first terms. Using this idea, we can obtain the following for the coefficients $u_{0n}(r, t)$ and $v_{0n}(r, t)$ at $r \leq a_c$: /96

$$u_{0n} = v_{0n} \frac{\left(n + \frac{1}{2}\right)}{n!\sqrt{\pi}} \left(\frac{2}{c}\right)^{n+1} \sum_{k=n}^{\infty} \frac{k!}{(2k+1)!\,(k-n)!} \times \left(\frac{r}{c}\right)^{2k} D^{2k-n-1}\{f(t)\}. \qquad (16)$$

Formula (16) was written on the assumption that N = ∞. For finite N, the form of the record changes somewhat, as we must use the Taylor series with remainder term for $f\left(t \pm \frac{a}{c}\right)$. However, it can be seen from (16) that not only a retention of many terms in the series for u_{0n} (or v_{0n}), but also a consideration of u_{0n} with higher numbers n are connected with a regard for terms of higher order in the sense of the inequality in (15). For example,

$$u_{01} = v_{01} \cong f(t)\frac{r}{2}, \quad u_{02} = v_{02} \cong \cdots \frac{\partial f}{\partial t}\cdot\frac{r^2}{18c}.$$

It is obvious [see (11)] that the relationships between $u_{0n}(v_{0n})$ in order of magnitude determine the relationships between u_n (v_n). If after integrating the principal part of the process we limit ourselves solely to the leading terms, then it suffices for us to

solve (12) only at n = 1:

$$\begin{aligned}(1+w)\frac{\Phi_1''}{c^2a}+(1+w)\frac{\Phi_1}{ca^2}+\frac{\Phi_1}{a^3}&\cong -f(t)+\frac{w}{2}\cdot\frac{\partial f}{\partial t}\left(\frac{a}{c}\right),\\ \left(1+\frac{1}{w}\right)\frac{\Psi_1''}{c^2a}+\left(1+\frac{1}{w}\right)\frac{\Psi_1'}{ca^2}+\frac{\Psi_1}{a^3}&\cong -f(t)+\frac{1}{2w}\cdot\frac{\partial f}{\partial t}\left(\frac{a}{c}\right).\end{aligned}\qquad(17)$$

In these equations, a = a(t) is the radius of the sphere, while the derivatives of the functions Φ_1 and Ψ_1 are taken by complete argument equal to $t - \frac{a(t)}{c}$. The second terms in the right-hand part can be substantial for extreme impedance values ($\underline{w} \to 0$ or $w \to \infty$).

The functions of Φ_1 and Ψ_1 found from (17) determine the principal part of the diffracted field, for a clear representation of which we must use the general formulas in (9). However, for physical interpretations it is simpler to consider that the secondary field (in the approximation assumed) consists of a field of an electric dipole at the center of the sphere, oriented in the direction of the axis OX, with moment equal to $\Phi_1(t)$, as well as the field of a magnetic dipole with moment $\Psi_1(t)$, directed along the axis OY. The proof for this is very elementary, and we will not stop to discuss it.

The problem we studied earlier in [5], concerning the pulsation of an ideally conducting ($w_0 = 0$) sphere in a constant uniform field is a particular case for the equations in (17). It is only necessary that, having considered the static uniform field as a superposition of two plane counterwaves, $f(t) = E_0$ in the first equation, while $f(t) = H_0$ in the second, where E_0 and H_0 are the magnitudes of the intensities of the constant fields. /97

Let us first examine movements of the sphere which are slow when compared to the speed of light (non-relativistic case). The function a(t) will then change slowly in the sense of (15). Naturally, a similar requirement can also be imposed on the impedance w(t), as its dependence on the time is generally connected with the velocity of the boundary. We will disregard the small derivatives of the time (in this case the difference between differentiation by $\underline{t}$ and $t - \frac{a(t)}{c}$ disappears), and then the equations in (17) are simplified:

$$\begin{aligned}\frac{\partial\Phi_1}{\partial t}+\frac{\Phi_1}{\tau_e}&=\frac{a^2}{\tau_e}\left\{-f(t)+\frac{1}{2}\cdot\frac{\partial f}{\partial t}\tau_e\right\},\\ \frac{\partial\Psi_1}{\partial t}+\frac{\Psi_1}{\tau_h}&=\frac{a^3}{\tau_h}\left\{-f(t)+\frac{1}{2}\cdot\frac{\partial f}{\partial t}\tau_h\right\}.\end{aligned}\qquad(18)$$

Here we have introduced the characteristic relaxation times: $\tau_e = \frac{wa}{c}$ for the electric dipole moment, and $\tau_h = \frac{a}{cw}$ for the magnetic one. They depend largely on the electromagnetic properties of the material of the sphere, and are not constant in time. For example, the solution to the first of the equations in (18) which satisfies the initial zero conditions has the following form:

$$\Phi_1\left(t-\frac{a(t)}{c}\right)=\int_0^t \frac{a^3(x)}{\tau_e(x)}\left\{-f(x)+\frac{1}{2}\cdot\frac{\partial f}{\partial x}\tau_e(x)\right\}e^{-\frac{t-x}{\tau_e(x)}}dx. \qquad (19)$$

In this case, when the characteristic time of the process f(t) greatly exceeds τ_e, integration with $\frac{1}{\tau_e}\exp\left\{-\frac{t-x}{\tau_e}\right\}$ can be replaced by multiplication by unity.

Let us discuss the case of w = 0 in more detail. It corresponds to the arisal of infinitely great conductivity in the system of coordinates which we agreed to call immobile. In this regard, $\tau_e = 0$, $\tau_h = \infty$ and

$$\begin{aligned}\Phi_1\left(t-\frac{a(t)}{c}\right)&\cong -a^3 f(t),\\ \Psi_1\left(t-\frac{a(t)}{c}\right)&\cong\int_0^t \frac{a^3(x)}{2}\cdot\frac{\partial f}{\partial x}dx.\end{aligned} \qquad (20)$$

The magnetic moment applied on the sphere decreases in a transfer toward slower fields $\left(\frac{\partial f}{\partial t}\to 0\right)$. It is not induced at all in the constant field. In other words, the constant magnetic field penetrates without hindrance inside the "arising" conductor. The formulas in (20) yield the functions Φ_1 and Ψ_1 only on the surface of the sphere; they are extended in space by the characteristics of (13), and the field at great distances from the sphere (in the zone of the emission) is determined by the second derivative of the dipole moment with accuracy up to the well-known geometric and polarization factors. Since

/98

$$\begin{aligned}\left[\vec{E}_e\right]_i=\left[\vec{H}_e\right]_k&\sim(a^3f''+6a^2a'f'+6a(a')^2f+3a^2a''f),\\ \left[\vec{E}_h\right]_i=\left[\vec{H}_h\right]_k&\sim\left(\frac{a^3}{2}f''+\frac{3}{2}a^2a'f'\right),\quad i,\ k=\theta,\ \varphi.\end{aligned} \qquad (21)$$

The spectral composition of the scattered field changes when compared to the incident one. The transformation of the spectrum is particularly substantial if the process in the incident wave

is slow when compared to the process of expansion of the sphere, i.e., if $\frac{df}{dt}\, a << f\, \frac{da}{dt}$. In this case, the spectrum of the scattered field is determined basically, not by the function f(t), but by the parametric interaction between the wave and the boundary. When the opposite inequality is fulfilled, the scattered field coincides in form (in first approximation) with the second derivative of the incident signal. The corrections here are not confined to formulas for the Doppler effect; thus, changes in amplitude which are commensurate in order of magnitude, together with phase displacements, are observed even for a monochromatic incident field in a diffracted wave.

The other extreme value for the impedance ($w \to \infty$) corresponds to the scarecely real case of a dielectric with a very high value of magnetic susceptibility $\mu >> \varepsilon > 1$. A constant electric field $\vec{E}_0$ would penetrate without hindrance into such a substance, and the magnetic field would be forced completely out of its space.

In the non-relativistic situation we have examined thus far, there is practically no difference between the motion of the substance and the motion of the state. As can be seen from (3), $w \to w_0$ for $\frac{U}{c} \to 0$.

Let us now turn to an analysis of the rules which hold for velocities of the expansion of the sphere on the order of the speed of light c. In this case, slowness in the change of the function f(t) does not guarantee slowness in the change of Φ_1 and Ψ_1, and integration of the equations in (17) is found to be a very complicated problem. However, for uniform expansion (compression) of the sphere, when $\frac{da}{dt} = V_0$ is constant, the arguments of the functions Φ_1 and Ψ_1 differ from the start time t_a only by the constant factor /99

$$x = t_a - \frac{a(t_a)}{c} = t_a(1-\beta), \quad \beta = \frac{V_0}{c},$$

In assuming invariability of w (the dependence of the impedance on the velocity does not presuppose its dependence on time in the case of constancy of the latter, according to (3), the equations in (17) are converted into Euler equations and can be rewritten in the following way:

$$\begin{aligned}
&\beta^2(1+w)(1-\beta)\,x^2\Phi_{1xx}'' + \beta(1+w)(1-\beta)^2\,x\Phi_{1x}' + \Phi_1(1-\beta)^3 = \\
&\quad = -V_0^3x^3\left\{f\left(\frac{x}{1-\beta}\right) - \frac{w}{2}\cdot\frac{\partial f}{\partial x}\,x\beta\right\}, \\
&\beta^2x^2\left(1+\frac{1}{w}\right)(1-\beta)\,\Psi_{1xx}'' + \beta\left(1+\frac{1}{w}\right)\beta x\,(1-\beta)^2\,\Psi_{1x}' + \Psi_1(1-\beta)^3 = \\
&\quad = -V_0^3x^3\left(f\left(\frac{x}{1-\beta}\right) - \frac{1}{2w}\cdot\frac{\partial f}{\partial x}\,x\beta\right).
\end{aligned} \tag{22}$$

In integrating (22) for the case of a sphere expanding uniformly from a "point", we must use the initial zero conditions. For a more complex "step-wise" expansion of the sphere, when the velocity is constant only during each of the steps in the process, the solution for the preceding step will also give the initial conditions for the subsequent step of the computations. It is also useful to consider that the condition in (15) of the slowness in change of the function f(t) for velocities of expansion on the order of c practically signifies constancy of f(t) over the entire step of the process under investigation (since the time a_0/c and the time for expansion of the sphere to a size of a_0 are values of one order). Considering the latter circumstance, the solution to (22) acquires the following form:

$$\Phi_1(x) = -\frac{V_0^3(1-\beta)^3 t_a^3}{K_e(\beta)}\left\{f(t) - \frac{w}{2}\cdot\frac{\partial f}{\partial t}\beta t_a\right\},$$
$$\Psi_1(x) = -\frac{V_0^3(1-\beta)^3 t_a^3}{K_h(\beta)}\left\{f(t) - \frac{2}{w}\cdot\frac{\partial f}{\partial t}\beta t_a\right\}, \qquad (23)$$

where

$$K_e(\beta) = (1-\beta)\{3(1+w)(\beta^2+\beta)+(1-\beta)^2\};$$
$$K_h(\beta) = (1-\beta)\left\{3\left(1+\frac{1}{w}\right)\beta(\beta+1)+(1-\beta)^2\right\}.$$

In the case of $1 - \beta \ll 1$, there is a substantial difference between the motion of the substance and the motion of the state. For example, if the ideal conductor moves, then $w = -\beta$ and $K_i(\beta) \sim (1-\beta)^2$; if infinitely great conductivity "arises" in a substance at rest, then $w = 0$, while $K_i(\beta) \sim (1-\beta)$. The arising dipole moments (and the fields connected with them) differ by order of magnitude of $(1-\beta)$. In movement of the conductor, there is a relative effect of the work of the body over the field displaced, which results in an abrupt increase in the emission fields. /100

For the sake of definiteness, let us examine a sphere which expands uniformly at a velocity of V_0 up to a certain radial dimension a_0 which is then maintained (the solution to such a problem is constructed by fitting two steps). Moreover, let the external field be uniform and electrostatic ($\vec{E} = E_0 \vec{e}_x$); then $\Psi_1 = 0$, or the magnetic moment is not induced. We will be interested in the field of emission. In calculating the fields, we must keep in mind that $\frac{\partial}{\partial t_a} \neq \frac{\partial}{\partial t}$ and, as follows from (13),

$$\left(\frac{\partial t_a}{\partial t}\right)_r = \frac{1}{1-\beta}.$$

The maximum intensity in the emission zone (at a distance r from the center) is then equal to the following in the case of a moving conductor (for $1-\beta \ll 1$):

$$\left[\vec{E}\right]_i = \left[\vec{H}\right]_k \cong -E_0 \frac{V_0}{r} \frac{(t - r/c)}{(1-\beta)^2}, \quad i, k = \theta, \varphi, \tag{24a}$$

In the case of conductivity arising in an unmoving medium, it is

$$\left[\vec{E}\right]_i = \left[\vec{H}\right]_k \cong -E_0 \frac{V_0}{r} \frac{(t - r/c)}{(1-\beta)}, \quad i, k = \theta, \varphi. \tag{24b}$$ /101

Formulas (24a) and (24b) are valid only for the first stage of the process, which corresponds at the observation site to the time interval from $t - \frac{r}{c}$ to $t - \frac{r}{c} + \frac{\alpha_0(1-\beta)}{V_0}$; both signals are linearly increase of the first (and, consequently, the amplitude attained at the end of the given stage) is $(1-\beta)^{-1}$ times greater.

When the sphere ceases to expand, the equation for the dipole moment acquires the following form:

$$\tau_0^2 \Phi_{1tt}'' + \tau_0 \Phi_{1t}' + \Phi_1 = -E_0 a_0^3; \quad \tau_0 = a_0/c.$$

The general solution, i.e.,

$$\Phi_1\left(t_a - \frac{a_0}{c}\right) = -E_0 a_0^3 + e^{-\frac{(t_a - a_0/c)}{2\tau_0}} \left\{C_1 \sin\left[\frac{\sqrt{3}(t_a - a_0/c)}{2\tau_0} + C_2\right]\right\}$$

contains two arbitrary constants determined from the condition of continuity in Φ_1 and $\partial\Phi_1/\partial t$ at the juncture of the two steps in the process. As a result, the form of the electromagnetic pulse in the emission zone ($\tau = t - \frac{r}{c} > \frac{\alpha_0}{V_0}(1-\beta)$) is found to be equal to the following in the two cases we have examined (we will consider, as before, that $1-\beta \ll 1$):

$$\left[\vec{E}\right]_i \cong \left[\vec{H}\right]_k \cong \frac{E_0 a_0}{r} e^{-\tau/2\tau_0} \sin\left\{\frac{\sqrt{3}\tau}{2\tau_0} - \frac{\pi}{6}\right\}, \tag{25a}$$

$$\left|\vec{E}\right|_i \cong \left|\vec{H}\right|_k \cong \frac{2E_0 a_0}{\sqrt{3} r} e^{-\frac{\tau}{2\tau_0}} \sin\left\{\frac{\sqrt{3}\tau}{2\tau_0} - \frac{\pi}{3}\right\}, \quad i, k = \theta, \varphi. \tag{25b}$$

The pulse lasts a time on the order of $\tau_0 = \frac{\alpha_0}{c}$ (natural oscillations of the dipole type take place in the external range, in respect to the ideally conducting sphere). There are no fundamental

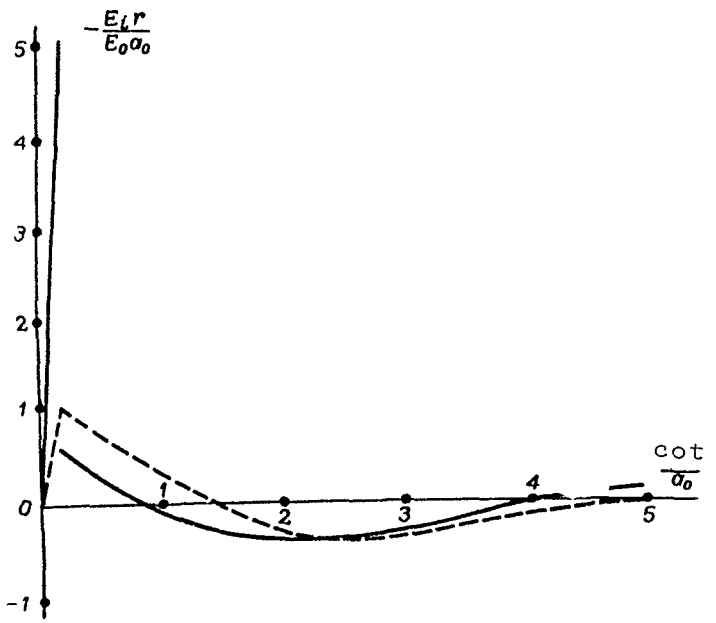

Fig. 2

differences between the fields of (25a) and (25b). The energy emitted by the natural damping vibrations at this stage is commensurable with the energy reserve $\frac{1}{6} E_0^2 a_0^2$ of the static field in the sphere with radius a_0. In the first step, the energy emitted by the moving conductor is an order [$(1 - \beta)^{-1}$ times] greater than this value. On the other hand, the conducting sphere with immobile substance emits energy which is $(1 - \beta)$ times less in its expansion. Figure 2 shows forms of signals arising in the emission field for $\beta = 0.8$. The solid curve corresponds to the case of motion of the substance, while the dotted curve corresponds to motion of the state.

Thus, even the simplest examples clearly show the uniqueness /102 of the process of wave diffraction on bodies of variable size. It is accompanied by the effects of transformation of the spectrum and parametric emission.

APPENDIX

Let us define which Debye potentials u_0 and v_0 correspond to the incident plane wave of (1). According to (5) and (6), we can find the following for the radial component of the incident field E_0:

$$(\varepsilon_0)_2 = \sin\theta\cos\varphi f\left(t-\frac{z}{c}\right) = -\frac{1}{c^2}\cdot\frac{\partial^2}{\partial t^2}(ru_0)+\frac{\partial^2}{\partial r^2}(ru_0). \qquad (I)$$

According to the theorem of expansion obtained in our study [4],

$$f\left(t-\frac{z}{c}\right)=\sum_{n=0}^{\infty} f_n(r,\ t)\,P_n(\cos\theta), \qquad (II)$$

where

$$f_n(r,\ t)=(-c)^{n+1}L_nD^{-(n+1)}\left(n+\frac{1}{2}\right)\left\{f\left(t-\frac{r}{c}\right)-f\left(t+\frac{r}{c}\right)\right\},$$
$$L_n=r^n\left(\frac{\partial}{r\partial r}\right)^n\frac{1}{r},$$

while $D^{-(n+1)}$ signifies integration by the variable t (n+1) times. The left-hand part of (I) can be converted in the following way with the aid of (II):

$$\sin\theta\cos\varphi f\left(t-\frac{z}{c}\right)=\frac{c}{r}\cos\varphi\frac{\partial}{\partial\theta}\int f\left(t-\frac{r\cos\theta}{c}\right)dt=$$
$$=-\frac{c}{r}\sum_{n=1}^{\infty}\int f_n(r,\ t)\,dtP_n^{(1)}(\cos\theta)\cos\varphi,$$

where we found that the following relationship holds for the Legendre polynomials:

$$\frac{\partial P_n}{\partial\theta}=-P_n^{(1)}(\cos\theta).$$

The right-hand part of (I) can also be represented in the form of expansion by spherical functions $P_n^{(1)}(\cos\theta)\cos\phi$. Following the general principle for solving a wave equation in the form of an expansion by non-stationary spherical waves [4], we can write out u_0 in the form of

$$u_0(\vec{r},\ t)=\sum_{n=1}^{\infty} L_n\{u_{0n}(r,\ t)\}\,P_n^{(1)}(\sin\theta)\cos\varphi,$$

and, to find the functions $u_{0n}(r, t)$ we will use (I). It follows from the orthogonality of the functions $P_n^{(1)}$ (cos θ) cos φ that

$$-\frac{c}{r}\int f_n(r, t)\,dt = \frac{\partial^2}{\partial r^2}(ru_{0n}) - \frac{1}{c^2}\cdot\frac{\partial^2}{\partial t^2}(ru_{0n}). \qquad \text{(III)}$$

In order to simplifty (III), we should note that (4) shows the fol-/103 lowing for ru_{0n}:

$$\frac{\partial^2}{\partial r^2}(ru_{0n}) - \frac{1}{c^2}\cdot\frac{\partial^2}{\partial t^2}(ru_{0n}) +$$
$$+ (ru_{0n})\left\{\frac{1}{r^2\sin\theta P_n^{(1)}(\cos\theta)}\cdot\frac{\partial}{\partial\theta}\left[\sin\theta\frac{\partial}{\partial\theta}P_n^{(1)}(\cos\theta)\right] - \frac{1}{r^2\sin^2\theta}\right\} = 0.$$

Let us also consider that $P_n^{(1)}$ (cos θ) is a solution to the equation

$$\frac{1}{\sin\theta}\cdot\frac{\partial}{\partial\theta}\left(\sin\theta\frac{\partial P_n^{(1)}}{\partial\theta}\right) + \left[n(n+1) - \frac{1}{\sin^2\theta}\right]P_n^{(1)} = 0.$$

As a result, (III) is reduced to the form of

$$-\frac{c}{r}\int f_n(r, t)\,dt = \frac{u_{0n}\cdot n(n+1)}{r}, \qquad \text{(IIIa)}$$

and the Debye potential $u_0(\vec{r}, t)$ of the incident wave for (I) can be represented in the following expansion by spherical functions:

$$u_0(\vec{r}, t) = \sum_{n=1}^{\infty}\frac{\left(n+\frac{1}{2}\right)}{n(n+1)}(-c)^{n+2}L_nD^{-(n+2)}\left\{f\left(t-\frac{r}{c}\right) - f\left(t+\frac{r}{c}\right)\right\}P_n^{(1)}(\cos\theta)\cos\varphi. \qquad \text{(IV)}$$

An almost analogous formula can be obtained for $v_0(\vec{r}, t)$;

$$v_0(\vec{r}, t) = \sum_{n=1}^{\infty}\frac{\left(n+\frac{1}{2}\right)}{n(n+1)}(-c)^{n+2}L_nD^{-(n+2)}\left\{f\left(t-\frac{r}{c}\right) - f\left(t+\frac{r}{c}\right)\right\}P_n^{(1)}(\cos\theta)\sin\varphi. \qquad \text{(V)}$$

REFERENCES

1. Landau, L.D. and Ye.M. Livshits: Teoriya polya (Field Theory). "Fizmatgiz", 1960.
2. Kovalev, A.S. and V.N. Krasil'nikov: Reflection of Electromagnetic Waves by a Moving Mirror. Zhur. Teoret. Fiz., Vol. XXXII, No. I, 1962.
3. Frank, F. and R. Mizes: Differential and Integral Equation of Mathematical Physics. ONTI, 1937.
4. Krasil'nikov, V.N.: Solving a Wave Equation in a Spherical System of Coordinates. This Collection, p. 77.
5. Krasil'nikov, V.N.: A Study of Electromagnetic Waves of an Ideally Conducting Sphere Pulsing in a Uniform Field. In the Collection: Problemy difraktsii i rasprostraneniya voln (Problems of Wave Diffraction and Propagation), No. 4, Leningrad State Univ. Press, 1965.

DIFFRACTION OF AN ELECTROMAGNETIC FIELD ON AN UNBOUNDED HOLLOW CYLINDER IN A CONDUCTING HALF-SPACE

O.G. Kozina and K.F. Filippov

ABSTRACT: The authors look for a field diffracted on a hollow cylinder of infinite length in the lower conducting half-space of a two-layered medium divided by a plane boundary, which is produced by vertical or horizontal magnetic dipoles in the lower half-space. It is found that a vertical magnetic dipole is more sensitive to all discontinuities than a horizontal one.

A two-layered medium divided by a plane boundary is investigated in this article. /10 A hollow cylinder of infinite length is located in the lower conducting half-space near the boundary. We are looking for the field diffracted on the cylinder which is produced by vertical or horizontal magnetic dipoles in the lower half-space.

We will consider that the lower conducting half-space is characterized by the parameters ε_1, μ_1 and σ_1. The upper half-space and the insides of the cylinder of radius a are characterized by the parameters ε_2 and μ_2 ($\sigma_2 = 0$).

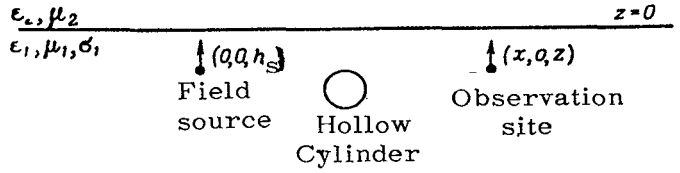

Fig. 1.

We will use the Cartesian system of coordinates in order that the plane z = 0 might coincide with the plane boundary between the media, and that the axis z might be perpendicular to the latter. The source of the field with coordinates (0,0, h_s) and the observation site (x, 0, z) are of lesser depth than their distance along the horizontal (Fig. 1).

$$z \ll x \text{ и } h_s \ll x. \qquad (1)$$

Here h_s is the depth of submersion of the transmitter.

The problem of the diffraction of a field on an unbounded cylinder in a uniform medium has been investigated for a long time [1]; the existence of a plane boundary complicates it to a great extent. In physical terms, the existence of such a boundary results in a situation where a system of multiply reflected waves arises between the cylinder and the boundary. If the secondary field due to the disturbing effect of the cylinder is small, then we can expect that the multiply "reflected" waves will be greatly weakened, and the waves which undergo a small number of reflections, which can be found by the method of successive approximations, will play the most important role.

Let us apply this method to a solution of our problem, and let us divide it into a number of steps. For the first step, we will consider that there is no cylinder, and there is only a two-layered medium with a field source in the form of a magnetic dipole. We will use the results obtained in [2] for this step, but the plane boundary will be replaced by fictitious sources in a uniform medium, with parameters of the lower half-space. These sources have different forms for vertical and horizontal emitting dipoles.

For the second step, we will solve the problem of the diffraction of an electromagnetic field on a hollow cylinder in a uniform conducting medium for each source separately.

For the third step, we will make the cylinder itself similar to some source of a field, and in solving the problem of diffraction of the field produced by this source there is a field reflected twice from the plane. The latter can be considered as the incident field, and we can again solve the problem of diffraction of a field on a cylinder. When the cylinder is a certain distance from the boundary, this process will rapidly converge, and it can be stopped after the third step.

Let us turn to a solution of the problem formulated and consider, first of all, the case when there is no cylinder, while there is a vertical magnetic dipole in the lower conducting half-space.

If we are interested in distances between the source of the field and the observation sites which are much less than the wavelength in the upper medium, i.e.,

$$x \ll \lambda_2, \tag{2}$$

then we can assume that $k_2 = 0$, and we will obtain an approximative expression for the Hertz vector. As shown in [2], this expression

has the following form:

$$\Pi_z^* = \frac{M_0}{4\pi}\left\{\frac{e^{ik_1R}}{R} - \frac{e^{ik_1R'}}{R'} - \frac{2}{k_1^2}\cdot\frac{\partial^2}{\partial z^2}\left(\frac{e^{ik_1R'}}{R'}\right) - \pi i\frac{\partial}{\partial z}J_0(n)H_0^{(1)}(m) - \right.$$
$$\left. - \frac{\pi i}{k_1^2}\cdot\frac{\partial^3}{\partial z^3}J_0(n)H_0^{(1)}(m)\right\} = \Pi_{z_1}^* + \Pi_{z_2}^* + \Pi_{z_3}^* + \Pi_{z_4}^* + \Pi_{z_5}^*, \quad (3)$$

where $R = \sqrt{x^2 + (z - h_s)^2}$ and $R' = \sqrt{x^2 + (z + h_s)^2}$ are the distances from the primary and mirror sources to the observation site; M_0 is the magnetic dipole moment; /106

$$n = \frac{k_1}{2}\sqrt{(R')^2 - (z + h_s)^2};$$
$$m = \frac{k_1}{2}\sqrt{(R')^2 + (z + h_s)^2};$$

J_0 and H_0 are Bessel functions; $k_1^2 = k_0^2\,\varepsilon'_{m_1}\mu_{m_1}$; k_0 is the wave number for vacuum; ε'_{m_1} and μ_{m_1} are the complex relative permittivity and relative magnetic susceptibility, respectively.

The first term in (3) describes the field of the primary source, while the remaining terms describe the field of fictitious sources due to the presence of a plane boundary. In this regard, $\Pi^*_{z_2}$ is the Hertz vector of the mirror source, $\Pi^*_{z_3}$ is the Hertz vector of the octupole, while Π_{z_4} and Π_{z_5} correspond to the field of two-dimensional sources producing waves which, in the future, we will call "refraction waves". We will use the formula

$$H = \text{grad div}\,\Pi + k^2\Pi \quad (4)$$

and substitute (3) into (4). We will then find all the components of the field, which we wi-l call the components of the "direct" field, while the field caused by the cylinder will be called the diffracted one.

Table 1 shows approximating expressions for the "direct" fields H_z and H_x with a consideration of (1) ($H_y = 0$ at the selected observation site for $y = 0$). It can be seen from the table that, in the vicinity of the surface ($h_s \approx z \approx 0$), the field of the primary and mirror sources is close to zero. This can be explained in physical terms by the fact that the waves are in opposite phase and compensate for each other. When the following condition is fulfilled,

$$|k_1R'| > 1 \quad (5)$$

the field of the octupole attenuates exponentially. Under these conditions, the components $\Pi^*_{z_4}$ and $\Pi^*_{z_5}$ make the principal contribution to the field at the observation point; for these components, there is no exponential attenuation with distance along the horizontal. In order to show the mechanism for propagation of these waves, let us turn to their phase, which has the form of

$$\varphi = \operatorname{Re} k_1 (h_s + z).$$

A wave with such phase can be ascribed the following path (Fig. 2). From the lower conducting medium, the wave goes to the surface, where it is propagated without attenuation ($k_2 = 0$) up to the projection of the receiving point on the plane boundary, and then again descends to the lower medium and is detected by the receiver.

TABLE 1 /1

Hertz Vector	Magnetic Field
$\Pi^*_{z_{1,2}} = \frac{M_0}{4\pi}\left[\frac{e^{ik_1R}}{R} - \frac{e^{ik_1R'}}{R'}\right]$ Primary and mirror source	$H_z = \frac{M_0}{2\pi} k_1^3 \frac{e^{ik_1R'}}{k_1 x} \cdot \frac{h_s z}{RR'}(1 - ik_1R'),$ $H_x = -\frac{M_0}{2\pi} k_1^3 \frac{e^{ik_1R'}}{k_1^3 RR'} \cdot \frac{h_s}{x^2}(1 - ik_1R' + ik_1x)$
$\Pi^*_{z_3} = -\frac{M_0}{2\pi} \cdot \frac{1}{k_1^2} \cdot \frac{\partial^2}{\partial z^2} \cdot \frac{e^{ik_1R'}}{R'}$ Octupole	$H_z = \frac{M_0}{2\pi} k_1^3 e^{ik_1R'}\left[-\frac{9}{(k_1R')^5} + \frac{9i}{(k_1R')^4} + \frac{4}{(k_1R')^3} - \frac{i}{(k_1R')^2}\right],$ $H_x = \frac{M_0}{4\pi} k_1^3 \frac{(h_s + z)x e^{ik_1R'}}{(R')^2}\left[\frac{45}{(k_1R')^5} - \frac{36i}{(k_1R')^4} - \frac{9}{(k_1R')^3}\right]$
$\Pi^*_{z_4} + \Pi^*_{z_5} = -\frac{M_0}{4} i\left[\frac{\partial}{\partial z} J_0(n) H_0^{(1)}(m) + \frac{1}{k_1^2} \cdot \frac{\partial^3}{\partial z^3} J_0(n) H_0^{(1)}(m)\right]$ Planar source	$H_z = \frac{9M_0}{2\pi} k_1^3 \frac{e^{ik_1(h_s+z)}}{(k_1x)^5},$ $H_x = -\frac{3M_0}{2\pi} k_1^3 \frac{e^{ik_1(h_s+z)}}{(k_1x)^4}$

According to Table 1, the refraction wave consists of two components:

$$H_x = -\frac{3M_0}{2\pi} k_1^3 \frac{e^{ik_1(h_s+z)}}{(k_1x)^4}, \quad (6)$$

$$H_z = \frac{9M_0}{2\pi} k_1^3 \frac{e^{ik_1(h_s+z)}}{(k_1x)^5}. \quad (7)$$

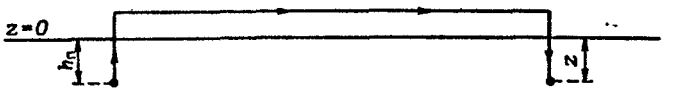

Fig. 2.

Turning to E_y, according to the formula

$$\text{rot}\, H = -i\omega\varepsilon' E$$

or

$$\frac{\partial H_x}{\partial z} - \frac{\partial H_z}{\partial x} = -i\omega\varepsilon' E_y \qquad (8)$$

and considering (6) and (7), we have the following: /10

$$E_{y_1} = \frac{3iM_0}{2\pi} k_1^3 \sqrt{\frac{\mu_0}{\varepsilon'}} \cdot \frac{e^{ik_1(h_S+z)}}{(k_1 x)^4}, \qquad (9)$$

$$E_{y_2} = \frac{45iM_0}{2\pi} k_1^3 \sqrt{\frac{\mu_0}{\varepsilon'}} \cdot \frac{e^{ik_1(h_S+z)}}{(k_1 x)^6}. \qquad (10)$$

Expressions (6), (7), (8), and (9) describe the field on the lines y = 0. In the future, we will consider that the field is defined by the same expressions for any y. In order to evaluate the admissable error, we should note that the refraction waves can be described by a set of two-dimensional sources with annular currents, as depicted in Figure 3. A disregard of the value y is equivalent to a situation where the annular current is replaced by the linear one (see the dotted line on Figure 3), and this corresponds to a replacement of a point source by a source in the form of a filament. It is clear from the physical materials that this type of substitution does not bring about a large error for a cylinder which is sufficiently removed from the source. In this case, we can find a quantitative estimate of the admissable error. For this purpose, the field incident on the cylinder is expanded by plane waves with such computations that the principal term of the

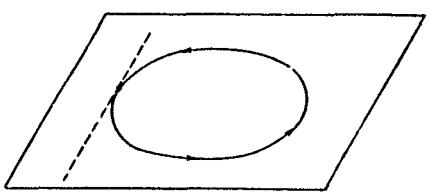

Fig. 3.

expansion coincides with the solutions we have obtained.[1] The evaluations show that the major term describes the field in full very well when the cylinder is a distance on the order of the wavelength in the lower medium from the observation site. This can be explained in physical terms by the fact that, for small radii of the cylinder, the induced currents are directed mainly along the axis of the cylinder; therefore, the form of the source is not of great significance [3, 4].

As the evaluations show, in fulfilling the condition

$$\frac{\omega d}{x_0} \ll 1,$$

i.e., for a small radius of the cylinder (compared to its distance from the source), we can consider that the value $k_1 x$ changes little along the cross section of the cylinder, and it can be replaced by $k_1 x_0$. We can then consider the fields from (6), (7) or (8) and (9) to be plane, which simplifies all further computations to a great extent. In this medium, there is an unbounded cylinder on which a plane wave falls, i.e., /109

$$E_y = -\frac{3M_0}{2\pi} ik_1^3 \sqrt{\frac{\mu_0}{\varepsilon'}} \cdot \frac{e^{ik_1(h_S+z)}}{(k_1 x_0)^4} \left[1 + \frac{15}{k_1 x_0}\right], \qquad (11)$$

The front of this wave is parallel to the axis of the cylinder.

In order to find the diffracted field, let us turn to the cylindrical system of coordinates for the following formula:

$$z = z_0 + r\cos\varphi,$$

where z_0 is the coordinate of the cylinder axis. We will consider that the axis y of the Cartesian system is parallel to the axis z of the cylindrical system. The problem of the incidence of a plane wave on the cylinder is then solved by the standard methods. Therefore, we will present the prepared solution for the diffracted field here directly:

$$E_{y\,\mathrm{dif}} = \sum_{m=0}^{\infty} A_m H_m^{(1)}(k_1 r)\cos m\varphi, \qquad (12)$$

[1] This solution is very cumbersome, and we therefore will not present it here.

where A_m contains a combination of Bessel functions and (11). When there is satisfaction of the condition

$$|k_1 a| \ll 1 \tag{13}$$

and m = 0, this field acquires the following form:

$$E_{y\,\mathrm{dif}} = -\frac{3}{8} M_0 k_1^3 \frac{(k_1 a)^2}{(k_1 x_0)^4} \sqrt{\frac{\mu_0}{\varepsilon'}} e^{ik_1(h_s + z_0)} H_0^{(1)}(k_1 r)\left[1 + \frac{15}{(k_1 x_0)^2}\right], \tag{14}$$

where x_0 is the distance from the axis of the cylinder to the transmitter. It can be seen from (14) that the field represented by the first term of the series is proportional to $(k_1 a)^2$, and the n-th term of the series contains the factor $(k_1 a)^{2(n+1)}$, which guarantees convergence of the series as a geometric progression when (13) is fulfilled, due to which the terms following it need not be considered. This is all the more valid if we consider that we have approximated the incident field in terms of the plane wave, as a result of which the admissable error is comparable to the discarded terms of the series for the diffracted field.

It can also be seen from (14) that the diffracted field which has been found represents a sky wave propagating directly in the conducting medium, where it attenuates exponentially. As a result of this, the field component which has been found makes a small contribution to the total field at the observation point.

The refraction wave produced by the cylinder itself will make a much greater contribution if the latter is at a small depth from the boundary, and if the following condition if fulfilled:

$$|k_1 z_0| < 1,$$

while its distance from the transmitter and receiver greatly exceeds the wavelength in the conducting medium. As mentioned above, this circumstance is due to the fact that the refraction waves undergo exponential attenuation only along the path corresponding to the shortest distance to the surface, while the sky waves undergo exponential attenuation over the entire course of propagation.

Figure 4 shows the course of propagation of refraction waves incident on a cylinder and diffracted on it.

In order to find the field of a refraction wave going from the cylinder along the surface to the receiving point, we will

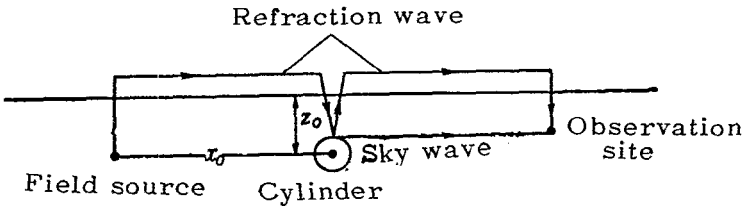

Fig. 4.

make the cylinder similar to a source in the form of a filament [5], and we will call this field an incident one, i.e.,

$$E_{y\,\mathrm{inc}} = A_i H_0^{(1)}(k_1 r). \tag{15}$$

Having solved the problem of the field of a filamentary source in the presence of a boundary, we can find the field reflected from it in the following form:

$$E_{y\,\mathrm{ref}} = -\frac{A_i}{4\pi}\int_{-\infty}^{\infty}\frac{\left[\sqrt{\mu^2-k_2^2}-\sqrt{\mu^2-k_1^2}\right]e^{-\sqrt{\mu^2-k_1^2}(z+z_0)+i\mu(x-x_0)}}{\sqrt{\mu^2-k_1^2}\left[\sqrt{\mu^2-k_1^2}+\sqrt{\mu^2-k_2^2}\right]}d\mu. \tag{16}$$

Considering that

$$\mathrm{rot}\,E = i\omega\mu_0 H,$$

we have the following expression for the vertical field component:

$$H_z = \frac{1}{i\omega\mu_0}\cdot\frac{\partial E_y}{\partial x} = -\frac{Ai}{\omega\mu_0 4\pi}\int_{-\infty}^{\infty}\frac{\mu\left[\sqrt{\mu^2-k_2^2}-\sqrt{\mu^2-k_1^2}\right]}{\sqrt{\mu^2-k_1^2}\left[\sqrt{\mu^2-k_2^2}+\sqrt{\mu^2-k_1^2}\right]}\times \\ \times e^{-\sqrt{\mu^2-k_1^2}(z+z_0)+i\mu(x-x_0)}d\mu. \tag{17}$$

In order to calculate this integral, we will draw divisions from the branching point $\mu = k_{1,2}$ on the complex plane in such a way that $\mathrm{Re}\sqrt{\mu^2 - k_1^2} = 0$ along the division, and we will call that sheet on which $\mathrm{Re}\sqrt{\mu^2 - k_{1,2}^2} > 0$ the upper one. This guarantees convergence and freedom of the deformation of the contour on the upper sheet. Calculations of the integral in (17) by the division k_2 then give the total field of the refraction wave in the follow- /111

ing form, considering (2):

$$H_{z_1}+H_{z_2}=\frac{3M_0}{\pi}\cdot\frac{k_1^3(k_1a)^2e^{ik_1(h_s+2z_0+z)}}{(k_1x_0)^4k_1^3(x-x_0)^3}\left[1+\frac{15}{(k_1x_0)^2}\right]. \tag{18}$$

Calculations of the integral in (17) by the division k_1 give sky waves, which are much less than the field from (18) for the condition in (5) due to exponential attenuation, and therefore are not presented here.

Thus, if the source of a field, the cylinder and the observation site are located in the neighborhood of the boundary, then refraction waves produced by various sources arise: (a) going from the primary source to the observation site (these waves produce the principal part of the "direct" field) and (b) going to the observation site from the cylinder itself (as a source of the field). These waves produce the main part of the diffracted field at the receiving point; nevertheless, this field is noticeably less than the direct field produced by refraction waves from the primary source. Actually, if we compare (7) and (18), then we can see that the diffracted field contains the factor $(k_1a)^2$, which is much less than unity, and the factor k_1x in the denominator, which is much greater than unity in modulus and has a higher power.

In order to better understand the magnitude of the diffracted field, we will compare it to the direct one, and assume that the hollow cylinder is in the middle between the transmitter and receiver, so that the following equality holds:

$$x=2x_0.$$

The field ratio of interest to us then acquires the following form:

$$\frac{H_z\,\text{dif}}{H_z\,\text{dir}}=\frac{64}{3}\left(\frac{a}{x_0}\right)^2\left[1+\frac{15}{(k_1x_0)^2}\right]. \tag{19}$$

The ratio obtained determines the maximum distance from the transmitter and receiver to the cylinder for a given radius a, for which the field differs greatly at the observation site from the field in the uniform two-layered medium.

Let us now find under which conditions we can disregard the subsequent reflections from the plane to the cylinder and back, and limit ourselves to the results obtained. For this purpose, we will compare the direct field of a refraction wave incident on a cylinder for the first time [see (11)] and the field of a refraction wave which is produced by the cylinder, reflected from the plane boundary, and again incident upon the cylinder [see (20)]. The purpose of this comparison is to lead directly to the surface of the cylinder, and we will therefore assume that $x = x_0$ and $z = z_0$ in (17). After calculating the integral in (17) by the division k_2, we will obtain the following field: /112

$$E_y = \frac{3M_0}{4\pi} \cdot \frac{k_1^3}{k_1 z_0} \sqrt{\frac{\mu_0}{\varepsilon'}} \cdot \frac{(k_1 a)^3}{(k_1 x_0)^2} e^{ik_1(h_S + 3z_0)} \left[1 + \frac{i}{k_1 z_0}\right]. \qquad (20)$$

TABLE 2

Hertz Vector	Magnetic Field
$\Pi_y^* = \frac{M_0}{4\pi}\left[\frac{e^{ik_1R}}{R} - \frac{e^{ik_1R'}}{R'}\right]$ Primary and mirror source	$H_y \approx \frac{M_0}{2\pi} k_1^3 e^{ik_1R} \frac{\overset{5}{h}_{\text{пр}} z}{RR'}\left[\frac{1}{k_1 x} + \frac{2i\overset{5}{h}_{\text{пр}} z}{x^2}\right]$
$\Pi_{z_1}^* = \frac{M_0 l}{4k_1^2} \cdot \frac{\partial^3}{\partial z^2 \partial y} J_0(n) H_0^{(1)}(m)$ Planar source	$H_y \approx -\frac{M_0}{2\pi} k_1^3 \frac{e^{ik_1(\overset{5}{h}_{\text{пр}} + z)}}{(k_1 x)^3}\left[1 + \frac{3}{(k_1 x)^2}\right]$
$\Pi_{z_1}^* = \frac{M_0}{2\pi k_1^2} \cdot \frac{\partial^2}{\partial z \partial y}\left(\frac{e^{ik_1R'}}{R'}\right)$ Octupole	$H_y \approx \frac{M_0}{2\pi} k_1^3 \frac{e^{ik_1R'}}{(k_1R')^3}\left[\frac{3}{(k_1R')^2} - \frac{3i}{k_1R'} - 1\right]$

Having compared the secondary refraction wave obtained to the refraction wave incident for the first time on the cylinder, we find that

$$\frac{E_{y(20)}}{E_{y(11)}} = \frac{1}{2}\left(\frac{a}{z_0}\right)^2 e^{i2k_1 z_0}. \qquad (21)$$

The condition for applicability of our method of successive approximations follows from the requirement that this ratio be small: $a < z_0$. Therefore, in deepening the cylinder z_0 by several of its radii a, we can disregard the subsequent reflections and limit ourselves to the result of (19).

All the calculations presented above were carried out for a vertical magnetic dipole. For a horizontal magnetic dipole, the calculations are carried out by similar methods; therefore, we will present here only the final results. It is considered that the horizontal dipole is directed along the y axis parallel to the axis of the cylinder.

The Hertz vector of the complete field, in its reflection from the plane boundary, when the dipole is in the uniform two-layered medium, has the following form for the same approximations:

$$\Pi_y^* = \frac{M_0}{4\pi}\left[\frac{e^{ik_1R}}{R} - \frac{e^{ik_1R'}}{R'}\right],$$

$$\Pi_z^* = \frac{M_0}{4\pi}\left\{\frac{2}{k_1^2}\cdot\frac{\partial^2}{\partial y\partial z}\cdot\left(\frac{e^{ik_1R'}}{R'}\right) + \frac{\pi i}{k_1^2}\cdot\frac{\partial^3}{\partial z^2\partial y}\left[J_0(n)H_0^{(1)}(m)\right]\right\}, \quad (22)$$

/113

Where the first term of Π_y^* described the field of the primary source, while the remaining terms of Π_y^* and Π_z^* are due to the presence of a plane boundary.

Expressions for the direct field in the approximation we are studying are given in Table 2. It can be seen from this table that the principal field component, as before, is produced by a refraction wave of the following type:

$$H_y = -\frac{M_0}{2\pi}k_1^3\frac{e^{ik_1(h_S+z)}}{(k_1x)^3}\left[1+\frac{3}{(k_1x)^2}\right]. \quad (23)$$

In the diffraction of this field on the cylinder, the latter produces a refraction wave, and this wave plays the major part at the receiving point. The ratio between the diffracted field from (23) and the direct field of the planar source then acquires the form of

$$\frac{H_{y\,\mathrm{dif}}}{H_{y\,\mathrm{dir}}} \approx \left(\frac{a}{x_0}\right)^2. \quad (24)$$

Having compared (24) and (19), we can conclude that a vertical magnetic dipole is more sensitive to all discontinuities than a horizontal one.

REFERENCES

1. Frank, F. and R. Mizes: Differentsial'nyye i integral'nyye uravneniya v matematicheskoy fizike (Differential and Integral Equations in Mathematical Physics). ONTI, 1937.
2. Kozina, O.G. and K.F. Filippov: Equivalent Sources in the Problem of the Field of a Magnetic Dipole in a Two-Layered Medium. In the Collection: Problemy difraktsii i rasprostraneniya voln (Problems of Wave Diffraction and Propagation), No. V. Leningrad State Univ. Press, 1966.
3. Wait, J.R.: "Some solution for electromagnetic problems involving spheroidal, spherical and cylindrical bodies." U.S. Nat. Bur. Stand. J. Res., Vol. 64B, No. 1, 1960.
4. Velikin, A.B. and G.S. Frantov: Eksperimental'nyye polya, primenyayemyye v induktsionnykh metodakh elektrorazvedki (Experimental Fields Applied in Induction Methods of Electrical Discharge). "Gostekhizdat", 1962.
5. Stratton, J.A.: Teoriya elektromagnetizma (Electromagnetism Theory). "Gostekhizdat", 1948.

DIFFRACTION OF AN ELECTROMAGNETIC WAVE ON A HOLLOW SPHERICAL DISCONTINUITY IN A CONDUCTING HALF-SPACE

O.G. Kozina, A.I. Pevzner and D.N. Chartorizhskiy

ABSTRACT: This article treats the problem of the case when there is a discontinuity in the form of a spherical shell located in the vicinity of the boundary surface in the conducting half-space of a two-layered medium. It is shown that the field of a vertical dipole is more sensitive to discontinuities than that of a horizontal one. It is also shown that, under certain conditions, the ratio between the field diffracted on a cylinder and the direct one is always greater than in the case of a sphere, and that this result can be anticipated by considering the geometry of the problem

The problems of the diffraction of an electromagnetic wave in/114 a two-layered medium consisting of conducting and nonconducting half-spaces divided by a plane surface were investigated in [1, 2]. In [2], the solution to the diffraction problem was applied to the case when there is a hollow cylinder of infinite length in the conducting half-space, in the vicinity of the boundary. We will examine a similar problem, for the case when there is a discontinuity in the form of a spherical shell located in the vicinity of the boundary surface in the conducting half-space. The source of the field is a magnetic dipole (horizontal or vertical, located in the conducting medium). The problem is solved on the assumption that the radius of the sphere is small in comparison to the wavelength in the conducting medium. It is also assumed that the distance from the magnetic dipole to the point at which the receiver is located, and the distance from each of these points to the sphere, are much greater than the wavelength in the conducting half-space but less than the wavelength in the nonconducting medium.

Let the lower conducting half-space in which the sphere is located be characterized by the parameters ε_1 μ_1 and σ_1. The upper half-space and the cavity of the sphere have parameters of ε_2 and μ_2 ($\sigma_2 = 0$). We will use the Cartesian system of coordinates in such a way that the plane $z = 0$ coincides with the plane of the division between the two media, while the axis 0z passes through the source of the field (see the figure). The coordinates of the source are $0,0,h_s$; the coordinates of the center of the sphere are $x_0,0,z_0$. We will be interested in the field at the receiving point located in the conducting medium which has coordinates of $x,0,z$.

The problem will be solved for the case of smallness of the sphere a in comparison to the wavelength in the lower medium, when the distances x_0, x and $(x-x_0)$ are much greater than the wavelenghts in the lower half-space λ_1 and much less than the wavelengths in the upper medium λ_2. Moreover, we will consider that the depth of /115 the dipole, sphere and receiving points is not substantial when compared to the horizontal distances, i.e.

$$\max\{h_S, z_0, z\} \ll \min\{x_0, x, (x-x_0)\}. \quad (1)$$

The field at the receiving point can be represented in the form of the sum of

$$\vec{H}=\vec{H}_{\text{dir}}+\vec{H}_{\text{dif}}, \quad (2)$$

where H_{dir} is that part of the field which is produced only because of diffraction of the field of the source on the surface of the boundary between the two media, in the absence of a sphere; in the future, we will call such a field a direct or undisturbed field; $\vec{H}_{dis}$ is the supplementary field (disturbance) caused by diffraction on the sphere of the field $\vec{H}_{dir}$. It is our task to calculate this value.

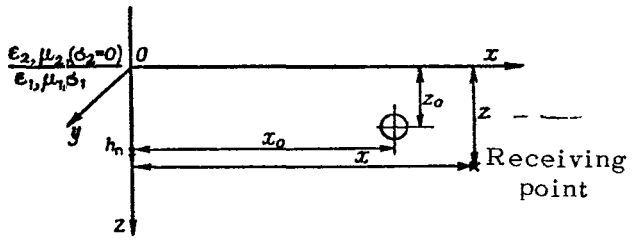

The first component can be found from the formulas obtained in [1]. In the case of vertical orientation of the dipole, the Hertz vector for the direct field in the lower medium has the following form:

$$\Pi_z^{\bullet}=\frac{M_0}{4\pi}\left\{\frac{e^{ik_1R}}{R}-\frac{e^{ik_1R'}}{R'}-\frac{2}{k_1^2}\cdot\frac{\partial^2}{\partial z^2}\left(\frac{e^{ik_1R'}}{k_1R'}\right)-\right.$$
$$\left.-\pi i\frac{\partial}{\partial z}\left[J_0(n)H_0^{(1)}(m)\right]-\frac{\pi i}{k_1^2}\cdot\frac{\partial^3}{\partial z^3}\left[J_0(n)H_0^{(1)}(m)\right]\right\}, \quad (3)$$

where M_0 is the magnetic dipole moment;

$$R = \sqrt{x^2 + (z - h_S)^2};$$
$$R' = \sqrt{x^2 + (z + h_S)^2};$$
$$n = \frac{k_1}{2}\sqrt{(R')^2 - (z + h_S)^2};$$
$$m = \frac{k_1}{2}\sqrt{(R')^2 + (z + h_S)^2};$$

J_0 and $H_0^{(1)}$ are the Bessel and Hankel functions of the first type, respectively;

$$k_1^2 = k_0^2 \varepsilon'_m \mu_{1m},$$

ε_m and μ_{1m} are the complex relative permittivity and relative magnetic susceptibility, $k_0 = 2\pi/\lambda$ is the wave number for vacuum. /116

We will solve this problem by the method of successive approximations, using the fact that the field in the lower medium can be represented as the result of multiple reflection of waves between the discontinuity and the surface of the boundary, when there is a discontinuity in it.

For example, we can construct the following qualitative picture for the case under investigation. A wave propagating from a source, after being reflected from the surface of the boundary, falls on a sphere; scattered by the sphere, it is again reflected from the boundary surface, and a wave which returns to the surface of the sphere is formed; this wave diffracts on the sphere a second time, etc. As a result, a field formed by the waves undergoing single, double, etc. reflection is added to the field $\vec{H}_{dir}$ at the observation site. From the mathematical point of view, these waves are terms of the series of successive approximations for the field $\vec{H}_{dif}$. As will be seen from subsequent calculations, this series converges very rapidly, which can be explained by the large amount of attenuation in a medium which has active losses due to the existence of conductivity.

We will calculate the results of reflections described above in order, and we will first define the field which produces a wave scattered once by the sphere at the observation site.

The values for the direct field are given in [1] in terms of $\vec{H}$ and $\vec{E}$. In view of the fact that these expressions are somewhat cumbersome, we will not write them out in full. We will only mention that, as was shown in [2], for distances between the sphere and the source of $x_0 >> \lambda_1$, which are small in comparison to the horizontal distance for the depths of submersion ($z_0 << x_0$), the field in the conducting medium is determined mainly by the refrac-

tion wave which has the following components:

$$H_x = -\frac{3M_0}{2\pi} k_1^3 \frac{e^{ik_1(h_S+z)}}{(k_1x)^4}; \tag{4}$$

$$H_z = \frac{9M_0}{2\pi} k_1^3 \frac{e^{ik_1(h_S+z)}}{(k_1x)^5}; \tag{5}$$

$$E_y = \frac{3M_0}{2\pi} ik_1^3 \sqrt{\frac{\mu}{\varepsilon'}} \frac{e^{ik_1(h_S+z)}}{(k_1x)^4}\left[1+\frac{15}{(k_1x)^2}\right]. \tag{6}$$

These expressions define the field of the incident wave on the lines y = 0. However, since the dimensions of the sphere are small ($|k_1a|<<1$), we can consider that the field is determined by the same expressions for all values of y on the surface of the sphere. The correctness of this assumption was discussed in [2]. In this case, a disregard of the dependence between the field and y in the neighborhood of the sphere results in even lesser errors. Moreover, when there is a satisfaction of the condition[1] /117

$$x_0 \gg 6a \tag{7}$$

we can consider that the field in the neighborhood of the sphere also does not change along the direction x, and that the wave incident on the sphere is plane. The components of this wave are found from (4), (5) and (6) by replacing k_1x by k_1x_0. The field of the wave scattered by the sphere is easily found by such simplifications.

The problem of the diffraction of a plane wave on a sphere is solved by the standard methods [3,4]. We will discuss the solution briefly in order to clarify the nature of the assumptions we have made. We will use the spherical coordinates r, θ and φ with origin at the center of the sphere; they are linked with the coordinates introduced above by the relationships

$$\begin{aligned} x &= x_0 + r\cos\varphi\sin\theta, \\ y &= r\sin\theta\sin\varphi, \\ z &= z_0 + r\cos\theta. \end{aligned} \tag{8}$$

It is convenient to describe the field in the spherical system of coordinates with the aid of Debye scalar potentials U and V, which are connected to the Hertz vector by the following formulas:

$$\begin{aligned} \vec{\Pi} &= \Pi_r\vec{e}_r = rU\vec{e}_r, \\ \vec{\Pi}^* &= \Pi_r^*\vec{e}_r = rV\vec{e}_r, \end{aligned} \tag{9}$$

[1] This condition follows in an obvious manner from the expansion of (6) into a Taylor series.

where Π_r and Π_r^* are the radial components of the electric and magnetic Hertz vectors, respectively.

In the case under investigation, a plane wave falls on the sphere, propagating in a direction parallel to the axis oz, and the solution for the wave scattered by the sphere can be written in the form of the following series:

$$U_{\text{ref}} = N_1 \sin\varphi \frac{\partial}{\partial\theta} \sum_{n=1}^{\infty} i^n a_n \frac{2n+1}{n(n+1)} \frac{\xi_n(k_1 r)}{k_1 r} P_n(\cos\theta); \tag{10}$$

$$V_{\text{ref}} = N_2 \cos\varphi \frac{\partial}{\partial\theta} \sum_{n=1}^{\infty} i^n b_n \frac{2n+1}{n(n+1)} \frac{\xi_n(k_1 r)}{k_1 r} P_n(\cos\theta) + \\ + N_3 \sum_{n=0}^{\infty} i^n b_n \frac{2n+1}{n(n+1)} \frac{\xi_n(k_1 r)}{k_1 r} P_n(\cos\theta), \tag{11}$$

Where N_1, N_2 and N_3 are constants depending on the amplitude of incident wave, i.e., /118

$$\xi_n(k_1 r) = \sqrt{\frac{\pi k_1 r}{2}} H^{(1)}_{n+\frac{1}{2}}(k_1 r);$$

$$a_n = -\frac{k_2 \psi_n'(k_1 a)\psi_n(k_2 a) - k_1 \mu_{2m} \psi_n(k_1 a)\psi_n'(k_2 a)}{k_2 \psi_n(k_2 a)\xi_n'(k_1 a) - k_1 \mu_{2m} \psi_n(k_1 a)\xi_n(k_2 a)};$$

$$b_n = -\frac{k_1 \mu_{2m} \psi_n'(k_1 a)\psi_n(k_2 a) - k_2 \psi_n(k_1 a)\psi_n'(k_2 a)}{k_1 \mu_{2m} \psi_n(k_2 a)\xi_n'(k_1 a) - k_2 \psi_n'(k_2 a)\xi_n(k_1 a)};$$

$$k_2^2 = k_0^2 \varepsilon_{2m} \mu_{2m},$$

ε_{2m} and μ_{2m} are the relative permittivity and relative magnetic susceptibility of the sphere;

$$\psi_n(k_1 r) = \sqrt{\frac{\pi k_1 r}{2}} J_{n+\frac{1}{2}}(k_1 r).$$

The small dimentions of the sphere allow us to consider only the first terms of the series in (10) and (11), i.e., the solution to the problem in a dipole approximation (see [5], for example). Having retained the first terms in the series in (10) and (11), having written out the coefficients N_1, N_2 and N_3 in explicit form, having replaced the functions $\psi_n(z)$ and $\xi_n(z)$ by their representations in the form of series, and having used the condition $|k_2 a| << |k_1 a|$, we can obtain the following expression for the field reflected by the sphere after a number of transformations:

$$U_{\text{ref}} = i \frac{3M_0}{4\pi} k_1 \sqrt{\frac{\mu}{\varepsilon}} (k_1 a)^3 \frac{e^{ik_1(n_S + z_0)}}{(k_1 x_0)^4} \left[1 + \frac{15}{(k_1 x_0)^2}\right] \times \\ \times \sin\varphi \sin\theta \frac{\partial}{\partial r}\left(\frac{e^{ik_1 r}}{k_1 r}\right), \tag{10a}$$

$$V_{\text{ref}} = -\frac{M_0}{2\pi} k_1 (k_1 a)^5 \frac{e^{ik_1(h_n+z_0)}}{(k_1 x_0)^4} \sin\theta\cos\varphi \frac{\partial}{\partial r}\left(\frac{e^{ik_1 r}}{k_1 r}\right) + \\ + \frac{3M_0}{2\pi} k_1 (k_1 a)^5 \frac{e^{ik_1(h_n+z_0)}}{(k_1 x_0)^5} \cos\theta \frac{\partial}{\partial r}\left(\frac{e^{ik_1 r}}{k_1 r}\right)^2 \qquad (11a)$$

It is easy to see that the field described by (10a) and (11a) can be represented as the sum of the fields produced by one electric and two magnetic dipoles located at the center of the sphere. Actually, we will use a Cartesian system of coordinates with origin at the center of the sphere which is connected to the spherical coordinate by the following relationships:

$$x' = r\sin\theta\cos\varphi,$$
$$y' = r\sin\theta\sin\varphi,$$
$$z' = r\cos\theta. \qquad (12)$$

Converting from the Debye potential U_{ref} to the Hertz vector with the aid of (9), we find that /119

$$\vec{\Pi} = i\frac{3M_0}{4\pi} k_1 \sqrt{\frac{\mu}{\varepsilon'}} (k_1 a)^3 \frac{e^{ik_1(h_S+z_0)}}{(k_1 x_0)^4}\left[1 + \frac{15}{(k_1 x_0)^2}\right] y' \operatorname{grad}\left(\frac{e^{ik_1 r}}{k_1 r}\right). \qquad (13)$$

Let us note the obvious equality of

$$y' \operatorname{grad}\left(\frac{e^{ik_1 r}}{k_1 r}\right) = \operatorname{grad}\left(y'\frac{e^{ik_1 r}}{k_1 r}\right) - \frac{e^{ik_1 r}}{k_1 r}\vec{e}_{y'}. \qquad (14)$$

Having substituted (14) into (13) and having rejected that part of the expression which contains the factor $\operatorname{grad}\left(y'\frac{e^{ik_1 r}}{k_1 r}\right)$, we find the following:

$$\vec{\Pi} = -i\frac{3M_0}{4\pi} k_1 \sqrt{\frac{\mu}{\varepsilon'}} (k_1 a)^3 \frac{e^{ik_1(h_S+z_0)}}{(k_1 x_0)^4}\left[1 + \frac{15}{(k_1 x_0)^2}\right] \frac{e^{ik_1 r}}{k_1 r}\vec{e}_{y'}. \qquad (15)$$

Expression (15) is a record of the field of the electric dipole which is located at the center of the sphere and directed along the axis y'. Having performed similar operations, we can convert from the potential V_{ref} to the magnetic Hertz vector, and we can represent the field described by the latter as a field of two magnetic dipoles, one of which is directed along the axis, z', while the other is directed along the axis x'. However, it is easy to see that

---

[2] In writing out (11a), we discarded the zero term in the second series in (11), since, in transferring to the Hertz vector with the aid of (9), it gives the complete gradient of the function and can be disregarded because of the gradient invariance of the Hertz vector.

the fields $\vec{E}$ and $\vec{H}$ produced by the magnetic dipoles are much smaller than the fields produced by the electric dipole, since the dipole moment of the magnetic dipoles contain the factor $(k_1 a)^5$, while the dipole moment of the electric dipole is proportional to $(k_1 a)^3$. Therefore, we will disregard the fields produced by the magnetic dipoles, and we will disregard the fields produced by the magnetic dipoles, and we will consider the field scattered by the sphere as the field of the electric dipole located at the center of the sphere and directed along the axis y'.

As was mentioned above, in order to determine the addition $\vec{H}_{dif}$ at the receiving point, we must consider the diffraction of the field scattered by the sphere at the boundary of the division between the conducting and nonconducting media. In this case, the problem is reduced to an investigation of the diffraction of the electric dipole field in the two-layered medium. This problem is solved by classical methods, and we will not discuss its solution here. We will only mention that, for distances of $x \ll \lambda_2$, the formulas for the fields have the same structure as the formulas presented in [1].

In the case under examination, the receiving point is removed from the sphere by a distance of $|x - x_0| \gg \lambda_1$; therefore, for shallow (compared to the horizontal distance) depths of submersion, the field at the receiving point will be produced because of the refraction wave going from the sphere, in a way similar to that for the cylinder in [2]. Computations give the following result for the vertical component of the wave undergoing single reflection from this sphere:

$$H_z \approx \frac{9M_0}{2\pi} k_1^3 (k_1 a)^3 \frac{e^{ik_1(h_S + 2z_0 + z)}}{(k_1 x_0)^4 k_1^4 (x - x_0)^4}. \qquad (16)$$ /120

A comparison between (16) and the field of the direct wave, the main part of which is given by (5), shows that, even for single reflection, the wave arrives at the receiving point in a greatly weakened state; a supplementary factor $(k_1 a)^3$ arises in the expression for the field in this case. Moreover, as can be seen from (16), the amplitude of the reflected wave decreases exponentially with an increase in the depth of submersion of the sphere. As was noted before, the addition of $\vec{H}_{dif}$ to the field at the receiving point, which arises because of the diffraction of the wave on the sphere, can be found as the sum of the fields of waves undergoing single, double, etc. reflections between the sphere and the boundary surface. However, it is easy to see that only the singly reflected wave should be considered. Actually, for a submersion of the sphere at a depth on the order of several of its radii (the latter condition is necessary in order to consider the sphere as a point source), the amplitude of the wave undergoing reflection twice contains the factor $(k_1 a)^6 e^{ik_1 4 z_0}$; that undergoing reflection three times contains the factor $(k_1 a)^9 e^{ik_1 6 z_0}$, etc., i.e., the fields of

these waves can be disregarded. This problem was discussed in more detail in [2] for a cylinder, and we will not stop on it. Thus, it can be considered that the addition to the field $\vec{H}_{dif} \approx H_z^{(1)}$.

In order to evaluate the ratio H_{zdif}/H_{zdir}, we will assume that $x = 2x_0$, i.e., we will consider that the sphere is located in the middle between the receiver and the emitter. For H_{zdir}, we will take its principal part determined by (5). Then

$$\frac{H_z \text{dif}}{H_z \text{dir}} = 32 (k_1 a)^3 \frac{e^{ik_1 2z_0}}{(k_1 x_0)^3}. \tag{17}$$

The ratio in (17) makes it possible to determine the maximum distance from the emitter and receiver to the sphere for which the field at the receiving point differs substantially from the "undisturbed" one.

The calculations presented were carried out for the case when the dipole of the source has vertical polarization. For a horizontal dipole, the problem is solved in a similar way, and we will present only the final result.

The direct field at the receiving point can be obtained from the Hertz vector describing the field in the lower medium. The expression for it is presented in [1], and has the following form:

$$\Pi_y^* = \frac{M_0}{4\pi} \left[\frac{e^{ik_1 R}}{R} - \frac{e^{ik_1 R'}}{R'} \right], \tag{18}$$

$$\Pi_z^* = \frac{M_0}{4\pi} \left\{ \frac{2}{k_1^2} \cdot \frac{\partial^2}{\partial y \partial z} \left(\frac{e^{ik_1 R'}}{R'} \right) + \frac{\pi i}{k_1^2} \cdot \frac{\partial^2}{\partial y \partial z^2} \left[J_0 (n) H_0^{(1)} (m) \right] \right\}. \tag{19}$$

The principal part of the field $\vec{H}_{dir}$ obtained from (18) and (19) with the aid of (3) for distances of $x >> \lambda_1$, for depths of submersion which are small in comparison to the horizontal distance, is determined by the refraction wave which has the y-th component, i.e., /12

$$H_y = -\frac{M_0}{2\pi} k_1^3 \frac{e^{ik_1 (h_S + z)}}{(k_1 x)^3} \left[1 + \frac{3}{(k_1 x)^2} \right]. \tag{20}$$

The addition to the direct field of $\vec{H}_{dif}$ is determined mainly by the wave reflected once from the sphere. The horizontal component of this wave is

$$\vec{H}_{y\,dif} = -\frac{M_0}{2\pi} k_1^3 (k_1 a)^3 \frac{e^{ik_1(h_S+2z_0+z)}}{(k_1 x_0)^3 k_1^3 (x - x_0)^3} + \\ + \frac{9M_0}{2\pi} k_1^3 (k_1 a)^3 \frac{e^{ik_1(h_S+2z_0+z)}}{(k_1 x_0)^4 k_1^4 (x - x_0)^4}. \quad (21)$$

The ratio H_{ydif}/H_{ydir} for the case of $x = 2x_0$ and sufficiently great distances has order of

$$\frac{H_{y\,dif}}{H_{y\,dir}} \approx 8 (k_1 a)^3 \frac{e^{ik_1 2z_0}}{(k_1 x_0)^3}. \quad (22)$$

A comparison of (22) and (17) allows us to conclude that the field of the vertical dipole is more sensitive to discontinuities than that of the horizontal one. The latter was already noted in [2] for the case when the discontinuity represented an unbounded hollow cylinder. Moreover, comparing (22) and (17) to the analogous expressions of (25) and (19) in [2], we can conclude that the ratio between the field diffracted on the cylinder and the direct one, for sufficiently small a/x_0, is always greater than in the case of a sphere. In addition, this result was anticipated by considering the geometry of the problem.

REFERENCES

1. Kozina, O.G. and K.F. Filippov: Equivalent Sources in the Problem of the Field of a Magnetic Dipole in a Two-Layered Medium. In the Collection: Problemy difraktsii i rasprostraneniya radiovoln (Problems of Radio-Wave Diffraction and Propagation), No. V. Leningrad State Univ. Press, 1966.
2. Kozina, O.G. and K.F. Filippov: Diffraction of an Electromagnetic Field on an Unbounded Hollow Cylinder in a Conducting Half-Space. This Collection, p. 104.
3. Fok, V.A.: The Field from a Vertical and Horizontal Dipole Held over the Surface of the Earth. Zhur. Eksper. i Teoret. Fiz., Vol. XIX, 1949.
4. Frank, F. and R. Mizes: Differentsial'nyye i integral'nyye uravneniya matematicheskoy fiziki (Differential and Integral Equations of Mathematical Physics). ONTI, 1937.
5. Morse, F.M. and H. Feshbach: Metody teoreticheskoy fiziki (Methods of Theoretical Physics), Vol. II. Foreign Literature Publishing House, 1960.

SOME FORMULAS FOR SHORT-WAVE ASYMPTOTICS IN THE THREE-DIMENSIONAL PROBLEM OF DIFFRACTION ON SMOOTH CONVEX BODIES

D. Sh. Mogilevskiy

ABSTRACT: This paper treats some formulas used for short-wave asymptotics in the three-dimensional problem of diffraction on smooth convex bodies. The studies of V.A. Fok and V.S. Buslayev in this regard are discussed, and combined formulas for these problems and the problems of light and shadow are given.

INTRODUCTION

Let S be the surface of a smooth convex body. The stationary problem of diffraction on the body S of waves from a point source located at point x' is then formulated in the following way: /122

$$(\Delta + k^2)\, U = -\delta(x - x'),$$

$$U|_S = 0,$$

$$r\left(\frac{\partial U}{\partial r} - ikU\right) \underset{r \to \infty}{\to} 0.$$

We are looking for the asymptotics of the function U for $k \to \infty$. It has been shown in studies treating this problem that the asymptotics differs greatly in regions of light and shadow. The asymptotics for the boundary layer near the surface of the body is found by the method of the parabolic equation developed mainly in the works of V.A. Fok (see [1], for example). Excellent formulas were obtained in [2] for the regions of light and shadow. However, these formulas lose their significance in the vicinity of the geometric boundary between the light and the shadow, as well as in shadow in the boundary layer around the surface of the body.

In 1962, V.S. Buslayev [3], using the method of the parabolic equation, obtained formulas for the two-dimensional problem which were valid in all regions and converted into Keller formulas where the latter had significance. In 1964, a detailed review of the work of V.S. Buslayev [4] was published. In this study, we will generalize some results of Buslayev for the three-dimensional case.

I. DERIVING THE ASYMPTOTICS IN SHADOW AT THE BOUNDARY LAYER /12

1. Geometry of Enveloping Waves

The phase of the enveloping wave is used for the region of the shade (Fig. 1), i.e.,

$$\Phi = t' + s + t,$$

where t' is the segment of the tangent from the source to the surface of the body; s is the geodesic segment; t is the segment of the tangent in the shaded region.

The phase Φ satisfys an eikonal equation

$$(\nabla\Phi)^2 = 1.$$

For the case when the observation point is on the surface of the body (for t = 0), we will use the designation Φ (t = 0) $\equiv$ u. The enveloping rays on the surface form a set of geodesic lines. We can use an orthoganal semi-geodesic system (u, v) with Lamé coefficients of $h_u = 1$ and $h_v = h_v(u, v)$.

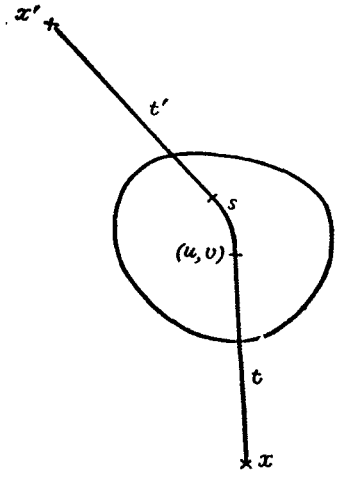

Figure 1.

In the neighborhood of the surface, on the boundary layer, we will expand Φ by powers n:

$$\Phi(u, v; n) = u + \delta_1 n^{\frac{3}{2}} + \\ + \delta_2 n^2 + O\left(n^{\frac{5}{2}}\right),$$

where n is the length along the normal to the surface at the point (u, v);

$$\delta_i = \delta_i(u, v).$$

Calculations show that

$$\frac{9}{4}\delta_1^2 = \frac{2}{\rho}, \qquad (1.1)$$

$$3\delta_1\delta_2 + \delta_1' = 0. \qquad (1.2)$$

Here ρ is the radius of curvature of the line u at the point (u, v);

$$\delta_1' = \frac{\partial\delta_1(u, v)}{\partial u}.$$

Let us introduce $\tau = -\delta_1 n^{\frac{3}{2}}$. Then,

$$\Delta(\Phi+\tau)|_{n=0} = 2\delta_2 + \frac{h_v'}{h_v}, \quad h_v' = \frac{\partial h_v}{\partial u}.$$

2. Calculation and Matching of Exponents

/124

We will look for the enveloping waves in the following form:

$$U = Ce^{ik(\Phi+\tau)}V.$$

We will write out $(\Delta + k^2)\,\underline{U}$ in the following way, considering that $(\nabla\Phi) = 1$:

$$(\Delta+k^2)\,U = Ce^{ik(\Phi+\tau)}\{\Delta V + ik\,[2(\nabla V,\ \nabla(\Phi+\tau)) + V\Delta(\Phi+\tau)] - k^2V\,[2(\nabla\Phi,\ \nabla\tau) + (\nabla\tau)^2]\}.$$

Consequently, the equation for $\underline{V}$ has the following appearance:

$$\Delta V + ik\,[2(\nabla V,\ \nabla(\Phi+\tau)) + V\Delta(\Phi+\tau)] - k^2V\,[2(\nabla\Phi,\ \nabla\tau) + (\nabla\tau)^2] = 0. \tag{1.3}$$

Let us examine (1.3) at the boundary layer. For this, we must substitute into (2.3) the expansions of Φ and τ by powers of $\underline{n}$, instead of those values themselves. At the boundary layer, high values of $\underline{k}$ will be compensated by low values of $\underline{n}$. Factors of the type $k^p\,n^{\frac{q}{2}}$ will be introduced into the coefficients of the equation. Arguments similar to those in [3] show that $n \sim k^{-\frac{2}{3}}$. The thickness of the boundary layer is then on the order of $k^{-\frac{2}{3}}$, while $\frac{\partial}{\partial n} \sim k^{\frac{1}{3}}$. The highest orders in the equation are $k^{\frac{4}{3}}$ and k.

We will write out only the terms for the two highest orders:

$$\underline{V_{nn}} + ik\left[\underline{2V_u} + 4\delta_2 n V_n + V\left(2\delta_2 + \frac{h_v'}{h_v}\right)\right] - k^2V\left[-\frac{9}{4}\delta_1^2 n - 6\delta_1\delta_2 n^{\frac{3}{2}} - 2\delta_1' n^{\frac{3}{2}}\right] = 0. \tag{1.4}$$

The terms containing $n^{\frac{3}{2}}$ are kept because of (1.2). The terms of the principle order ($k^{\underline{4}}$) are underlined. The remaining terms are of order $k^{\underline{3}}$.

3. Deriving the Parabolic Equation and Calculating the Smooth Factors

Let us introduce new variables

$$\lambda = \left(\frac{k}{2}\right)^{\frac{1}{3}} \int_{u'}^{u} \left(\frac{9}{8}\delta_1^2\right)^{\frac{2}{3}} d\sigma,$$
$$\mu = k^{\frac{2}{3}} n \left(\frac{9}{4}\delta_1^2\right)^{\frac{1}{3}}, \qquad (1.5)$$
$$\mu' = k^{\frac{2}{3}} n' \left(\frac{9}{4}\delta_1^2\right)^{\frac{1}{3}}.$$

The variables μ', u' and n' relate to the source, while the variables μ, u and n relate to the receiver. In determining λ, integration is carried out along the geodesic line v = const. For subsequent symmetrization, we will consider that the source is also on the boundary layer, $n' \sim k^{-\frac{2}{3}}$. /12

We will look for the solution in the form of

$$\dot{V} = \varphi(u, v)\Psi(\lambda, \mu, \mu').$$

We must again consider the differential operations for the new variables (only in the two highest orders) and substitute them into (1.4). We then find that

$$k^{\frac{4}{3}} \left(\frac{9}{4}\delta_1^2\right)^{\frac{2}{3}} \varphi \left[\Psi_{\mu\mu} + i\Psi_\lambda + \mu\Psi\right] +$$
$$+ ik\varphi\mu\Psi_\mu \left[4\delta_2 + \frac{4}{3}\delta_1^{-1}\delta_1'\right] + ik\Psi\left[2\varphi' + \varphi\left(2\delta_2 + \frac{h_v'}{h_v}\right)\right] = 0. \qquad (1.6)$$

The second brackets in (1.6) is equal to zero because of (1.2). Having made the first brackets equal to zero, we obtain the following for the equation for Ψ:

$$\Psi_{\mu\mu} + i\Psi_\lambda + \mu\Psi = 0. \qquad (1.7)$$

Equation (1.7) is often found in studies on diffraction. It is usually called "parabolic", although it is actually a Schrödinger equation. The terms of the principle order (k^3) are kept in the equation for $\underline{V}$ because of Ψ, while the terms of the next order (k) are kept because of ϕ. We can obtain the equation for ϕ by making the third brackets in (1.6) equal to zero:

$$2\varphi' + \varphi\left(2\delta_2 + \frac{h_v'}{h_v}\right) = 0. \tag{1.8}$$

We have obtained an ordinary differential equation. Having integrated it, and having considered (1.1) and (1.2), we find that

$$\varphi = C\rho^{-\frac{1}{6}} h_v^{-\frac{1}{2}} \tag{1.9}$$

4. Final Formula for the Boundary Layer

We still must integrate (1.7), with a consideration of the boundary condition that $\Psi|_{\mu=0} = 0$ and a condition for $\mu \to \infty$ equivalent to the condition for emission. Moreover, we must consider the reciprocity theorem: There should be symmetry relative to the rearrangements of the source and receiver. Let us write out the solution for Ψ, following [4]. The final formula has the following appearance:

$$U = Ce^{ik(\Phi+\tau)}\rho^{-\frac{1}{6}}(u)\,\rho^{-\frac{1}{6}}(u')\,h_v^{-\frac{1}{2}}\Psi(\lambda, \mu, \mu'), \tag{1.10}$$

/126

where

$$\begin{aligned}
\tau &= \delta_1(u)\,n^{\frac{3}{2}} - \delta_1(u')\,n'^{\frac{3}{2}};\\
\delta_1 &= \frac{2}{3}\sqrt{\frac{2}{\rho}};\\
\Psi &= \int_{-\infty}^{+\infty} d\zeta e^{i\zeta\lambda}\,\frac{w_1(\zeta-\mu')}{w_1(\zeta)}\,G(\zeta, \mu);\\
G(\zeta, \mu) &= w_2(\zeta-\mu)\,w_1(\zeta) - w_2(\zeta)\,w_1(\zeta-\mu) =\\
&= -2i\,[v(\zeta-\mu)\,w_1(\zeta) - v(\zeta)\,w_1(\zeta-\mu)].
\end{aligned} \tag{1.11}$$

The definitions and properties of the Airy functions w_1, w_2 and $\underline{v}$ can also be found in [4].

II. MOVING FROM THE BOUNDARY LAYER IN DEEP SHADOW

1. Geometry of the Enveloping Rays

Let us use a radial shadow coordinate system. The point is determined by the coordinates (u, v; Φ); (u, v) are the coordinates of the point of separation of the ray; Φ = u + t. The beam system is orthogonal. Φ = const is the wave surface, the principal radii of curvature of which are

$$\rho_1 = t, \quad \rho_2 = \rho_2^0 + t.$$

The Lamé coefficients are

$$h_\Phi = 1, \quad h_u = \frac{t}{\rho}, \quad h_3 = h_v \frac{\rho_2^0 + t}{\rho_2^0}.$$

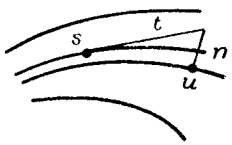

Figure 2

Here h_3 is the third Lamé coefficient of the radial system in space, while h_v relates to the radial system on the surface; low is the radius of curvature of the line u at the point of separation of the ray;

$$\frac{1}{\rho_2^0} = \frac{1}{h_v} \cdot \frac{\partial h_v}{\partial u}.$$

All of these formulas are obtained by the methods of differential geometry.

We will express the variable boundary layers in the neighborhood of the surface in terms of the radial variables (Fig. 2) thus:

$$\begin{gathered} \rho(u) = \rho(s) + O\left(n^{\frac{1}{2}}\right), \\ 2\rho n = t^2 + O\left(n^{\frac{3}{2}}\right), \\ \int_{u'}^{u} \rho^{-\frac{2}{3}} d\sigma = \int_{s'}^{s} \rho^{-\frac{2}{3}} d\sigma + \rho^{-\frac{2}{3}}(s)\, t + \rho^{-\frac{2}{3}}(s')\, t' + O(n). \end{gathered} \tag{2.1}$$

Here u is the basis of the normal, while s is the coordinate of the point of separation.

2. Buslayev Formula

/127

Let us replace the variable boundary layers (n) by the radial variables (t) in the boundary-layer formulas, according to (2.1):

$$\begin{aligned}
\mu \to Y &= \left(\frac{k}{2\rho^2(s)}\right)^{\frac{2}{3}} t^2, \\
\mu' \to Y' &= \left(\frac{k}{2\rho^2(s')}\right)^{\frac{2}{3}} t'^2, \\
\lambda \to X &= Y^{\frac{1}{2}} + Y'^{\frac{1}{2}} + Z, \\
Z &= \left(\frac{k}{2}\right)^{\frac{1}{3}} \int_{s'}^{s} \rho^{-\frac{2}{3}} d\sigma, \\
k\tau &= -\frac{2}{3} Y^{\frac{3}{2}} - \frac{2}{3} Y'^{\frac{3}{2}}.
\end{aligned} \tag{2.2}$$

After substitutions, we obtain the following Buslayev formula:

$$U = Ce^{ik\Phi} \rho^{-\frac{1}{6}}(s) \rho^{-\frac{1}{6}}(s') h_3^{-\frac{1}{2}} e^{-i\left(\frac{2}{3} Y^{\frac{3}{2}} + \frac{2}{3} Y'^{\frac{3}{2}}\right)} \Psi^{(s)}(X, Y, Y'). \tag{2.3}$$

Here h_3 is the Lamé coefficient in the radial system, while the superscript (S) for Ψ signifys the enveloping wave.

Formula (2.3) also has significance beyond the limits of the boundary layer. It satisfies the equation only in the principal order [and not in two orders, as in (1.10)]. Beyond the limits of the boundary layer, (2.3) converts into the Keller formula. In order to show this, we must take the integral for Ψ by deductions, and substitute the asymptotics of the Airy functions, as was done in [4]. The Buslayev formula loses significance near the caustic ($h_3 \to 0$ for a formal sign). In these regions, it can be specified by one of the famous examples (see [6], for example). If we assume that h_3 = const, we obtain the Buslayev formula for the plane case.

III. FORMULAS FOR THE ASYMPTOTICS IN LIGHT, LIGHT-SHADOW BOUNDARY AND SEWING OPERATION

1. Geometry of the Reflected Rays

Within the framework of geometrical optics, the following formula is valid for the amplitude of a wave from a point source (spherical) reflected from a smooth convex body:

$$P = \left[(t'+t)^2 + 2tt'(t'+t)\left(2H\cos\gamma + \Gamma\frac{\sin^2\gamma}{\cos\gamma}\right) + 4Kt^2t'^2\right]^{-\frac{1}{2}}. \tag{3.1}$$

This formula was derived in [5]. We will write out the symbols: /128
t' is the length of the incident ray (Fig. 3); t is the length of the reflected ray (Fig. 3); γ is the angle of reflection (Fig. 3); f_1 and f_2 are the principal radii of curvature of the reflector at the point of reflection; α is the angle between the plane of reflection and the principal section of curvature with the radius f_1; H is the average curvature,

$$2H = \frac{1}{f_1} + \frac{1}{f_2};$$

Γ is the curvature of the normal section in the reflection plane,

$$\Gamma = \frac{\cos^2\alpha}{f_1} + \frac{\sin^2\alpha}{f_2};$$

K is the total (Gaussian) curvature,

$$K = \frac{1}{f_1 f_2}.$$

The principal radii of curvature of the reflected front at the reflection point are:

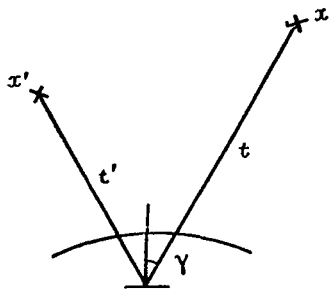

Figure 3

$$\frac{1}{\rho^0_{1,2}} = \frac{1}{t'} + \frac{a \pm a_1}{\cos\gamma},$$
$$a = 2H\cos^2\gamma + \Gamma\sin^2\gamma, \qquad (3.2)$$
$$a_1 = \sqrt{a^2 - 4K\cos^2\gamma}.$$

2. Buslayev Formula for the Reflected Wave and the Sewing Operation

We will use the symbol

$$b = \frac{2}{a + a_1}. \qquad (3.3)$$

We will call the smaller radius of curvature of the reflected front b, i.e.,

$$\frac{1}{\rho^0_1} = \frac{1}{t'} + \frac{2}{b\cos\gamma}. \qquad (3.4)$$

Let us use the following "reflected-ray" variables:

$$M=\left(\frac{kb}{2}\right)^{\frac{1}{3}},\quad T=\left(\frac{M}{b}\right)t,\quad T'=\left(\frac{M}{b}\right)t',\quad S=M\cos\gamma,$$
$$X=T+T',\quad Y=T(T+2S),\quad Y'=T'(T'+2S). \tag{3.5}$$

The value b is a continuous extension of the shadow radius ρ. All the variables X, Y and Y' are extended continuously from shadow to light. The Lamé coefficient h_3 is determined in the following way:

in shadow,

$$h_3=h_0\frac{\rho_2^0+t}{\rho_2^0}, \tag{3.6}$$

in light,

$$h_3=t'\frac{\rho_2^0+t}{\rho_2^0}. \qquad \text{/129}$$

We did not define h_v unambiguously before. In order that h_3 be extended continuously from shadow to light, we must assume that h_v equals t' at the boundary between light and shadow. The phase of the reflected wave, i.e.,

$$\Phi_R=t'+t$$

is a continuous extension in light of the enveloping phase

$$\Phi_S=t'+s+t.$$

We will continue the enveloping wave into the light range with the aid of (2.3), in which the variables were determined by (3.5), and with (3.6).

Thus, the enveloping wave

$$U^{(S)}=Ce^{ik\Phi_S}\left(\frac{k}{2}\right)^{\frac{1}{6}}\rho^{-\frac{1}{6}}(s)\rho^{-\frac{1}{6}}(s')h_3^{-\frac{1}{2}}e^{-iF_S}\Psi^{(S)}(X,\ Y,\ Y'), \tag{3.7}$$

where

$$F_S=\frac{2}{3}\left(Y^{\frac{3}{2}}+Y'^{\frac{3}{2}}\right);$$
$$\Psi^{(S)}=\frac{e^{i\frac{\pi}{4}}}{2\pi^{\frac{1}{2}}}\int_{-\infty}^{+\infty}d\zeta e^{i\zeta X}\frac{w_1(\zeta-Y')}{w_1(\zeta)}G(\zeta,\ Y).$$

Compared to (2.3), there are other constants here, including $(\frac{k}{2})^{\frac{1}{6}}$. This was done for the sake of convenience in the sewing operation. We will extend $U^{(S)}$ into the light region with the following formula:

$$U = Ce^{ik\Phi_R}\left(\frac{k}{2}\right)^{\frac{1}{6}} b^{-\frac{1}{3}} h_3^{-\frac{1}{2}} e^{-iF_R}\Psi^{(S)}(X,\ Y,\ Y'), \tag{3.8}$$

where

$$F_R = -S^2X + \frac{2}{3}(Y+2S)^{\frac{3}{2}} + \frac{2}{3}(Y'+2S)^{\frac{3}{2}} - \frac{4}{3}S^3. \tag{3.9}$$

We will now write out $\Psi^{(S)}$ in the form of the sum of two terms, using (1.11):

$$\Psi^{(S)} = \frac{e^{-\frac{\pi i}{4}}}{\pi^{\frac{1}{2}}}\int_{-\infty}^{+\infty} d\zeta e^{i\zeta X} w_1(\zeta - Y)\, v(\zeta - Y') - \tag{3.10}$$
$$- \frac{e^{-\frac{\pi i}{4}}}{\pi^{\frac{1}{2}}}\int_{-\infty}^{+\infty} d\zeta e^{i\zeta X} w_1(\zeta - Y)\frac{v(\zeta)}{w_1(\zeta)} w_1(\zeta - Y').$$

The first integral is calculated precisely according to the formula derived by V. A. Fok [1], i.e., /130

$$\frac{e^{-\frac{\pi i}{4}}}{\pi^{\frac{1}{2}}}\int_{-\infty}^{+\infty} d\zeta e^{i\zeta X} w_1(\zeta - Y)\, v(\zeta - Y') = X^{-\frac{1}{2}} e^{i\Omega}, \tag{3.11}$$

where

$$\Omega = -\frac{1}{12}X^3 + \frac{1}{2}X(Y'+Y) + \frac{(Y'-Y)^2}{4X}. \tag{3.12}$$

Correspondingly, be dividing $\Psi^{(S)}$ we can represent U in the form of the sum of two terms, i.e.,

$$U = U^{(\Phi)} + U^{(R)},$$

Where $U^{(\Phi)}$ corresponds to the direct wave. Using (3.11) and (3.12), it is easy to find that

$$U^{(\Phi)} = Ce^{i(k\Phi_R + \Omega - F_R)} h_3^{-\frac{1}{2}} \Phi_R^{-\frac{1}{2}}.$$

At the light-shadow boundary and on the surface of the reflector,

$$U^{(\Phi)} = C\frac{e^{ik\Phi_0}}{\Phi_0},$$

i.e., $U^{(\Phi)}$ there coincides with the direct wave, if we specify that

$$C = \frac{1}{4\pi}.$$

Φ_0 is the phase of the direct wave (length of the direct beam in light). The second term $U^{(R)}$ corresponds to the reflected wave, i.e.,

$$U^{(R)} = \frac{1}{4\pi} e^{ik\Phi_R} \left(\frac{k}{2}\right)^{\frac{1}{6}} b^{-\frac{1}{3}} h_3^{-\frac{1}{2}} e^{-iF_R} \Psi^{(R)}(X, Y, Y'), \tag{3.13}$$

where

$$\Psi^{(R)} = -\frac{e^{-\frac{\pi i}{4}}}{\pi^{\frac{1}{2}}} \int_{-\infty}^{+\infty} d\zeta e^{i\zeta X} w_1(\zeta - Y) \frac{v(\zeta)}{w_1(\zeta)} w_1(\zeta - Y'). \tag{3.14}$$

3. Converting the Buslayev Formula into a Formula of Geometrical Optics

We can calculate $\Psi^{(R)}$ asymptotically for regions far from the shadow:

$$e^{-iF_R} \Psi^{(R)}(X, Y, Y') \to -\left(\frac{S}{XS + 2TT'}\right)^{\frac{1}{2}}. \tag{3.15}$$

These calculations are presented in [4].

Having substituted the values for the variables in (3.5) into (3.13), and having considered (3.15), we can find the following asymptotically:

$$U^{(R)} \to -\frac{1}{4\pi} e^{ik\Phi_R} h_3^{-\frac{1}{2}} \left(t' + t + \frac{2tt'}{b\cos\gamma}\right)^{-\frac{1}{2}}.$$

If we substitute b and h_3 in (3.3) and (3.6) into the latter formula, /131 we obtain (3.1), i.e. a formula of geometrical optics. Naturally, there are no phase factors or coefficients $\frac{1}{4\pi}$ in (3.1).

IV. SUMMARY OF THE RESULTS OBTAINED

Let us consider the function U*:

$$U^* = \begin{cases} U^{(S)} & \text{In shadow} \\ \frac{1}{4\pi} \cdot \frac{e^{ik\Phi_0}}{\Phi_0} + U^{(R)} & \text{In light} \end{cases}$$

$U^{(S)}$ is determined by (3.7), while $U^{(R)}$ is determined by (3.13). This formula converts into a formula of geometrical optics in the region of bright light, while it converts into a Keller formula in the region of deep shade when the latter has significance. The function U* satisfys the boundary condition precisely, and the condition for emission when going to infinity. It is continuous at the boundary between light and shadow; however, the derivative for the normal to the shadow boundary has a discontinuity. All this allows us to confirm that the function U* is a precision of the previously-known formulas and combines them into one in a certain sense. It was proven in [4] that a function analogous to U* in the two-dimensional case satisfys the equation in the principal order in all the regions. These arguments are transposed for the three-dimensional case with trivial changes. In conclusion, we should mention that (1.10) represents the asymptotics more precisely than (3.7) in the boundary layer in shadow, since it satisfies the equation for the two principal orders.

REFERENCES

1. Fok, V.A.: Fresnel Diffraction from Convex Bodies. Uspekhi Fiz. Nauk, Vol. 43, No. 4, 1951.
2. Levy, B.R. and J.B. Keller: Diffraction by a Smooth Object, Comm. Pure Appl. Math., Vol. 12, No. 1, 1959.
3. Buslayev, V.S.: Formulas for Short-Wave Asymptotics in the Problem of Diffraction on Convex Bodies. Vestnik L.G.U., No. 13, 1962.
4. Buslayev, V.S.: Short-Wave Asymptotics in the Problem of Diffraction on Smooth Convex Contours. Trudy Matem. Instit. imeni Steklova, Vol. 73, 1964.
5. Friedlander, F.: Zvukovyye impul'sy (Sound Impulses). Foreign Literature Publishing House, 1962.
6. Landau, L.D. and Ye.M. Lifshits: Teoriya polya (Field Theory). "Fizmatgiz", 1962.

EFFECT OF A STEPLIKE DISCONTINUITY ON A FIELD IN A PLANE WAVEGUIDE

B.V. Nerinovskiy

ABSTRACT: This article treats the effect of a steplike discontinuity in a plane unbounded waveguide with ideal walls. The problem is reduced to solutions to Maxwellian equations which satisfy definite boundary conditions, solved by the method of successive approximations, using the Schwarz algorithm.

In this article we will attempt to consider the effect of a steplike discontinuity in a plane unbounded waveguide with ideal walls. /132

We will consider that the waveguide, unbounded in the plane (x,y) of the Cartesian system of coordinates x, y, z, appears as shown in figures 2 to 4. Moreover, we will assume that the waveguide is excited by a filamentary source passing through the point x = 0, z = a along the y axis (parallel to the step). Thus, the problem amounts to finding a solution to Maxwellian equations which satisfies the following condition on the surface of the waveguide S:

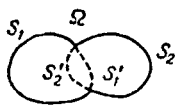

Fig. 1.

$$E|_S = 0. \tag{1}$$

We will construct the solution by the method of successive approximations, using the Schwarz algorithm.

Let us make some comments relative to this method. We will assume that we want to find a solution to the equation

$$-Au = \frac{\partial^2 u}{\partial x^2} + \frac{\partial^2 u}{\partial y^2} + \frac{\partial^2 u}{\partial z^2} + k^2 u = 0 \tag{2}$$

in a certain region Ω, as depicted in Figure 1, for the extreme condition

$$u|_S = \Psi|_S, \tag{3}$$

where Ψ is the function defined in Ω. Furthermore, we will assume that we cannot solve this boundary problem, but that we can solve the boundary problem for (2) in regions Ω_1 and Ω_2, which are bounded by the surfaces S_1US_1' and S_2US_2', respectively, whereas $S_1US_2 = S$.

The Schwarz process consists in the construction of a sequence of approximative solutions $\{u^{(k)}\}$ according to the following scheme. The function $u^{(1)}$ is found as a solution to (2) in the region Ω_1 under the boundary conditions of

$$u^{(1)}|_{S_1US_1'} = \psi|_{S_1US_1'} \tag{4}$$

and is defined supplementarily by the condition $u^{(1)} \equiv \psi$ in the region $\Omega \setminus \Omega_1$. Subsequently, assuming that

$$u^{(2k)}|_S = \psi|_S, \quad u^{(2k)}|_{S_2'} = u^{(2k-1)}|_{S_2'} \tag{5}$$

and

$$u^{(2k+1)}|_S = \psi|_S, \quad u^{(2k+1)}|_{S_1'} = u^{(2k)}|_{S_1'}, \tag{6}$$

we can construct the sequence of the functions $\{u^{(k)}\}$, $k = 2, 3, \ldots$, which are definite over the entire range Ω and which also satisfy (2) everywhere in Ω, except for the surface S_1' and S_2'.

It was shown in [1] that, in the case when the range is finite, the operator is positive definite $\Psi \in L_2(\Omega)$, the sequence of $\{u^{(k)}\}$ converges in $L_2(\Omega)$ to a solution of the formulated problems for u (x, y, z), whereas $u^{(k)} \to u$ uniformly in any internal subregion of Ω.

Generally speaking, the finiteness of the region Ω is not a fundamental condition for the convergence of the Schwarz process [2]. In our case of an unbounded waveguide, the solution to the problem should describe a field which attenuates at $x = \pm \infty$, which naturally implies the existence of a positive imaginary part (although very small) for the wave number k.

We will discuss three different cases for the relative position of a source and discontinuity below; they are illustrated by Figures 2-4, respectively. In the future we will agree that, if h_j is the altitude of the j-th part of the waveguide, then $h_j \leq h_k$ for $j < k$.

1. Constructing the Solution

I. Let us begin with the case of a steplike connection between two waveguides at different heights, when the source is the lower one (see Fig. 2). In correspondence with the scheme of the Schwarz method, we will divide the space inside the waveguide by the imaginary surfaces S_{12} and S_{21}, and then we will construct the sequence of the solution, i.e.,

$$E^{(1)}, E^{(2)}, E^{(3)}, \ldots, \tag{7}$$

where $E^{(1)}$ satisfies the condition

$$E^{(1)}|_{S_{1B} \cup S_{12}} = E^{(1)}|_{S_{1H} \cup S_{2H}} = 0; \tag{8}$$

$E^{(2)}$ satisfies the conditions

$$E^{(2)}|_{S_{2B}} = E^{(2)}|_{S_{2H}} = 0 \text{ and } E^{(2)}|_{S_{21}} = E^{(1)}; \tag{9}$$

$E^{(3)}$ satisfies the conditions

$$E^{(3)}|_{S_{1H} \cup S_{2H}} = E^{(3)}|_{S_{1B}} = 0 \text{ and } E^{(3)}|_{S_{12}} = E^{(2)} \tag{10}$$

etc.

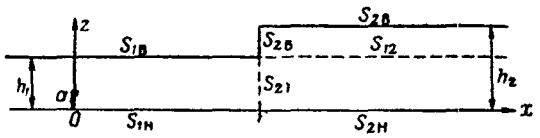

Fig. 2.

Each term in the sequence of $E^{(k)}$ (k = 1, 2, 3 ...) satisfies the boundary conditions of (1), as well as the Helmholtz equation in (2) - everywhere inside the waveguide, except for the surfaces S_{12} and S_{21}.

We will introduce the functions

$$Z_{nj}(z) = \sin\left(\frac{\pi n z}{h_j}\right) \tag{11}$$

and

$$k_{nj} = \sqrt{k^2 - \left(\frac{\pi n}{h_j}\right)^2}, \tag{12}$$

Then, for x $\geq$ 0,

$$E^{(1)} = \sum_{n=1}^{\infty} C_{p1} Z_{p1}(z)\, e^{ik_{p1}x}. \tag{13}$$

Further, we can note that the function

$$\varphi_2^+ = \begin{cases} \frac{i}{h_2} \sum_{n=1}^{\infty} \frac{Z_{n2}(z)\, Z_{n2}(z_0)}{k_{n2}} \left(e^{ik_{n2}(x+x_0) - 2ik_{n2}r} - e^{ik_{n2}(x_0-x)} \right) \\ \text{for} \quad x < x_0 \\ \frac{i}{h_2} \sum_{n=1}^{\infty} \frac{Z_{n2}(z)\, Z_{n2}(z_0)}{k_{n2}} \left(e^{ik_{n2}(x+x_0) - 2ik_{n2}r} - e^{ik_{n2}(x-x_0)} \right) \\ \text{for} \quad x > x_0 \end{cases} \tag{14}$$

In the region of x, $x_0 \geq r$; $0 \leq z, z_0 \leq h_2$ satisfies the equation /13

$$\Delta\varphi + k^2\varphi = \delta(x - x_0)\,\delta(z - z_0) \tag{15}$$

and the condition

$$\varphi_2^+ |_{S_{2B} US_{21} US_{2H}} = 0; \tag{16}$$

Consequently, considering (9), we have the following for x $\geq$ r:

$$E^{(2)} = -\int_0^{h_1} \left(E^{(1)} \frac{\partial \varphi_2^+}{\partial x_0} \right)_{x_0 = r} dz_0 \tag{17}$$

or

$$E^{(2)} = \sum_{n=1}^{\infty} T_{n2} Z_{n2}(z)\, e^{ik_{n2}(x-r)}, \tag{18}$$

where

$$T_{n2} = \sum_{p=1}^{\infty} C_{p1}\tau_{np}e^{ik_{p1}r}; \qquad (19)$$

$$\tau_{np} = \frac{2}{h_2}\int_0^{h_1} Z_{n2}(z_0)\,Z_{p1}(z_0)\,dz_0 = \frac{2p\xi}{\pi(n^2\xi^2 - p^2)}\sin[\pi(\xi n - p)] \qquad (20)$$

For the sake of convenience, we introduced the parameter $\xi = h_1/h_2$, where $0 < \xi \leq 1$.

The function

$$\varphi_1 = \begin{cases} -\frac{i}{h_1}\sum_{m=1}^{\infty}\frac{Z_{m1}(z)\,Z_{m1}(z_0)}{k_{m1}}e^{ik_{m1}(x-x_0)} & \text{for } x > x_0 \\ -\frac{i}{h_1}\sum_{m=1}^{\infty}\frac{Z_{m1}(z)\,Z_{m1}(z_0)}{k_{m1}}e^{ik_{m1}(x_0-x)} & \text{for } x_0 > x \end{cases} \qquad (21)$$

satisfies (15) and the condition

$$\varphi_1|_{S_{1B}US_{12}} = \varphi_1|_{S_{1H}US_{2H}} = 0, \qquad (22)$$

Therefore,

$$E^{(3)} = E^{(1)} + \int_r^{\infty}\left(E^{(2)}\frac{\partial\varphi_1}{\partial z_0}\right)_{z_0=h_1}dx_0 \qquad (23)$$

or, considering (13), (18) and (21) for $0 < x \leq r$,

$$E^{(3)} = \sum_{m=1}^{\infty} C_{m1}Z_{m1}(z)e^{ik_{m1}x} + \sum_{m=1}^{\infty} R_{m1}Z_{m1}(z)\,e^{ik_{m1}(r-x)}, \qquad (24)$$

/136

where

$$R_{m1} = -\frac{\pi m(-1)^m}{h_1^2\left[k^2 - \left(\frac{\pi m}{h_1}\right)^2\right]}\sum_{n=1}^{\infty}\frac{T_{n2}}{1+\frac{k_{n2}}{k_{m1}}}\sin(\pi n\xi). \qquad (25)$$

On the whole, the functions $\phi_1(x, z; x_0, z_0)$ and $\phi_2^+(x, z; x_0, z_0)$ allow us to construct any term for the sequence in (7).

II. We can consider the case when the source is located on a higher waveguide in a similar way (Fig. 3).

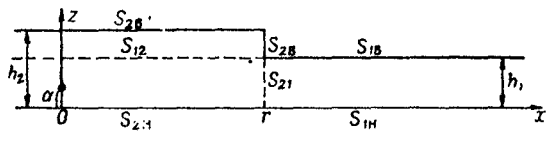

Fig. 3.

Assuming, for the sake of definiteness, that $0 < a \leq h_1$, we will find the sequence $\{E^{(k)}\}$, as before, by the conditions of (8), (9), (10), etc. However, in this case, it is useful to use the following function, together with the already-applied function ϕ_1:

$$\varphi_2^- = \begin{cases} \frac{i}{h_2}\sum_{n=1}^{\infty}\frac{Z_{n2}(z)\,Z_{n2}(z_0)}{k_{n2}}\left(e^{2ih_{n2}r-ih_{n2}(x+x_0)} - e^{ih_{n2}(x-x_0)}\right) \\ \qquad \text{for} \quad x_0 < x \\ \frac{i}{h_2}\sum_{n=1}^{\infty}\frac{Z_{n2}(z)\,Z_{n2}(z_0)}{k_{n2}}\left(e^{2ih_{n2}r-ih_{n2}(x+x_0)} - e^{ih_{n2}(x_0-x)}\right) \\ \qquad \text{for} \quad x < x_0, \end{cases} \tag{26}$$

In the region of $x, x_0 \leq r$, $0 \leq z, z_0 \leq h_2$ it satisfies (15) and (16).

The approximation of $E^{(1)}$ for $x \geq 0$ has the form of (13). $E^{(2)}$ is determined by the following relationship:

$$E^{(2)} = D\varphi_2^-(x, z; 0, a) + \int_0^{h_1}\left(E^{(1)}\frac{\partial\varphi_2^-}{\partial x_0}\right)_{x_0=r} dz_0 \tag{27}$$

(here D is the normalization factor), or, considering (13) and (26), /137

$$E^{(2)} = \begin{cases} \sum_{n-1}^{\infty} C_{n2}Z_{n2}(z)\,e^{ih_{n2}x} + \sum_{n-1}^{\infty} R_{n2}Z_{n2}(z)\,e^{ih_{n2}(r-x)} \\ \qquad \text{for} \quad 0 < x \leqslant r \\ \sum_{n-1}^{\infty} C_{n2}Z_{n2}(z)\,e^{-ih_{n2}x} + \sum_{n=1}^{\infty} R_{n2}Z_{n2}(z)\,e^{ih_{n2}(r-x)} \\ \qquad \text{for} \quad x < 0, \end{cases} \tag{28}$$

where

$$C_{n2} = -\frac{iD}{h_2} \cdot \frac{Z_{n2}(a)}{k_{n2}} \tag{29}$$

and

$$R_{n2} = -\left(C_{n2} e^{ik_{n2}r} - T_{n2}\right). \tag{30}$$

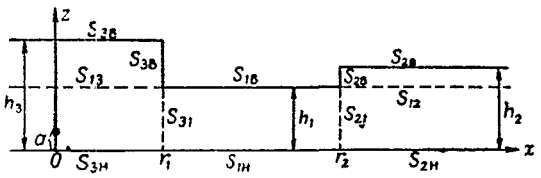

Fig. 4.

We can then find $E^{(3)}$ for $0 \leq z \leq h_1$:

$$E^{(3)} = E^{(1)} + \int_{-\infty}^{'} \left(E^{(2)} \frac{\partial \varphi_1}{\partial z_0}\right)_{z_0 = h_1} dx_0. \tag{31}$$

Let us assume that $x \geq r$; then

$$E^{(3)} = \sum_{m=1}^{\infty} A_{m1} Z_{m1}(z)\, e^{ik_{m1}x} + \sum_{m=1}^{\infty} B_{m1} Z_{m1}(z)\, e^{ik_{m1}(x-r)}. \tag{32}$$

The coefficients A_{m1} and B_{m1} have the form of

$$A_{m1} = C_{m1} - \frac{2\pi m(-1)^m}{h_1^2 k_{m1}^3} \sum_{n=1}^{\infty} \frac{k_{n2} C_{n2} \sin(\pi n \xi)}{1 - \left(\frac{k_{n2}}{k_{m1}}\right)^2}, \tag{33}$$

$$B_{m1} = \frac{\pi m(-1)^m}{h_1^2 k_{m1}^2} \sum_{n=1}^{\infty} \left(\frac{C_{n2} e^{ik_{n2}r}}{1 - \frac{k_{n2}}{k_{m1}}} + \frac{R_{n'}}{1 + \frac{k_{n2}}{k_{m1}}}\right) \sin(\pi n \xi). \tag{34}$$

E_4 is determined in a similar way, etc.

III. Finally, let us discuss the case when there is a rectangular protrusion between two waveguides of different heights. /1
Having made a mental division of the space inside such a waveguide by the surfaces S_{13}, S_{31}, S_{21} and S_{12}, as shown in Figure 4, we can determine the sequence of $\{E^{(k)}\}$ by the following conditions:

$$E^{(1)}|_{S_{13}US_{1B}US_{12}} = E^{(1)}|_{S_{3H}US_{1H}US_{2H}} = 0; \tag{35}$$

$$E^{(2n)}|_{S_{3B}} = E^{(2n)}|_{S_{3H}} = E^{(2n)}|_{S_{2B}} = E^{(2n)}|_{S_{2H}} = 0,$$

$$E^{(2n)}|_{S_{31}} = E^{(2n-1)} \text{ и } E^{(2n)}|_{S_{21}} = E^{(2n-1)}; \tag{36}$$

$$E^{(2n+1)}|_{S_{3H}US_{1H}US_{2H}} = E^{(2n+1)}|_{S_{1B}} = 0, \quad E^{(2n+1)}|_{S_{13}} = E^{(2n)}$$

$$\text{и } E^{(2n+1)}|_{S_{12}} = E^{(2n)}, \tag{37}$$

where n = 1, 2, 3,...

As before, $E^{(1)}$ is determined by (13). If we now introduce the function ϕ_3 as was done for (26) and we assume that $r = r_1$, as well as the function ϕ_2, as was done for (14), and we assume that $r = r_2$, then

$$E^{(2n)}|_{x \leqslant r_1} = D\varphi_3(x, z; 0, a) + \int_0^{h_1} \left(E^{(2n-1)} \frac{\partial \varphi_3}{\partial x_0}\right)_{x_0 = r_1} dz_0, \tag{38}$$

$$E^{(2n)}|_{x > r_2} = -\int_0^{h_1} \left(E^{(2n-1)} \frac{\partial \varphi_2}{\partial x_0}\right)_{x_0 = r_2} dz_0, \tag{39}$$

$$E^{(2n+1)} = E^{(1)} + \int_{-\infty}^{r_1} \left(E^{(2n)} \frac{\partial \varphi_1}{\partial z_0}\right)_{z_0 = h_1} dx_0 + \int_{r_2}^{\infty} \left(E^{(2n)} \frac{\partial \varphi_1}{\partial z_0}\right)_{z_0 = h_1} dx_0 \tag{40}$$

$$0 \leqslant z \leqslant h_1$$

Thus, for example,

$$E^{(2)}|_{x < r_1} = \begin{cases} \sum_{n=1}^{\infty} C_{n3} Z_{n3}(z) e^{-ik_{n3}x} + \sum_{n=1}^{\infty} R_{n31} Z_{n3}(z) e^{ik_{n3}(r_1 - x)} \\ \text{for } x < 0 \\ \sum_{n=1}^{\infty} C_{n3} Z_{n3}(z) e^{ik_{n3}x} + \sum_{n=1}^{\infty} R_{n31} Z_{n3}(z) e^{ik_{n3}(r_1 - x)} \\ \text{for } x > 0, \end{cases} \tag{41}$$

$$E^{(2)}|_{x > r_2} = \sum_{n=1}^{\infty} T_{n21} Z_{n2}(z) e^{ik_{n2}(x - r_2)}; \tag{42}$$

/139

$$E^{(3)}|_{r_1<x<r_2} = \sum_{n=1}^{\infty} A_{n12} Z_{n1}(z) e^{ih_{n1}x} +$$

$$+ \sum_{n=1}^{\infty} B_{n13} Z_{n1}(z) e^{ih_{n1}(x-r_1)} + \sum_{n=1}^{\infty} R_{n12} Z_{n1}(z) e^{ih_{n1}(r_2-x)}. \qquad (43)$$

The coefficients T_{n21}, R_{n31}, A_{n13}, B_{n13} and R_{n12} are determined by (19), (30), (33), (34) and (25), respectively. E^4 is found in the same way, etc.

2. Discussion of the Results

Let us begin with case 1. Although we wrote out approximative $E^{(1)}$ in the form of a series in (13), we actually have a finite sum for $x \neq 0$, because the walls have ideal characteristics. It follows from the expression in (18) for $E^{(2)}$ that the local "waves" play a significant role in the satisfaction of the boundary conditions of (9), which are fulfilled, as are all the others, in the corresponding distance function L_2. Since the theories in (18)

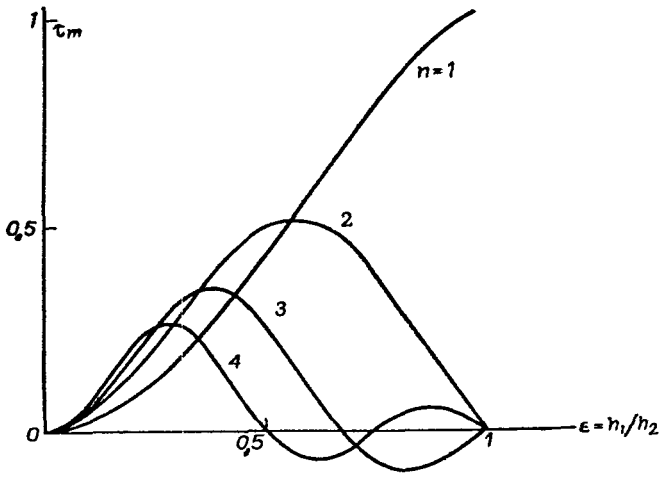

Fig. 5.

$$\tau_{np}|_{n>p/\xi} \simeq \frac{2p(-1)^p \sin(\pi n\xi)}{\pi n^2 \xi}, \qquad (44)$$

converges, and it is suitable that we consider the case when the number of propagating normal waves in the lower waveguide is small, while the heights h_1 and h_2 do not differ greatly. /140

Equation (18) allows us to treat the field in the higher waveguide as overexcited by the discontinuity. The coefficients T_{n2}

imply the coefficients of transmission, and depend naturally on the phases and amplitudes of the propagating modes in the incident field, as well as the coefficients of overexcitation of the modes τ_{np}. If $1 < \lambda/h_1 < 2$, then the first mode alone propagates in the lower waveguide, and T_{n2} are determined by the coefficients τ_m. The behavior of several of the first coefficients τ_m, which depends on the height ratio of the waveguides, is shown in Figure 5, which illustrates the tendence to relative equilibrium of the coefficients of overexcitation with a decrease in the parameter $\xi = h_1/h_2$.

In order to consider the effect of reflection from the discontinuity, we should use the term $E^{(3)}$. It can be seen from (24) that $E^{(3)}$ represents the field for $x \leq r$ as the sum of the incident and reflected fields with coefficients of reflection of R_{m1}, while each R_{m1} is determined by all the propagated and local modes of the higher waveguide for $x = r$ and is a complex value.

Further, if we consider the term $E^{(4)}$, it would allow us to describe the process of passage to the upper waveguide, considering the reflection from the discontinuity for $x = r$.

In case II the basic step of $E^{(1)}$ has the same form, while $E^{(2)}$ describes the reflection from a rectangular projection. We can see from (28) - (30) that the reflection effect can be interpreted in this situation as the difference between the field reflected from an ideal wall at $x = v$ and the field which passed to the upper waveguide from the lower one from some imaginary source arranged at $z = z$, $x = 2r$.

The approximation of $E^{(3)}$ allows us to describe the effect of the step on the field in the lower waveguide. Since $a \leq h_1$, the source can be seen from any point in the region $x \geq r$, and therefore the field here is combined both of a "direct" and "diffracted" step [see (32) - (34)]. The diffracted field is determined by the combination of modes which are incident on the step and reflected.

Case III can be reduced largely to cases I and II. Thus, the expressions in (41) illustrate the process of reflection from a protrusion, formula (43) shows that the field in the region below the protrusion is represented by the sum of the "direct" field from the source, the field diffracted on the protrusion for $x = r_1$, and the field reflected from the end of the protrusion for $x = r_2$. Finally, (42) characterizes the field in the waveguide behind the protrusion. However, (41) and (42) do not consider, for example, /141 the reciprocal effect of waveguides arranged along both sides of the protrusion. Therefore, for a more complete description of the phenomenon, we should consider $E^{(4)}$, etc.

REFERENCES

1. Mikhlin, S.G.: Problema minimuma kvadratichnogo funktsionala (Problem of the Minimum of a Quadratic Functional). G.I.T.T.L., 1952.
2. Sobolev, S.: Schwarz Algorithm in the Theory of Elasticity. Doklady Akad. Nauk S.S.S.R., Vol. IV, No. 6, 1936.

THE PROPAGATION OF LONG RADIO WAVES AND THE NONHOMOGENEOUS IONOSPHERE

E.M. Gyunninen and I.N. Zabavina

ABSTRACT: The authors discuss the propagation of long radio waves and the nonhomogeneous ionosphere in terms of a model they used in a previous study. It is shown that the method of constructing the solution to the problem of wave propagation with the aid of "rays" for the earth-ionosphere waveguide channel with subsequent approximation is valid when the dependence of the waveguide height on the distance along the earth's surface is considered.

The problem of the propagation of radio waves in a waveguide /14
channel formed by the spherical surface of the Earth and the nonhomogeneous (in altitude) ionosphere was examined in an earlier study of ours [1]. Its solution was approximative, in the sense that we used the impedance of a plane wave incident on a layer of the ionosphere which was nonuniform in terms of depth. It was constructed in the form of an expansion by "rays", which allowed us to consider the dependence of the impedance on the angle of incidence.

In the case of an isotropic ionosphere and vertically polarized wave, the impedances can be calculated by numerical integration of the following equation (see [2]):

$$\frac{d\delta_s(z)}{dz} = -ik\left\{\varepsilon'_m(z)\,\delta_s^2(z) - \frac{\varepsilon_m(z) - \sin^2\psi}{\varepsilon'_m(z)}\right\}, \qquad (1)$$

where k is the wave number in the air; $\varepsilon'_m(z)$ is the relative complex permittivity of the ionosphere, depending on a single coordinate z; ψ is the angle of incidence of the wave on the layer of the ionosphere, and Equation (1) itself is obtained from the first equation in (6) in [2] after replacing A_{11} by $\frac{1}{\delta_s}$ (the time dependence of all the values is determined by the factor $e^{-i\omega t}$).

As we showed in [1], a similar equation can be obtained for "spherical" impedance, and then the solution to this problem becomes a strict one. We will compare both solutions in this article, and we will attempt to evaluate the accuracy of the approximative one.

For the sake of convenience, we will formulate the problem briefly. Let r, θ, ϕ be spherical coordinates with origin at the center of the globe of radius a, let a vertical electric dipole be located at the point r = a, θ = 0, let the space for a < r < c be filled with a uniform atmosphere, and for r > c let there be a nonuniform (in terms of r) isotropic ionosphere whose electrical properties are characterized by the relative complex permittivity $\varepsilon'_m(r)$. We will look for the field of the dipole in air. /143

Let us introduce the single-component electric Hertz vector $\vec{\Pi} = \Pi \frac{\vec{r}}{r}$ by the following formulas:

$$\vec{E} = \frac{1}{\omega\varepsilon'(r)} \operatorname{rot}\operatorname{rot}\vec{\Pi} + \frac{\vec{j}}{i\omega\varepsilon'(r)}, \qquad \vec{H} = \operatorname{rot}\vec{\Pi}, \tag{2}$$

where $\vec{j}$ is the current density at the source; $\varepsilon'(r) = \varepsilon'_m(r)\,\varepsilon_0$, $\varepsilon_0 = \frac{1}{36\pi}\cdot 10^{-9}$ f/m. For the vectors of the fields $\vec{E}$ and $\vec{H}$, we will impose an impedance boundary condition at the air-earth division (r = a), and we will impose precise boundary conditions at the air-ionosphere division (r = c). The solution constructed for such assumptions can be written in the following form (for r = a) (see [1], formulas (79)-(83)):

$$\Pi = \sum_{m=0}^{\infty} \Pi^{(m)}, \tag{3}$$

$$\Pi^{(m)} = \frac{j_0}{2\pi}\cdot\frac{1}{ka^2}\cdot\frac{\sqrt{2}\,e^{i\frac{\pi}{4}}}{\sqrt{\pi\sin\theta}}\times$$

$$\times\int_\Gamma \sqrt{\nu}\left[\frac{\zeta^{(1)}_{\nu-\frac{1}{2}}(kc)}{\zeta^{(2)}_{\nu-\frac{1}{2}}(kc)}\right]^m\left[\frac{\zeta^{(2)}_{\nu-\frac{1}{2}}(ka)}{\zeta^{(1)}_{\nu-\frac{1}{2}}(ka)}\right]^{m-1}\frac{F^m_\nu\Phi^{m-1}_\nu e^{i\nu\theta}d\nu}{\left[\zeta^{(1)\prime}_{\nu-\frac{1}{2}}(ka)+i\delta\zeta^{(1)}_{\nu-\frac{1}{2}}(ka)\right]^2}, \tag{4}$$

where m = 1, 2, 3, ...; F_ν and Φ_ν are the "spherical" coefficients of reflection for the earth's surface and the lower boundary of the ionosphere, respectively, expressed by the formulas

$$F_\nu = \frac{\dfrac{i\zeta^{(1)\prime}_{\nu-\frac{1}{2}}(kc)}{\zeta^{(1)}_{\nu-\frac{1}{2}}(kc)} - \delta_\nu(c)}{\dfrac{i\zeta^{(2)\prime}_{\nu-\frac{1}{2}}(kc)}{\zeta^{(2)}_{\nu-\frac{1}{2}}(kc)} + \delta_\nu(c)}, \tag{5}$$

$$\Phi_\nu = \frac{\dfrac{\zeta^{(2)'}_{\nu-\frac{1}{2}}(ka)}{i\zeta^{(2)}_{\nu-\frac{1}{2}}(ka)} - \delta}{\dfrac{i\zeta^{(1)'}_{\nu-\frac{1}{2}}(ka)}{\zeta^{(1)}_{\nu-\frac{1}{2}}(ka)} + \delta} \qquad (6)$$

The first term in (3) characterizes the field for a uniform atmosphere, and is not written out in an explicit form. The dipole current is designated by j_0, δ shows the reduced surface impedance of the earth's surface, and $\zeta^{(1)}_{\nu-\frac{1}{2}}$, $\zeta^{(2)}_{\nu-\frac{1}{2}}$ — are "spherical" Bessel functions. The symbol $\delta_\nu(c)$ in (5) designates the "spherical" impedance at the air-ionosphere boundary ($r = c$), /144

$$\delta_\nu(c) = -\frac{i}{k\varepsilon'_m(c)} \cdot \frac{R'_\nu(c)}{R_\nu(c)}, \qquad (7)$$

where $R_\nu(r)$ are radial functions in the expansion of the field in the ionosphere. They satisfy the following equation:

$$\frac{d^2R_\nu}{dr^2} - \frac{1}{\varepsilon'_m(r)} \cdot \frac{d\varepsilon'_m(r)}{dr} \cdot \frac{dR_\nu}{dr} + \left(k^2\varepsilon'_m(r) - \frac{\nu^2-\frac{1}{4}}{r^2}\right)R_\nu = 0. \qquad (8)$$

If we are interested in the field in the air, then the function R_ν can be disregarded, since it is sufficient to know the impedance of (7) in this case, for which we can find the following equation with the aid of (8), as was shown in [1]:

$$\frac{d\delta_\nu(r)}{dr} = -ik\left\{\varepsilon'_m(r)\,\delta^2_\nu(r) - \left[1 - \frac{\nu^2-\frac{1}{4}}{k^2\varepsilon'_m(r)\,r^2}\right]\right\}. \qquad (9)$$

It is easy to see that (9) converts into (1) if we assume that

$$\sin^2\psi = \frac{\nu^2-\frac{1}{4}}{k^2r^2} \approx \frac{\nu^2}{k^2c^2}\left(1 - \frac{2h}{c}\right), \qquad (10)$$

where $\underline{h} = \underline{r} - \underline{c}$. Since in our problem $\underline{h} << \underline{c}$ always, then the value of ν obtained from (10) coincides with the saddle point of the integrand from (4), i.e.,

$$\nu_m = ka \sin \varphi_m = kc \sin \psi_m \qquad (11)$$

(see Fig. 1).

For the initial condition in integration of (9), we can select such a value of $\delta_\nu(r_1)$ that the layers of the ionosphere above r_1 have no effect on the field in the air. We can then consider the ionosphere for $\underline{r} > \underline{r}_1$ to be uniform, (8) is degenerated into a Bessel equation, and, considering the conditions for emission at $\underline{r} \to \infty$, we find that

$$\delta_\nu(r_1) = -\frac{1}{\sqrt{\varepsilon'_m(r_1)}} \cdot \frac{\zeta^{(1)'}_{\nu-\frac{1}{2}}\left(k\sqrt{\varepsilon'_m(r_1)}\, r_1\right)}{\zeta^{(1)}_{\nu-\frac{1}{2}}\left(k\sqrt{\varepsilon'_m(r_1)}\, r_1\right)}, \qquad (12)$$

where the prime in the function $\zeta^{(1)}_{\nu-\frac{1}{2}}$ signifies differentiation over the entire argument. However, in practice it is sufficient to assume the following [2]: /145

$$\delta_\nu(r_1) = \frac{1}{\sqrt{\varepsilon'_m(r_1)}}. \qquad (13)$$

In order to compare the solutions for "plane" and "spherical" impedances, we carried out numerical calculations, the results of which are discussed below.

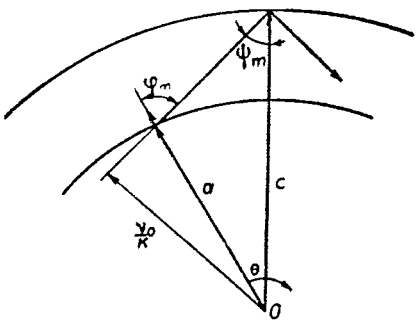

Fig. 1.

Equation (9) was solved by numerical integration on an electronic computer. The permittivity $\varepsilon_m(r)$ in the ionosphere was determined on the basis of averaged ionospheric profiles for the electron concentration and number of electron collisions [2]. We examined the diurnal and nocturnal ionosphere, and the latter was distinguished by a sharper gradient for the electron concentration.

If we compare the solutions to (1) and (9) for certain fixed angles of ψ ($\nu = kc \sin \psi$), then we can hardly expect a great

difference, as can be seen from (10). Actually, this difference does not exceed 1% in the case of the nocturnal ionosphere for values of ψ in the range from 1.0 to 1.45 and for frequencies from 5 to 60 KHz, and it does not exceed 3% in the case of the diurnal ionosphere (when the wave penetrates more deeply into the ionosphere).

The solutions to (9) for real ν, which can be associated with definite angles of incidence on the layer of the ionosphere with the aid of (11), depend in different ways on the angle of incidence for the nocturnal and diurnal models of the ionosphere. For low frequencies (5-15 KHz), this difference is not very substantial, but at higher frequencies the same change in the angle of incidence causes a much greater change in the impedance for the diurnal layer than for the nocturnal one (Fig. 2). A similar dependence is also maintained for complex ν. Figures 3-6 show graphs of the dependence of the real and imaginary parts of the "spherical" impedance, as well as the real and imaginary parts of the integrand of the variable for integration along the contour for the first "ray" ($m = 1$) at a distance from the source of 3,000 km.[1] In this regard, we are examining frequencies of 5 and 60 KHz for the diurnal and nocturnal models of the ionosphere. The integration contour consists of two lines emerging from the origin of the coordinates at angles of $\frac{3\pi}{4}$ and $\frac{\pi}{6}$ to the real axis. The integration variable t is connected to ν by the following relationship: /146

$$t=\left(\frac{2}{ka}\right)^{\frac{1}{3}}(\nu-ka), \tag{14}$$

since in calculating the diffraction rays of the Bessel function, they were replaced by asymptotic representations in terms of the Airy functions [3].

Using the graphs in Figures 3-6, we can assume that the assumptions we made in [1] in calculating the diffraction "rays" ("plane" impedance which does not depend on the integration variable ν) yield the greatest error for the highest frequencies of this range and the diurnal conditions for propagation. This is confirmed by the results of numerical computations presented in the table for "spherical" and "plane" impedances.[2]

Thus, the solution obtained in [1] is found to be completely satisfactory (at least in the range of 5-60 KHz). Obviously, this allows us to use the method of constructing the solution with the

---

[1] The integrand of (4) is designated by ϕ in Figures 3-6.

[2] The moduli and arguments of values of V_m which imply the functions of attenuation for the "rays" are given in the Table (see [1]).

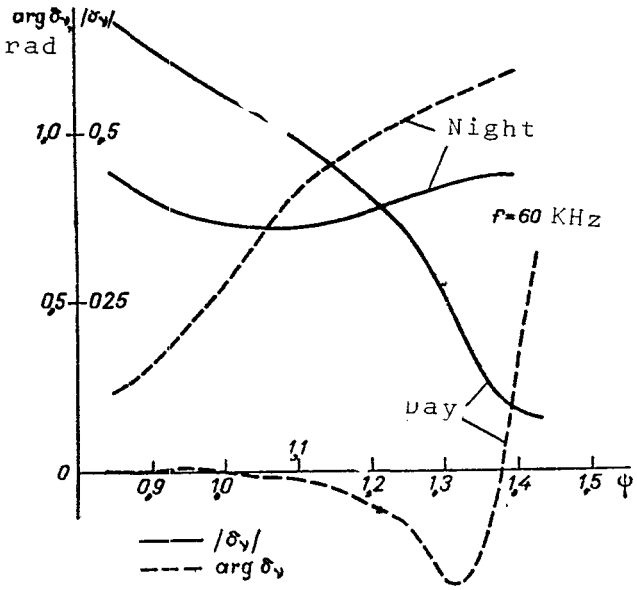

Fig. 2

aid of "rays" for the earth-ionosphere waveguide channel with subsequent approximation, considering the dependence of the waveguide height on the distance along the earth's surface.

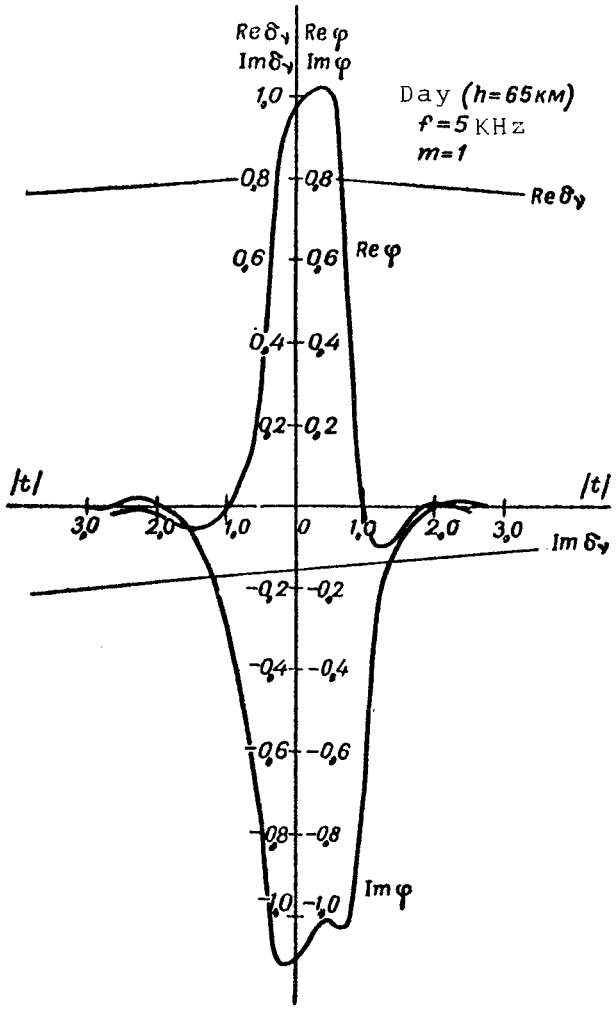
Re δy
Im δy
Re φ
Im φ
Day (h=65км)
f=5 KHz
m=1
1,0
0,8
0,6
0,4
0,2
Re δy
Re φ
/t/
/t/
3,0
2,0
1,0
0
1,0
2,0
3,0
Im δy
-0,2
-0,4
-0,6
-0,8
-1,0
Im φ

Fig. 3

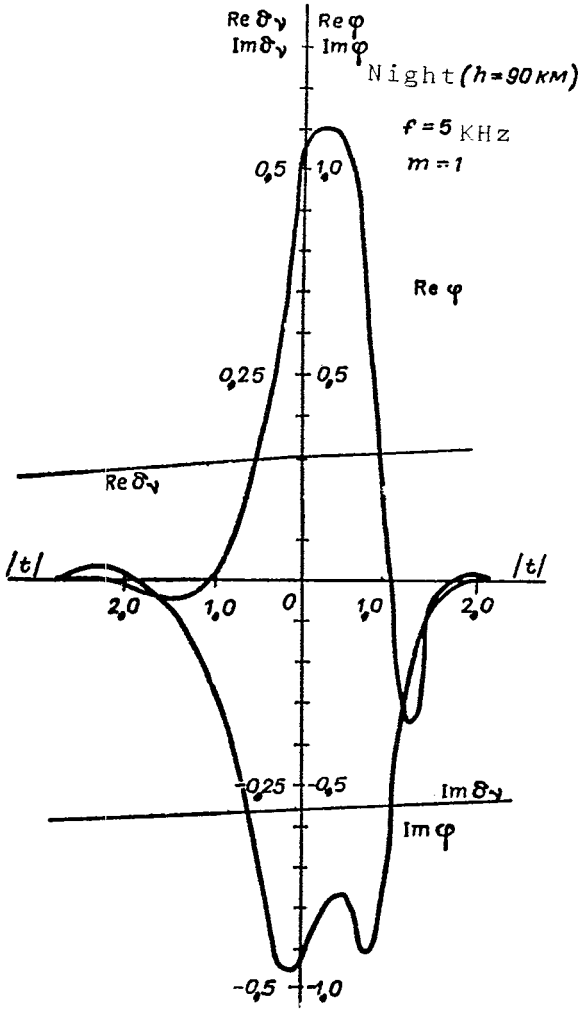
Re δ_v
Im δ_v
Re φ
Im φ
Night (h=90 км)
f=5 KHz
m=1
0,5
1,0
Re φ
0,25
0,5
Re δ_v
/t/
/t/
2,0
1,0
0
1,0
2,0
-0,25
-0,5
Im δ_v
Im φ
-0,5
-1,0

Fig. 4

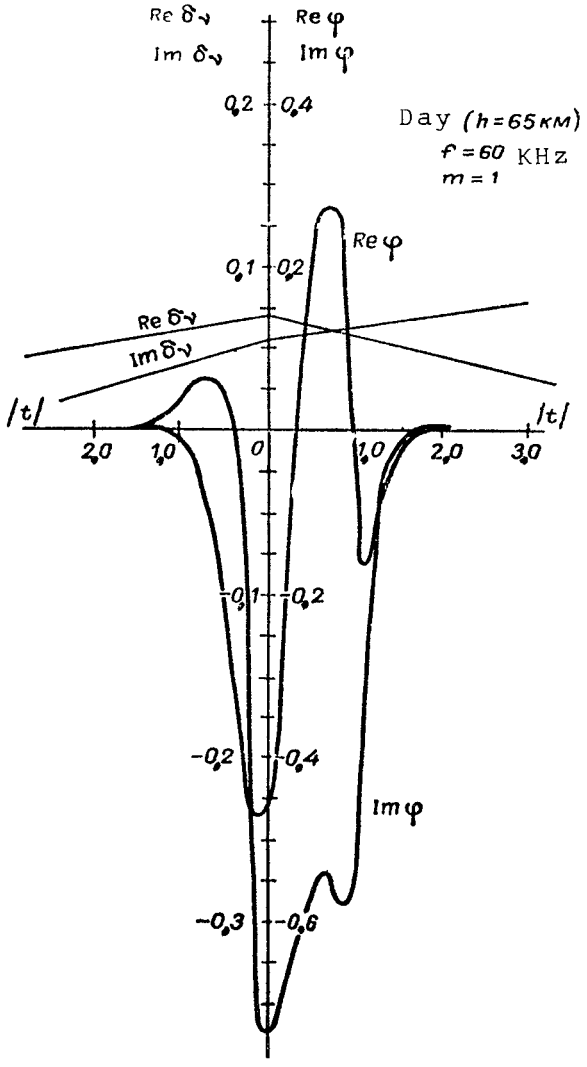
Re δ-ν
Im δ-ν
Re φ
Im φ
0,2
0,4
Day (h=65км)
f=60 KHz
m=1
Re φ
0,1
0,2
Re δ-ν
Im δ-ν
/t/
/t/
2,0
1,0
0
1,0
2,0
3,0
-0,1
-0,2
-0,2
-0,4
Im φ
-0,3
-0,6

Fig. 5

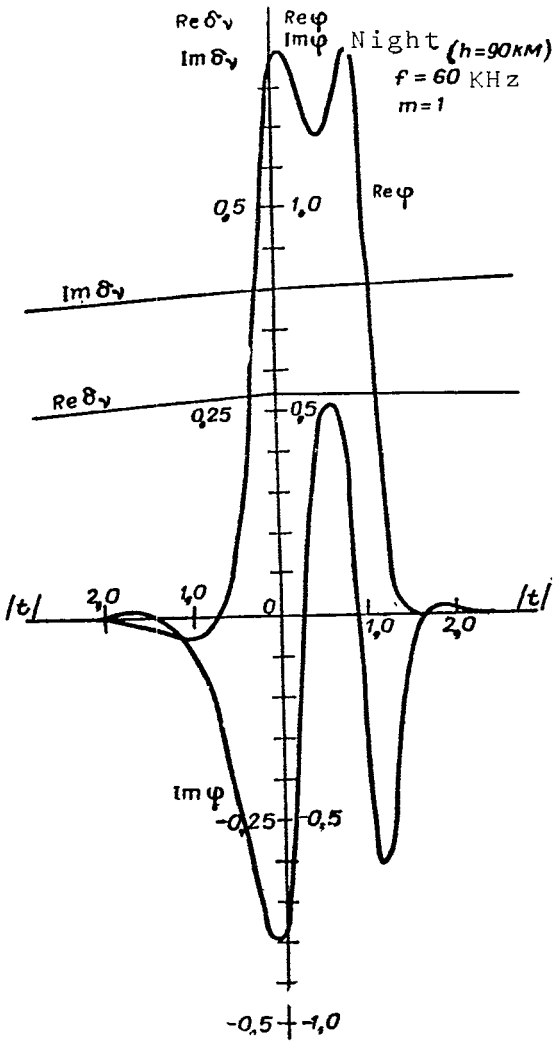
Re δ_v
Im δ_v
Re φ
Im φ
Night (h=90км)
f = 60 KHz
m = 1
Re φ
0,5
1,0
Im δ_v
Re δ_v
0,25
0,5
/t/
2,0
1,0
0
1,0
2,0
/t/
Im φ
-0,25
-0,5
-0,5
-1,0

Fig. 6

MODULUS AND ARGUMENT OF THE ATTENUATION FUNCTION V_m FOR DISTANCE OF 3,000 KM

Impedance	Night		Day	
	Modulus V_m	Argument V_m	Modulus V_m	Argument V_m
	5 KHz			
	m=1		m=1	
δ_ν	0.7853	2.444	0.8353	3.136
δ_s	0.7839	2.442	0.8397	3.137
	m=2		m=2	
δ_ν	0.8125	3.666	0.968	5.070
δ_s	0.8121	3.667	0.968	5.075
	60 KHz			
	m=1		m=1	
δ_ν	0.9166	5.682	0.3778	1.213
δ_s	0.9152	5.681	0.3280	1.203
	m=2		m=2	
δ_ν	1.0941	2.468	0.2135	5.186
δ_s	1.0962	2.467	0.2570	5.005

REFERENCES

1. Gyunninen, E.M. and M.N. Zabavina: In the Collection: Problemy difraktsii i rasprostraneniya voln (Problems of Wave Diffraction and Propagation), No. V, 1966.
2. Gavrilov, N.S. and V.V. Kirillov: Same, p. 31.
3. Fok, V.A.: Difraktsiya radiovoln vokrug zemnoy poverkhnosti (Radio-Wave Diffraction around the Earth's Surface). Academy of Sciences U.S.S.R.,1946.

TAKING ACCOUNT OF THE NONUNIFORMITY OF THE IONOSPHERE IN THE PROBLEM OF SUPER-LONG WAVE PROPAGATION IN THE WAVEGUIDE CHANNEL EARTH-IONOSPHERE

S. T. Rybachek

ABSTRACT: This article is a continuation of a study on the problem of the field of a vertical electric dipole in a waveguide whose walls are formed by the Earth, characterized by finite conductivity, and a uniform isotropic ionosphere, expanded for the cases of an ionosphere which is non-uniform in terms of the radial coordinates. The difficulties encountered with this problem are cited, and methods of overcoming them are suggested.

The problem of the field of a vertical electric dipole in a waveguide whose walls are formed by the Earth, characterized by finite conductivity, and the uniform isotropic ionosphere was investigated in [1]. This study is a direct continuation and generalization of the results of [1] for the case of the ionosphere which is non-uniform in terms of the radial coordinates. /152

1. We will consider the source of the elctromagnetic field to be a radial electric dipole which has moment of P_0 and which is located on the surface of the Earth at the point $r = a$, $\vartheta = 0$ (we will use the spherical system of coordinates (r, ϑ, ϕ) with origin at the center of the Earth). We will approximate the Earth, whose electrical properties are characterized by the reduced surface impedance δ, by a sphere of radius $\underline{a}$. The ionosphere, which we will consider to be an isotropic and nonuniform (in terms of the radial coordinate $\underline{r}$) medium, is arranged at $r > c$ ($c = a + h$, where h is the height of the waveguide).

As is well known [2], this problem is reduced to a solution to the wave equation for the Hertz function $\underline{u}$:

$$\nabla^2 u + \tilde{k}^2 u = -\frac{P_0}{2\pi\varepsilon}\,\frac{\delta(r-a)\,\delta(\vartheta-0)}{r^3\sin\vartheta}, \qquad (1)$$

where $\tilde{k}^2 = k^2$ at $a < r \leq c$;

$$\tilde{k}^2 = k_u^2 - k_u \frac{d^2}{dr^2}\cdot\frac{1}{k_u} \quad \text{for } r > c.$$

The boundary conditions have the following appearance:

(1) $\frac{\partial(ru)}{\partial r} = -ik\delta ru$ at $r = a$;

(2) u and $\frac{\partial u}{\partial r}$ are continuous at the boundary $r = c$ (we will assume that k_u and $\frac{\partial k_u}{\partial r}$ are continuous at $r = c$). The function u has a pole of first order at the points where the source is located, and it should satisfy the conditions for emission to infinity. /153

The solution to the boundary problem formulated above is constructed by standard methods in a way similar to what was done for the case of a uniform ionosphere, the wave number of which k_u did not depend on the radial coordinate r [1]. Therefore, we will not reconstruct the solution in this study, but will only present the final formulas and discuss the difficulties encountered in considering a non-uniformity in the ionospheric layer.

Expansion by normal waves results in the following type of solution for the function of attenuation V connected with the function u by the relationship $u = 2\frac{e^{ika\partial}}{a\partial} V$:

$$V = -\sqrt{\frac{2\pi}{\sin\vartheta}} \cdot \frac{\vartheta}{ka} e^{i\frac{\pi}{4}} \sum_{m=1}^{\infty} \times$$

$$\times \frac{\sqrt{\nu_m}\left[\zeta^{(1)}_{\nu_m-1/2}(ka) - \zeta^{(2)}_{\nu_m-1/2}(ka) A_{\nu_m-1/2}\right] e^{i(\nu_m - ka)\vartheta}}{\left[\zeta^{(1)'}_{\nu_m-1/2}(ka) + i\delta\zeta^{(1)}_{\nu_m-1/2}(ka)\right] \frac{\partial}{\partial\nu}\left[1 - A_{\nu-1/2}B_{\nu-1/2}\right]_{\nu=\nu_m}}, \quad (2)$$

where

$$A_{\nu-1/2} = \frac{\zeta^{(1)}_{\nu-1/2}(kc)}{\zeta^{(2)}_{\nu-1/2}(kc)} R^u_{\nu-1/2};\ R^u_{\nu-1/2} = \frac{\frac{\zeta^{(1)'}_{\nu-1/2}(kc)}{\zeta^{(1)}_{\nu-1/2}(kc)} - i\delta_u}{-\frac{\zeta^{(2)'}_{\nu-1/2}(kc)}{\zeta^{(2)}_{\nu-1/2}(kc)} + i\delta_u}; \quad (3)$$

$$B_{\nu-1/2} = \frac{\zeta^{(2)}_{\nu-1/2}(ka)}{\zeta^{(1)}_{\nu-1/2}(ka)} R^3_{\nu-1/2};\ R^3_{\nu-1/2} = \frac{\frac{\zeta^{(2)'}_{\nu-1/2}(ka)}{\zeta^{(2)}_{\nu-1/2}(ka)} + i\delta}{-\frac{\zeta^{(1)'}_{\nu-1/2}(ka)}{\zeta^{(1)}_{\nu-1/2}(ka)} - i\delta}. \quad (4)$$

The values $R^3_{\nu-1/2}$ and $R^u_{\nu-1/2}$ signify the spherical coefficients of reflection from the Earth and the ionosphere. The value δ_u, which defines the coefficient of reflection from the ionosphere, has the following form:

$$\delta_u = \frac{1}{ik} \cdot \frac{f'_{\nu-1/2}(r)}{f_{\nu-1/2}(r)}\Big|_{r=c}, \quad (5)$$

where $f_{\nu-1/2}$ satisfies the equation

$$f''_{\nu-1/2}(r)+\left\{k_u^2(r)-k_u(r)\frac{d^2}{dr^2}\cdot\frac{1}{k_u(r)}-\frac{\nu^2-\frac{1}{4}}{r^2}\right\}f_{\nu-1/2}(r)=0, \tag{6}$$

in which /154

$$k_u^2(r)=k^2\varepsilon'_{mu}(r)=k^2\left\{1-\frac{4\pi e^2N(r)\left[1-i\frac{\nu_{eff}(r)}{\omega}\right]}{m\left[\omega^2+\nu^2_{eff}(r)\right]}\right\},$$

as well as the condition for emission to infinity.

In calculating the electromagnetic field by the method of normal waves, the basic difficulty is to determine the zeros of the transcendental equation

$$1-A_{\nu-\frac{1}{2}}B_{\nu-\frac{1}{2}}=0, \tag{7}$$

which contains Hankel functions of the first and second type of arbitrary index and argument, the radial functions $f_{\nu-\frac{1}{2}}(r)$ and the derivative of these functions by the argument. In solving this problem, we used numerical methods which permitted us to determine the zeros of (7) with the requisite accuracy. The method of calculating Hankel functions and determining the roots of (7) was expanded in detail in [1]. In this study, we will describe the method of calculating the radial functions. We should mention that, in calculating the coefficients of reflection from the ionosphere, which are determined by these radial functions, it was suggested that we use the experimental dependences of the electron concentration and the effective number of collisions between electrons and neutral molecules on the height. This problem can be solved solely by numerical methods. However, after integration of (6) we must carry out numerical differentiation of the function given by tables ($\frac{d^2}{dr^2}\cdot\frac{1}{k_u(r)}$). This can be avoided if we introduce the new function $\underline{y}$ by the formula

$$y=\frac{\frac{d}{dr}\left(\sqrt{\varepsilon'_{mu}}f_{\nu-\frac{1}{2}}(r)\right)}{\left(\varepsilon'_{mu}\right)^{3/2}f_{\nu-\frac{1}{2}}(r)}. \tag{8}$$

We will then convert from a second-order differential equation for the function $f_{\nu-1/2}(r)$ to a first-order differential equation for the function $y(r)$, in which there is no term of the type

$\frac{d^2}{dr^2} \cdot \frac{1}{k_u(r)}$:

$$\frac{dy}{dr} = \varepsilon'_{mu} + \left\{ k^2 - \frac{\nu^2 - \frac{1}{4}}{r^2 \varepsilon'_{mu}} \right\} y^2. \qquad (9)$$

We took the value $y = \frac{\sqrt{\varepsilon' mu}}{ik}$ at the level $r = c + h_0$ as the initial data for (9). This corresponds to a solution to the differential equation in (6) for the function $f_{\nu-1/2}(r)$ in a WKB approximation on the level $c + h_0$. The value h_0 is selected in such a way that the layer of the ionosphere located above it does not affect the values of the function y, and consequently, has no effect on the values of the "spherical impedance" δ_u at the boundary of the ionosphere, which is connected with y by the following relationship:

$$\delta_u = -\frac{i}{ky}\Big|_{r=c}.$$

Analytical and numerical investigations of the error in initial data were prevented in [3] for a similar equation describing the coefficients of reflection of plane electromagnetic waves from a plane-layered anisotropic plasma. We carried out analogous numerical studies for (9), which showed that, in order to calculate the value of δ_u with accuracy up to 0.1% (in the frequency range of 5-60 KHz), we must take a value of h_0 which does not exceed 20 km.

2. In order to illustrate the dependences of the damping, which is determined by the value $\mathrm{Im}\nu_m$, and the phase velocity c_{fm} of the wave mode of number m, determined by the ratio $\frac{c}{c_{fm}} = \frac{\mathrm{Re}\nu_m}{ka}$, as well as that of the modulus and phase of the attenuation function V on the properties of the ionosphere and the frequency of the electromagnetic field, we carried out our computations on an electronic computer.

In order to account for the effect on the field in air of a highly conductive layer of ground waters, we selected a two-layered model of the Earth: the upper layer, of thickness l = 10 m, had relative permittivity of $\varepsilon/\varepsilon_0 = 20$ and conductivity of $\sigma = 10^{-2}$ 1/Ohm·m; the lower "layer" (sphere of radius a - l) had $\varepsilon/\varepsilon_0 = 25$, $\sigma = 5 \cdot 10^{-2}$ 1/Ohm·m (meter-kilogram-second unit system).

The dependence of the electron concentration N[el/cm^3] and ν_{eff} [1/sec] on the altitude (starting with the level r = a) of the ionospheric layer for which the calculations of the coefficients of reflection from the ionosphere were carried out, is depicted in Figure 1. The curve for ν_{eff} (dotted) was obtained according to the Nicolet formula [4], while we used approximations by third-power polynomials obtained in [3] in calculating the curves of N(r-a) which

are averaged models of the diurnal and nocturnal layer. Figure 2 shows the dependence of the attenuation of the first normal wave on the frequency for different manners of calculating the coefficients of reflection from the ionosphere. Curve 1 corresponds to

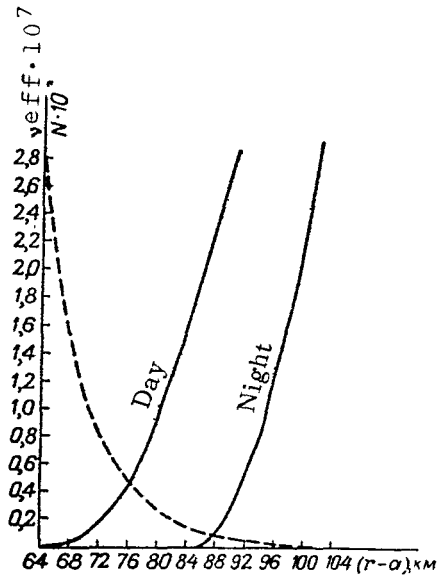

Fig. 1

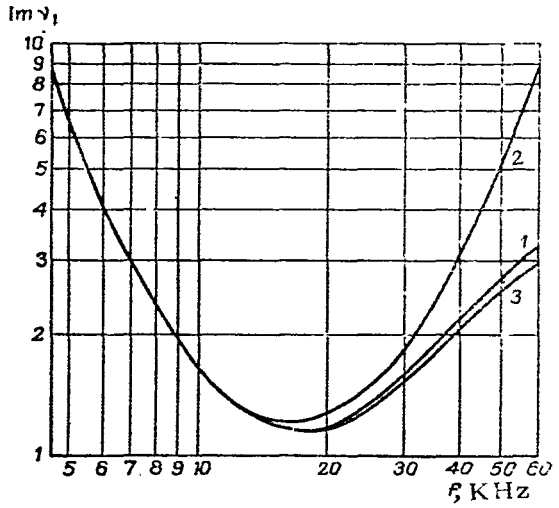

Fig. 2

/156

calculations with "point" coefficients of reflection [y was determined by integration of the differential equation in (9)]. In calculating Curve 2 (which was done in [1]), we used the Fresnel coefficients of reflection of a plane wave from a plane boundary of the ionosphere. Finally, in calculating Curve 3, we used coefficients of reflection from a plane air-ionosphere boundary (this corresponds to integration of the differential equation for y of the type

/157

$$\frac{dy}{dr} = \varepsilon'_{mu} + \left\{k^2 - \frac{\nu^2 - \frac{1}{4}}{r^2 \varepsilon'_{mu}}\right\} y^2).$$

In calculating the coefficients of reflection from the ionosphere by these methods, the phase velocities obtained for the normal waves did not differ substantially; therefore, the corresponding dependences of $\frac{c}{c_{fl}}$ are not presented in this work.

The dependences of the damping and the ratio $\frac{c}{c_{fm}}$ of the first two modes on the frequency are shown in Figures 3(a) and 3(b) for the day. The corresponding dependences for the nocturnal condition of the ionosphere are shown in Figures 4(a) and 4(b).

A consideration of the non-uniformity of the ionosphere in terms of altitude resulted in a situation where a clearly pronounced minimum (Fig. 3(a)) was observed in the damping of the modes corresponding to the diurnal state of the ionosphere; the position of this minimum shifted toward higher frequencies with an increase in the number of the wave mode. The nocturnal curves for the damping (Fig. 4a) in the frequency range under investigation did not have such sharp minima for the selected model of the ionospheric layer. We could also mention that, in going from day to night, the curves for attenuation of various normal waves converged. Correspondingly, for frequencies higher than 10-15 KHz, the electromagnetic field oscillated more during the night than during the day. At lower frequencies, the field was determined by one mode both during the day and the night; therefore, the dependence of the field on the distance and properties of the ionosphere obviously was of a monotonous nature.

Figures 5(a) and 5(b) show the modulus of the damping function and supplementary phase of the electromagnetic field ϕ_{sup} for the first two modes in dependence on the distance (in Fig. 5b the left-hand scale corresponds to the solid lines, while the right-hand one corresponds to the dotted lines). As the frequency increases the role of the second mode becomes more substantial: if $|V_1|$ is greater than $|V_2|$ at low frequencies, then they become comparable at higher frequencies; then $|V_2|$ begins to exceed $|V_1|$, and thus the second mode becomes the principal one.

The dependences of $|V|$ and the supplementary phase of the electromagnetic field on the distance are shown in Figures 6-13 (for frequencies of 10, 12, 14, 16, 18 and 20 KHz). Figures 6 and 7 correspond to the diurnal condition of the ionosphere at an altitude of 64 km, while Figures 8 through 13 correspond to the nocturnal condition, for altitudes of 85 and 90 km. We will not discuss the dependences depicted in Figures 6-13 in detail; we will only mention some of the rules for them. At low frequencies, both $|V|$ and ϕ_{sup} are monotonous functions of the distance. As the frequency increases, the oscillations in the electromagnetic field are magnified. A transition from the diurnal to the nocturnal conditions results in a situation where oscillations in the field arise at lower frequencies. When the properties of the ionosphere are kept unchanged, an increase in the height of the waveguide also causes oscillations in the field at lower frequencies. Thus, if ϕ_{sup} changes almost linearly throughout the entire range under investigation (3-10,000 km), at a frequency of 14 KHz for an altitude of 85 km, i.e., if the phase velocity does not depend on the distance, then the range for a linear change in ϕ_{sup} becomes much narrower (8-10,000 km) for the same frequency but for an altitude of 90 km (see Fig. 12).

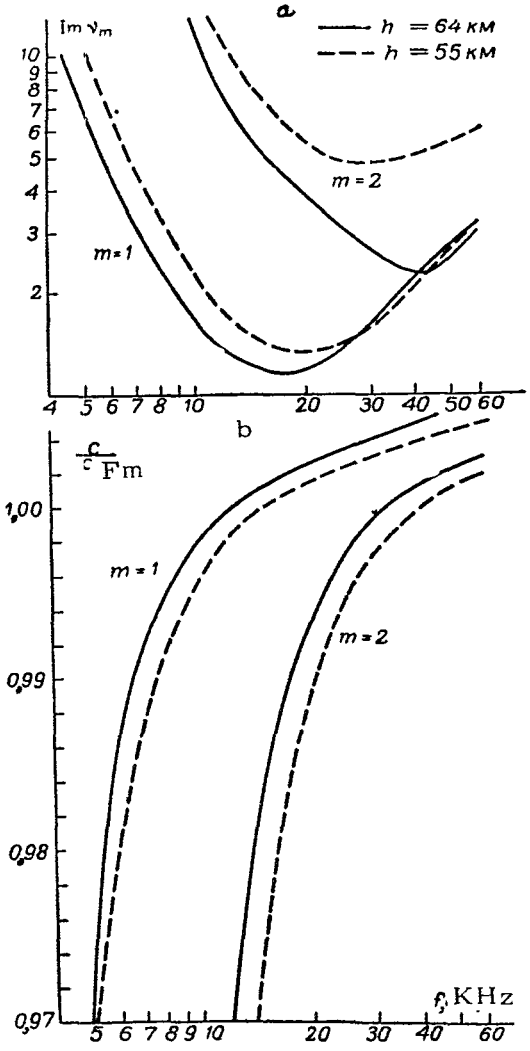
a
h = 64 км
h = 55 км
Im ν_m
10
9
8
7
6
5
4
3
2
m=1
m=2
4 5 6 7 8 10 20 30 40 50 60
b
c/c Fm
1,00
0,99
0,98
0,97
m=1
m=2
f, KHz
5 6 7 8 9 10 20 30 40 60

Fig. 3

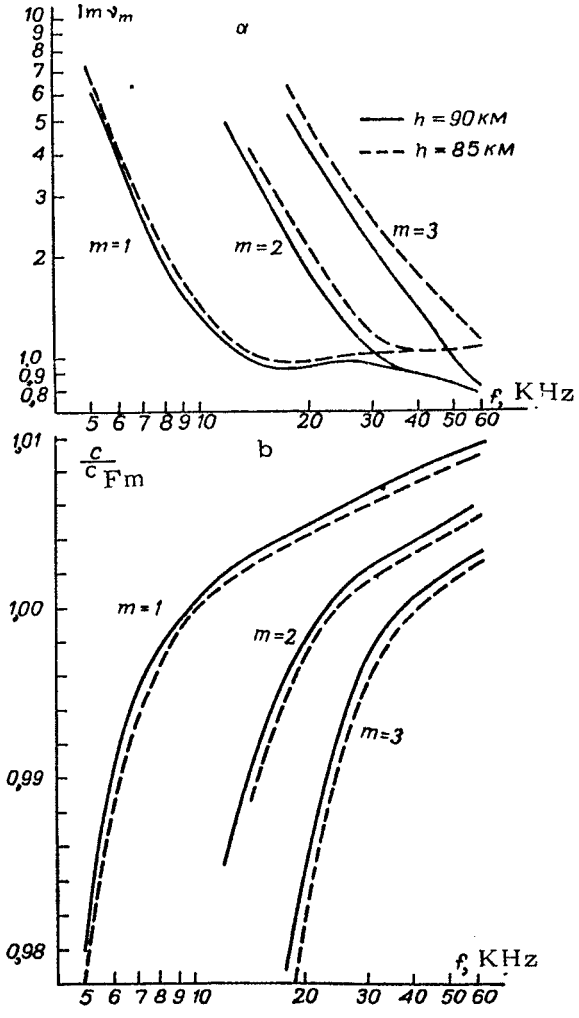

Fig. 4

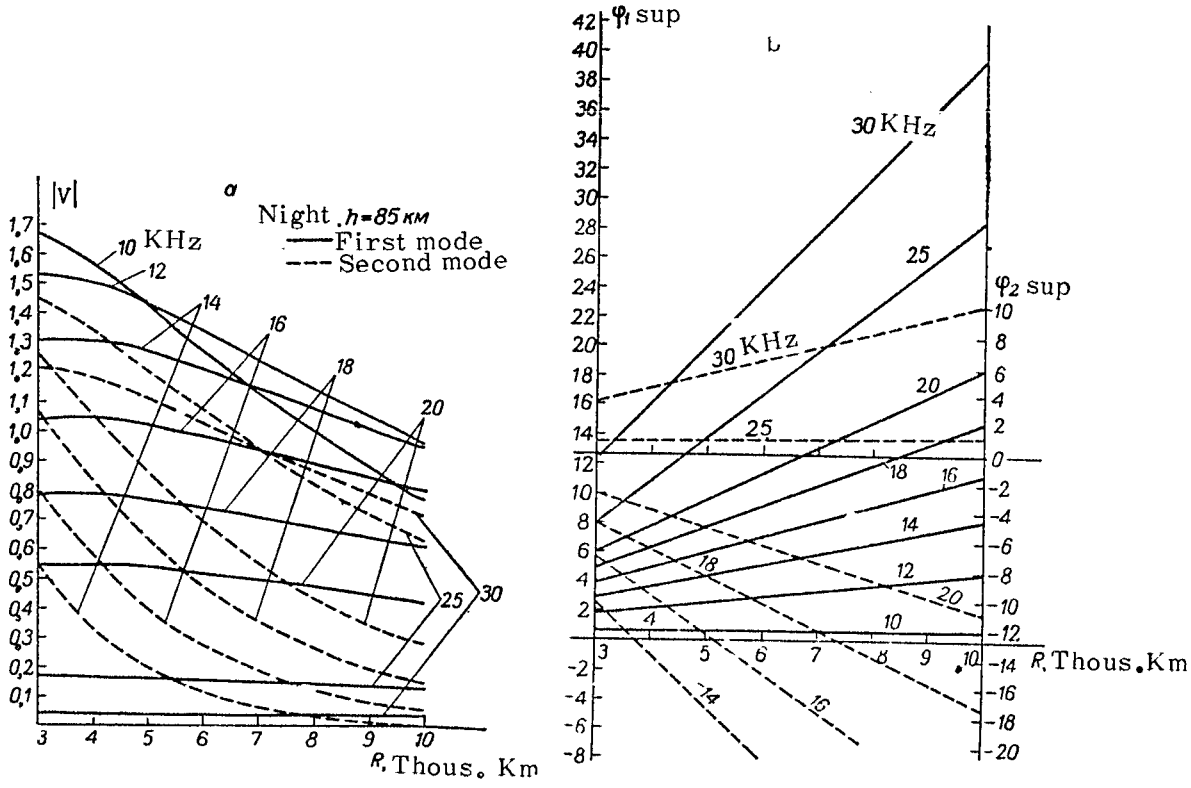
a
|V|
Night, h=85 км
First mode
Second mode
10 KHz
12
14
16
18
20
25
30
R, Thous. Km
b
φ1 sup
30 KHz
25
30 KHz
25
φ2 sup
20
18
16
14
12
10
R, Thous.Km

Fig. 5

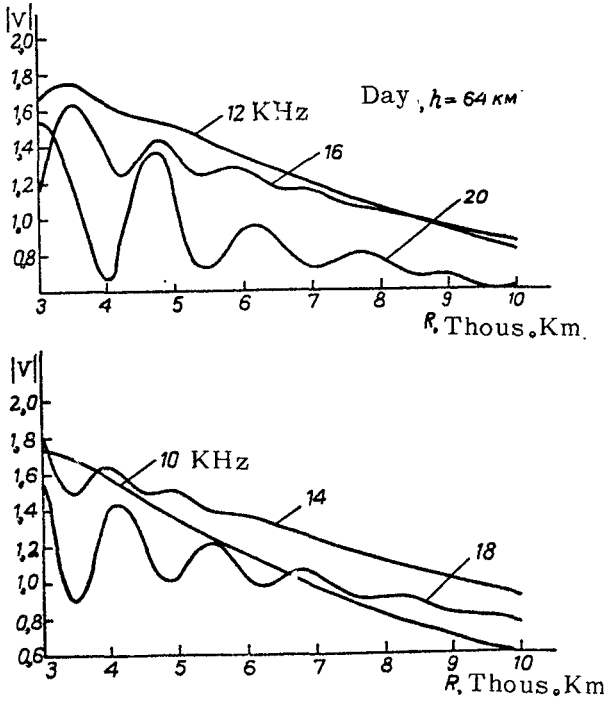

Fig. 6

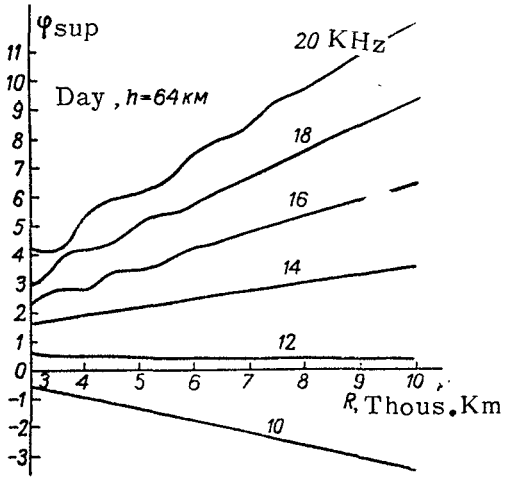

Fig. 7

/161/

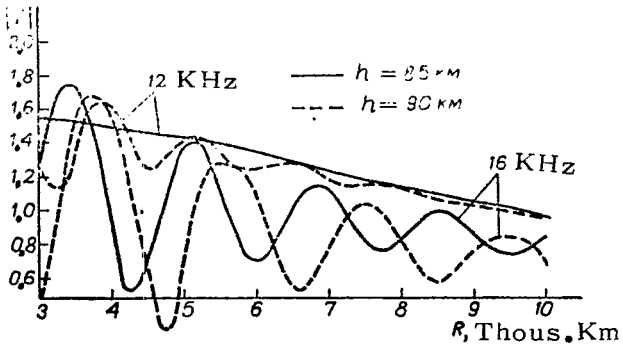

/16

Fig. 8

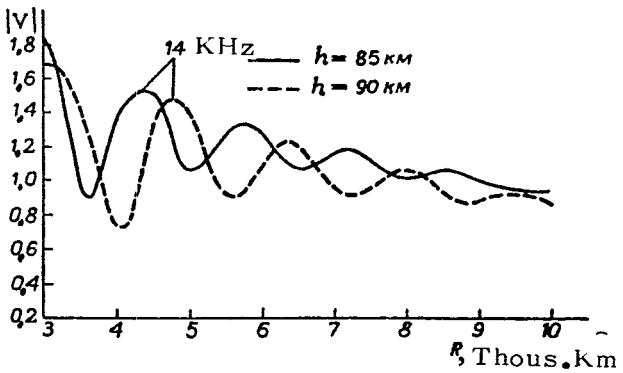

Fig. 9.

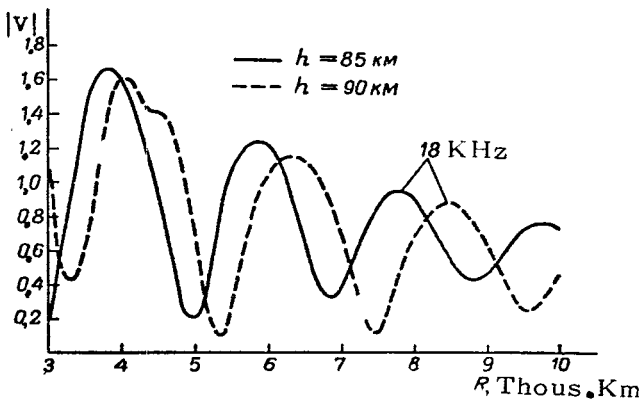

Fig. 10.

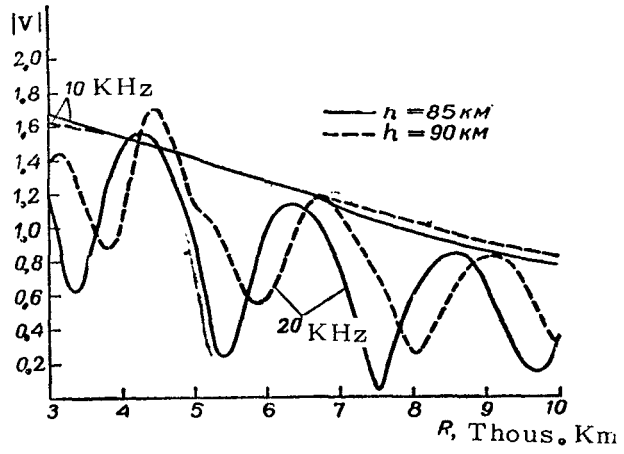

Fig. 11.

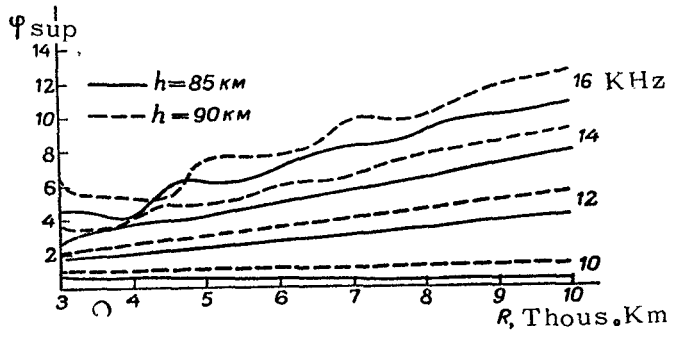

Fig. 12.

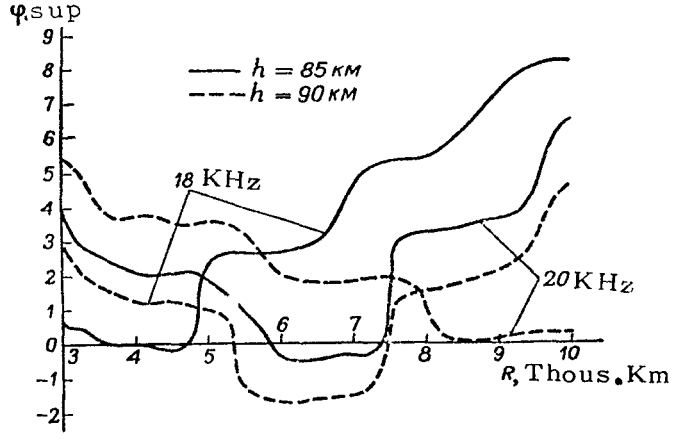

Fig. 13.

In conclusion, we must mention that we have presented numerous /164 graphs, thinking that they might be of independent interest for those carrying out studies on the propagation of super-long waves.

REFERENCES

1. Rybachek, S. T. and E. M. Gyunninen: Propagation of Long and Superlong Radio Waves in the Waveguide Channel Earth-Ionosphere. In the Collection: Problemy difraktsii i rasprostraneniya voln (Problems of Wave Diffraction and Progagation), No. VI. Leningrad State University Press, 1966.
2. Bremmer, H.: Terrestrial Radio-Waves. New York, 1949.
3. Gavrilova, N.S. and V. V. Kirillov: Propagation of Superlong Waves. Calculation of the Coefficients of Reflection of Plane Waves from a Nonuniform Anisotropic Plasma. In the Collection: Problemy difraktsii i rasprostraneniya voln (Problems of Wave Diffraction and Propagation), No. V. Leningrad State University Press, 1966.
4. Nicolet, M.J.: J. of Atmospherical and Terrestrial Physics, Vol. 3, 1953.

THE REFLECTION OF A "BELL" PULSE FROM A SYMMETRICAL EPSTEIN MEDIUM

L.I. Bezruchenko

ABSTRACT: The problem of the reflection of a "bell" pulse from a symmetrical Epstein medium is discussed in relation to the use of ground-based radiophysical methods of obtaining real profiles for the electron concentration in the ionosphere. The criteria for formulation of the problem are cited, and the "spreading" of a reflected pulse, the displacement of the maximum of the reflected signal and the frequency modulation of this signal are examined.

In using ground-based radiophysical methods of obtaining real /165 profiles for the electron concentration in the ionosphere, it is necessary to solve the problem of the reflection of radio-frequency signals from nonuniform and anisotropic layers. It is a complicated task to obtain simple formulas controlling the most characteristic physical effects with a strict formulation of the problem. Therefore, having specified the formulation of the problem, we will consider that the model of the layer and the shape of the probing pulse satisfy the following prerequisites:

(1) The pulse has a narrow-band spectrum;
(2) The non-uniformity is "localized" in some layer with a maximum of electron concentration on the level of z = 0;
(3) The transmitter and receiver are a great distance from the maximum of the layer;
(4) The distribution of the electron concentration is such that it can be modeled by an Epstein layer [1];
(5) The medium is isotropic and has no damping ($\nu_{eff} = 0$).

We will show the mathematical criteria for limitations 2 and 3 below.

In the case when conditions 2, 3 and 4 are fulfilled, we can characterize the layer under investigation with a graat deal of accuracy by some coefficient of reflection R (iω) which does not depend on the coordinates. For a symmetrical Epstein layer, when the limiting value for the concentration $N(z \to \pm \infty) = 0$, R (iω) has the following form [2]

$$R(i\omega)=\frac{\Gamma\left(\frac{1}{2}-id_1-i\omega\Omega\right)\Gamma\left(\frac{1}{2}+id_1-i\omega\Omega\right)\Gamma(1+i\omega\Omega)}{\Gamma(1-i\omega\Omega)\,\Gamma\left(\frac{1}{2}+id_1\right)\Gamma\left(\frac{1}{2}-id_1\right)}, \qquad (1)$$

where $\Gamma(z)$ is a gamma function; $\Omega = \frac{2s}{c}$ (normal incidence of the wave on the layer); /166

$$d_1 = \frac{1}{2}\sqrt{\omega_к^2 \Omega^2 N_3 - 1}. \quad (2)$$

$$\omega_к^2 = \frac{4\pi e^2 N_3}{mc}; \quad (3)$$

s is a parameter characterizing the thickness of the Epstein layer; N_3 is the concentration of the layer at the maximum (z = 0).

A harmonic dependence on time of the type $e^{i\omega t}$ is assumed.

We will be interested in the envelope and microstructure of the reflected pulse, considering the following as the probing pulse with "bell-shaped" envelope and high-frequency loading ω_0:

$$E(t) = e^{-\alpha^2(t-t_0)^2} e^{i\omega_0 t}. \quad (4)$$

The spectrum of this pulse has the following form:

$$F(i\omega) = \frac{\sqrt{\pi}}{\alpha} e^{-\frac{1}{4\alpha^2}(\omega-\omega_0)^2} e^{-i(\omega-\omega_0)t_0}. \quad (5)$$

In view of the assumptions we made earlier, the reflected field of a plane monochromatic wave is expressed by the formula

$$E_{ref}(i\omega) = E_0 e^{i\omega\left(t+\frac{2z}{c}\right)} R(i\omega). \quad (6)$$

It is obvious that, for the field of the reflected pulse in (4), we can write out the relationship in the form of a Fourier integral, i.e.

$$E_{ref}(t) = \frac{1}{2\pi}\int_{-\infty}^{\infty} E_{ref}(i\omega) F(i\omega) e^{i\omega t} d\omega \quad (7)$$

or, considering (5) and (6), we find that

$$E_{ref}(t) = E_0 R(i\omega_0) e^{i\omega_0\left(t+\frac{2z}{c}\right)} e^{-i\omega_0 t_0} \frac{\sqrt{\pi}}{\alpha} \Phi(t), \quad (8)$$

where

$$\Phi(t) = \frac{1}{2\pi}\int_{-\infty}^{\infty}\frac{R(i\omega)}{R(i\omega_0)}e^{-\frac{1}{4\alpha^2}(\omega-\omega_0)^2+i\omega\left(t+\frac{2z}{c}\right)}d\omega. \quad (9)$$

Let us calculate Φ (t) on the assumption that the layer is sufficiently "thick" in terms of the wavelength, and that the load frequency ω_0 is less than the critical one ("reflecting layer") i.e., the following conditions are fulfilled:

$$\text{a)}\quad k_\kappa s \gg 1, \quad k_0 s \gg 1, \quad k \equiv \frac{\omega}{c}; \quad k_k = \frac{\omega_k\sqrt{N_3}}{c}; \quad (10)$$

$$\text{b)}\quad \omega_\kappa > \omega_0; \quad (11)$$

$$\text{c)}\quad |\omega_0\Omega - d_1| \simeq |\omega_0\Omega - \omega_\kappa\Omega| \geqslant 5. \quad (12)$$

Then, if the conditions in (10) - (12) are fulfilled, an asymptotic expression is valid for the Γ (z)-functions in (1) when the argument has high values.

Since the spectrum of the probing pulse is a narrow-band one, a substantial contribution to (9) in integration is made only by some region in the neighborhood of the point + $i\omega_0$. Using the relationship for Γ (z) in [3], i.e.,

$$\ln\Gamma(z+a) = \ln\Gamma(z) + a\ln z - \frac{a-a^2}{2z} + \ldots, \quad (13)$$

which is valid at $|z + a| >> 1$ and $|a| << |z|$, we can obtain the following asymptotic expression in the neighborhood of $\omega = \omega_0 \pm \delta$ for the ratio $\frac{R(i\omega_0)}{R(i\omega_0)}$:

$$\ln\frac{R(i\omega)}{R(i\omega_0)} \simeq (i\delta\Omega)^2 A - i\delta\Omega(B-C), \quad (14)$$

where

$$\operatorname{Re} A \simeq -\frac{1}{4}\cdot\frac{1}{(\omega_\kappa+\omega_0)^2\Omega^2} + \frac{1}{4}\cdot\frac{1}{(\omega_\kappa-\omega_0)^2\Omega^2} + \frac{1}{2(\omega_0\Omega)^2}; \quad (15)$$

$$\operatorname{Im} A \simeq \frac{1}{2(\omega_\kappa+\omega_0)\Omega} - \frac{1}{2(\omega_\kappa-\omega_0)\Omega} - \frac{1}{\omega_0\Omega}; \quad (16)$$

$$\operatorname{Re} C \simeq \frac{1}{4(\omega_\kappa+\omega_0)^2\Omega^2} + \frac{1}{4(\omega_\kappa-\omega_0)^2\Omega^2} - \frac{1}{2(\omega_0\Omega)^2}; \quad (17)$$

$$\operatorname{Im} C \simeq -\frac{1}{2}\cdot\frac{1}{(\omega_\kappa+\omega_0)\Omega} - \frac{1}{2}\cdot\frac{1}{(\omega_\kappa-\omega_0)\Omega} + \frac{1}{\omega_0\Omega}; \quad (18)$$

$$\operatorname{Re} B \simeq \ln\left[\left(\frac{\omega_\kappa}{\omega_0}\right)^2 - 1\right]; \quad (19)$$

$$\operatorname{Im} B = \operatorname{arc\,tan2}(\omega_k+\omega_0)\Omega + \operatorname{arc\,tan2}(\omega_k-\omega_0)\Omega - \operatorname{arc\,tan}\omega_0\Omega - \frac{\pi}{2}. \quad (20)$$

Having placed (14) under the sign of the integral of (9), we find that

$$\Phi(t) \simeq \frac{1}{2\pi} \int_{-\delta_0}^{\delta_0} e^{-\delta^2\left(\frac{1}{4\alpha^2} + A\Omega^2\right) - i\delta[\Omega(B-C) - (\tau - t_0)]} d\delta, \tag{21}$$

where

$$\tau \equiv t + \frac{2z}{c}$$

and δ_0 determines the boundaries of the region where the integrand makes a substantial contribution to (21).

The integral of Φ (t) can now be calculated with the aid of the integrals of probability from the complex argument in [4]. However, having replaced the limit in (21) by infinity, we can find the following for the field of the reflected pulse, with a great deal of accuracy:

$$E_{\text{refl}}(\tau) \cong R(i\omega_0)\, e^{i\omega_0\tau} \frac{1}{2\alpha D} e^{\frac{\sigma^2}{4D^2}} = F(\tau)\, e^{i\theta(\tau)}, \tag{22}$$

where /168

$$\sigma^2 \quad \Omega(B - C) - (t - t_0); \tag{23}$$

$$D^2 \quad \frac{1}{4\alpha^2} + \Omega^2 A. \tag{24}$$

Considering that σ^2 and D^2 are complex values, we can obtain the following expressions after rather simple conversions:

$$\psi(\tau) \equiv \operatorname{Re}\frac{\sigma^2}{4D^2} = \gamma^2(1 + 4\operatorname{Re} A\alpha^2\Omega^2)\left\{[\tau - t_0 - \tau_0]^2 - \right.$$
$$\left. - (\Omega q)^2\left[1 + \left(\frac{4\operatorname{Im} A\alpha^2\Omega^2}{1 + 4\operatorname{Re} A\alpha^2\Omega^2}\right)^2\right]\right\};$$
$$\varphi(\tau) \equiv \operatorname{Im}\frac{\sigma^2}{4D^2} = -\gamma^2 4\operatorname{Im} A\,\alpha^2\Omega^2\left\{(\tau - t_0 - \tau_0)^2 + \right. \tag{25}$$
$$+ 2(\tau - t_0 - \tau_0)\left(\frac{4\operatorname{Im} A\,\alpha^2\Omega^2}{1 + 4\operatorname{Re} A\,\alpha^2\Omega^2} + \frac{1 + 4\operatorname{Re} A\,\alpha^2\Omega^2}{4\operatorname{Im} A\,\alpha^2\Omega^2}\right)\Omega q +$$
$$\left. + \left[1 + \left(\frac{4\operatorname{Re} A\,\alpha^2\Omega^2}{1 + 4\operatorname{Re} A\,\alpha^2\Omega^2}\right)^2\right](\Omega q)^2\right.,$$

(26)

where

$$\tau_0 = \Omega p + \frac{4\operatorname{Im} A\,\alpha^2\Omega^2}{1 + 4\operatorname{Re} A\,\alpha^2\Omega^2}\Omega q; \tag{27}$$

$$\gamma^2 = \frac{\alpha^2}{(1 + 4\operatorname{Re} A\alpha^2\Omega^2) + (4\operatorname{Im} A\,\alpha^2\Omega^2)^2}; \tag{28}$$

$$p \equiv \operatorname{Re}(B - C), \quad q \equiv \operatorname{Im}(B - C). \tag{29}$$

Obviously, $\Psi(\tau)$ and $\phi(\tau)$ contain all the characteristics of the pulsed effect and describe the envelope of $\underline{F}(\tau)$ and the phase $\theta(\tau)$ in time, respectively. The value τ_0 characterizes the displacement of the maximum of the reflected signal relative to the time $\tau-t_0$. It follows from (26) that the minimum attenuation of the amplitude of the reflected signal (for $\tau-t_0 = \tau_0$) is determined by the value

$$\Psi[\tau-t_0=\tau_0]=-\gamma^2(1+4\operatorname{Re}A\alpha^2\Omega^2)\left[1+\frac{4\operatorname{Im}A\alpha^2\Omega^2}{1+4\operatorname{Re}A\alpha^2\Omega^2}\right](\Omega q)^2. \qquad (30)$$

Having studied (28) and (29), we can draw the following conclusions concerning some of the physical parameters of the reflected signal.

1. "Spreading" of the reflected pulse. If we determine the duration of the probing pulse Δt_i on the level where the envelope is incident $\underline{e}$ times, i.e. $\alpha^2(t-t_0)^2 = 1$, then for t_i = 100 μsec, the parameter $\beta = 2\cdot10^4$ sec^{-1}.

It can be seen form (25) that the curvature of the envelope for the reflected pulse is characterized by the parameter β:

$$\beta^2=\alpha^2\gamma^2. \qquad (31)$$

Disregarding the values of second order, we find the following approximating expression for the "spreading" of the pulse, for "thick" layers:

$$\Delta\simeq\frac{\alpha}{2(\omega_к-\omega_0)^2} \qquad (32)$$

on the condition that $\omega_к-\omega_0<\omega_0$ or /16

$$\Delta\simeq\frac{\alpha}{\omega_0^2} \qquad (33)$$

in the case when the load frequency is far from the critical frequency of the layer.

Thus, the magnitude of the anticipated spreading of the reflected pulse for "thick" layers satisfys the following inequality:

$$\frac{\alpha}{\omega_0^2}<\Delta<\frac{1}{2}\cdot\frac{\alpha}{(\omega_к-\omega_0)^2}. \qquad (34)$$

It can be seen from (34), in particular, that the spreading increases as the load frequency approaches the critical frequency. However, we should note that the inequality in (34) is of an asymptotic nature, connected with the limitations of (10) - (12), and the limit

transition $\omega_0 \to \omega_k$ is forbidden.

2. Displacement of the maximum of the reflected signal. It can be seen from (25) that the maximum of the reflected signal displaces by a value of τ_0 determined by (27). It follows from (27) that

$$\tau_0 \simeq -\frac{1}{\Omega}\left[\frac{1}{4(\omega_k-\omega_0)^4}-\Omega^2\ln\left[\left(\frac{\omega_k}{\omega_0}\right)^2-1\right]\right]. \quad (35)$$

In view of the limitation of (12) and (13), the solution is valid on the condition that $\omega_0 > \frac{\omega_k}{\sqrt{2}}$. In this regard, it is found that $\tau_0 < 0$ on the whole, and, consequently, the maximum of the reflected signal arises with some delay relative to the moment of time $\tau = t_0 + \frac{2z}{c}$.

3. Frequency modulation of the reflected signal. The expression in (26) for the phase $\phi(\tau)$ contains a term which changes in time according to the quadratic law.

If we define the load frequency of the reflected signal $\omega_{0\ ref}$ as the derivative in time of the phase of the reflected signal, then it is obvious that

$$\omega_{0\ ref} = \omega_0 - \Delta\omega - 2\gamma^2 \cdot 4\,\mathrm{Im}\,A\,\alpha^2\Omega^2(\tau - t_0 - \tau_0), \quad (36)$$

$$\Delta\omega = 2\gamma^2 \cdot 4\,\mathrm{Im}\,A\,\alpha^2\Omega^2\left(\frac{4\,\mathrm{Im}\,A\,\alpha^2\Omega^2}{1+4\,\mathrm{Re}\,A\,\alpha^2\Omega^2}+\frac{1+4\,\mathrm{Re}\,A\,\alpha^2\Omega^2}{4\,\mathrm{Im}\,A\,\alpha^2\Omega^2}\right)\Omega q. \quad (37)$$

Expression (37) defines the magnitude of the constant shift in load frequency of the reflected signal in relation to ω_0, and the following for thick layers:

$$\Delta\omega \simeq 2\gamma^2\Omega q. \quad (38)$$

If the duration of the reflected pulse $t_{i\ ref}$ is also defined on the level where the envelope decreases e times, then

$$t_{i\ ref} = \frac{1}{\gamma(1+4\,\mathrm{Re}\,A\,\alpha^2\Omega^2)^{1/2}} \quad (39)$$

and

$$\omega_{0\,ref} = \omega_0 - \Delta\omega - \omega_M \text{ при } \tau - t_0 = t_{i\ ref} + \tau_0, \quad (40)$$

where

$$\omega_M = +2\gamma\frac{4\,\mathrm{Im}\,A\,\alpha^2\Omega^2}{[1+4\,\mathrm{Re}\,A\,\alpha^2\Omega^2]^{1/2}}. \quad (41)$$

/170

Thus, the load frequency of the reflected signal $\omega_{0\ ref}$ changes linearly in time, and, since Im A < 0 for "thick" layers, $\omega_{0\ ref}$ increases from a value of $\omega_0-\Delta\omega-\omega_m$ at $\tau-t_0 < \tau_0$ to a value of $\omega_0-\Delta\omega+\omega_m$ at $\tau-t_0>\tau_0$.

The effect of the frequency modulation of the reflected signal can be explained by the dispersion properties of the reflected layer.

Finally, let us evaluate the order of magnitude of Δ, τ_0, $\Delta\omega$ and ω_m in that case when the reflection originates from a layer of the ionosphere modeled by the Epstein layer. An analysis of the experimental data on the profiles of the electron concentration [5, 6, 7] gives the following characteristic dimensions of the parameters s for various altitudes:

for the upper branch of the F-layer ($h > 250$ km), $s \sim 90$ km,
for the lower branch of the F-layer (120 km $< h < 250$ km), $s \sim 30$ km,
for the lower branch of the E-layer (80 km $< h < 120$ km), $s \sim 5$ km.

We can obtain the following criterion for validity of the limitations imposed earlier from an investigation of the strict solution for the Epstein layer [2]:

$$\ln\left|\frac{d_1^2}{\omega_0\Omega}\right| \ll \frac{z}{s}; \qquad (42)$$

From the point of view of the apparatus of the standard equations, the significance of the inequality in (42) consists in the great distance between the reversal point and the observation site. Evaluations show that, in the range of probing frequencies on the order of 1 - 3 MHz, the requisite [according to (42)] distance between the observation site z and the maximum of the layer ($z = 0$) is equal to:

For the E-layer, $z \geq 50$ km,
For the F-layer, $z \geq 220$ km.

Since the maxima of the electron density of the E- and F-layers are located at altitudes of approximately 120 and 250 km, respectively, then the condition of "localization of the non-uniformity" is easily fulfilled in many cases of real N(h) -profiles, all the more so when the gradients of the electron concentration are higher.

Using specific values of s, we can obtain the following values of the parameters of the reflected pulse of interest to us in the case of "thick layers" (see the table).

As can be seen from the table, the effects concerning the layers of the ionosphere discussed before are not arbitrarily great. However, the values for the frequency modulation ω_m becomes substantial, and it is interesting, that for frequencies of $\omega_0 < \omega_k - \omega_0$,

Parameters of the Layer	Parameters of Reflected Pulse	f, MHz						
		1	2	3	4	5	6	7
$s = 55{,}8$ км $\omega_к =$ $= 7{,}57 \cdot 10^7$ сек$^{-1}$	$\Delta\omega$, сек$^{-1}$ $\omega_м$, сек$^{-1}$ τ_0, сек β^2, сек$^{-2}$	$-7{,}78 \cdot 10^{-4}$ $-3{,}82 \cdot 10^3$ $1{,}85 \cdot 10^{-3}$ 0,999	$-9{,}71 \cdot 10^{-5}$ $-1{,}95 \cdot 10^3$ $1{,}33 \cdot 10^{-3}$ 0,999	$-2{,}86 \cdot 10^{-4}$ $-1{,}35 \cdot 10^3$ $1{,}01 \cdot 10^{-3}$ 0,999	$-1{,}19 \cdot 10^{-5}$ $-1{,}07 \cdot 10^3$ $7{,}77 \cdot 10^{-4}$ 0,999	$-5{,}92 \cdot 10^{-6}$ $-9{,}16 \cdot 10^2$ $5{,}84 \cdot 10^{-4}$ 0,999	$-2{,}92 \cdot 10^{-6}$ $-8{,}40 \cdot 10^2$ $4{,}12 \cdot 10^{-4}$ 1,000	$-1{,}49 \cdot 10^{-6}$ $-8{,}18 \cdot 10^2$ $2{,}50 \cdot 10^{-4}$ 1,000
$s = 36{,}9$ км $\omega_к =$ $= 4{,}51 \cdot 10^7$ сек$^{-1}$	$\Delta\omega$, сек$^{-1}$ $\omega_м$, сек$^{-1}$ τ_0, сек β^2, сек$^{-2}$	$-1{,}77 \cdot 10^{-3}$ $-2{,}69 \cdot 10^3$ $9{,}66 \cdot 10^{-4}$ 0,996	$-2{,}2 \cdot 10^{-4}$ $-1{,}36 \cdot 10^3$ $6{,}10 \cdot 10^{-4}$ 0,998	$-6{,}23 \cdot 10^{-5}$ $-1{,}01 \cdot 10^3$ $3{,}83 \cdot 10^{-4}$ 0,999	$-2{,}07 \cdot 10^{-5}$ $-9{,}10 \cdot 10^2$ $1{,}97 \cdot 10^{-4}$ 0,999			
$s = 31{,}6$ км $\omega_к =$ $= 3{,}78 \cdot 10^7$ сек$^{-1}$	$\Delta\omega$, сек$^{-1}$ $\omega_м$, сек$^{-1}$ τ_0, сек β^2, сек$^{-2}$	$-2{,}42 \cdot 10^{-3}$ $-2{,}21 \cdot 10^3$ $7{,}51 \cdot 10^{-4}$ 0,997	$-2{,}87 \cdot 10^{-4}$ $-1{,}21 \cdot 10^3$ $4{,}40 \cdot 10^{-4}$ 0,999	$-7{,}70 \cdot 10^{-5}$ $-9{,}56 \cdot 10^2$ $2{,}34 \cdot 10^{-4}$ 0,999				
$s = 26{,}4$ км $\omega_к =$ $= 7{,}77 \cdot 10^7$ сек$^{-1}$	$\Delta\omega$, сек$^{-1}$ $\omega_м$, сек$^{-1}$ τ_0, сек β^2, сек$^{-2}$	$-3{,}48 \cdot 10^{-3}$ $1{,}80 \cdot 10^3$ $8{,}83 \cdot 10^{-4}$ 0,998	$-4{,}27 \cdot 10^{-4}$ $-9{,}19 \cdot 10^2$ $6{,}36 \cdot 10^{-4}$ 0,999	$-1{,}28 \cdot 10^{-4}$ $-6{,}34 \cdot 10^2$ $4{,}87 \cdot 10^{-4}$ 1,000	$-5{,}33 \cdot 10^{-5}$ $-5{,}00 \cdot 10^2$ $3{,}77 \cdot 10^{-4}$ 1,000	$-2{,}64 \cdot 10^{-5}$ $-4{,}28 \cdot 10^2$ $2{,}87 \cdot 10^{-4}$ 1,000	$-1{,}42 \cdot 10^{-5}$ $-3{,}90 \cdot 10^2$ $2{,}07 \cdot 10^{-4}$ 1,000	$-7{,}11 \cdot 10^{-6}$ $-3{,}76 \cdot 10^2$ $1{,}32 \cdot 10^{-4}$ 1,000

the parameter ω_m practically does not depend on ω_k, and consequently, on N_{stag}, and is directly proportional to the parameter s, which characterizes the gradient of the electron concentration profile. /17

An experimental observation of the effect of frequency modulation of the reflected signal would give additional information on the rate of the change in electron concentration with altitude in the neighborhood of the maximum of the reflecting layer.

REFERENCES

1. Epstein, P.S.: Reflection of Waves in an Inhomogeneous Absorbing Medium. Proc. Nat. Acad. Sci. Amer., Vol. 16, 1930.
2. Bezruchenko, L. I. and G. I. Makarov: Propagation of a Pulsed Signal in an Epstein Layer of the Ionosphere. In the Collection: Problemy difraktsii i rasprostraneniya voln (Problems of Wave Diffraction and Propagation), No. 5. Leningrad State Univ. Press, 1966.
3. Whittaker, E.T. and J. Watson. Kurs sovremennogo analiza (Course in Modern Analysis), Part II. "Fizmatgiz", 1963.
4. Faddeyeva, V.N. and N. M. Terent'yev: Tablitsy znacheniy integrala veroyatnostey ot kompleksnogo argumenta (Tables of Values of the Probability Integral of a Complex Argument). Academy of Sciences U.S.S.R., 1954.
5. Gringauz, K.I.: Rocket Measurements of the Electron Concentration in the Ionosphere with the Aid of an Ultrashort-Wave Dispersion Interferometer. In the Collection: Iskusstvennyye sputniki Zemli (Artificial Earth Satellites), No. 1, Academy of Sciences U.S.S.R., 1958.
6. Kazachevskaya, T.V. and G. S. Ivanov-Kholodnyy: Rocket Data on the Behavior of the Electron Concentration in the Ionosphere at Altitudes of 100-300 km. Geomagnetizm i Aeronomiya, Vol. 5, No. 6, 1965.
7. Jekulin, L.A.: Radio-Wave Propagation Characteristics of a Simple Ionospheric Model Based on Rocket Data. Planet. Space Sci., Vol. 2, 1960.

PERTURBATION OF ELECTROMAGNETIC FIELDS BY MOVING BODIES

V.S. Gerasimov and V.N. Krasil'nikov

ABSTRACT: The authors discuss the perturbation of electromagnetic fields by moving bodies. The calculations in this article show that, if a body is extended into an ellipsoid with axis orthogonal to the field (electric or magnetic), maintaining a constant volume, then the disturbances it undergoes (in correspondence with the electric or magnetic field) decrease with an increase of this axis.

The motion of bodies in electromagnetic fields causes certain /173 disturbances whose nature is determined by the physical properties of the medium and circumstances of the motion. In this report, we will investigate one particular case which lends easily to mathematical description.

Let a body which has the shape of an ellipsoid move at a constant velocity $\vec{V}$ through a uniform magnetic field existing in vacuum $\vec{H}_0$.[1] We will assume that the substance of the body is conductive ($\sigma > 0$), while its magnetic susceptibility is constant.

The method for the solution is based on a successive examination of two reference systems with parallel spatial axes: a system K with coordinates x, y, z (relative to which the body moves) and a system K' with coordinates 'x, 'y, 'z (in which the body is at rest).

We will assume that a uniform magnetostatic field $\vec{H}_0$ assigned in the system K is directed along the z axis, i.e.,

$$\vec{H}_0 = H_0\vec{e}_z \tag{1}$$

(for the symbols, $\vec{e}_x$, $\vec{e}_y$ and $\vec{e}_z$ are the basis vectors of the system K; $\vec{e}'_x$, $\vec{e}'_y$ and $\vec{e}'_z$ are the basis vectors of the system K'), while the rate of movement of the body $\vec{V}$ is given by the formula

$$\vec{V} = v_x\vec{e}_x + v_y\vec{e}_y + v_z\vec{e}_z. \tag{2}$$

[1] The movement through an electrostatic field can also be examined with the same success.

Using the Lorentz transform for the field in (1), we can find the vectors $\vec{E}'_0$ and $\vec{H}'_0$ describing the field in (1) in the system K:

$$\vec{H}'_0 = \vec{H}_{0\parallel} + \gamma \vec{H}_{0\perp}, \tag{3}$$

$$\vec{E}'_0 = \frac{\gamma}{c}\left(v_y H_0 \vec{e}'_x - v_x H_0 \vec{e}'_y\right), \tag{4}$$

/1

where c is the speed of light in vacuum;

$$\gamma = \frac{1}{\sqrt{1 - V^2/c^2}};$$

the indices $\parallel$ and $\perp$ signify that we are taking the component of the corresponding vector as parallel to the velocity of relative movement of the reference systems, or perpendicular to it [2]; the field $\vec{E}'_0$ is orthogonal to the vectors $\vec{V}$ and $\vec{H}_0$.

Now we must find the electric and magnetic disturbances in the system K' which are caused by putting in the field of (3)-(4) an immobile conducting ellipsoid of a magnet. The relevant static problem has a well-known [3] solution which permits us to express the unknown potentials Φ' and Ψ' in terms of the elliptical integral of type II. For the sake of brevity in the presentation, we will limit ourselves to an investigation of the following particular case.

Let the major semi-axis a of the revolving ellipsoid be directed along the axis 'x; the origin of the reference system is in the middle between the foci of the ellipsoid, and the system K' moves relative to K in such a way that the axis 'x slides along the axis x at a velocity of $v_x \vec{e}_x$. In this case, the field disturbances arising outside the body are described by the following potentials [3]:

$$\Phi' = \Phi'_0\left[1 - \frac{1}{\int_0^\infty \frac{d\xi}{(\xi + b^2)R_\xi}} \int_\xi^\infty \frac{d\xi}{(\xi + b^2)R_\xi}\right] \tag{5}$$

$$\Psi' = \Psi'_0\left[1 - \frac{\frac{ab^2}{2} \cdot \frac{\mu - 1}{\mu} \int_\xi^\infty \frac{d\xi}{(\xi + b^2)R_\xi}}{1 + \frac{ab^2}{2} \cdot \frac{\mu - 1}{\mu} \int_\xi^\infty \frac{d\xi}{(\xi + b^2)R_\xi}}\right] \tag{6}$$

where $R_\xi = (\xi + b^2)\sqrt{\xi + a^2}$; ξ is a variable in the ellipsoidal system of coordinates determined by the equation [3]

$$\frac{'x^2}{a^2+\xi}+\frac{'y^2}{b^2+\xi}+\frac{'z^2}{b^2+\xi}=1; \tag{7}$$

a is the major semi-axis; b is the minor semi-axis of the ellipsoid;

$$\Phi_0'=-E_0'y=\frac{\gamma}{c}v_xH_0y; \tag{8}$$

$$\Psi_0'=-H_0'z=\gamma H_0z; \tag{9}$$

μ is the magnetic susceptibility of the body.

By identity conversions (which we will not carry out here), (5) and (6) can be simplified. For example, the following representation is valid for Φ': /175

$$\Phi'=\Phi_0'\left(1-\frac{\frac{2u}{u^2-f^2}+\frac{1}{f}\ln\frac{u-f}{u+f}}{\frac{2a}{a^2-f^2}+\frac{1}{f}\ln\frac{a-f}{a+f}}\right), \tag{10}$$

where f is one half the interfocal distance;

$$u=\sqrt{\xi+a^2}=\frac{1}{2}(r_1'+r_2')= \\ =\frac{1}{2}\left[\sqrt{('x+f)^2+'y^2+'z^2}+\sqrt{('x-f)^2+'y^2+'z^2}\right]; \tag{11}$$

r'1 and r'2 are the focal radii of the ellipsoids representing the coordinate surfaces. The components of the electric field vector in the system K' are found according to the following formulas:

$$E_x'=\frac{32E_0'f^{2'}x'y}{Ar_1'r_2'(r_1'+r_2')\left[(r_1'+r_2')-4f^2\right]}, \tag{12}$$

$$E_z'=\frac{32E_0'f^{2'}z'y\,(r_1'+r_2')}{Ar_1'r_2'\left[(r_1'+r_2')-4f^2\right]^2}, \tag{13}$$

$$E_y'=E_0'-\frac{E_0'}{A}\left[\frac{4(r_1'+r_2')}{(r_1'+r_2')^2-4f^2}+\frac{1}{f}\ln\frac{r_1'+r_2'-2f}{r_1'+r_2'+2f}\right]+ \\ +\frac{32E_0'f^{2'}y^2(r_1'+r_2')}{Ar_1'r_2'\left[(r_1'+r_2')^2-4f^2\right]^2}, \tag{14}$$

where

$$A=\frac{2a}{a^2-f^2}+\frac{1}{f}\ln\frac{a-f}{a+f}.$$

Using the Lorentz transforms a second time, it is easy to determine the components of the electric field in the system K:

$$E_x = \frac{32\gamma E_0' f^2 (x - \tau)\, \nu \cos\theta}{A r_1 r_2 (r_1 + r_2)\,[(r_1 + r_2)^2 - 4f^2]}, \tag{15}$$

$$E_z = \frac{16\gamma E_0' f^2 \nu^2 \sin 2\theta\, (r_1 + r_2)}{A r_1 r_2\,[(r_1 + r_2)^2 - 4f^2]^2}, \tag{16}$$

$$E_y = -\frac{\gamma E_0'}{A}\left[\frac{4(r_1 + r_2)}{(r_1 + r_2)^2 - 4f^2} + \frac{1}{f}\ln\frac{r_1 + r_2 - 2f}{r_1 + r_2 + 2f}\right] + \frac{32\gamma E_0' f^2 \nu^2 \cos^2\theta\, (r_1 + r_2)}{A r_1 r_2\,[(r_1 + r_2)^2 - 4f^2]^2}, \tag{17}$$

where we used the symbols $y = \nu\cos\theta$; $z = \nu\sin\theta$; $\tau = v_x t$. At $f \to 0$, we find the formula for a sphere.

Let us select some plane which is orthogonal to the trajectory of movement, for example $x = 0$. We can select the observation points on this plane, fixing the values of ν and θ, and then find the change in value of the field components at these points in dependence on the time. These changes are caused by two factors: a turn of the /17

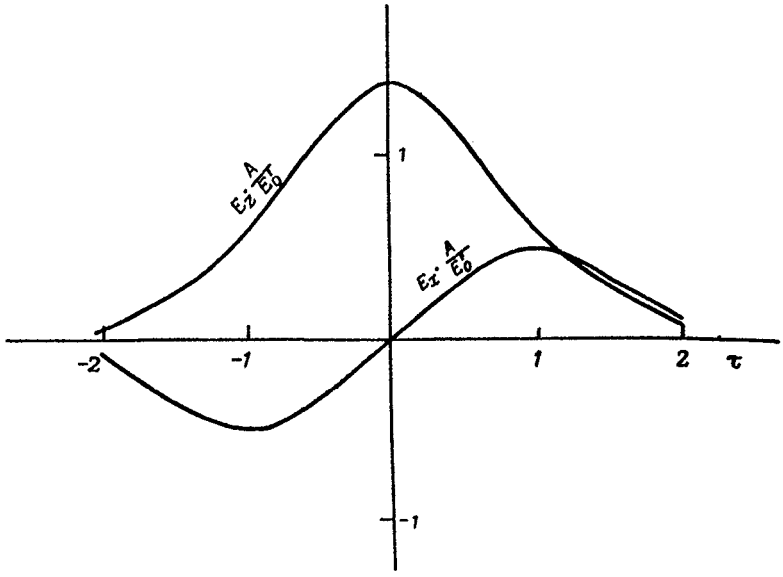

Fig. 1.

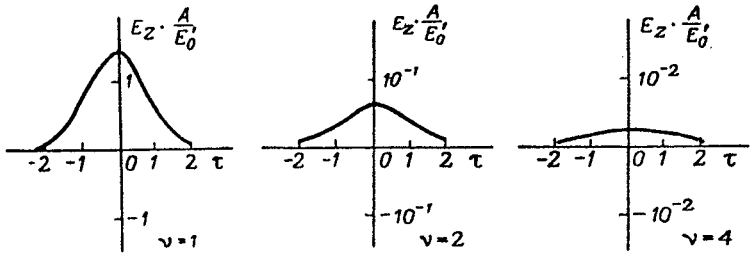

Fig. 2.

vector E in space and a decrease in field intensity with the distance. For example, let us take the points $\theta = \pi/4$; $\nu = 1$. The changes of the field in it appear as shown in Figure 1.

The process is lengthened in time when the distance ν increases. Figure 2 shows the change in E_z for $\nu = 1$, $\nu = 2$ and $\nu = 4$.

The intensity of the field decreases according to a law close to ν^{-3}.

The electrical polarization of the body by the effect of the Lorentz force (from the point of view of the observer at rest) is proportional to V/c. The magnetic polarization of the body does not depend on the value of V/c, and therefore the magnetic field disturbances are greater in order of magnitude (in the Gaussian unit system) than the electrical values for low velocities. They can be written out with the aid of formulas similar to (15)-(17), if $\mu >> 1$:

$$H_x = \frac{32\gamma H_0' f^2 (x-\tau)\nu \sin\theta}{A[(r_1+r_2)^2-4f^2](r_1+r_2)r_1r_2}; \quad (18)$$

$$H_y = \frac{32\gamma H_0' f^2 \nu^2 \sin^2\theta (r_1+r_2)}{A[(r_1+r_2)^2-4f^2]^2 r_1 r_2}; \quad (19)$$

$$H_z = \frac{\gamma H_0'}{A}\left[\frac{4(r_1+r_2)}{(r_1+r_2)^2-4f^2} + \frac{1}{f}\ln\frac{r_1+r_2-2f}{r_1+r_2+2f}\right] - \frac{16\gamma H_0' f^2 \nu^2 \sin 2\theta (r_1+r_2)}{A[(r_1+r_2)^2-4f^2]^2 r_1 r_2}. \quad (20)$$

Formulas (15)-(17) and (18)-(20) permit us to compare disturbances arising as a result of motion of ellipsoids with different interfocal distances and eccentricities. For example, we can compare a sphere with radius equal to the minor semiaxis b of an ellipsoid to an ellipsoid for which the major semiaxis a is equal to 10 b.

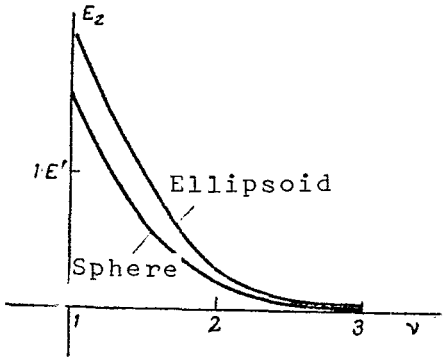

Fig. 3.

Let us consider the maximum disturbances at the moment of time $\tau = 0$ at $\theta = \pi/4$ (Fig. 3) for the component E_z, in dependence on the distance. It follows from the formulas obtained that, if a body is extended into an ellipsoid with axis 2a orthogonal to the field (electric or magnetic), maintaining a constant volume, then the disturbances it undergoes (in correspondence with the electric or

magnetic field) decrease with an increase of the axis 2a. If we consider that case when the major semi-axis of an ellipse extends along the field, then the disturbances increase. We should also mention that, for velocities comparable to the speed of light, there is an increase in the amplitude of the change in field by a factor of γ^2 and "contraction" in time by a factor of γ.

REFERENCES

1. Landau, L.D. and Y.M. Lifshits: Teoriya polya (Field Theory). "Fizmatgiz", 1959.
2. Matveyev, A.N.: Elektrodinamika i teoriya otnositel'nosti (Electrodynamics and the Theory of Relativity). "Vysshaya shkola", 1964.
3. Stratton, J.A.: Teoriya elektromagnetizma (Electromagnetism Theory). "Gostekhizdat", 1948.

ERRORS IN DETERMINING THE CHARACTERISTICS OF SUPERLONG-WAVE PROPAGATION BY THE METHOD OF HARMONIC ANALYSIS OF THE FORMS OF ATMOSPHERICS

V.A. Krivoshein and A.B. Orlov

ABSTRACT: The errors involved in determining the characteristics of superlong-wave propagation by the method of harmonic analysis of the forms of atmospherics are discussed, and methods of eliminating them are investigated. The article contains a detailed analysis of the algorithms for determining the attenuations and phase velocities with the purpose of finding the sources of possible errors, the specific characteristics of these errors, and estimates of their magnitude.

The method of studying the rules for propagation of superlong /178 radio-frequency waves (frequency of 1 - 30 KHz) which is based on an analysis of the spectral composition of atmospherics is well known. The studies in this field are numerous: among the most important ones, we should mention [1-5]. However, the authors of these studies did not make a detailed investigation of the algorithms for determining the attenuations and phase velocities with the purpose of finding the sources of possible errors, the specific characteristics of these errors and estimates of their magnitude. We will attempt to carry out such an investigation and evaluation in this study. The first section contains a generalization of the methods and algorithms proposed earlier. The materials presented in the subsequent sections are partially based on works [6, 7] which appeared recently, and they apply statistical methods to the problems cited above.

Section 1. Algorithms for Calculating the Propagation Characteristics

As is well known (see [8, 9], for example), the spectrum of the vertical component of an electric field E (jω, D) of atmospherics can be described well within the framework of a single-mode representation of the propagation processes for great distances D from the source (D > 1000 - 2000 km) and for frequencies lower than 12 - 13 KHz (depending on the state of the course day-night and its length). It has the following form:

$$E(j\omega, D) = \frac{C(j\omega)}{\sqrt{\sin D/a}} e^{-\alpha(\omega) D + j\beta(\omega) D}, \qquad (1)$$

where C (jω) is a frequency-dependent factor which does not depend on the distance and which includes, in particular, the characteristics of the emission source and the coefficient of excitation of the waveguide earth-ionosphere; α(ω) is a frequency-dependent parameter which characterizes the velocity of exponential attenuation of the spectral components of a signal in its propagation along the course; β(ω) is the increase in phase of the spectral component of the atmospherics in propagation per unit length; a is the radius of the earth. /179

The spectrum F (jω, D) of the signal fixed on the oscillograph recorder is connected with the spectrum of the field E (jω, D) calibrated by the factor k, and can be calculated by a time oscillogram f(t, D) by way of a Fourier transformation:

$$F(j\omega, D) = kE(j\omega, D) = \int_0^{T_s} f(t, D)\, e^{-j\omega t}\, d\omega, \quad (2)$$

Where T_s is the interval for observation of the signal f(t, D). We should mention that (1) and (2) presuppose a selection of the beginning of time reading t = 0, in examining the dependence of the field of the atmospherics on time, at the point of the mathematical front propagating at the speed of light c. The supplementary factor $e^{j\frac{\omega}{c}D}$ is not needed in (1) for such a selection of the beginning of the time reading.

The algorithms for calculating attenuation α(ω) are simplest (see [4], for example). Using the spectra of two atmospherics recorded from the same source, which are distances of D_1 and D_2 from it ($D_2 > D_1$), we can determine α(ω):

$$\alpha(\omega)\,[\text{db/thous. km}] = \frac{G(\omega, D_1) - G(\omega, D_2)}{D_2 - D_1} + \frac{10}{D_2 - D_1} \log \frac{\sin \frac{D_2}{a}}{\sin \frac{D_1}{a}}, \quad (3)$$

Where G (ω, D_i) is the modulus of the signal spectrum in decibels relative to some measurement unit E_0,

$$G(\omega, D_i) = 20 \log \frac{F(j\omega, D_i)}{k_i E_0},$$

while D and a are expressed in thousand kilometers.

A study of the rules for the phase change with distance is greatly complicated by the ambiguity of the 2 πl values for the phase of the signal spectrum:

$$\varphi_l(\omega,\ D) = \arg F(j\omega,\ D) + 2\pi l, \qquad (4)$$

where $l = 0, \pm 1, \pm 2 \ldots$ In this regard, the problem of an unambiguous determination of the phase velocities V_{ph} (ω) can be solved only by using additional information:

(1) Continuity of the theoretically calculated dependence $V_{ph}=V_{ph}$ (ω) [1, 2] or, which is the same, the continuity of the dependence $\beta = \beta(\omega)$;

(2) The relatively small (compared to $\frac{\partial \beta}{\partial \omega} D$) value of the curvature for the dependence arg C ($j\omega$) on the frequency and the continuity of this dependence (for the phase characteristics of the atmospherics of the nearest zone, see [10], for their relatively small contribution to ϕ_l (ω, D), see [11], and for the argument of the coefficient of excitation, (see [9]); /180

(3) The provisional value (the requisite precision will be shown below) of the velocity V_{ph} for some definite frequency, which is obtained theoretically or experimentally according to observations of superlong-wave signals by radio stations.

Considering points 1 and 2, the phase spectrum ϕ (ω, D) can always be represented in the form of a smooth curve by matching single parts of the phase characteristic (due to a corresponding selection of the calculated values of arg F ($j\omega$, D) of number l). Running ahead [see (18) and (26) in section 3], we should mention that the rather smooth nature of ϕ (ω, D) can be destroyed, in principle, as a result of errors in the calculation, which can complicate the matching operation. As will be shown, the interval for correlation of $\Delta\omega k$ by frequency is equal to $\frac{2\pi}{T_s}$ for these errors. This distorting effect of noises must be considered only for errors involved in a calculation of $\sigma\phi$ which are commensurate with π; for example, for $\sigma\phi \geq \frac{\pi}{3}$. Naturally, the matching operation requires rather close adjacent values of the argument ω_k and $\omega k + 1$ in calculating the dependence $\phi_l^{(k)} = \phi_l(\omega_k, D)$ by points. Their closeness is determined in practice determined by the following conditions:

$$|\omega_{k+1} - \omega_k| \cdot \left|\frac{\partial \beta}{\partial \omega}\right|_{\omega=\omega_k} D \ll \pi,$$

$$|\omega_{k+1} - \omega_k| < \frac{2\pi_0}{T_s} \quad \text{for } \sigma_\varphi \geqslant \frac{\pi}{3}.$$

Thus, as a result of the application of the Fourier transform to f(t, D), we can obtain a set of continuous curves for $\phi_l(\omega, D)$ which was displaced from one another by $2\pi l$.

Using the spectral phase characteristics of two synchronous atmospherics, we can find [1, 2] the parameter of $\beta(\omega)$ (for a corresponding method with a single-point recording of atmospherics, see [2]):

$$\beta_m(\omega) = \frac{\varphi_{l_2}(\omega, D_2) - \varphi_{l_1}(\omega, D_1)}{D_2 - D_1} + \frac{2\pi m}{D_2 - D_1}, \qquad (5)$$

where $m = l_2 - l_1 = 0, \pm 1, \pm 2 \ldots$

The parameter $\beta(\omega)$, which signifies an additional phase (per unit length) is connected with the phase velocity by the following expression:

$$\beta(\omega) = \frac{\omega}{c}\left(1 - \frac{c}{V_{ph}}\right). \qquad (6)$$

An ambiguous calculation of $\beta(\omega)$ results in corresponding ambiguity /181 in determining V_{ph}. Considering (6) and $\left|1 - \frac{c}{V_{ph}}\right| \ll 1$, we have the following:

$$\left(\frac{V_{ph}}{c} - 1\right)_m \simeq \frac{c}{\omega} \cdot \frac{\varphi_{l_2}(\omega, D_2) - \varphi_{l_1}(\omega, D_1)}{D_2 - D_1} + \frac{m2\pi c}{(D_2 - D_1)\omega}. \qquad (7)$$

Therefore, the a priori accuracy of the representation $\frac{V_{ph}}{c} - 1$ should be much better than $2\pi c/(D_2 - D_1)\omega$. This imposes a limitation on the maximum value of $D_2 - D_1$ for given accuracy Δ_a of the a priori value of $\frac{V_{ph}}{c} - 1$. Thus, for $\omega/2\pi = 20$ KHz and $\Delta_a \leq 0.25 \cdot 10^{-2}$, it is necessary that $D_2 - D_1 \leq 6000$ km. For $D_2 - D_1 \geq 6000$ km, an unambiguous determination of the phase velocity is virtually impossible. This remark also holds for the single-point method of determining V_{ph} in [2]; in this case, $D_2 - D_1$ implies the removal of the receiving point from the source of emission.

Being interested in the physical accuracy of the values obtained for α and β, we should mention that the algorithms in (3) and (5) presuppose identical properties of paths with lengths of D_1 and D_2 (this is particularly essential in the case of $D_2 - D_1 \ll D_1$). Therefore, it is most important for which the source of emission and the points of the record are located on one line (on the arc of the greater circle). When there are more than two points on the record, (3) and (5) can be replaced by the formulas of regression analysis, which determines the parameters α and β best of all (in terms of the minimum of the sum of squares of deviations).

Section 2. Statistical Nature of the Problem of Determining Attenuations and Phase Velocities. Errors Connected with Calibration of the Apparatus.

The statistical nature of the problem of determining α and β experimentally is obvious. The discrepancy observed in calculating α and β by different initial data (different signals, different experimental conditions, etc.) is due, first of all, to variations in the properties in the propagation path (mainly the ionosphere) and, secondly, to the different types of errors in recording and reading the oscillograms of the atmospherics.

An evaluation of the variations and properties of the path is almost of the same interest as a determination of the average laws. As a rule, the latter are found by regular averaging. In this regard, we must emphasize that

$$\overline{\alpha(\omega)} = \frac{1}{N}\sum_{1}^{N}\alpha_i(\omega) \text{ and } \overline{\beta(\omega)} = \frac{1}{N}\sum_{1}^{N}\beta_i(\omega),^{1} \qquad (8)$$

which are measured when there are no noises or distortions, signify the average parameters (averaging over different conditions of the path) only of monochromatic oscillations. A description of the propagation processes of a pulsed signal is unreliable when $\bar{\alpha}$ and $\bar{\beta}$ are used. Moreover, $\bar{\alpha}$ and $\bar{\beta}$, as functions of the frequency, may not correspond, generally speaking, to any of the specific real conditions of the path (ionosphere). /182

When we must describe the processes of propagation of pulsed broad-band signals under certain average conditions with the aid of $\overline{\alpha(\omega)}$ and $\beta(\omega)$, the only correct method of obtaining $\bar{\alpha}$ and $\bar{\beta}$ is the operation of averaging, not by the set of functions $\alpha_i(\omega)$, $\beta_i(\omega)$ but by the parameters $\vec{p}_i = p_1^{(i)}, p_2^{(i)}, \ldots, p_M^{(i)})$ on which they depend: $\alpha_i(\omega) = A(\omega, \vec{p}_i)$, $\beta_i = (\omega) = B(\omega, \vec{p}_i)$. The parameters $p_1, p_2, \ldots, p_M$ should be independent, and it is desirable that they have a definite physical significance. The problem of determining the explicit form of the functions $A(\omega, \vec{p})$ and $B(\omega, \vec{p})$ is reduced either to an M-parametric approximation by the set $\alpha_i(\omega)$, $\beta_i(\omega)$, which is satisfactory from the point of view of further usage, or to finding the analytical dependences $A(\omega, \vec{p})$, $B(\omega, \vec{p})$ by theoretical calculations. The second way involves a determination of the approximative functional dependence of the eigen-values of the zero, first and higher normal waves on such parameters as the altitude of the ionosphere, its effective conductivity, and the conductivity of the earth; thus we can immediately separate out the unknown independent parameters p_1,

---

[1] Here and in the future, a line over an expression signifies averaging over a set period.

p_2 ... p_M with clear physical meaning.

We will assume below that the properties of the path are independent within the framework of one experiment (group of measurements) in recording N pairs of synchronous atmospherics, and we will give special attention to the errors involved in recording and reading their oscillograms. Considering the different types of errors, the logarithmic modulus $\widetilde{G}(\omega, D)$ and phase $\widetilde{\phi}(\omega, D)$ of the calculated spectrum of the atmospherics can be written out in the following way:

$$\begin{aligned} \widetilde{G}(\omega, D) &= G(\omega, D) + \Pi + \mu(\omega), \\ \widetilde{\varphi}(\omega, D) &= \varphi(\omega, D) + \omega\tau + \nu(\omega), \end{aligned} \qquad (9)$$

where G (ω, D) and φ (ω, D) are the spectral characteristics of the atmospherics when there are no errors (we omitted the index 1 for ϕ, since we will be interested in random errors in its determination); Π is the error in calibration of the absolute sensitivity of the recorder in terms of the field; μ and ν are the errors due to the superposition of additive atmospheric noises on the atmospherics, geometric distortions in the oscillograph recording and inaccuracies in reading the shape of the signal; $\omega\tau$ is some addition to the phase of the signal connected with error in determining the beginning of the time reading $t = \tau$ on the oscillogram under investigation. /1

We must make the following comments regarding the selection of the beginning of the time reading. As was shown above, the parameter $\beta(\omega)$ in (1) was introduced for the case of selecting a beginning of the time reading at the point of the mathematical front, since (6) and (7), which connect $\beta(\omega)$ with $V_{ph}(\omega)$, are only then valid. However, the point corresponding to the mathematical front on a real oscillogram actually cannot be shown, particularly for distances greater than 2-3 thous. km from the source. Therefore, a precise determination of the absolute value of V_{ph} is possible, in principle, only when there is a precision time-unit system at the two recording points (accuracy no worse than microsecond units). When there is no such system, the problem of determining β can be solved, but with accuracy up to some unknown term $\Delta\beta = \overline{\omega\tau}$ [see (5), (8) and (9)], where $\overline{\tau} = \frac{1}{N} \cdot \frac{\sum (\tau_{2i} - \tau_{1i})}{D_2 - D_1}$. Correspondingly, the phase velocities V_{ph} can be obtained for different frequencies with accuracy up to some constant

$$\Delta\left(\frac{V_{ph}}{c} - 1\right) = c\overline{\tau}.$$

When the experiment is carried out on fixed courses (constant value of $D_2 - D_1$) and there is a substantial distance from the emission source, the beginning of the time reading must be selected in identical zero transitions of two synchronous atmospherics. Identity of the zero transitions can be established at $D_2 - D_1 \leq$ 2-3 thous. km. We will not discuss the corresponding method in detail in this work. We will only mention that a selection of zero transitions at the beginning part of the atmospherics is experient, since the ionospheric reflections caused by their formation are more stable for variations in properties of the ionosphere than are reflections of high numbers, which form the middle and tail parts of signal. The velocities of propagation of the "prime" zero transitions, as certain characteristic points of the signal, can be calculated theoretically by synthesis of the forms of the atmospherics [12]. We should expect that these velocities are determined largely by the properties of the Earth's surface (finite conductivity and sphericity). Therefore, a theoretical diagnosis is most precise in this case. The method /184
proposed is expedient even in the case when there is no information on the value for the velocity of propagation of the selected characteristic point on the signal. The relative stability in velocity of propagation of the initial zero transitions then aids in making the best comparison between results obtained under different conditions of the ionosphere, and thereby in evaluating the effect of its variations on the phase characteristics of propagation.

The existence of an error in calibration of the sensitivity of the apparatus [determination of the factor k, see (2)] results in the arisal of some constant unknown term $\Delta\alpha$, with accuracy up to which the dependence $\alpha(\omega)$ is determined, i.e.,

$$\Delta\alpha = \frac{\Pi_1 - \Pi_2}{D_2 - D_1}.$$

It follows from the formulas given above for determining $\Delta\beta$, $\Delta\left(\frac{V_{ph}}{c} - 1\right)$ and $\Delta\alpha$ that the effect of errors in calibration of Π and determination of the beginning of the time reading τ is most substantial for small $D_2 - D_1$. An evaluation of the accuracy (reliability interval) for the calculated values of $\bar{\alpha}$, $\bar{\beta}$, and $\bar{V}_{ph}$ does not cause any difficulties when there are definite standards for deviations in Π and τ.

We can have a very good idea of the accuracy in determinations of $\alpha(\omega)$ and $\beta(\omega)$ only after having examined the errors in $\mu(\omega)$ and $\nu(\omega)$ of the calculated spectra of the atmospherics. A study of the statistical characteristics of these spectra is carried out in the following section.

Section 3. Statistical Characteristics of the Spectra of Pulsed Signals Recorded Against a Noise Background.

Having examined the errors which occur in calculating the spectra of pulsed signals, let us use the following two models for their arisal. The first will be connected with the existence of additive noise which is independent of the signal and stationary during one session of observations. This noise will describe the atmospheric noises against the background of which the atmospherics are recorded, as well as errors in taking the data from the oscillogram. In order to describe these errors, the proposed model is an idealization, since actually the "noise" of taking data depends on the shape of the signal (the dispersion of the noise should increase where the curvature of the signal increases). The second model will describe specific distortions arising in the oscillograph recording (error in plotting the zero line and misalignment of the plates of the electron-beam tube in the oscil- /185
lograph).

Let us turn to an analysis of the errors of the first type. For this, we will examine a group of signals $f(t)$ which are the sum of the time function of the signal shape $f_0(t)$ and the selective realization $\xi(t)$ of a stationary random process with average zero value and autocorrelation function $B_\xi(\tau)$ determined as $B_\xi(\tau)=\overline{\xi(t)\,\xi(t+\tau)}$. For the sake of convenience in mathematical analysis, we will take a symmetric time interval in calculating the spectrum of the signal, i.e., one describing a signal distorted by noise, and the function $f(t) = f_0(t) + (t)$ given for the interval $(-T, T)$, and we will take the following [similar to (2)]:

$$F(j\omega)=\int_{-T}^{T} f(t)\,e^{-j\omega t}dt=X(\omega)+jY(\omega).. \qquad (10)$$

The complex function is represented in the form of the sum of the real and imaginary parts, and it is very convenient in evaluating its statistical properties that X and Y not be correlated. As can be shown, there is no correlation between X and Y when the symmetric time interval (-T, T) in (10) is selected. For any unsymmetric interval of the same length 2T, the relative correlation coefficient for X and Y is, generally speaking, non-zero. This is an opportune moment to mention that a specific selection of the time interval is not fundamental from the point of view of calculating the signal spectrum. Actually, the modulus of the spectrum $|F(j\omega)|$ is invariant for the beginning of the time reading, while the phase acquires the determined supplement ωT in its transfer.

Let us find the dispersions of X and Y, for which we will use the expressions of the autocorrelation functions presented in [6]:

$$B_X(\omega_1, \omega_2) = \int_0^{2T} (2T-\tau) B_\xi(\tau) \cos \omega_c \tau \frac{\sin \Delta\omega (2T-\tau)}{\Delta\omega (2T-\tau)} d\tau + \quad (11)$$
$$+ \int_0^{2T} (2T-\tau) B_\xi(\tau) \cos \Delta\omega\tau \frac{\sin \omega_c (2T-\tau)}{\omega_c (2T-\tau)} d\tau,$$

$$B_Y(\omega_1, \omega_2) = \int_0^{2T} (2T-\tau) B_\xi(\tau) \cos \omega_c \tau \frac{\sin 2\omega (2T-\tau)}{\Delta\omega (2T-\tau)} d\tau - \quad (12)$$
$$- \int_0^{2T} (2T-\tau) B_\xi(\tau) \cos \Delta\omega\tau \frac{\sin \omega_c (2T-\tau)}{\omega_c (2T-\tau)} d\tau,$$

where $\Delta\omega = \frac{|\omega_2 - \omega_1|}{2}$; $\omega_c = \frac{\omega_2 + \omega_1}{2}$. Assuming that $\Delta\omega = 0$, we can find the dispersions of the values X and Y from (11) and (12): /186

$$\sigma_X^2 = \int_0^{2T} (2T-\tau) B_\xi(\tau) \cos \omega\tau d\tau + \frac{1}{\omega} \int_0^{2T} B_\xi(\tau) \sin \omega (2T-\tau) d\tau; \quad (13)$$

$$\sigma_Y^2 = \int_0^{2T} (2T-\tau) B_\xi(\tau) \cos \omega\tau d\tau - \frac{1}{\omega} \int_0^{2T} B_\xi(\tau) \sin \omega (2T-\tau) d\tau. \quad (14)$$

We will be interested in the cases when $\sigma_X^2 \approx \sigma_Y^2$. Let us establish which limitations result in this approximative equality. For this, we will take the autocorrelation function in the simplest form $B\xi(\tau)=B(0)e^{-\frac{|\tau|}{\tau_k}}$, which is frequently required in describing real processes, and we will calculate the first and second terms in (13) and (14):

$$\int_0^{2T} B(0) e^{-\frac{\tau}{\tau_k}} (2T-\tau) \cos \omega\tau d\tau = \frac{B(0)\tau_k 2T}{1+\omega^2\tau_k^2} \times$$
$$\times \left[1 + \frac{\tau_k}{2T}\left(\gamma_1 e^{-\frac{2T}{\tau_k}} + \gamma_2\right)\right],$$
$$\frac{1}{\omega} \int_0^{2T} B(0) e^{-\frac{\tau}{\tau_k}} \sin \omega (2T-\tau) d\tau = \frac{B(0)\tau_k}{\omega(1+\omega^2\tau_k^2)} \times$$
$$\times \left[\sin 2\omega T \left(1 + \gamma_3 e^{-\frac{2T}{\tau_k}} + \gamma_4 e^{-\frac{2T}{\tau_k}} \omega\tau_k\right) - \right.$$
$$\left. - \cos 2\omega T \left(\omega\tau_k + \gamma_5 e^{-\frac{2T}{\tau_k}} + \gamma_6 e^{-\frac{2T}{\tau_k}} \omega\tau_k\right)\right],$$

where $|\gamma i| \leq 1$.

If

$$2T \gg \tau_k \text{ and } e^{-\frac{2T}{\tau_k}} \omega\tau_k \ll 1, \quad (15)$$

then the ratio between the second term and the first does not exceed $\frac{1 + \omega\tau k}{\omega \cdot 2T}$. Subsequently, considering only those cases when actually more than one period of analyzed frequency is included in the interval 2T, and when, consequently, this ratio is much less than unity, we can find the following, omitting the second terms in (13) and (14):

$$\sigma_X^2 = \sigma_Y^2 = \sigma^2. \tag{16}$$

Let us establish the relation between the value σ^2 and the spectral intensity of the noise N (ω):

$$\sigma^2(\omega) = \int_0^{2T} (2T - \tau) B_\xi(\tau) \cos \omega\tau d\tau \simeq$$
$$\simeq 2T \int_0^{2T} B_\xi(\tau) \cos \omega\tau d\tau \simeq 2T\pi N(\omega).$$

The functions B_X and B_Y can be calculated only for some specific representation of the function $B\xi(\tau)$. Let us evaluate the correlation interval for X and Y in the simplest case, assuming that the noise is delta-correlated ($B_\xi(\tau)=\delta(0-\tau)$, "white" noise). Using this assumption, the correlation coefficient σ_{X1X2} is /187

$$\rho_{X_1X_2} = \frac{B_{X_1X_2}}{\sigma_{X_1}\sigma_{X_2}} \simeq \frac{B_{X_1X_2}}{\sigma_X^2(\omega_c)} \simeq \frac{\sin 2T\Delta\omega}{2T\Delta\omega}. \tag{17}$$

In obtaining (17), we also assumed that $\sigma_{X1}\sigma_{X2} \quad \sigma_X^2(\omega_c)$ and $1/2T\omega_c << 1$. A result similar to (17) can be obtained for ρ_{Y1Y2}. Thus, the real and imaginary parts of this spectrum are actually not correlated for frequencies of ω_1 and ω_2, when the following condition is fulfilled:

$$\Delta\omega = \frac{|\omega_1 - \omega_2|}{2} > \frac{\pi}{2T}. \tag{18}$$

Let us find the form of the common distribution of X and Y. In that case when $\xi(t)$ has a normal distribution, X and Y are also distributed normally. In the case of other types of distributions of $\xi(t)$ the distribution of X and Y is of an asymptotically normal nature (relative to 2T). Assuming that the distribution of X and Y is normal, and considering the lack of correlation between them, we find the following expression for the probability density of common distribution:

$$p(X, Y) = \left(\frac{1}{\sqrt{2\pi}\sigma}\right)^2 \exp\left\{-\frac{1}{2\sigma^2}[(X - X_0)^2 + (Y - Y_0)^2]\right\}, \qquad (19)$$

where X_0 and Y_0 are the values for the absence of noise.

Thus, the problem of the spectrum of the function representing the sum of the signal and some noise can be reduced to the famous problem of the statistical characteristics of the amplitude and phase of a two-dimensional normally distributed vector [7]. We will find the characteristics of interest to us by the method of numerical integration, which is more convenient for solving the formulated problem. In order to signify the modulus and phase of the spectrum (10), we will introduce the functions $A(\omega)$ and $\phi(\omega)$, respectively, which characterize the signal and, in the case of absence of noise, are written out in the form of $A_0(\omega)$ and $\phi_0(\omega)$. Turning to the distribution function of (19) in polar coordinates, we can calculate some important statistical characteristics. Let us find the average value for the modulus of the spectrum $\overline{A}$:

$$\overline{A} = \int_0^\infty Ap(A)\,dA = \frac{1}{\sigma^2}\int_0^\infty \rho^2 e^{-\frac{1}{2}\left(\frac{\rho - A_0}{\sigma}\right)^2} I_0\left(\frac{\rho A_0}{\sigma^2}\right) e^{-\frac{\rho A_0}{\sigma^2}}\,d\rho.$$

We will use the symbol $\sigma/A_0 = n$, which signifies the noisesignal ratio, and we will finally obtain the following:

$$\overline{A} = A_0 \int_0^\infty \frac{q^2}{n^2} e^{-\frac{1}{2}\left(\frac{q-1}{n}\right)^2} I_0\left(\frac{q}{n^2}\right) e^{-\frac{q}{n^2}}\,dq = A_0[1 + g_1(n)]. \qquad (20)$$

The function $g_1(n) = \frac{\overline{A} - A_0}{A_0}$ describes the relative deviation of the average value for the amplitude of the spectral components from its value when there is no noise. The function $g_1(n)$ obtained by numerical integration of (20) is shown in Figure 1. For a small values of n, the function $g(n) \approx \frac{n^2}{2}$. We should not that, since $g_1(n) \geq 0$, the existence of noise always increases the average value for the amplitudes of the spectral components.

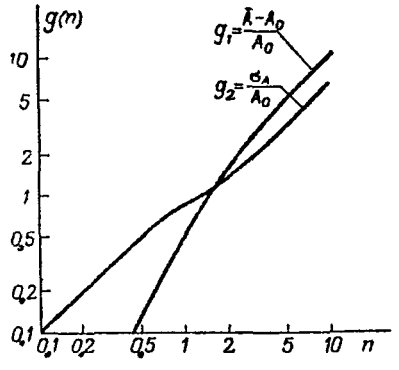

Fig. 1

As is easy to find, $\overline{A^2} = A_0^2 + 2\sigma^2$; therefore, the dispersion of the amplitude of the spectral component is equal to

$$\sigma_A^2 = \overline{A^2} - \overline{A}^2 = A_0^2[2n^2 - 2g_1 \times (n) - g_1^2(n)] = A_0^2 g_2^2(n). \qquad (21)$$

The function $g_2(n)$ is shown in Figure 1.

For low values of $\underline{n}$, we can represent $\underline{A} = \sqrt{\underline{X}^2 + \underline{Y}^2}$ in the form of part of a series by deviations $\underline{X} - X_0$ and $\underline{Y} - Y_0$ and, limiting ourselves to the quadratic terms, we can find the approximative value for the correltion between $A(\omega_1)$ and $A(\omega_2)$ for low noise-signal ratios:

$$B_{A_1A_2} = \overline{A(\omega_1)A(\omega_2)} - \overline{A(\omega_1)}\cdot\overline{A(\omega_2)} \simeq$$
$$\simeq \frac{1}{A_0(\omega_1)A_0(\omega_2)}\left[X_0(\omega_1)X_0(\omega_2)B_X(\omega_1, \omega_2) + Y_0(\omega_1)Y_0(\omega_2)B_Y(\omega_1, \omega_2)\right]. \qquad (22)$$

It follows from (22) that, in the case of low delta-correlated noise, the correlation interval for $A(\omega_1)$ and $A(\omega_2)$ is also determined by (18).

In order to determine α, it is of interest to calculate the average value for the logarithm of the modulus of the spectrum and to evaluate its dispersion. A consideration of the non-linear nature of the logarithm operations is very important in examining average values. Let us calculate $\overline{\ln A}$, expressing (19) in terms of /189 polar coordinates:

$$\overline{\ln A} = \frac{1}{\sigma^2}\int_0^\infty \rho \ln \rho\, e^{-\frac{1}{2}\left(\frac{\rho - A_0}{\sigma}\right)^2} I_0\left(\frac{\rho A_0}{\sigma^2}\right) e^{-\frac{\rho A_0}{\sigma^2}} d\rho.$$

In order to obtain the displacement relative to $\ln A_0$, we will make the following transformations:

$$\overline{\ln A} = \frac{1}{\sigma^2}\int_0^\infty \rho \ln \frac{\rho}{A_0}\, e^{-\frac{1}{2}\left(\frac{\rho - A_0}{\sigma}\right)^2} I_0\left(\frac{\rho A_0}{\sigma^2}\right) e^{-\frac{\rho A_0}{\sigma^2}} d\rho +$$
$$+ \frac{\ln A_0}{\sigma^2}\int_0^\infty \rho e^{-\frac{1}{2}\left(\frac{\rho - A_0}{\sigma}\right)^2} I_0\left(\frac{\rho A_0}{\sigma^2}\right) e^{-\frac{\rho A_0}{\sigma^2}} d\rho. \qquad (23)$$

Let us examine the second term in (23), representing it in the form of:

$$\ln A_0 e^{-\frac{1}{2n^2}}\int_0^\infty q e^{-\frac{1}{2}q^2} I_0\left(\frac{q}{n}\right) dq.$$

In this expression, the integral is equal to $e^{\frac{1}{2n^2}}$ (see [13]). Considering this, we will again write out (23) in the following form:

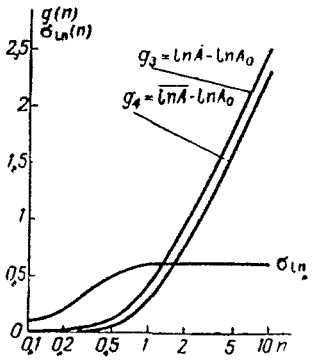

Fig. 2

$$\overline{\ln A} - \ln A_0 = \frac{1}{n^2}\int_0^\infty q \ln q e^{-\frac{1}{2}\left(\frac{q-1}{n}\right)^2} \times$$

$$\times I_0\left(\frac{q}{n^2}\right)e^{-\frac{q}{n^2}}dq \quad g_3(n). \qquad (24)$$

The result of a calculation of $g_3(n)$ is shown in Figure 2. We should note that $\overline{\ln A} - \ln A_0$ is always greater than zero.

Let us turn to a calculation of the dispersion of lnA:

$$\sigma_{\ln}^2 = \overline{(\ln A)^2} - \overline{(\ln A)}^2.$$

Using methods similar to those applied in calculating lnA, we find the following expression for the unknown dispersion:

$$\sigma_{\ln}^2 = g_4^2(n), \qquad (25)$$

where

$$g_4^2(n) = \frac{1}{n^2}\left[\int_0^\infty q(\ln q)^2 e^{-\frac{1}{2}\left(\frac{q-1}{n}\right)^2} I_0\left(\frac{q}{n^2}\right)e^{-\frac{q}{n^2}}dq - g_3(n)\right].$$

The graph depicted in Figure 2 was constructed according to the results of a numerical calculation of the integral in (25). We should mention that the dispersion $\sigma_{\ln}^2$ increases when the noise-signal ratio is increased, and it tends towards an asymptotic value (see [7]) $\sigma_\infty^2 = g_4^2(\infty) = \pi^2/24$.

It is interesting to compare different averaging methods and /190 their effectiveness. Figure 2 illustrates the behavior of the differences $\overline{A} - \ln A_0 \equiv \ln[1 + g_1(n)]$ and $\overline{\ln A} - \ln A_0 \equiv g_3(n)$ in dependence on n. It can be seen that any averaging method yields values which exceed $\ln A_0$; however, in the case of averaging lnA the accuracy in obtaining the modulus of the spectrum is found to be somewhat better, particularly for $n < 0.5$. This circumstance must always be taken into account in calculating the average values in that case when the moduli of the spectra should change potentially in a broad range with a change in the frequency. The parts of the modulus of the signal spectrum with relatively little significance (relative to the maximum of the modulus) "float" in obtaining the average value. Therefore, the observer cannot obtain a precise modulus

of the signal spectrum $f_0(t)$ for any volume of the initial sample, in principle. The results can be corrected somewhat by considering the magnitude of this "floating". This is done more simply in the case of calculating $\overline{\ln A}$. Then, having obtained σ_{1n} from a preliminary statistical analysis, we can calculate $\underline{n}$ from (25) and further determine the unknown correction for "floating" according to (24). The "floating" of $\overline{A}$ in relation to A_0 can also be calculated with the aid of (20) and (21).

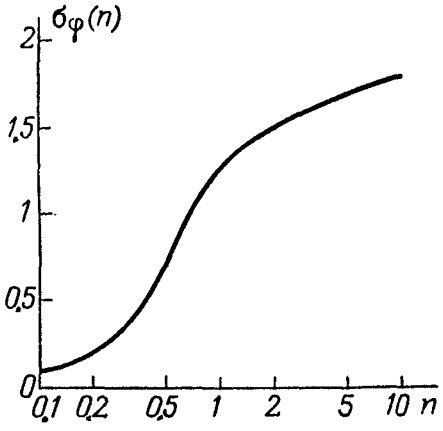

Fig. 3

Let us examine the phase of the spectrum defined as $\phi(\omega) = \arg F(j\omega)$. The average value of the phase is not shifted, i.e., $\phi(\omega) = \phi_0(\omega)$, which is substantial in determining V_{ph}. The dispersion of the phase is found in [7], while its dependence on the noise-signal ratio is shown in Figure 3. For low values of $\underline{n}$, this dependence is expressed approximatively by the formula $\sigma_\phi \simeq n$. Let us find the approximate value for the correlation of spectral components of different frequencies for low $\underline{n}$. For this, we will expand the expression for the phase into a series by deviations $\Delta X = X - X_0$ and $\Delta Y = Y - Y_0$, limiting ourselves to the quadratic terms (in this regard we will not consider $X_0(\omega_i) = A_{0i}$ and $Y_0(\omega_i) = 0$, which does not depreciate the generality in the case when conditions resulting in (16) are fulfilled:

$$\varphi_1 = \arctan\frac{Y_1}{X_1} \simeq \frac{1}{A_{01}}\Delta Y_1 - \frac{1}{A_{01}^2}\Delta Y_1 \Delta X_1,$$

$$\varphi_2 = \arctan\frac{Y_2}{X_2} \simeq \frac{1}{A_{02}}\Delta Y_2 - \frac{1}{A_{02}^2}\Delta Y_2 \Delta X_2, \qquad (26)$$

$$B_\varphi(\omega_1, \omega_2) = \overline{\varphi_1\varphi_2} \simeq \frac{B_Y(\omega_1, \omega_2)}{A_{01}A_{02}} + \frac{B_X(\omega_1, \omega_2)B_Y(\omega_1, \omega_2)}{A_{01}^2 A_{02}^2}.$$

/191

Let us consider the second model of noise, which describes the specific distortions in shapes of the signal when the narrow line is drawn incorrectly--with a pedestal and slope. The pedestal shows up when the symmetric time interval is selected only on the real part of the signal spectrum. The term added to the signal spectrum is given by the following formula:

$$(\Delta X)_n = h\int_{-T}^{T}\cos\omega t\, dt = \frac{2h}{\omega}\sin\omega T,$$

where h is the magnitude of the pedestal.

In the case of inclination of the zero line, only the imaginary part of the signal spectrum changes:

$$(\Delta Y)_z = k \int_{-T}^{T} t \sin \omega t \, dt = \frac{2k}{\omega^2} (\sin \omega T - \omega T \cos \omega T),$$

where k is the tangent of the angle of inclination of the zero line. In correspondence with the assumption that $\omega T >> 1$, the approximate value of $(\Delta Y)_z$ can be determined according to the following formula:

$$(\Delta Y)_z \simeq \frac{2kT}{\omega} \cos \omega T = \frac{2h}{\omega} \cos \omega T,$$

where 2h signifies the span of the misalignment. Assuming that the value h is distributed normally with the average zero line and dispersion σ_h^2, we find that $(\Delta X)_p$ and $(\Delta Y)_p$ are also distributed normally with average value equal to zero, and

$$\overline{(\Delta X)}_p^2 = \frac{4\sigma_h^2}{\omega^2} \sin^2 \omega T, \quad \overline{(\Delta Y)}_z^2 = \frac{4\sigma_h^2}{\omega^2} \cos^2 \omega T. \qquad (27)$$

Since distortions of the pedestal and slope type have duration equal to that of the signal 2T, which is a random value, we can also carry out averaging by T in evaluating the dispersions in $\overline{(\Delta X)}_p^2$ and $\overline{(\Delta Y)}_p^2$, on the assumption that the distribution is uniform. Then we finally obtain the following:

$$\overline{(\Delta X)}_p^2 = \overline{(\Delta Y)}_z^2 = \frac{2\sigma_h^2}{\omega^2},$$

and, due to the presence of errors of the pedestal and misaligment type, all we said above for the case of additive noise $\xi(t)$ will hold, while the value σ^2 signifies only $2\sigma_h^2/\omega^2$. We should note that complete averaging of $\sin\omega T$ and $\cos\omega T$ in (27) is possible only for /192 frequencies which satisfy the condition $\omega \Delta T >> \pi$, where ΔT is the interval of uniformly distributed deviations and duration of the signals. Thus, for ΔT = 100 μsec, we will have $f \geq 5$ KHz. For lower frequencies, we must use (27) directly, whereas, since the dispersions in the real and imaginary parts are not equal, generally speaking, there can be a shift in the average value for the phase. Having considered the most disadvantageous case, where $\overline{(\Delta X)}_p^2 = 4\sigma_h^2/\omega^2$ (or $\overline{(\Delta Y)}_z^2 = 4\sigma_h^2/\omega^2$) and $\phi_0 = \frac{\pi}{4}$, we can obtain the following approximating expression, using an expansion similar to (26):

$$|\bar{\varphi} - \varphi_0| \simeq 2n^3,$$

where $n^2 = \frac{4\sigma_h^2}{\omega^2} \Big/ A_0^2$.

Figures 4 and 5 serve as illustration of the materials in this section. Figure 4 depicts the modulus of a specific theoretical spectrum of atmospherics at a distance of 5 thous. km [14] on the assumption that $|C(j\omega)| = 1$ (Curve 1) and the results of its distortions by noises of two types (Curves 2 and 3). The first noise is white, comprising 10%(-20 db) of the spectral intensity of this signal at a frequency of 10 KHz (Curve 4)[2], while the second corresponds to atmospheric noise, the spectral intensity of which was taken from [15], and is also -20db in relation to the signal at a frequency of 10 KHz (Curve 5). Figure 5 shows the dispersion of the spectral phase of the atmospherics under the conditions of Figure 4.

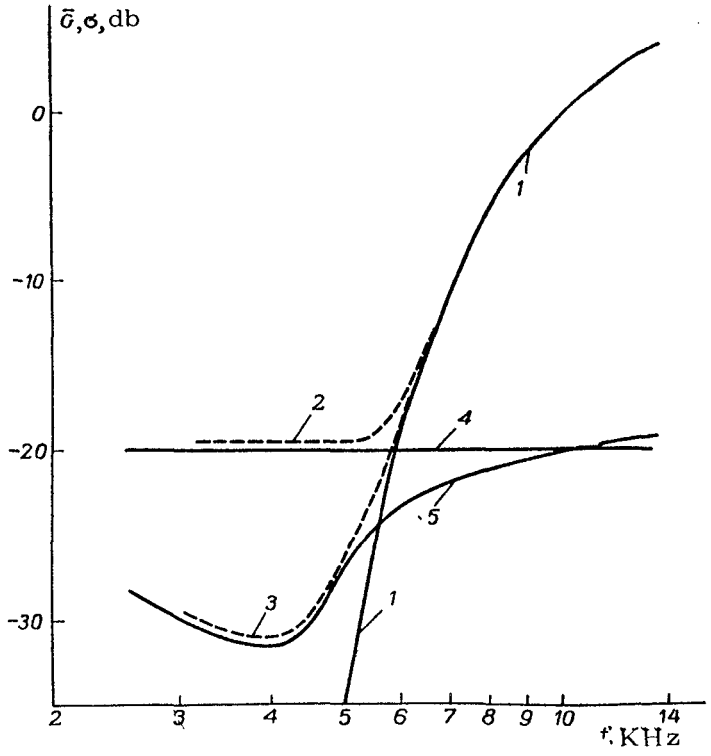

Fig. 4

[2] We can obtain from the experimental data an approximating expression which connects the ratio between the root-mean-square value of the noise and the amplitude of the atmospherics A_{max} with the value n for a frequency of 10 KHz. Thus, in the case of $B(\tau) = B(0)e^{-\frac{|\tau|}{\tau_k}}$ and for values of the parameters of $2T = 4 \cdot 10^{-4}$ sec, $\tau_k = 5 \cdot 10^{-5}$ sec, it is found that $n|_{10KHz} \cong \sqrt{B(0)}/A_{max}$.

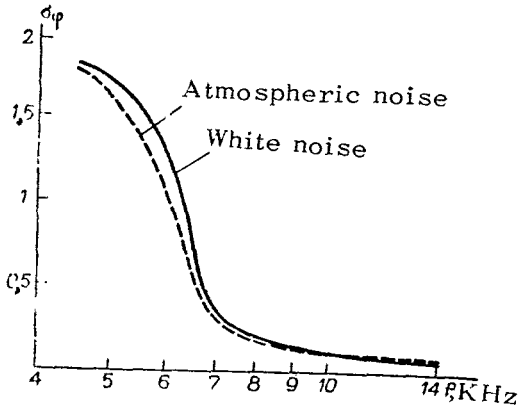

Fig. 5

4. Evaluating the Possible Accuracy in Determing the Parameters α and β. Illustrative Examples.

Knowing the requisite statistical characteristics of the spectra of the analyzed signals, we can now evaluate the accuracy in determining the propagation characteristics $\alpha(\omega)$ and $\beta(\omega)$ according to them.

Being interested in the average values of $\alpha(\omega)$, we find the following, using (3), (9) and (24) and considering the errors in μ_1 and μ_2 at the first and second observations sites as not correlated:

$$\bar{\alpha} \quad \alpha_0 + \frac{20 \log e}{D_2 - D_1} \left(g_3^{(1)} - g_3^{(2)}\right), \tag{28}$$

where α_0 is the "real" attenuation determined by (3) in the case of $\mu_1 = \mu_2 = 0$, while $g_3^{(1)}$ and $g_3^{(2)}$ are the values of the function $g_3(n)$ at the first and second sites respectively.

Further, let us analyze two cases. The first will correspond to a consideration solely of atmospheric noises, which we will assume to be identical at both recording points for the atmospherics (Curve 3 on Fig. 6). The second case will illustrate a consideration of the "noises" of the sample of data, the spectral distribution of which will be uniform in a certain frequency band (levels 4 and 5 on Fig. 6). Curves 1 and 2 correspond to the spectrum of the signal at distances of D_1 = 2 thous. km and D_2 = 5 thous. km from the source. These curves, just as the curves in Figures 5 and 4, are calculated on the basis of the theoretical data in [14] on the assumption that $|C(j\omega)| = 1$.

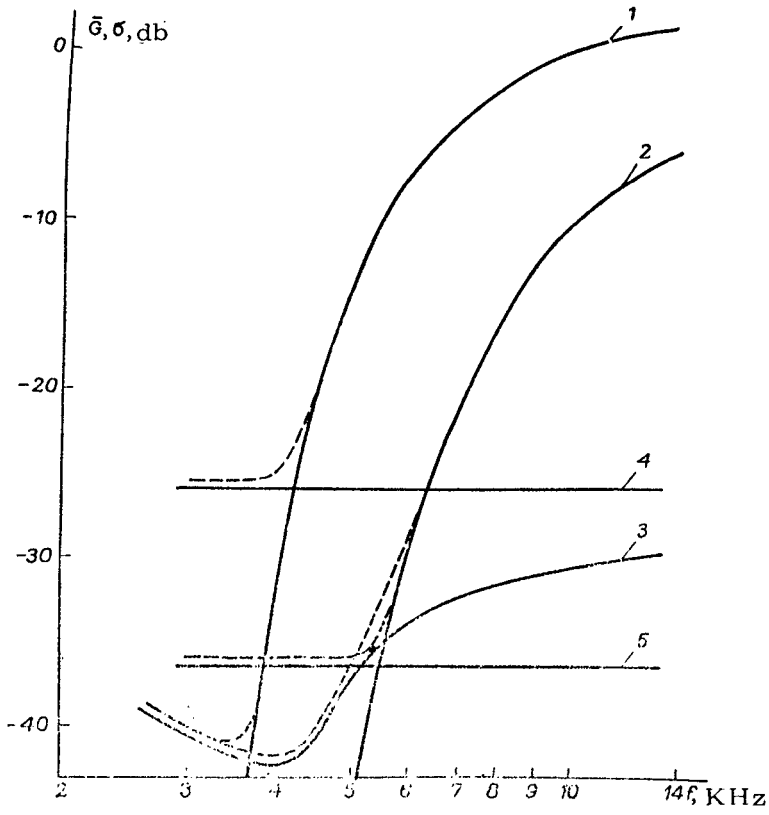

Fig. 6

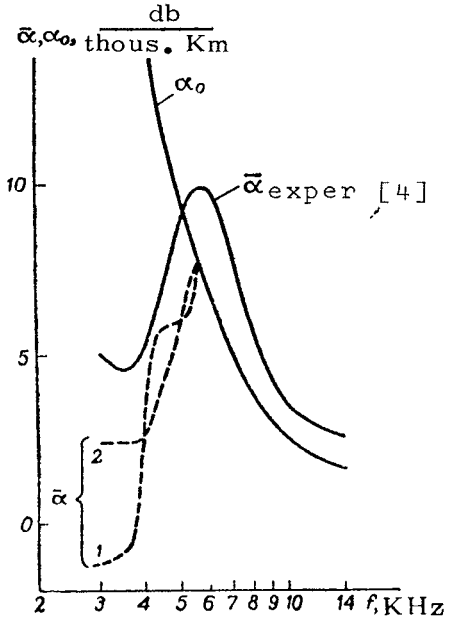

Fig. 7

In order to make the calculations more specific, we will consider the level of atmospheric noise at a frequency of 10 KHz to be equal to 10% of the signal level at a further point, while the level of "noise" in the sample of data at the same frequency is equal to 5% of the signal level at each point. This level corresponds to 5% accuracy in analyzing the time oscillograms of atmospherics (in percentages of the maximum amplitudes) for distances of 2-5 thous. km. with a time for correlation of the "noise" of the data on the order of 50 sec. We can find the noise-signal ratio $n = \sigma(\omega)/A_0(\omega)$ for all the cases of interest to us with the aid of Figure 6.

/195

Figure 7 shows the curves of

$\alpha_0(\omega)$ for the "real" dependence of attenuation on frequency [14] and the dependence $\overline{\alpha(\omega)}$ obtained according to (28) for cases where the distorting effect of atmospheric noises (Curve 1) and "noises" of the sample of data (Curve 2) are considered. Moreover, Figure 7 also shows the dependence $\overline{\alpha(\omega)}$ according to the experimental data of [4] (in this experiment, $D_1 \sim 1.5$ and $D_2 \sim 5$ thous. km). Naturally, Curves 1 and 2 represent a somewhat artificial situation, and less distorting effects of noises can be observed in practice. However, even despite its illustrative nature, the example cited indicates that there must be a very careful statistical approach to the data on attenuations of $\bar{\alpha}$ formerly obtained according to (3), in order to discuss the objectivity and reality of the results obtained.

A qualitative evaluation of the closeness of the dependences of $\overline{\alpha(\omega)}$ obtained to some real $\alpha_0(\omega)$ can be carried out on the basis of an investigation of the standards for deviation in $\alpha(\omega)$:

$$\sigma_\alpha \approx \frac{20 \log e}{D_2 - D_1} \sqrt{\sigma^2_{\ln A_1} + \sigma^2_{\ln A_2}}.$$

Thus, if the derivative of $\sigma_\alpha(D_2-D_1)$ is on the order of 6 db (see the expression for σ_∞ on p. 212, the result of $\overline{\alpha(\omega)}$ actually has no physical significance. For smaller values of $\sigma_\alpha(D_2 - D_1)$ on the basis of the recommendations made in the preceding sections. /196

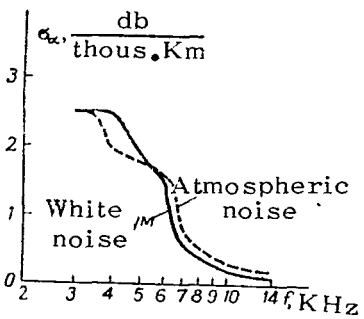

Fig. 8

Figure 8 shows the dependence $\sigma_\alpha = \sigma_\alpha(\omega)$. The symbols and the initial conditions are the same here as for Figures 6 and 7.

It follows from the preceding section that the algorithm for calculating $\beta(\omega)$ gives an unchanged estimate of $\overline{\beta(\omega)}$, except for the very lowest frequencies (see p. 215). The average quadratic deviation of $\beta(\omega)$ is determined by the following formula:

$$\sigma_\beta = \frac{1}{D_2 - D_1} \sqrt{\sigma^2_{\varphi_1} + \sigma^2_{\varphi_2}}$$

A sharp increase in the dispersion for frequencies lower than 4-5 KHz (see Fig. 5) should be taken into account in carrying out the matching operating (Section 1) and in evaluating the significance of the results obtained for $\overline{\beta(\omega)}$ and $\overline{V_{ph}(\omega)}$.

In conclusion, we should mention that, together with the method of determining the attenuations (and phase velocities) accord-

ing to calculated spectral characteristics of atmospheric waves, there are also widely-used methods based on direct apparatus changes in the spectral characteristics of atmospherics. Studies of the errors in such methods have much in common with the problems examined above, and the authors suggest they be completed in the nearest future.

The authors consider it their privilege to express their appreciation to G. I. Makarov and V. V. Novikov for their constant attention and useful advice in discussing this work.

REFERENCES

1. Mikhaylova, G.A.: The Spectra of Atmospheric Waves and the Phase Velocity of Electromagnetic Waves at Superlow Frequencies. Geomagnetizm i Aeronomiya, Vol. 2, No. 2, 1962.
2. Mikhaylova, G.A. and T. I. Kurakina: The Phase Velocity of Electromagnetic Waves in the Range of 1-25 KHz. Geomagnetizm i Aeronomiya, Vol. 3, No. 2, 1963.
3. Mikhaylova, G.A.: Distribution Function and Average Phase Velocity of Electromagnetic Waves at Superlow Frequencies. Geomagnetizm i Aeronomiya, Vol. 5, No. 1, 1965.
4. Taylor, W.L.: VLF Attenuation for East-West and West-East Daytime Propagation using Atmospherics. J. Geophys. Res., Vol 65, No. 7, 1960.
5. Jean, A.G., W. L. Taylor and J. R. Wait: VLF Phase Characteristics Deduced from Atmospheric Waveforms. J. Geophys. Res., Vol. 65, No. 3, 1960.
6. Vasyuk, G.I. and V. I. Chaykovskiy: Statistical Characteristics of the Selective Spectral Capacitive Density of a Stationary Random Process. Vestnik Kiyevskogo Politekhn. Instit., No. 2, Kiev, 1965.
7. Levin, B.R.: Teoreticheskiye osnovy statisticheskoy radiotekhniki (Theoretical Principles of Statistical Radio-Engineering). "Sovetskoye Radio", 1966.
8. Krasnushkin, P. Ye. and N. A. Yablochkin: Teoriya rasprostraneniya sverkhdlinnykh voln (Theory of the Propagation of Superlong Waves) VTs Akad. Nauk S.S.S.R., 1963.
9. Wait, J.R.: Influence of Finite Ground Conductivity on the Propagation of VLF Radio-Waves. J. Res. NBS, Vol. 69D, No. 10, 1965.
10. Taylor, W.L.: Radio Field Characteristics of Lightning Discharges in the Bank 1 kc/s. J. Res. NBS, Vol. 67D, No. 5, 1963.
11. Sao, K.: A Note on the Phase-Frequency Spectra Analysed from Waveforms of Atmospherics. J. Atm. a. Terr. Physics, Vol. 24, 196
12. Figel', D.S.: Synthesis of Atmospheric Waveforms. Trudy IZMIRAN, No. 17, (27), 1960.
13. Ryzhik, I.M. and I.S. Gradshteyn: Tablitsy integralov, summ, ryadov i proizvedeniy (Tables of Integrals, Sums, Series and Derivatives). 4th Ed., Supp. "Fizmatgiz", 1962.
14. Rybachek, S.T. and E.M. Gyunninen: Propagation of Long and Superlong Radio Waves in the Waveguide Channel Earth-Ionosphere.

In the Collection: Problemy difraktsii i rasprostraneniya voln (Problems of Wave Diffraction and Propagation), No. VI. Leningrad State Univ. Press, 1966.
15. Watt, A.D. and E.L. Maxwell: Proc. IRE, Vol. 45, No. 6, 1957. Russian Translation: Kharakteristiki atmosfernykh pomekh v diapazone chastot ot 1 do 1000 kgts. In the Collection: Rasprostraneniye dlinnykh i sverkhdlinnykh radiovoln (Propagation of Long and Superlong Radio Waves) Foreign Literature Publishing House, 1960.

EXPERIMENTAL STUDY OF THE DIPOLE AND CURRENT MOMENTS OF LIGHTNING DISCHARGES

Yu.V. Shtennikov

Part I. Methods of Studying a Dipole Model of Emission Sources

ABSTRACT: Two methods of studying the dipole and current moments of lightning discharges are described in this study. It is shown that the method of direct recording with the aid of filters has definite advantages, particularly for short-period signals.

Introduction

/19

This work discusses studies of lightning discharge as a source of electromagnetic waves. In 1926, P. Lejey [1] first suggested that lightning be examined as an emitter of electromagnetic waves in the form of a vertical electric dipole. This model was used in a number of studies [2,3] in order to determine the parameters of an equivalent source according to an electric and magnetic field; however, there was no attempt at testing the correctness of this model. This work is an attempt at filling in the gaps in studies of lightning discharges.

We used the model of a vertical point dipole for lightning discharge in our study. It can be shown that any complex emitter of electromagnetic waves can be replaced by the equivalent dipole which produces the same field as the original source at a given point. However, if the original emitter is not a dipole in terms of its physical nature, then the equivalent dipole must be ascribed a dipole moment whose dorm depends on the distance to the observation point. Thus, the nature of the emission source can be determined by examining the structure of its electromagnetic field.

By analyzing oscillograms of synchronous atmospherics, we succeeded in showing the correctness of the dipole model for the principal discharges of lightning at a distance greater than 30 km from the discharge, within the limits of experimental errors, which were 16%. The possibility of representing such an extensive emitter in the form of a vertical dipole can be explained by the fact that the emission of branched horizontal segments of lightning is just as ineffective as the emission of a horizontal dipole for observation points located on the ground.

We will be making a comparative analysis of two methods for

measuring and calculating the dipole and current moments of discharges in relation to their precision and interference resistance, /1 and we will present the preliminary results of the experiment. In the second part of the article, we intend to present the results of experimental measurements of the dipole and current moments of different types of discharges. This article contains materials which are part of a dissertation written by the author under the direction of G.I. Makarov.

Section 1. Methods of Reconstructing the Dipole Moments of Emission Sources

For the field of a vertical electric dipole located on the ground, we can write out an equation which connects the vertical components of the electrical field $E_z(t)$ with the dipole moment of the source P(t) in the following way:

$$E_z(t) = -\frac{\mu}{2\pi r}[P''(t) + \alpha P'(t) + \alpha^2 P(t)], \qquad (1)$$

where $\mu = 4\pi \cdot 10^{-7}$ H/m; $\alpha \equiv \frac{c}{r}$; $c = 3 \cdot 10^5$ km/sec; r is the distance to the emitter. The solution to this equation can be written in the form of a convolution, i.e.,

$$P(t) = \frac{4\pi r^2 \varepsilon_0 c}{\sqrt{3}} \int_0^t E_z(t-\tau) e^{-\frac{\alpha\tau}{2}} \cdot \sin\frac{\alpha\sqrt{3}}{2}\tau d\tau. \qquad (2)$$

In order to determine the dipole moment, we can use two methods (two plans) according to (2).

1. The method of numerical calculations of the dipole moment. For this, the oscillograms of the electric field $E_z(t)$ obtained in the recording are tabulated, and the integral of (2) is calculated on a digital computer by numerical methods.

2. The method of direct recording, which immediately yields an oscillogram of the dipole moment, by the insertion of special filters between the antenna and the recorder; the arrangement of these filters is determined by the distance to the source.

Let us examine these methods in more detail. In using the first method (Fig. 1a), the signal from antenna 1 enters the input device 2 which is intended for separating the signals of lightning discharges from against the background of industrial interference and interference from radio stations. Its coefficient of transmission is close to unity in the frequency band ΔF occupied by the signals of the lightning discharges, and decreases sharply outside of it. On the screen of the oscillograph 3 which is in-

stalled behind the input device 2, we find the oscillogram of the vertical components of the electric field $E_z(t)$, which we tabulated /20 and introduced to the digital computer 5 in order to calculate the dipole moment P(t) according to (2).

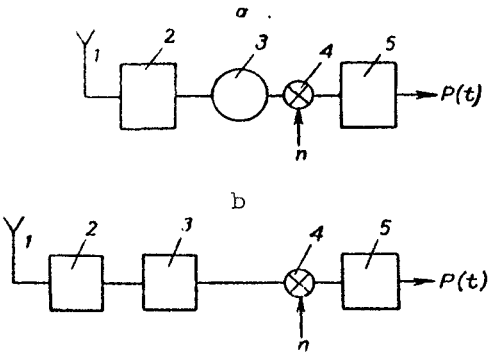

Fig. 1.

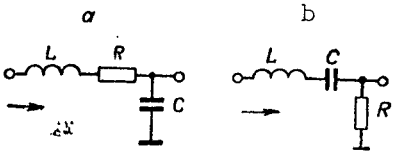

Fig. 2.

Let us consider the scheme of the operation according to the second method (Fig. 1b). It differs from the scheme in Figure 1(a) in that the signal goes from the output of the input device 2 to the filter 3 with impulse characteristics of the type

$$h(t)=\frac{2\alpha}{\sqrt{3}}e^{-\frac{\alpha t}{2}}\sin\frac{\sqrt{3}}{2}\alpha t, \qquad (3)$$

where $\alpha = c/r$.

The filter carries out the operation which was done by the digital computer in the first scheme (Fig. 1a), and the parameters of this filter are determined only by the distance to the source of emission. The voltage $U_p(t)$ at the output of filter 3 is proportional to the dipole moment P(t) only in that case when the distance over which the signal has came corresponds to the distance by which the filter was tuned. When there is detuning, the signal $U_p(t)$ must be subjected to an additional analysis with the digital computer 5 in order to eliminate the effect of the detuning, as is shown in Figure 1(b).

We should mention that, as is easy to show, the filter with pulse characteristics described by (3) can be made in the form of a successive oscillational contour (Fig. 2a). Its parameters are connected with the parameters of the filter in the following way:

$$\omega_0=\frac{1}{\sqrt{LC}}=\alpha=\frac{v}{r} \quad \text{at} \quad Q=\frac{\rho}{R}=1$$

$$\rho = \sqrt{\frac{L}{C}}. \qquad (4)$$

The transmission coefficient of this filter can be written out in the following way:

$$K_p = \frac{\alpha^2}{p^2 + \alpha p + \alpha^2}. \qquad (5)$$

It is obvious that we can thus have a filter which reconstructs the current moment of the source, i.e.,

$$I(t) = \frac{dP}{dt}. \qquad (6)$$

It also has the form of an ordered oscillational contour, and only the output voltage is taken from the active element (Fig. 2b), while the relationships between the parameters remain the same.

Let us compare these methods from the point of view of accuracy in the final results and convenience in using them. It is difficult to carry out such an analysis in the general case without specifying the frequency properties of the receiving circuit, the signals under investigation and the interference.

The spectral properties of the signal from lightning discharges are characterized by the curves on Figure 3a. The maxima of spectral density are found at a frequency of 4-8 KHz for the principal discharges (Curves 1 and 2 on Fig. 3a) and at a frequency of 12-15 KHz for leader discharges (Curves 3 on Fig. 3a), which are recorded in the wave zone at a distance of 50-100 km from the source.

Let us examine the properties of interference which can affect the results of our calculations and measurements. The interference can be divided into external and internal types. In relation to external interference imposed on an antenna, both of the methods under investigation are equivalent, and the only difference is found in relation to internal supplementary errors which can arise in analyzing the oscillograms. They can be divided into random errors, connected with the finite accuracy in reading, and systematic ones, obtained, for example, as a result of an incorrect plotting of the zero line on the oscillogram. These errors are equivalent in their effect to the inclusion of some internal interference. We should mention that this interference will also play a major role in view of the fact that the signals examined in this study greatly exceed the level of atmospheric noise interference.

Let us describe the spectral properties of internal noises. Random errors arising because of the finite thickness of the line on the oscillogram result in supplementary interference of the random type for a discrete selection of the reading points; we will call this type of interference the noise of sampling of the data. This noise can have a uniform spectrum in the transmission end of the input device (Curve 4 on Fig. 3b). Systematic errors, or a distortion of the zero line on the oscillogram in the form of a jump or sag, have a spectrum with maximum spectral density at zero frequency. The spectra of interference of these types are shown in Figure 3b (Curve 5 for the jump and Curve 6 for the sag).

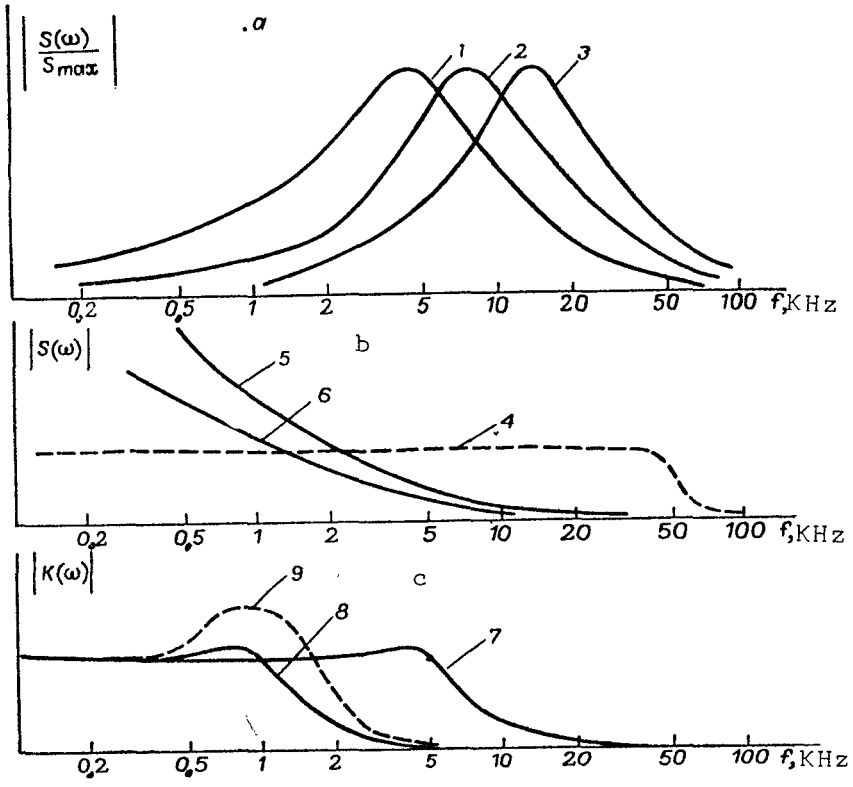

Fig. 3.

The dipole moments P(t) can be reduced according to the electrical field with any of the methods examined above, for the equivalent operation of linear filtration by an upper-frequency filter with limit frequency of $f_0 = \frac{c}{2\pi r}$. The frequency characteristics of the receiving circuit are shown in Figure 3(c) for distances of 10 and 50 km from the source of emission (Curves 7 and 8, respectively).

Let us now attempt to draw qualitative conclusions on how the signal-noise ratio changes in passing through the receiving circuit. As was already mentioned, both methods are equivalent in /203
relation to external interference. However, different types of internal interference have different effects, since they are connected at various points on the diagrams as shown in Figures 1(a) and 1(b).

In the diagram (Fig. 1a), the "connection" of interference takes place at point 4 in tabulation of the signal. It can be seen from an examination of the spectral properties of the signals, interference and receiving circuit (Fig. 3) that, in the passage of signals and interference through filter 3 (Fig. 1b) there can only be a worsening of the signal-noise ratio, because the signal is richer in higher frequencies than the interference under investigation (a particular worsening can be expected for high-frequency signals of the leader discharge type for lightning). Thus, we can conclude that the introduction of an additional processing can result in substantial errors in the final result, which are absent in using the second method--the method of direct recording. However, when there is detuning between the distance over which the signal has come and the distance by which the filter is tuned, and when the second method is used, we must carry out an additional analysis of the signal in order to compute the corrections for detuning, which is also equivalent to the connection of some additional interference at point 4 on Figure 1(b). However, if filter 3 is tuned at a rather great distance, e.g., 50 km, then the basic filtration, i.e., separation of the low-frequency part of the signal spectrum, is already carried out by filter 3 with the frequency characteristic presented on Figure 3c (Curve 7 or 8), while the operation carried out on the signal with the digital computer 5 is equivalent to filtration by some filter whose frequency characteristic is also represented in Figure 3(c) for some detuning (Curve 9). From examining the frequency properties of the signal $U_p(t)$ and Figure 3(c), we can conclude that the latter operation changes the signal-noise ratio very little and only brings about some correction for the form of the signal $U_p(t)$ due to the detuning. Thus, the connection of "interference" (additional processing) behind filter 3 decreases the error in the final results substantially, compared to the first method. Therefore, we can draw a definite conclusion concerning the advantage of the second method--the method of direct recording with the aid of filters--in relation to the accuracy and interference resistance. Moreover, this method has an indisputable advantage in terms of the clarity of the data and the speed at which it is obtained.

The conclusion we have derived may seem strange since, at first glance, both methods are physically equivalent if we disregard the effect of interference, because the operation carried out on the digital computer in using the first method (Fig. 1a) is equivalent to the linear filtration by filter 3 in using the second method

(Fig. 1b). However, the internal interference and limitedness of the dynamic range for the oscillographic recording have different effects on the final results, depending on whether or not they are imposed on the signal before or after filter 3 (Fig. 1), which changed the spectral composition of the signal substantially.

Let us present some quantitative evaluations of the effect of /204
the noise of data samplings on the restoration of dipole moments by the method of numerical calculations. For this, we will calculate the change in dispersion of white noise in its passage through the filter with pulse characteristics of (3). If we compare these results to the attenuation of typical atmospherics by the same filter, then we can use the following expression to evaluate the relative errors due to the noise of sampling of the data:

$$\frac{\frac{\sqrt{D_{вых}}}{P_{max}}}{\frac{\sqrt{D_{вх}}}{E_{z\,max}}} = \left(\frac{f_m}{f_0}\right)^2 \sqrt{\frac{2f_0}{\Delta F} F(x)}, \qquad (7)$$

where

$$F(x) = 1 - e^{-x}\left(\frac{2}{3}\sin^2\frac{\sqrt{3}}{2}x + \frac{1}{\sqrt{3}}\sin\sqrt{3}x + 1\right);$$

$x = \alpha t$; D_{out} is the known dispersion at the output of the filter; D_{in} is the dispersion of noise at the input of the antenna; ΔF = 50 KHz is the band width of the recording apparatus; P_{max} is the maximum value of the dipole moment P(t); $E_{z\,max}$ is the maximum amplitude of the signal $E_z(t)$; f_m is the frequency of the maximum spectral density of the atmospherics; $f_0 = \frac{c}{2\pi r}$ is the limit frequency of filter 3; r is the distance to the emission source; t is the time for observation, starting with the beginning of the signal.

r, км	f_0, KHz	$x = \alpha t$, $t = 0{,}3$ msec	Errors		
			$f_m = 5$ KHz	$f_m = 10$ KHz	$f_m = 15$ KHz
10	5	9,5	0,3	1,2	2,7
20	2,5	4,8	0,9	3,5	8
50	2	1,9	3	12	27
100	0,5	0,9	5	20	45
200	0,25	0,45	6,2	25	56

The graph for the function F(x) is shown in Figure 4. It demonstrates how the error increases with an increase in the observation time. The results of calculations according to (7) for a moment of time of 300 μsec with bandwidths of the recording

apparatus of 50 KHz given in the Table show by what factor the relative error in calculating the dipole moment exceeds the relative error in the measurements. The calculations were made for the principal (f_m = 5 and 10 KHz) and leader (f_m = 15 KHz) lightning discharges. The errors increase with an increase in the distance, particularly for short-period signals. If we take a value equal to 5% for the average error in recording the forms of the atmospherics, then we can see that, for long-period atmospherics with maximum spectral density occurring in the range of 5 KHz, the reduction of dipole moments in calculations with accuracy up to 30% can possibly be up to 160 km, while that for short-period ones is only up to 20 km.

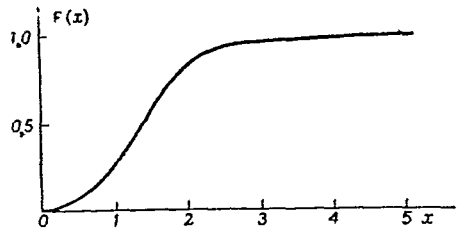

Fig. 4.

Calculations evaluating the effect of errors in sampling the data when using the method of direct recording (Fig. 1b) show that the relative error in determining the dipole moment increases by no more than a factor of 1.4, compared to the relative errors in measuring the signal $U_p(t)$, even for detuning by 50%. The calculations were carried out for a moment of time 300 μsec after the beginning of the signal, for filters tuned by 50 and 100 km. It can be seen from a comparison of the data presented in the Table that, under the same conditions, the error in the method of numerical calculations increases by a factor of 5-45. This indicates that the method of direct recording by the aid of filters has a definite advantage.

Section 2. Preliminary Results of Experimental Studies

The purpose of our experimental studies was to find the validity of using the model for lightning discharge and to define its principal characteristics. We will present only the preliminary results; they touch mainly on a clarification of the dipolar nature of the source. The principal results of the experiments will be published at a later time.

The experimental study was carried out at Voyeykovo, part of the Leningrad region, in the summer, when local storms were observed in radius of 200 km. The dipole and current moments of the discharges were reduced both with the aid of numerical calculations according to the oscillograms of the vertical component of the electrical field and by the method of direct recording with the aid of filters.

In order to find the nature of the source, we carried out calculations of the dipole moments of synchronous atmospherics

recorded by the receiving site of the Main Geophysical Observatory /2
at Voyeykovo and Roshchino (Curves 1 and 2 on Fig. 5, respectively). A comparison of the dipole moments of the synchronous atmospherics, with accuracy up to the experimental error, showed that the dipole model for the lightning discharge as the emitter of electromagnetic waves at distances greater than 30 km was valid. The calculations were carried out for 12 pairs of synchronous atmospherics, and the distances they spanned changed from 30 to 140 km. The errors in the oscillographic recording were equal to 5% in this case, while the errors in determining the distance with the bearing network of the Main Geophysical Observatory were 10%.

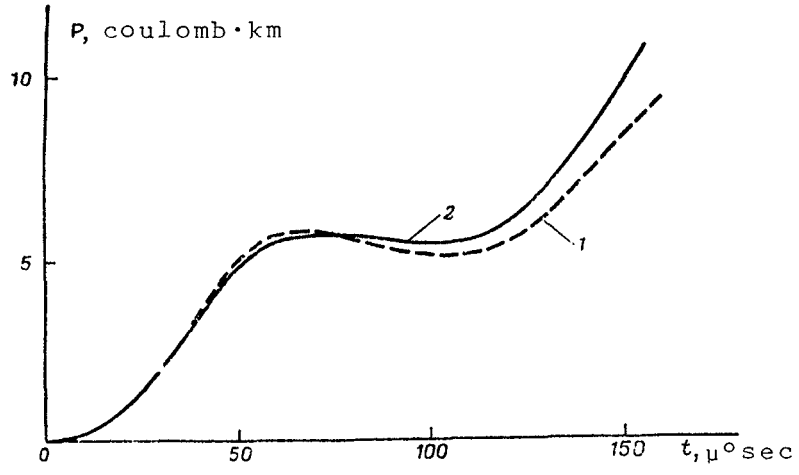

Fig. 5.

We used the arrangement whose blocks-diagram is given in Figure 6 in order to determine the dipole and current moments of the discharges by the method of direct recording.

The signal was received on a collapsible-whip antenna 1 of a 10 m-length and through a remote cathode follower 2 to the delay line 3, and then through the amplifier 4 to filters 5 and 6, for separation of the dipole and current moments. The signals whose amplitude was proportional to the dipole and current moments of the source were photographed from the screen of a dual-beam oscillograph 7 equipped with photographic adjuster 8. The scanning of the oscillograph 7 was started up by a threshold device 9. The correction for detuning between the filter alignment and the real distance to the lightning discharge, determined with the aid of the bearing network of the Main Geophysical Observatory imeni Voyeykovo [4], was carried out by calculations on a digital computer. The oscillograms of the dipole and current moments of dis- /2
charges recorded experimentally with the aid of filters tuned for a distance of 50 km are shown in Figures 7(a) and 7(b), respectively;

the results of calculations of corrections for detuning are also depicted there by the dotted line. As can be seen from the figure, they are not very great, particularly for the current moments, and they often can be disregarded. The average values for the maxima

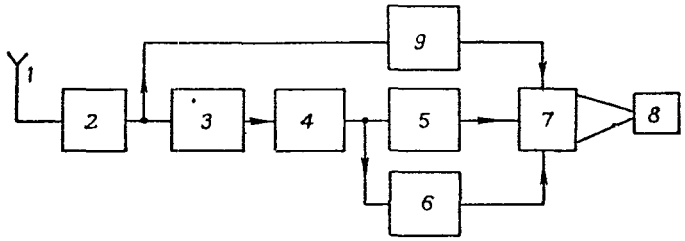

Fig. 6.

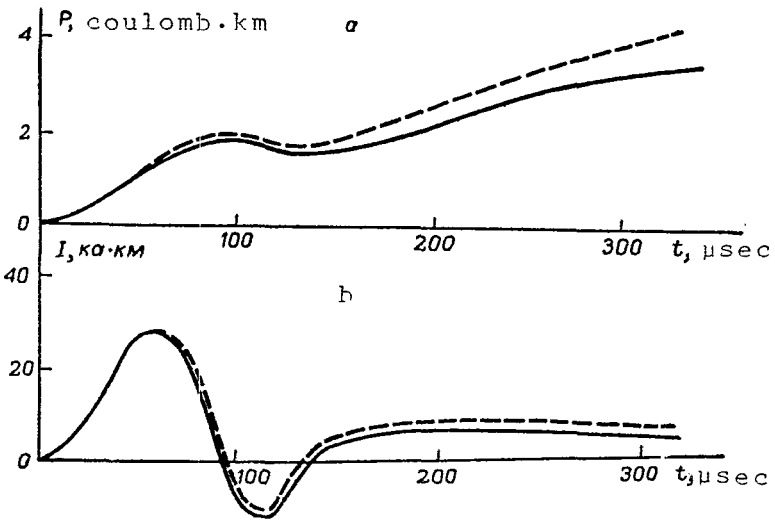

Fig. 7.

of the dipole and current moments were determined; they were found to be equal to 3 coulomb·km for the dipole moment and 32 ka·km for the current moment. They were recorded at the start level for scanning ± 1-0.8 V/m, and it was mainly the principal lightning discharges with greatest amplitude which were recorded. We should /208 point out the characteristic features of the shape of the dipole moments--the presence of a bend in the curves. This can be explained in terms of the superposition of two processes with dipole moments which have different speeds of change in time. Two stages can be separated: a rapid one with maximum dipole moment at 80-120 μsec causing the signal which, naturally, is called the atmospherics

(this stage can be connected with the movement of the discharge along the channel), and a slow one, with maximum dipole at 500-880 μsec, which is possible the source of the low-frequency part of the atmospherics--the so-called "tail". In physical terms, it is due to the dissipation of the charged column around the channel of the discharge.

Conclusions

Two methods of studying the dipole and current moments of lightning discharges are described in this study. Definite advantages in using the method of direct recording with the aid of filters, particularly for short-period signals, are demonstrated. By restoration of dipole moments according to synchronous oscillograms, the validity of using the dipole moment for a lightning discharge as the emitter of electromagnetic waves at distances greater than 30 km is shown. The dipole and current moments of the principal discharges are presented.

In conclusion, I would like to express my appreciation to G.I. Makarov and V.V. Novikov for their attention and help in the study, as well as the co-workers of the Division of Atmospheric Electricity of the Main Geophysical Observatory imeni A.I. Voyeykovo for kindly lending us oscillograms of synchronous atmospherics and data on the direction-finding of neighboring storms.

REFERENCES

1. Lejey, P.: Les perturbations oranges du champ electrique et leur propagation a grande distance (Orange Disturbances of the Electrical Field and Their Propagation at Great Distances). L'onde Electrique, Vol. 5, Paris, 1926.
2. Norinder, H. and O. Dahle: Measurements by Frame Aerials of Current Variations in Lightning Discharges. Arkiv Mat. Astr. Fys., Vol. 32A, No. 2, 1945.
3. Muller-Hillebrand, D.: Magnetic Field of Lightning Discharges. Proc. Intern. Conf. Gas Discharge and Electric Supply. London, 1962.
4. In'kov, B.K.: Rezul'taty registratsii form blizhnikh atmosferikov (Results of Recording the Forms of Neighboring Storms). GGO (Main Geophysical Observatory), No. 177, 1965.

Translated for the National Aeronautics and Space Administration by:
Aztec School of Languages, Inc.,
Research Translation Division (333)
Maynard, Massachusetts.
NASw-1692.